The Siemens Hybrid Process:

Mathematical Modeling and Analysis of an Innovative and Sustainable Pilot Wastewater Treatment Process

by

Michelle Nichole Young

A Thesis Presented in Partial Fulfillment
of the Requirements for the Degree
Master of Science

Approved November 2011 by the
Graduate Supervisory Committee:

Bruce E. Rittmann, Chair
Peter Fox
Rosa Krajmalnik-Brown

ARIZONA STATE UNIVERSITY

December 2011

ABSTRACT

To address sustainability issues in wastewater treatment (WWT), Siemens Water Technologies (SWT) has designed a "hybrid" process that couples common activated sludge (AS) and anaerobic digestion (AD) technologies with the novel concepts of AD sludge recycle and biosorption. At least 85% of the hybrid's AD sludge is recycled to the AS process, providing additional sorbent for influent particulate chemical oxygen demand (PCOD) biosorption in contact tanks. Biosorbed PCOD is transported to the AD, where it is converted to methane. The aim of this study is to provide mass balance and microbial community analysis (MCA) of SWT's two hybrid and one conventional pilot plant trains and mathematical modeling of the hybrid process including a novel model of biosorption.

A detailed mass balance was performed on each tank and the overall system. The mass balance data supports the hybrid process is more sustainable: It produces 1.5 to 5.5x more methane and 50 to 83% less sludge than the conventional train. The hybrid's superior performance is driven by 4 to 8 times longer solid retention times (SRTs) as compared to conventional trains. However, the conversion of influent COD to methane was low at 15 to 22%, and neither train exhibited significant nitrification or denitrification. Data were inconclusive as to the role of biosorption in the processes.

MCA indicated the presence of *Archaea* and nitrifiers throughout both systems. However, it is inconclusive as to how active *Archaea* and nitrifiers are under anoxic, aerobic, and anaerobic conditions.

Mathematical modeling confirms the hybrid process produces 4 to 20 times more methane and 20 to 83% less sludge than the conventional train under various operating conditions. Neither process removes more than 25% of the influent nitrogen or converts more that 13% to nitrogen gas due to biomass washout in the contact tank and short SRTs in the stabilization tank. In addition, a mathematical relationship was developed to describe PCOD biosorption through adsorption to biomass and floc entrapment. Ultimately, process performance is more heavily influenced by the higher AD SRTs attained when sludge is recycled through the system and less influenced by the inclusion of biosorption kinetics.

ACKNOWLEDGMENTS

My path to the point of writing a thesis and obtaining a Master degree has been a long, surreptitious journey. I received my Bachelor degree in Chemical Engineering in 1997 from Arizona State University. Quickly after that, I began a successful career in packaging engineering and manufacturing. However, I found this career hollow and miserable. I realized obtaining a chemical engineering degree had more to do with hubris than enjoyment. It was then I realized I needed a change.

When I began my graduate studies in 2009, I had an avid interest in both water and energy. As I perceive it, these two things represent the greatest obstacles to humanity over the next hundred years. There is not enough drinkable water available to hydrate all of humanity. As we have become more advanced as a species, our fates have become even more intertwined with the availability of energy to make life manageable, easier, and longer.

In November 2009, Dr. Bruce Rittmann interviewed me for a research assistant position on the Siemens hybrid project. I could not have found a better fit for my interests. The project's objective of creating affordable energy from wastewater addresses both energy and discharging clarified water into watersheds. In addition, I have always enjoyed computer programming and the concept of modeling. Dr. Rittmann placed me in the tutelage of Dr. Seongjun Park, one of the most gifted biological systems modelers in the world. At the same time this project began, I happened to be taking Biological Wastewater Treatment with Dr.

Peter Fox. After every class, I picked his brain for knowledge which would help me with modeling SWT's systems. Dr. Rosa Krajmalnik-Brown has been essential in educating me on microbial ecology. Dr. Andrew Marcus and Michal Ziv-El have been essential sounding boards during this process. Finally, I must acknowledge the guidance and support of Dr. Rittmann. Dr. Rittmann has been simply an inspiration. It has been an honor to work with him over the last year and a half. His amazing innovation, intelligence and prominence in the field of biological water treatment are well known. However, it is his humility and zeal for biological water treatment which is both contagious and inspiring. His goal in life seems to be taking complex fundamental concepts and applying them for the better of us all. I am notorious for simply showing up at his office and asking (and praying) for help. He never turns you away when you have a question. Plus, the man is has a wonderful sense of humor and is incredibly funny. We should all be thankful for his dedication to this field.

This journey began with one simple introduction. In August of 1996, I began a life changing internship in Northern California where I met my husband, James Wambold. Jim has maintained a beautiful, calming presence in my life since that point. It is his encouragement and sacrifice which have allowed me to pursue a new path in life in a field I was passionate about. Jim's incredible patience and even temper have been tested countless times over the last two years, and I am blessed to have him in my life. I must also acknowledge the love and support of my parents, Melvin and Cynthia Young. My father encouraged my

passion for science and math. My mother taught me compassion and love for everything around me, including the Earth. At the age of six, it was my mother that encouraged me to take my first steps into the environmental realm when I organized the neighborhood children to clean up the surrounding desert. Thank you also to my sister, Heather, and her family for their patience over the last two years.

Finally, this project would not have happened without the financial funding by Siemens Water Technologies, Inc., (SWT) along with the Swette Center for Environmental Biotechnology at Arizona State University. This project provided me with exposure to many typical water and wastewater treatment technologies and their real world applications. In particular, I want to thank Dr. Wenjun Liu, SWT's project leader, and Dr. Bobby Ding, pilot plant manager, for their incredible patience and support on this.

TABLE OF CONTENTS

Page

CHAPTER Page

CHAPTER Page

LIST OF TABLES

Table Page

Table Page

LIST OF FIGURES

Figure Page

Figure Page

Figure Page

Figure Page

Figure Page

1. Introduction and Significance

1.1 Wastewater Treatment's Effect on Sustainability is Under Scrutiny

There is little debate that municipal and industrial wastewater treatments are critical processes in the preservation of watersheds and the environment. The 2008 United States Environmental Protection Agency's (EPA) Clean Watersheds Needs Survey estimated that more than 226 million people in the United States have their wastewater treated by one of more than 14,000 wastewater treatment plants (WWTPs). A total of 11.7 billion gallons of wastewater are treated every year in the United States and released to watersheds and land as diverse as golf courses, oceans, rivers, and aquifers (U. S. Environmental Protection Agency, 2008).

The quest for energy efficiency has become an industry-wide focus in wastewater treatment. Wastewater treatment plants account for 3% of the total electricity usage in the United States, and it is estimated that their energy usage will increase by 20% in the next fifteen years (Carns, 2005). Figure 1.1 illustrates how electrical energy is used in a typical WWTP that employs activated sludge. Not surprisingly, the largest consumer of electricity in a typical activated sludge wastewater treatment plants is aeration, which is estimated to consume more than 54% of the required operational electricity for the plant for the support of aerobic treatment processes. Energy usage in wastewater treatment continues to climb as technologies with higher energy consumption, such has UV disinfection and

membrane filters, are introduced to help facilities meet more stringent treatment guidelines.

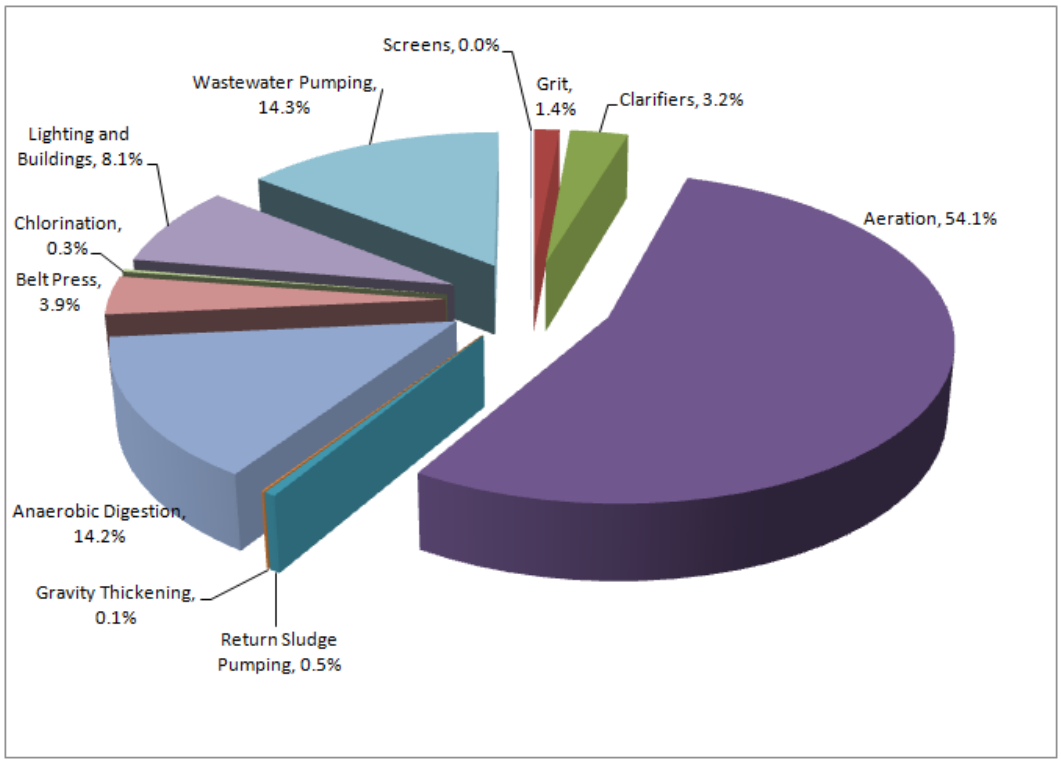

Figure 1.1. Typical electricity use for a WWTP that employs the activated sludge process. Source: O'Callaghan (2009).

Along with energy efficiency, the wastewater industry's is equally concerned about the fate of biosolids. It is estimated that 8 million dry tons of sludge were produced by U.S. wastewater treatment facilities in 2005, with 41% being applied to land application, 22% incinerated, and 17% being disposed of at landfills (Center for Sustainable Systems, University of Michigan, 2009). While wasted sludge produced during wastewater treatment is nutrient-rich, processes by which the solids are conditioned for reuse as soil nutrients or incineration are highly energy intensive.

Concerns also have grown over the relationship between sludge and the EPA's ever-increasing list of emerging environmental contaminants. The most prominent question is whether waste sludge from wastewater treatment contains these contaminants and if the contaminants can be transferred from sludge to the soil, seep into water tables, permeate ecosystems, and end up in food at our table. In June 2009, the United States Supreme Court refused to hear arguments in a 10-year old legal case regarding Kern County, California's refusal to allow Los Angeles County to dispose of biosolids at a farm purchased in Kern County for that specific reason (Sahagun, 2010).

1.2 The "Conventional" Activated Sludge Process

The activated sludge process is the most widely used biological treatment process for municipal and industrial wastewater in the United States, Europe, and Japan. The activated sludge process normally is located after primary sedimentation in wastewater treatment plants. It is a synergy of biological, physical, and chemical processes to remove one or more biotransformable pollutants from wastewater. Although the basic concept of conventional activated sludge treatment is strictly an aerobic process to remove chemical oxygen demand (COD), this is no longer a restriction: in the last twenty years, commercial processes have incorporated a variety of non-aerobic processes to address denitrification, phosphorus removal, and sludge reduction (Metcalf & Eddy, 2003).

The basic activated sludge process consists of four parts, as illustrated in Figure 1.2: an aeration tank, a settling tank (or clarifier), a solids recycle line that returns sludge to the aeration tank, and a sludge wasting line (Rittmann & McCarty, 2001). The aeration tank is a suspended growth reactor where COD is aerobically oxidized by facultative heterotrophs. In some instances, ammonium-oxidizing bacteria (AOB) and nitrite-oxidizing bacteria (NOB) may be present in the aeration tank and oxidize nitrogen compounds like ammonium (NH_4^+), and nitrite (NO_2^-). Aeration and mixing are critical processes in the aeration tank: they provide the necessary oxygen for the bacteria to perform aerobic oxidation. Mixed liquor leaves the aeration tank and flows to the settling tank or clarifier. In

the clarifier, the flocs of bacteria settle to the bottom, and treated effluent is removed from the top. The sludge at the bottom can then be returned to the aeration tank via the solids recycle line to maintain the appropriate level of microorganisms in the aeration tank. Excess sludge is removed from the process through the sludge wasting line.

The solids retention time (SRT) is the fundamental design parameter to control the performance of an activated sludge process. It is defined as the average time that the active biomass spends in the system, and it is the reciprocal of the specific growth rate (Rittmann & McCarty, 2001). Typically, the SRT of a basic activated sludge process ranges from 4 to 10 days for temperate climates (Rittmann & McCarty, 2001), and this ensures efficient removal of COD. Longer SRTs are used to accumulate AOB and NOB so that the nitrogenous oxygen demand (NOD) also is removed.

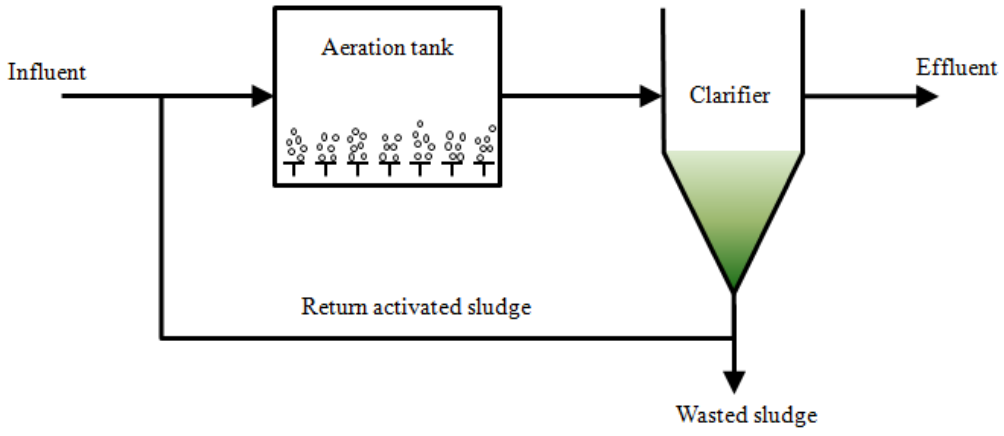

Figure 1.2. The basic activated sludge process.

Activated sludge processes have become more sophisticated as environmental regulations require increased removal of nitrogen and phosphorus

from plant effluents to prevent eutrophication in watersheds. One example is the incorporation of anoxic tanks for denitrification, as illustrated in Figures 1.3 a and b. During denitrification, facultative heterotrophs oxidize COD by nitrate (NO_3^-) respiration to produce nitrogen gas (N_2). The anoxic tank can be incorporated directly before or after the aeration tank. When the anoxic tank follows the aeration tank (Figure 1.3a), total Kjeldahl nitrogen (TKN) present in the influent is oxidized to nitrate first. Then, endogenous decay of biomass or an added organic substrate provides the electron donor to drive denitrification in the anoxic tank. Classical pre-denitrification, as illustrated in Figure 1.3b, places the anoxic tank before the aerobic tank. This configuration allows the influent to be the source for COD for denitrification of NO_3^- that is recycled from the aeration tank. Locating the anoxic tank before the aeration tank ensures that enough COD will be present to convert the NO_3^- to N_2 without needed to supply organic substrate.

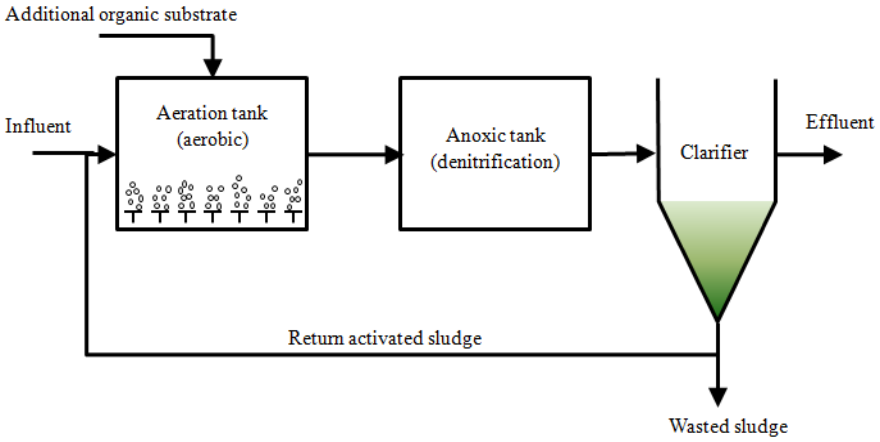

(a)

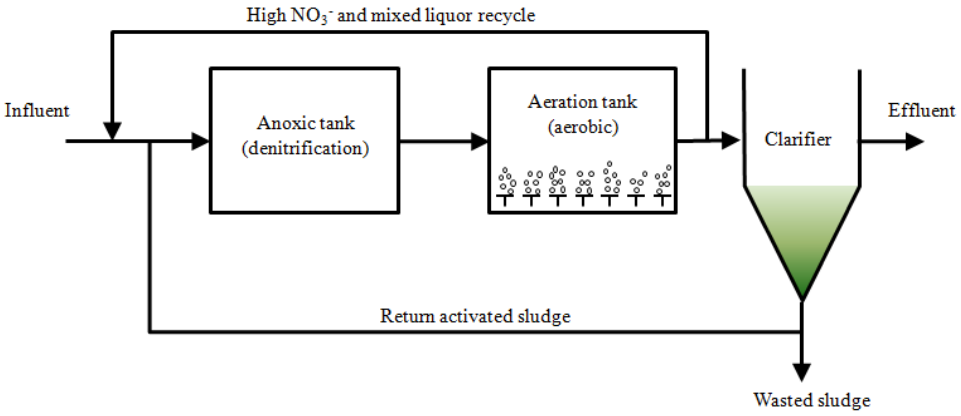

(b)

Figure 1.3. Two common activated sludge processes configurations that include anoxic tanks for denitrification. (a) The anoxic tank follows the aeration tank so that biomass decay and an additional organic substrate are the electron donor for denitrification of NO_3 produced in the aeration tank. (b) In pre-denitrification, the anoxic tank precedes the aeration tank so that the influent COD can be the electron donor for NO_3^- produced in the aerobic tank and recycled back to the anoxic tank.

Contact stabilization is a variation on the activated sludge process that utilizes two separate tanks for aeration and sludge stabilization, as seen in Figure 1.4. In the contact tank, the influent has a relatively short contact time with oxygen of 15-60 minutes. This allows for only the most readily biodegradable COD to be removed in the contact tank. The returned sludge from the clarifier is aerated has a residence time of 1-2 hours in the stabilization tank for sludge stabilization to occur (Metcalf & Eddy, 2003). The advantage of this process is that less overall tank volume is required to achieve the same levels of COD removal as a completely mixed conventional activated sludge process, resulting in a smaller plant footprint.

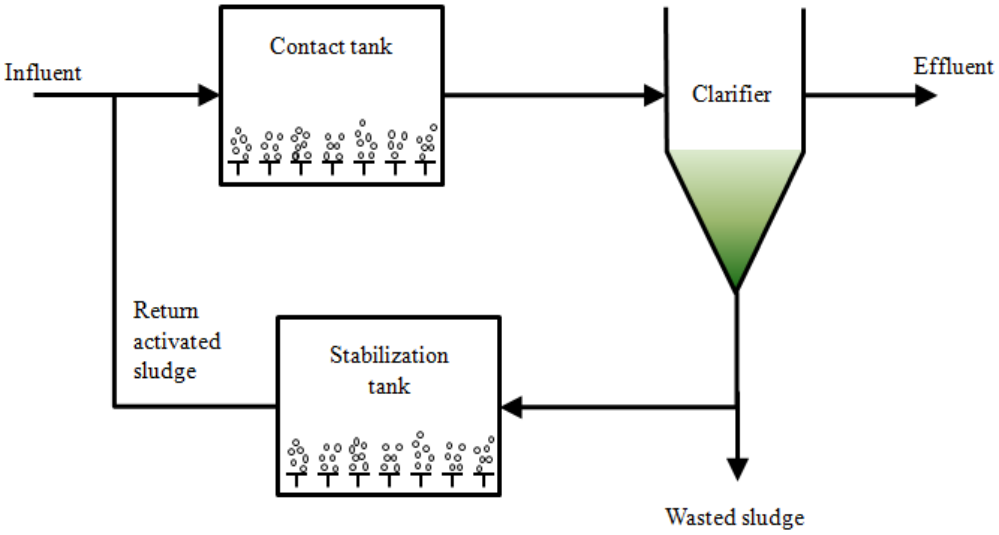

Figure 1.4. The contact stabilization process features aeration in two separate tanks, which reduces the overall tank volume required for COD removal.

Biosorption is an underutilized mechanism in activated sludge processes. Biosorption is a physio-chemical process defined as "the removal of substances from solution by biological material" (Gadd, 2009). It is most often utilized for

heavy metals and organics removal during primary treatment, when these contaminants are captured during the settling of the heavier solids. However, biosorption has potential to enhance COD removal in activated sludge. Particulate COD (PCOD) can be adsorbed or enmeshed in activated sludge flocs in the anoxic, biosorption and stabilization tanks. The PCOD can be carried to the anaerobic digester, where it can be converted to soluble COD (SCOD) as in intermediate and methane as an end product.

Anaerobic digesters are seeing increased use as a method of stabilizing biosolids produced during activated sludge treatment. Anaerobic digestion is a natural process in which methane gas (CH_4) is produced in the absence of oxygen. As shown in Figure 1.5, an anaerobic digester typically is fed thickened sludge from the clarifier. In the digester, the sludge is decomposed and converted to CH_4 by a three-step process: hydrolysis of solid and macromolecular organics or soluble fermentation products, fermentation of the hydrolysis products to simple organic products and H_2 gas, and methanogenesis of the fermentation products to CH_4. Fermenters and methanogens are slow-growing microorganisms, and typical SRTs for anaerobic digesters exceed 20 days (Metcalf & Eddy, 2003).

One advantage of anaerobic digestion is the significant reduction in solids needing to go for disposal at a landfill, by land application, or by incineration. The second advantage is the energy value of the captured CH_4, which is natural gas that can be combusted on site to produce heat and electricity.

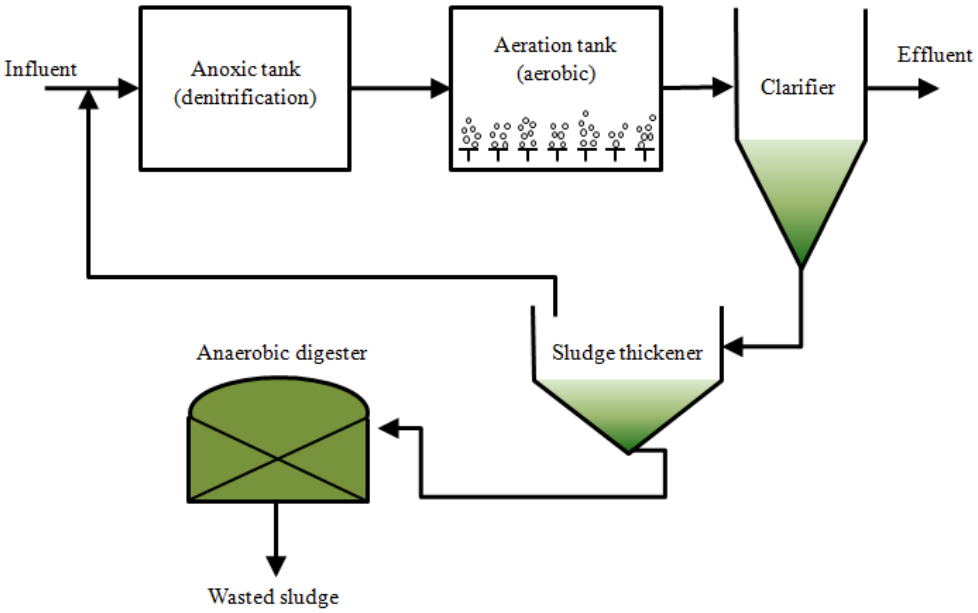

Figure 1.5. The activated sludge process with anaerobic digestion of waste biosolids.

1.3 The SWT Hybrid Wastewater Treatment Process

Siemens Water Technologies (SWT) has proposed the hybrid wastewater treatment process shown in Figure 1.6. It is called a hybrid process because it combines aerobic biosorption of particulate COD with anaerobic digestion to increase the amount of methane produced in the anaerobic digester. It does this by diverting most of the influent COD to the digester system so that it is not aerobically oxidized. Thus, SWT's goals for the hybrid system are to reduce energy consumption through increased methane production and decreased aeration while decreasing waste sludge production. If successful, the hybrid process will achieve a lower energy intensity and carbon footprint versus a traditional activated sludge process. Of course, these goals must be met while maintaining excellent effluent water quality, being both robust and easy to control, and being easily retrofitted into existing activated sludge processes.

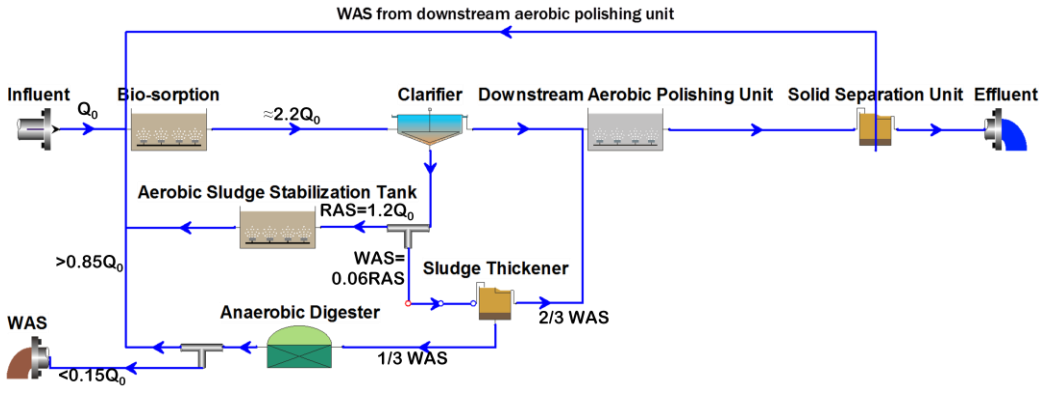

Figure 1.6. The SWT Hybrid Wastewater Treatment Process.

The hybrid process is centered on the concept of removing COD in the anaerobic digester rather than in the aerobic tank. SWT proposes that this could be achieved through quick and efficient biosorption of particulate COD to the

mixed liquor in the biosorption tank. The biosorbed particulate COD is transported to the anaerobic digester (via the settler and the thickener), where it is converted to CH_4 via methanogenesis. Preliminary modeling by SWT indicated the potential for 87% of the biodegradable COD in the influent stream to the anaerobic digester can be converted to methane, making the hybrid process an energy-production, not an energy-consumption process.

The hybrid system has another large difference from a conventional activated sludge system with an anaerobic digester. The critical difference is that about 85% of the anaerobic digester's sludge is recycled back to the stabilization tank. The expected benefits of wasting sludge recycling are three. The most obvious benefit is a decrease in waste-sludge removal for disposal. Siemens modeling predicts a 40% decrease in waste-sludge generation. Second, the recycling should increase the overall amount of biomass in the hybrid system. This should enhance the efficiency of biosorption of particulate COD in the contact tank. Consequently, the biosorption tank's retention time has been reduced to one hour for the typical 1 to 8 hours in traditional contact stabilization (Metcalf & Eddy, 2003). Third, the shorter retention time reduction in the biosorption tank should decrease aerobic oxidation of COD.

While it is undeniable that the hybrid system offers significant potential benefits, little is currently understood about several of the mechanisms involved. Specifically, research on biosorption mechanisms has been focused on the biosorption of metals to biomass (Gadd, 2009; Aksu, 2005), not on biosorption of

particulate COD. Likewise, the effects of recycling anaerobic-digester solids back to the aerobic system have not been evaluated. Biosorption and recycling should have profound effects on the mass flows of COD and N, and these effects will determine if the goals of energy efficiency, low solids wasting, and good effluent quality can be achieved in reality.

Successful commercialization of the hybrid process will require a better understanding of the process and the mechanisms involved in the hybrid process. SWT is operating two hybrid systems and one conventional system at a municipal wastewater treatment plant in Singapore. SWT initialized a research program with Arizona State University to provide, among other functions, mass balance modeling (not electron balances) of the hybrid and conventional systems and analysis of the systems' performance.

1.4 Objective

The main objective of my work is to provide a detailed analysis of the performance of SWT's hybrid water treatment process, compared with the conventional process being operated in Singapore. This requires a comprehensive evaluation of the roles of biosorption, contact stabilization, and anaerobic digestion in the hybrid configuration. The evaluation is carried out using a robust mass-balance model to assess the performance of both processes. I apply to the model data obtained by SWT to determine if the hybrid process provides the expected sustainable benefits in wastewater treatment.

My thesis is organized to achieve the goals outlined for the following chapters:

1. In Chapter 2, I discuss in more detail the functions occurring in biosorption, contact stabilization, and anaerobic digestion. These functions are combined and applied as the foundation of SWT's hybrid process. In addition, I provide information on tools, methods, and measurements being utilized by SWT to quantify the performance of both processes.
2. In Chapter 3, I provide the theoretical background for my mass-balance model of the performance of the hybrid and conventional processes. I focus the modeling on comprehensive mass balances of soluble and solid compounds in each vessel and the overall performance of the systems. I also develop unique yield analysis to provide critical information on biomass trends in each vessel

and the system. These methods form the foundation of my performance analysis in the subsequent chapters.

3. In Chapter 4, I review and interpret the results of modeling using SWT's data. Specifically, I address the fate of COD, nitrogen, and total iron, as well as biomass yields, for individual vessels in each system and the overall system. I correlate COD and nitrogen removal rates to gain a mechanistic understanding of system performance. Since methane production and sludge reduction are key objectives for SWT, I compare their performances between the anaerobic digesters of the hybrid and conventional processes.
4. In Chapter 5, I review my approach to non-steady state mathematical model of the hybrid system using MATLAB. I discuss my model formulation and assumptions and the sources for all kinetic and modeling parameters. I also present the mathematical models for novel mechanisms, like the combined theory of biosorption and flocculation and the application of switch factors in computer modeling.
5. In Chapter 6, I present the results from the non-steady state modeling. I begin by discussing conclusions obtained from performing mass balance closure on each individual tank and the overall system. I perform a sensitivity analysis on biosorption flocculation constants. I apply the results of this sensitivity analysis to perform non-steady state modeling at various operating conditions on the hybrid and conventional processes with and without biosorption

kinetics. I assess the modeling trends and determine the effect that biosorption kinetics has on modeling results.

6. In Chapter 7, I summarize this document and make recommendations as to how SWT can improve the pilot plant process and the performance of the hybrid system.

2. Critical Mechanisms for SWT's Hybrid Process

As SWT developed the hybrid process, it became apparent that three processes/mechanisms play crucial roles in increased methane production and decreased sludge production: contact stabilization, anaerobic digestion, and biosorption. In traditional activated sludge processes, contact stabilization processes are applied to decrease the size of aerobic tanks while improving biosorption and metabolizing most biodegradable COD within the aerobic system. The role of contact stabilization in the hybrid process is different: rather than consuming COD in the aerobic system, the contact stabilization tanks are sized specifically to maximize COD biosorption to biomass that is routed to anaerobic digestion, a process by which complex organic compounds are converted to methane. The recycling of anaerobic digester sludge provides additional biosorbent for COD biosorption while altering the microbial community composition versus a traditional activated sludge process.

In this chapter, I provide background on anaerobic digestion, contact stabilization, and biosorption. Each of these concepts is then applied in a discussion of SWT's hybrid process.

2.1 Anaerobic Digestion and Methane Production

Concerns continue to increase over the finite supply of fossil fuels and global climate change as a result of the accumulation of carbon dioxide (CO_2) in the atmosphere. As society attempts to address these issues, we often seek to commercialize the "low hanging fruit," or easily exploitable technologies that are

being under-utilized. One such process is anaerobic digestion: the anaerobic biodegradation of organic solids to produce methane gas. While anaerobic digestion has become popular in WWTPs in the past century, it is hardly a new concept: biogas from anaerobic digestion was utilized in 10^{th} century BC to heat bath water in Assyria. In 1776, Volta was the first person to note that "combustible air" was being produced from sediments in lakes, ponds and streams as a result of biological anaerobic digestion of organic materials to methane (McCarty, 2001). Today, anaerobic digestion is utilized as a critical process for the recovery of biogas and the reduction sludge that must be disposed of.

2.1.1 Microbiology

Anaerobic digestion involves a diverse community of microorganisms whose metabolism requires an atmosphere devoid of oxygen to biologically degrade complex organic compounds and transfer their COD to CH_4 gas. Anaerobic digestion is built upon on a series of syntrophic relationships between microorganisms in two different biological kingdoms, *Archaea* and *Bacteria*, who together perform the functions of hydrolysis, fermentation, and methanogenesis. For these relationships to be successful, each set of microorganisms produces a product that is metabolized by another set of microbes or consumes products that would otherwise prevent the other microorganisms from thriving and surviving. This food chain is illustrated in Figure 2.1.

Hydrolysis is the critical first step in anaerobic digestion, because essentially all of the organic matter is sludge is solid. During hydrolysis,

hydrolytic enzymes produced by fermenting bacteria hydrolyze, or use H_2O to split the organic solids into smaller pieces. Eventually, the hydrolysis products become soluble sugars, proteins, and lipids, which are the basic building blocks of biomass. Common bacteria that produce hydrolytic enzymes are in the genera *Clostridium, Peptococcus, Vibrio, Micrococcus*, and *Bacillus* (Mara & Horan, 2003). While these bacteria can grow at moderate growth rates when they ferment the hydrolysis products, often the hydrolysis step is the rate-limiting step in anaerobic digestion, as many types of organic solids that reach an anaerobic digester are not readily hydrolysable.

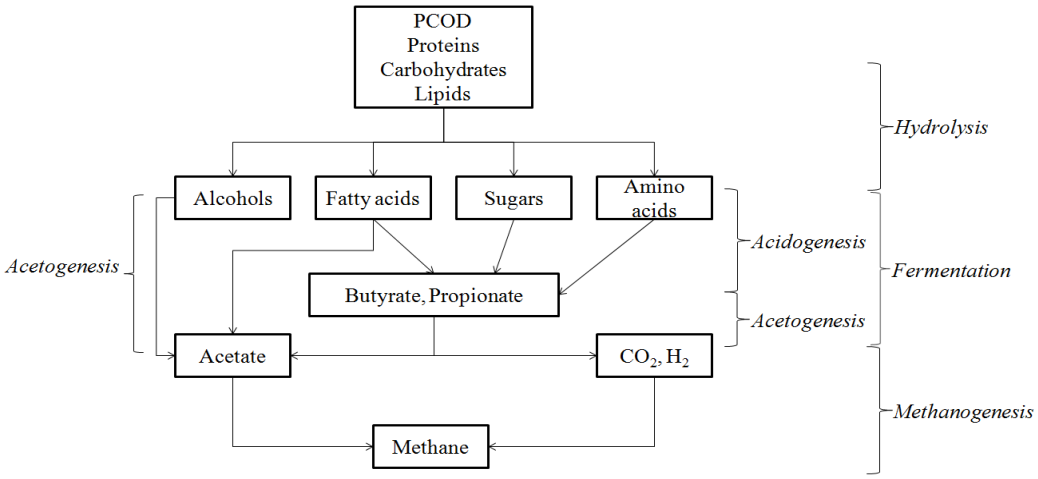

Figure 2.1. The metabolic processes by which complex organic substrates are converted to methane during anaerobic digestion.

Fermentation is the second step in anaerobic digestion. Fermentation is a form of metabolism in which part of the organic molecule is oxidized, while another part is reduced. Thus, the fermentation substrate is the cell's electron donor and electron acceptor, meaning that the fermenting bacteria do not utilize respiration to gain energy. Instead, oxidation and reduction of different parts of

the organic substrate releases energy that the fermenters can capture through substrate-level phosphorylation (Madigan & Martinko, 2006; Rittmann & McCarty, 2001). Acidogenic and acetogenic bacteria ultimately ferment the compounds produced during hydrolysis, mostly to acetate, propionate, butyrate, CO_2, and H_2. Fermenters have relatively fast reaction and growth rates, and often the rate of fermentation is limited by the amount of substrate available from hydrolysis.

While both are fermenters, acidogens and acetogens have different functions in the fermentation process. The first group of fermenters called acidogens include many fermentative genera, such as *Clostridium, Bacteroides, Ruminococcus, Butyribacterium, Propionibacterium, Eubacterium, Lactobactillus, Streptococcus, Desulfomacter, Micrococcus*, *Escherichia* and *Bacillus* (Mara & Horan, 2003). Acidogens metabolize fatty acids, amino acids, and sugars to organic acids, alcohols, and ketones. Key products include acetate, propionate, butyrate, and ethanol, as well as CO_2 and H_2 (Bitton, 2005).

As their name implies, acetogens convert products from hydrolysis and acidogenesis to acetate; they also produce CO_2 and H_2, depending on their substrate. Acetogens can be classified into two groups: H_2-producing acetogens and homo-acetogens (Mara & Horan, 2003). H_2-producing acetogens are facultative anaerobes that metabolize fatty acids likes propionate and butyrate, as well as alcohols through the following reactions:

Ethanol to acetate: $CH_3CH_2OH + H_2O \rightarrow CH_3COOH + 2H_2$ (1)

Propionate to acetate: $CH_3CH_2COOH + 2H_2O \rightarrow CH_3COOH + CO_2 + 3H_2$ (2)

Butyrate to acetate: $CH_3CH_2CH_2COOH + 2H_2O \rightarrow 2CH_3COOH + 2H_2$ (3)

Common H_2-producing acetogens are in the *Syntrophomonas* and *Syntrobacter* genera (Bitton, 2005). High levels of H_2 gas thermodynamically inhibit these bacteria from converting substrate to acetate.

Homo-acetogens are strict anaerobes that produce only acetate directly from CO_2 and H_2. Common genera of homo-acetogens include *Acetobacterium, Acetoanaerobium, Acetogenium,* and *Butribacterium*. Homo-acetogens are critical in maintaining low H_2 concentrations so that the metabolism of proton-reducing acetogens is not inhibited from producing fatty acids and alcohols (Mara & Horan, 2003).

Methanogenesis is the formation of methane through consumption of acetate or CO_2 and H_2. Methanogens are fastidious strict anaerobes that are phylogenetically members of the *Archaea* kingdom. This contrasts with the microorganisms involved in hydrolysis and fermentation, which are members of the *Bacteria* kingdom. Members of the *Archaea* kingdom are the only organisms capable of methane production.

Methanogens are divided into two categories: H_2-oxidizing and acetoclastic. H_2-oxidizing methanogens are often associated with the genera *Methanococcus* and *Methanobacterium*. They use H_2 as their electron donor and CO_2 as their electron acceptor to produce methane via this respiration reaction:

$$CO_2 + 4H_2 \rightarrow CH_4 + 2H_2O \quad (4)$$

H_2-oxidizing methanogens are the source of approximately 28-30% of the methane produced in a typical anaerobic digester (Mara & Horan, 2003; McCarty & Smith, 1986).

Aceotclastic methanogens convert acetate to methane and CO_2 via a fermentation reaction:

$$CH_3COOH \rightarrow CH_4 + CO_2 \quad (5)$$

The two main genera of acetoclastic methanogens are *Methanosarcina* and *Methanosaeta*. Acetoclastic methanogens generate the remaining 70-72% of the methane produced in typical anaerobic digesters (Mara & Horan, 2003; McCarty & Smith, 1986; Parkin & Owen, 1986).

Methanogens have slower growth rates than fermenting bacteria, and the solids retention time (SRT) in the system often is determined by retention of methanogens. However, methanogenesis is not necessarily the rate-limiting step for methane generation, as hydrolysis may control the rate at which acetate and H_2 are provided to the methanogens.

2.1.2 Process Fundamentals

Anaerobic digesters (ADs) have a reputation for being unreliable. This reputation, however, has as much to do with a lack of understanding and training on the part of wastewater engineers and technicians as it does with the complexity of anaerobic processes themselves. Proper understanding of processes fundamentals is essential to the sustained and controlled operations of ADs. As

reviewed by Parkin and Owen (1986) and Rittmann and McCarty (2001), the parameters that govern microbial growth and stability in ADs include adequate SRT and mixing, proper pH, proper temperature control, adequate nutrient levels, the absence of toxic materials, and proper feed characteristics.

Adequate SRT is essential for reliable operation of any biological process. The SRT is defined as the ratio of active biomass in the system to the production rate of active biomass, but it also is the reciprocal of the specific growth rate of the biomass (Rittmann & McCarty, 2001). The SRT must be long enough for the microorganisms with the rate-limiting kinetics to have sufficient time to metabolize substrate and to avoid wash out from the system. Because methanogens are slow growing, they require a relatively long SRT, typically 15 – 30 days when the temperature is maintained at around 37°C. For most ADs, the SRT equals the hydraulic retention time (HRT), as they are completely mixed tanks. In this case, the SRT is equivalent to HRT, which also is important for controlling the degree of hydrolysis of the input organic solids. SRT is indirectly affected by mixing efficiency in the AD. Although a well-mixed AD has a typical SRT = HRT of 15-30 days, unstirred ADs have HRTs of 60 days or longer because they utilize their volume less effectively than stirred reactors (Parkin & Owen, 1986).

Maintaining proper pH is somewhat complex in ADs. A pH range of 6.6 to 7.6 is ideal for methanogenesis (Rittmann & McCarty, 2001), but anaerobic systems naturally acidify due to the production of carbonic and organic acids.

CO_2 produced during fermentation and methanogenesis of acetate dissolves in water as carbonic acid (H_2CO_3), which is a weak acid (pK_a of 6.35 at 25˚C (Masters & Ela, 2008)) that dissociates to form bicarbonate (HCO_3^-) in proportion to the amount of alkalinity in the water. The pH of the water is mainly controlled by the concentration of bicarbonate in the water. The production of H_2CO_3 can be troublesome during start up, when methanogens in the system may be insufficient to metabolize the CO_2 being produced by fermenters in the system. Alkalinity can be added to the digester to buffer the pH and counter the effects of H_2CO_3.

More troublesome is a buildup of organic acids, including acetic, propionic, and butyric. They are stronger acids than H_2CO_3 and can consume bicarbonate alkalinity and lower the pH to dangerous levels. The buildup of these organic acids is caused by the methanogenic reactions being out of balance with the acidogenesis and acetogenesis reactions. The decrease in pH due to build up of organic acids is called a "pickled digester."

Temperature can greatly affect reaction rates and microbial growth rates in ADs. As reviewed in Rittmann and McCarty (2001), the growth rates of mesophilic microorganisms roughly double for every 10˚ between 10 and 35˚C, but remain constant between 35 and 40˚C. Thermophilic microbes that thrive at optimal temperatures ranging from 55 to 60˚C, but most ADs are operated between 30 and 40˚C (Metcalf & Eddy, 2003), since it can take more energy to maintain the higher temperatures for thermophilic operations. Operating at temperatures above 35˚C offers an additional benefit of pathogens destruction,

which reduces the needs for further sludge processing for land applications. ADs can be run at ambient temperatures ranging between 10 and 20˚C if it is too costly to operate at the mesophilic temperature range. The consequence of operating at lower temperatures include decreased substrate utilization rates which result in lower methane production and, consequently, larger reactor volumes to treat the same amount of substrate.

Adequate nutrients are required to maintain healthy microorganisms for anaerobic digestion. Like for all microorganisms, nitrogen and phosphorus are essential nutrients for biological growth of fermenters and methanogens. Methanogens have additional nutrient requirements, including sulfur and trace metals. For example, methanogens require sulfur at about the same order of magnitude as phosphorus. Additional sulfur supplied in sulfate form must be monitored closely, as excess sulfate can suppress methane generation if it is reduced to sulfides that also create complexes with metals, as well as odors. Trace metals, including iron, cobalt, and nickel, are vital for the activation of key enzymes required for methanogenesis. The required levels of these metals must be determined experimentally or during operation as systems often have varying requirements (Rittmann & McCarty, 2001).

As mentioned previously, methanogens are fastidious microorganisms that require specific combinations of conditions to survive. Because of this, ADs are susceptible to poisoning or inhibition by toxic materials. The levels and constancy of toxic materials can be complicated by a myriad of source points for

the influent stream to the WWTP. These source points can include a wide variety of contaminants, including synthetic detergents, pesticides, high concentrations of alkali and alkaline earth salts produced by industrial processes, and extremely high levels of ammonia as produced from slaughterhouses and piggery wastes. Toxic or inhibitory materials can temporarily or permanently affect the microbial digestion kinetics. Some plants with consistent contaminant streams can opt to add processes like activated carbon and crystallization to remove contaminants. Plants with influent stability can increase their SRTs to compensate for intermittent disturbances. Long SRTs can diminish the effects of inhibitory materials by employing extended operations under wash out conditions that may be required to relieve the AD of the contaminants.

Feed characteristics have an effect on ADs operations. Parameters like pH, alkalinity, temperature, and flow rate are inherently part of the feed characteristics and can affect the operations of the AD. However, an even larger effect is felt from fluctuating degrees of substrate biodegradability. For example, waste activated sludge, which is recycled back to the AD in some systems, has inherently lower levels of biodegradability than primary sludge (Parkin & Owen, 1986). The steadiness of feeding into the AD can also affect the AD's operations. Due to their slow growth rate, methanogens cannot respond quickly to a large upswing in organic loading, compared to fermenting bacteria, which adjust more readily to feast/famine conditions. Thus, intermittent feeding can result in the fluctuations in carbonic acid, organic acid, and pH levels that might adversely

affect the methanogens, which cannot respond quickly. These fluctuations lead to inconsistent methane production and sludge stabilization.

Sludge stabilization and reduced sludge production are major advantages of anaerobic digestion. As discussed previously, anaerobic digestion biodegrades complex organic solids, in some cases more efficiently than in aerobic processes. Anaerobic reactions have less negative free energy compared to their corresponding values in aerobic environments. Since so little energy is available to the microorganisms from anaerobic reactions, anaerobes use most of the energy for respiration of large amounts of CH_4, rather than biomass synthesis. For biomass synthesis, anaerobes have growth yield coefficients ranging from 0.03 to 0.20 g VSS/g COD, which is much lower when compared with activated sludge heterotrophic bacteria yields which range from 0.30 to 0.50 g VSS/g BOD_L (Metcalf & Eddy, 2003; Rittmann & McCarty, 2001). Consequently, anaerobic digestion yields large amounts of CH_4 with a high net loss of volatile solids.

2.2 Contact Stabilization

Contact stabilization, a variation on the activated sludge process, originally was developed in England in the early 20th century. It has experienced widespread application in the United States and Europe since the 1950s as a method for aerobically treating wastewater with lower contact times and aeration tank volumes compared to traditional activated sludge aeration tanks (Dermissi, 1991). Contact stabilization is characterized by two separate tanks for aeration and sludge stabilization, and Figure 2.2 shows a typical contact stabilization system. Biosorption of COD is carried out in the contact tank, while oxidation is carried out in the stabilization tank. Contact stabilization is critical in SWT's hybrid process: It is here that more complex organic compounds are adsorbed by particulate matter for transport to the AD for conversion to methane.

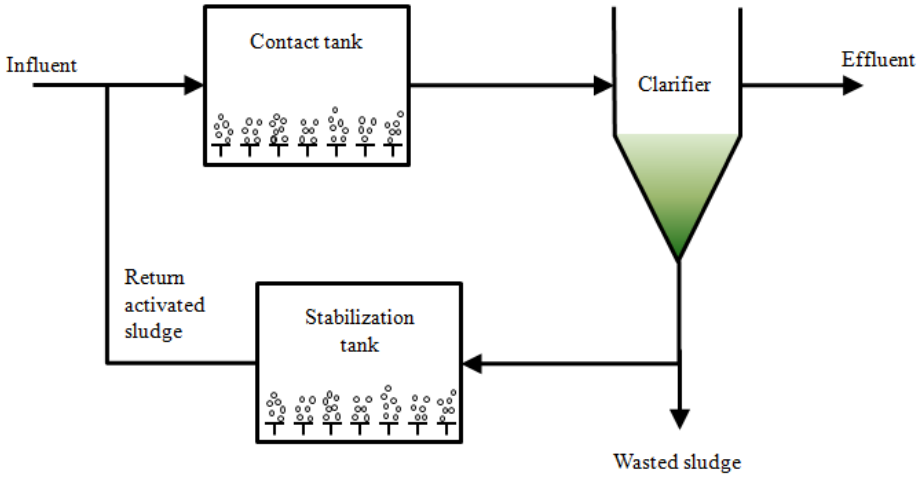

Figure 2.2. The typical contact stabilization process.

2.2.1 Microbiology

Like in any activated sludge processes, contact stabilization employs heterotrophic bacteria that utilize oxygen as an electron acceptor and organic compounds as electron donors. Activated sludge microbial communities are defined by two attributes: a diverse ecosystem of prokaryotes and eurkaryotes and the tendency to aggregate in flocs that are bound together by extracellular polymers and electrostatic forces. Heterotrophic bacteria are the primary consumers in activated sludge and dominate the microbial community population. Common genera present in activated sludge include *Pseudomonas, Arthrobacter, Comamonas, Lophomonas, Zoogloea, Sphaerotilus, Azotobacter, Chromobacterium, Achromobacter, Flavobacterium, Bacillus,* and *Nocardia* (Rittmann & McCarty, 2001).

Within the heterotrophic community, different bacteria consume various organics by different rates and methods. Some heterotrophs have diverse appetites, having the capability to consume a variety of organic compounds; other heterotrophic bacteria can consume only specific organic substrates. Heterotrophs have large maximum specific growth rates that allow them to function well with a relatively low SRT or relatively fast specific growth rates (Rittmann & McCarty, 2001). For example, the typical SRT for a conventional activated sludge is around 5 days, which is much shorter than for anaerobic digestion. Secondary consumers feed off the materials either released by primary consumers or produced as part of cell lysis and death or are predators of other bacteria.

Heterotrophs can be categorized as oligotrophs (or K-strategists) or copiotrophs (or r-strategists) (Rittmann & McCarty, 2001). While oligotrophs do not have the fastest maximum specific growth rates, their high affinity for their substrate makes them excellent scavengers of substrate under low loading and steady-state conditions. Oligotrophs are referred to as K-strategists since their high affinity for substrate can be described by a small value for the half-maximum rate concentration, or K as it is notated in the Monod-based substrate-utilization equation:

$$r_{ut} = -\frac{rS}{K+S}X_a \qquad (6)$$

In Eqn. 6, r_{ut} is the rate of substrate utilization ($M_s/T/L^3$), r is the maximum specific rate of substrate utilization ($M_sM_x^{-1}T^{-1}$), S is the substrate concentration (M/L^3), X_a is the biomass concentration in the system (M_x/L^3), and K is the half-maximum rate concentration (M_s/L^3).

As opposites of oligotrophs, copiotrophs are well suited for thriving under feast-famine conditions. Copiotrophs are referred to as r-strategists, since faster specific growth rates are often associated with a high r value in Eqn. 6. Copiotrophs use one of three strategies to cope in feast-famine conditions: utilize a faster specific growth rate to outgrow and outcompete oligotrophs for substrates present in high levels, take up and sequester substrate during feast conditions for utilization during fasting conditions, and dormancy during fasting conditions. The coexistence of r- and K-strategists in activated sludge lead to functional redundancy within the heterotrophic bacteria community. This functional

redundancy provides activated sludge systems to sustain consistent effluent quality under varying influent conditions (Rittmann & McCarty, 2001).

Although it is not always a primary function in activated sludge, nitrification is often present in contact stabilization to remove high levels of nitrogen compounds that would otherwise be detrimental to discharge environments. The two types of nitrifiers present in aerobic environments are AOB and NOB. AOB oxidize NH_4^+ to nitrite by the following reaction (Rittmann & McCarty, 2001):

$$NH_4^+ + 1.5O_2 = NO_2^- + 2H^+ + H_2O \quad (7)$$

All AOB include *Nitroso-* in the prefix of their genus. While the most recognized genus of AOB is *Nitrosomonas*, other ammonia oxidizers include *Nitrosococcus, Nitrosopira, Nitrosovibrio* and *Nitrosolobus*.

NOB oxidize NO_2^- to nitrate by the following reaction (Rittmann & McCarty, 2001):

$$2NO_2^- + O_2 = 2NO_3^- \quad (8)$$

All NOB have a specific prefix for their genus: *Nitro-*. *Nitrobacter* and *Nitrospira* are the most prevalent NOB in activated sludge processes. Because of the close association of their metabolite byproducts, AOB and NOB have evolved to be present in many of the same environments since NOB metabolize AOB's metabolic product, NO_2^-.

From Rittmann and McCarty (2001), a typical overall reaction for nitrifiers producing biomass is:

$$NH_4^+ + 1.815O_2 + 0.1304CO_2 = 0.0261C_5H_7O_2N + 0.973NO_3^- + 0.921H_2O + 1.973H^+ \quad (9)$$

Eqn. 9 indicates that a large amount of oxygen is consumed to produce a small amount of biomass: 4.14 g of O_2 for each gram of NH_4^+ consumed by nitrifiers. Another conclusion is that a high amount of alkalinity is consumed during nitrification due to the production of acid (H^+). In common alkalinity units, this chemical equation requires

$$1.973 \text{ mol } H^+ \left(\frac{1 \text{ eq}}{1 \text{ mol } H^+}\right)\left(\frac{50 \text{ g } CaCO_3}{1 \text{ eq}}\right)\left(\frac{1}{14 \text{ g } NH_4^+}\right) = 7.05 \frac{\text{g } CaCO_3}{\text{g } NH_4^+} \quad (10)$$

or 7.05 g $CaCO_3$ (alkalinity) per gram of NH_4^+ consumed by nitrifiers. The AOB reaction generates the H^+. Unless the input alkalinity is sufficient, the high alkalinity consumption can cause a nitrifying process to become acidic, generating an uninhabitable environment for heterotrophs and nitrifiers. From the equation above, the nitrifiers also require 0.1304 moles of CO_2 to nitrify 1 mole of NH_4^+.

Heterotrophs and nitrifiers have critical similarities and differences. Both microorganisms are aerobic, utilizing O_2 as their electron acceptor, but many heterotrophs have the ability to use other electron acceptors, such as nitrate and nitrite. Heterotrophs and nitrifiers produce soluble microbial products (SMP), but only the heterotrophs can reuse SMP as an electron donor and carbon source. Unlike heterotrophs, nitrifiers have not evolved to metabolize organic molecules, and, therefore, nitrifiers do not use SMP as their carbon source. While the production of SMP ultimately benefits the reproduction of heterotrophs, it is an

energy sink for nitrifiers. Nitrifiers are much slower growing than heterotrophs due their much smaller yields: AOB have a yield of 0.1 g VSS_a/g OD, versus 0.45 g VSS/g OD for heterotrophs. The maximum specific growth rate of nitrifiers is around 11-fold less than for typical heterotrophs in activated sludge (Rittmann and McCarty, 2001). Due to their inherently slower specific growth rates, nitrifiers are more sensitive to low temperature conditions. The higher specific growth rate and diversity of the heterotrophic bacteria generally makes them more resilient to lower temperatures.

2.2.2 Process Description

During contact stabilization, return activated sludge is mixed with the influent as it enters the contact aeration tank. In the contact tank, the mixed liquor has a relatively short detention time: 15 to 60 minutes, versus that of a conventional aeration tank, which is 6-8 hours (Rittmann & McCarty, 2001; Benefield & Randall, 1976). The short contact time allows the aerobic biomass to oxidize only the most readily biodegradable organic substrates. Instead, the heterotrophic bacteria store organic substrates for future oxidation by one of two mechanisms. The first is adsorption of particulate COD to the flocs, a process often called biosorption. The particulate COD is broken down extracellularly before being utilized as substrate by heterotrophs (Gray, 1989). The second is rapid uptake of simple soluble compounds with low molecular weights (like acetate) and their conversion to intracellular storage products, such as polyhydroxybutyrate (PHB) (Majone et al., 1998). Since most of the organic

matter in wastewaters is particulate, the dominant storage mechanisms in contact stabilization is biosorption. I focus on the mechanisms of biosorption in the next section.

The mixed liquor, which contains stored COD, flows to the clarifier, where the activated sludge is concentrated and separated from the treated wastewater. The concentrated activated sludge is discharged from the clarifier to the stabilization tank. The purpose of the stabilization tank is two-fold: to oxidize stored organic contaminants and to provide a sufficient SRT for the aerobic microorganisms. The stabilization tank has a residence time much longer than that in the contact tank: e.g., 1 - 8 hours (Metcalf & Eddy, 2003; Gray, 1989). The mixed liquor is discharged as returned activated sludge and reintroduced to the influent as it enters the contact tank.

The contact and stabilization tanks have key similarities and differences. As previously mentioned, the contact times are significantly different: less than 1 hour for the contact tank and 1-2 hours for the stabilization tank. The stabilization tank has a much higher mixed liquor volatile suspended solids (MLVSS) concentration than the clarifier, since it receives settler underflow. The higher MLVSS concentration makes it possible to have a sufficiently large SRT with a relatively short HRT for the system, thus reducing the overall volume required for COD removal. For example, at a typical SRT of 8 days for conventional activated sludge, a contact stabilization process with 75% of the biomass residing in the stabilization tank requires a total volume of 44% smaller

than a conventional activated sludge process (Rittmann & McCarty, 2001). Thus, the concentrated MLVSS level in the stabilization is key to reducing overall reactor volume for the normal application of contact stabilization.

Contact stabilization processes are not without their disadvantages. The operation of a contact stabilization process is considerably more complex than the basic activated sludge process: two tanks require monitoring and control. In addition, contact tank's smaller volume makes it more susceptible to upsets due to high variability in loading conditions (Rittmann & McCarty, 2001). Therefore, operators must be more skilled and pay closer attention to the operations.

In the SWT process, the contact stabilization process provides a second benefit beyond a lower HRT for the same SRT. That second benefit is routing stored COD to anaerobic digestion. The sludge from the clarifier is high in intracellular stored COD and particulate COD that has been enmeshed in the flocs. In a conventional contact stabilization processes, this COD is utilized as substrate for aerobic heterotrophs in the stabilization tank. With SWT's system, a minimum of 6% of the clarifier's sludge is diverted to the sludge thickener and anaerobic digester, with the remaining sludge cycled to the stabilization tank. When the COD is exposed to anaerobic conditions, it is hydrolyzed to simpler organic compounds that provide the basis for fermentation and methanogenesis. Therefore, more methane is produced by diverting more COD to the anaerobic digester.

2.3 Biosorption and Flocculation

2.3.1 Biosorption

Biosorption is one of the most promising, but poorly understood areas of environmental engineering research. A physio-chemical process, biosorption can be simply defined as "the removal of substances from solution by biological material" (Gadd, 2009). Perhaps reflecting the vagueness of as this definition, biosorption is all-encompassing: It addresses the removal of organic and inorganic contaminants through a variety of common physio-chemical mechanisms, including sorption, ion exchange, surface complexation, precipitation, and chelation (Aksu, 2005). Over the last decade, biosorption has become a hot topic in remediation and wastewater research because of its potential to selectively remove non-biodegradable contaminants using biological material that would otherwise be present without additional energy inputs (Gadd, 2009).

Traditionally, sorption processes, e.g., activated carbon, have been used to remove contaminants from water. While terms like adsorption and absorption are commonly applied, these terms can often cause confusion as to what types of bonding and phases are present. The term sorption is often applied as a simplification to encompass many physio-chemical processes that accumulate substances (sorbates) at an interface (sorbent). Many solid surfaces include functional groups -- such as –SH, -OH and –COOH, as well as deprotonated ligands -- that act as Lewis bases. These groups form complexes with the

complementary functional groups on the contaminant, forming new surface-associated species that can be referred to as surface complexes or precipitates. It is important to note that biosolids, such as the biomass aggregates in activated sludge, possess these functional groups on their surfaces, which allows them to participate in sorption of this type.

Gadd (2009) expanded the simple definition: "… biosorption can describe any system where a sorbate (e.g., an atom, molecule, a molecular ion) interacts with a biosorbent (i.e., a solid surface of a biological matrix) resulting in an accumulation at the sorbate–biosorbent interface, and therefore a reduction in the solution sorbate concentration." These physio-chemical processes take outside of biomass rather than through metabolic processes inside the microorganism. The outside of the biomass includes the cell wall, the cell membrane, and the extracellular polymeric substances (EPS) that are especially important in aggregates. While biosorption is not inherently a metabolite process, the byproducts of the metabolite process, such as EPS and the cells' exterior surfaces, are involved in biosorption.

The primary sorbates of interest up to now have been metals and complex organic solutes, like heavy metals, radioisotopes, textile dyes, and pesticides. Aksu (2005) reviewed several biosorption models and found that the Freundlich isotherm can model metals and organic compounds on sorbents with heterogeneous site energies, which surely exist in microbial biomass. Kinetic parameters have been modeled as first order by Lagergren (1898) and pseudo-

second-order by Aksu (2005). Gadd (2009) and Aksu (2005) emphasized that kinetics are affected by temperature, pH, and microbial community constituents. Therefore, understandings community and environmental conditions are key for modeling biosorption kinetics and how they change with varying conditions.

An example of the application of dynamic biosorption kinetics to organic contaminants is Aksu and Tezer's (2005) paper on, "Biosorption of reactive dyes on the green alga *Chlorella vulgaris*". Here, they combine first- and pseudo-second-order rate kinetics for adsorption density;

First order:

$$\frac{dq}{dt} = k_{1,ad}(q_{eq} - q_c) \tag{11}$$

Second order:

$$\frac{dq}{dt} = k_{2,ad}(q_{eq} - q_c)^2 \tag{12}$$

where q_{eq} is the equilibrium concentration of adsorbed solid (PCOD) on solid biomass (M/L^3), q_c is the actual amount of adsorbed solid (PCOD) on the sorbent at time t (M/L^3), $k_{1,ad}$ is the rate constant of first-order biosorption (1/t), and $k_{2,ad}$ is the rate constant of second-order biosorption (1/t). The equilibrium concentration is determined by allowing the sorbent to accumulate sorbate until the bulk liquid concentration is constant. An equilibrium isotherm can be established by plotting the equilibrium value of sorbate update, q_{eq}, against the equilibrium sorbate concentration in the bulk liquid (Gadd, 2009). For their study, Aksu and Tezer (2005) found that pseudo-second-order kinetics gave a better correlation to experimental results.

Aksu and Tezer (2005) also reiterated that the first-order adsorption rate constant follows an Arrhenius relationship with temperature:

$$k_{ad} = A_0 \exp\left(-\frac{E_A}{RT}\right) \quad (13)$$

where A_0 is the frequency factor of adsorption (unitless), and E_A activation energy of adsorption (usually represented in kJ/mol). If the adsorption coefficient is known at a reference temperature, the temperature dependence can also be represented by the simplified "theta" relationship, which is value for small changes in temperature:

$$k_{ad} = k_{ad,ref}\theta^{T-T_{ref}} \quad (14)$$

where $k_{ad,ref}$ (M/M) is the adsorption rate constant determined at a reference temperature T_{ref}.

For SWT's process, the biosorption mechanism is novel compared to the studies discussed in Aksu (2005) and Gadd (2009). SWT's process focuses on the biosorption of PCOD rather than metals and synthetic and organic pollutants such as pesticides and textile dyes. Metals are ionic species that favor biosorption to charged surfaces like microbial cells (Aksu, 2005). Synthetic and organic pollutants are generally hydrophobic molecules with large molecular weights that are attracted to other hydrophobic molecules, including collections of microbial cells or sludge. A microbial cell wall is hydrophilic, but its small size deters them from being attracted individually to large molecules (Bitton, 2005).

PCOD and much of the SCOD are large components that are not particularly hydrophobic, but can aggregate to cells via polymer bridging or being trapped by floc particles, which is explained in the next section. While early theory (Buswell, 1928) regarded aggregation mechanisms as functions of surface charge, Pavoni et al. (1972) established that biosorption of COD is heavily influenced by the presence of EPS and the mechanism of polymer bridging. EPS is a main component in the organic fraction of activated sludge, providing an extensive surface area for polymer bridging and microorganism aggregation (Wilen et al., 2003a). Pavoni et al. (1972) defines polymer bridging of EPS as the attachment of EPS with bacterial cells so that polyelectrolytes bridge individual cells together in a floc. As Wilen et al. (2003b) summarized, EPS is comprised of different negatively charged groups are bound together by divalent and trivalent charged cations, like Ca^{2+}. Keiding and Nielsen (1997) determined that decreasing Ca^{2+} concentration leads to an increase in negative surface charge on EPS and a resulting deflocculation of biomass and other "molecular entities." Jimenez et al. (2005) further established that EPS promotes particulate COD entrapment or attachment to the floc surface. The microbial cells then benefit from the being able to store PCOD for hydrolysis.

The biosorption process is further complicated by its competition with hydrolysis of the PCOD. As cells absorb PCOD, the PCOD can be hydrolyzed into SCOD, which then can be used by the cells as substrate for active biomass

growth. Hydrolysis kinetics are often represented by the first-order relationship (Rittmann & McCarty, 2001)

$$r_{hyd} = -k_{hyd} PCOD_a \quad (15)$$

where r_{hyd} is the hydrolysis rate ($M/L^3/t$), k_{hyd} is the first-order hydrolysis rate coefficient (1/t), and $PCOD_a$ is the adsorbed PCOD concentration (M/L^3). This model accounts for decreased PCOD concentration with increased biomass utilization. If we interpret these as competing mechanisms, the surface sorbate concentrations can be combined into a single model for biosorption kinetics with

$$\frac{dq}{dt} = -k_{hyd} PCOD_a - k_{1,ad}(q_{eq} - q_c) \quad (16)$$

Based on currently available data, it will be difficult to separate hydrolysis kinetics from biosorption to model only the biosorption kinetics; key to doing this is knowing the first-order hydrolysis rate coefficient. The first approach to establishing PCOD adsorption coefficients is to develop a linear model of the PCOD adsorbed concentration at various concentrations. If the provided information does not support a linear relationship, plots of $\ln(q_{eq} - q)$ vs. time and t/q vs. q should provide an estimate of whether the behavior is first or second order, respectively.

2.3.2 Flocculation

Flocculation is probably involved in biosorption processes in contact stabilization. The connection is that the PCOD attaches to flocs as they are formed in the stabilization tank and later removed in the clarifier during differential settling.

Smoluchowski (1917) developed the first major theory for coagulation and flocculation, and it has formed the basis for all theories subsequently developed. Smoluchowski described the rate of overall particle collisions as

$$r_k = \frac{dn_k}{dt} = \frac{1}{2}\alpha \sum_{j=1;i+j=k}^{j=k-i} \beta_{ij} n_i n_j - n_k \alpha \sum_{i=1}^{N} \beta_{ik} n_i \qquad (17)$$

where r_k is the net formation rate of k-sized particles (particles/L^3t); n_i, n_j and n_k are the number of particles size i, j, k (respectively) per volume (particles/L^3); t is time; α is the efficiency of collisions to make larger particles (unitless); β is the collision frequency for the particles of the class size designated (unitless); and N is the total number of particles. Smoluchowski's paper included collision frequencies based on perikinetic (β_{peri}) and orthokinetic (β_{ortho}) flocculation.

Camp and Stein (1943) further developed the orthokinetic and differential settling (β_{DS}) collision frequencies through a simplified interpretation of the varied velocity gradients in a system. They employed the root-mean-square (RMS) velocity gradient to compute the collision frequency. The RMS velocity gradient (G) is a measure of the amount of strain a particle undergoes to travel in a viscous fluid (with units 1/t). RMS velocity gradient can be calculated by

$$G = (\varepsilon/\nu)^{1/2} \qquad (18)$$

where ε is the rate of energy dissipation (L^2/t^3)and υ is kinematic viscosity (L^2/t).

The overall collision factor is the sum of the perikinetic, orthokinetic, and differential-settling factors:

$$\beta = \beta_{peri} + \beta_{ortho} + \beta_{DS} \qquad (19)$$

Perikinetic flocculation (β_{peri}), orthokinetic flocculation (β_{ortho}), and differential settling (β_{DS}) are described as (Thomas et al., 1999):

$$\beta_{peri} = \left(\frac{2kT}{3\mu}\right)\left(\frac{1}{d_i} + \frac{1}{d_j}\right)\left(d_i + d_j\right) \tag{20}$$

$$\beta_{ortho} = (G/6)\left(d_i + d_j\right)^3 \tag{21}$$

$$\beta_{DS} = \left(\frac{g\pi}{72\mu}\right)\left(\rho_p - \rho_l\right)\left(d_i + d_j\right)\left|d_i - d_j\right| \tag{22}$$

where k is Boltzmann's constant ($ML^2 t^{-2} K^2$), T is the absolute temperature of the fluid in Kelvin, μ is the water viscosity (M/L/t), d is the diameter of the particle type specified (i or j) (L), G is the RMS velocity gradient (1/t), g is the gravity constant (L/t^2), ρ_p is the density of the particle (ML^3), and ρ_l is the density of the fluid (M/L^3).

The rate of floc formation can be converted from a particle to a mass concentration using the following relationship

$$C_i = n_i M_i \qquad \text{or} \qquad n_i = C_i/M_i \tag{23}$$

where C_i is the concentration of PCOD particles of size i in the system (M/L^3) and M_i is the mass of PCOD of size i (M/particle). Substituting Eqn. 23 into Eqn. 17,

$$\frac{1}{M_k}\frac{dC_k}{dt} = \frac{1}{2}\alpha \sum_{j=1;i+j=k}^{j=k-i} \beta_{ij}\frac{C_i}{M_i}\frac{C_j}{M_j} - \frac{C_k}{M_k}\alpha \sum_{i=1}^{N} \beta_{ik}\frac{C_i}{M_i} \tag{24}$$

An advantage of this approach is that is quantifies all of the applicable floc mechanisms. However, it is difficult to apply Eqn. 24 to real-world systems, because the particle masses (M_i, M_j, M_k), particle-size distributions, and particle density (ρ_p) are difficult to quantify.

In *Wastewater Treatment: Biological and Chemical Processes*, Henze et al. (1995) develop a first-order relationship for floc analysis in the chapter on phosphorus removal. It can be extended to PCOD removal. The floc formation velocity, r_f, is equal to the velocity at which primary particles are being removed, $-r_p$.

$$r_f = \frac{dn_p}{dt} = k_{floc} n_p \Phi G \tag{25}$$

where r_f is the floc formation velocity (particles built into floc/ L^3 water t), k_{floc} is the formation constant (L^3 water/L^3 floc), n_p is the number of primary particles per unit volume (particles/L^3 water), Φ is the volume of flocs per unit volume of water (L^3 floc/ L^3 water), and G is the RMS velocity gradient. The flow regime in the tank is assumed to be turbulent so that the RMS velocity gradient can be calculated based on the power supplied to the tank

$$G = (W/\mu_a)^{1/2} \tag{26}$$

where W is the power supplied per unit volume of liquid ($W/L^3/t$) and μ_a is the absolute viscosity of the liquid (M/L/t). Since particle-size distribution is difficult to quantify, the authors relate the particle concentration to mass concentration using Eqn. 23.

$$r_f = \frac{dC_{PCOD}}{dt} = k_{floc}(PCOD_s/M_{PCOD})\Phi G \tag{27}$$

where $PCOD_f$ is the concentration of PCOD in floc (M/L^3) and M_{PCOD} is the mass of PCOD particle (M).

Henze et al. (1995) also describe floc removal or breakdown using

$$r_p = k_{p,f} PCOD_f \Phi G^p \quad (28)$$

where r_p is the primary particle formation velocity (primary particles formation velocity/ L^3/t), $k_{p,f}$ is the removal constant based on the size of particle p ($M/L^3/t^{p-1}$), and p is a dimensionless constant. While Henze does not provide a dimensionless constant for PCOD, the value for p usually ranges between 1 and 3 (often based on fractal geometries). Thus, the net formation of floc, r_n, with PCOD particles can be described as

$$r_n = r_f - r_p = \Phi G \left(k_{floc} \frac{C_{\text{single particles of PCOD}}}{M_{PCOD}} - k_{p,f} \frac{C_{\text{PCOD in floc}}}{M_{PCOD}} G^{p-1} \right) \quad (29)$$

The assumption of a first-order relationship may seem unusual, but has been successfully applied for PCOD removal by flocculation in several articles by Jimenez and La Motta (2005, 2007).

Flocculation rates and (specifically) constants can be affected by several factors. Agitation can affect the formation and breakup of floc, and is taken into account in the RMS velocity gradient (Henze et al., 1995). The amount of EPS in microbial aggregates has been shown to increase flocculation rates in activated sludge systems, which may result in the flocculation constant K_f being a function of EPS concentration. Due to the unavailability of data on PCOD and EPS contents of sludges, this relationship will have to be explored later in this work and in subsequent works. Should K_f depend on temperature, it can be modeled using the Arrhenius relationship mentioned in Eqn. 13.

2.4 SWT's Hybrid and Conventional Processes

The coupling of aerobic and anaerobic processes has been going on for decades. In the last fifty years, anaerobic digesters have been added to conventional activated sludge processes to stabilize sludge from the clarifier prior to disposal (Metcalf & Eddy, 2003). In the last twenty years, the coupling of anaerobic and aerobic processes has used sludge recycle from the anaerobic digester to facilitate nutrient removal from wastewaters. Anaerobic pre-treatment reactors are utilized prior to aeration tanks for enhanced phosphorus biological removal (Rittmann & McCarty, 2001). The PhoStrip^{TM} process recycles some sludge from the anaerobic digester to the activated sludge after it has been stripped of phosphorus via precipitation with lime (Metcalf & Eddy, 2003). The precipitate and sludge are removed from the digester for further processing. The SWT hybrid process is a novel expansion of the concept of coupling aerobic and anaerobic processes.

In June 2009, SWT installed three pilot plant trains in Singapore to provide data to understand and ultimately model hybrid system performance. Each train is capable of running either conventional and hybrid strategies, as illustrated in Figures 2.3a-c. Each train is fed 600 L/day of influent wastewater from the same source. Each train contains several processes that are present in activated sludge WWTPs: an anoxic tank, a contact tank, clarifier, stabilization tank, sludge thickener and AD. Influent enters the system at the anoxic tank. Effluent leaves the system as treated wastewater from the clarifier and sludge

from the AD. The target operating parameters are summarized in Table 2.1, and reflect values supplied by SWT. Actual flows, return activated sludge rate (RAS), and wasted activate sludge rate (WAS) are summarized in Table 2.2. In SWT's systems, WAS is defined as the flow rate to the sludge thickener.

In December 2010, train 1 was modified to increase denitrification in the system. The rationale behind these changes is that the stabilization tank is not supporting denitrification processes due to higher consumption of COD in the tank. The stabilization tank was removed while the anoxic and contact tanks were expanded in volume. A recycle was added from the effluent to the contact tank to the influent of the anoxic tank at a rate of 3 to 4 times the influent volumetric flow rate. Plastic packing was also added to the contact tank to provide another 32 m^2 of surface area for biofilm growth.

SWT's hybrid process is similar to and differs from the conventional contact stabilization processes in several ways. Conventional contact stabilization processes, as illustrated in Figure 2.2, send sludge from the clarifier to either the stabilization tank for sludge stabilization or sludge processing, with return activated sludge percentages to the stabilization tank ranging between 50 to 150% of the influent flow (Metcalf & Eddy, 2003). Consistent with normal practice, SWT's conventional and hybrid processes have a RAS of 120%. In SWT's conventional process, 1% of the RAS is diverted to anaerobic digestion, from which the sludge is eventually wasted, while 99% flows to the stabilization tank.

There is no recycle of anaerobic sludge back to aerobic processes in a conventional treatment process.

The hybrid process varies from conventional contact stabilization by performing sludge stabilization in parallel via an aerobic stabilization tank and an anaerobic digester. The return activated sludge rate ranges 100 to 120% of the influent flow rate and flows into the stabilization tank. The hybrid process diverts an additional 6% of the clarifier sludge to anaerobic digestion. The hybrid process also recycles anaerobic sludge back to the aerobic processes at rate which is 85% or more of the influent flow rate to the anaerobic digester.

When sludge is routed to the stabilization tank, the PCOD is provided with a longer SRT to biodegrade more complex organic compounds. A benefit of the stabilization tank may be nitrification, but aerobic biodegradation of PCOD prevents energy capture in methane. Routing sludge directly from the clarifier to the anaerobic digester allows for PCOD to be converted to methane through the processes described in earlier sections. Using BioWin 3.01, SWT projected that 50 to 87% of the COD entering the anaerobic digester will be removed when 2 to 20% of the RAS is diverted to the anaerobic digester, respectively (Liu, 2008). During hybrid operations, at least 85% of the sludge that would normally be wasted sludge from the anaerobic digester is recycled to the stabilization tank to increase the amount of biomass available for biosorption in the contact tank. For the purposes of this project, SWT targeted 17 L/day of wasting sludge from the anaerobic digester during conventional operations. The hybrid system targeted a

recycle rate of 15 L/day anaerobic sludge to the stabilization tank and discharge of 2 L/day of waste sludge. This equates to approximately 2% of RAS being transferred to the anaerobic digester.

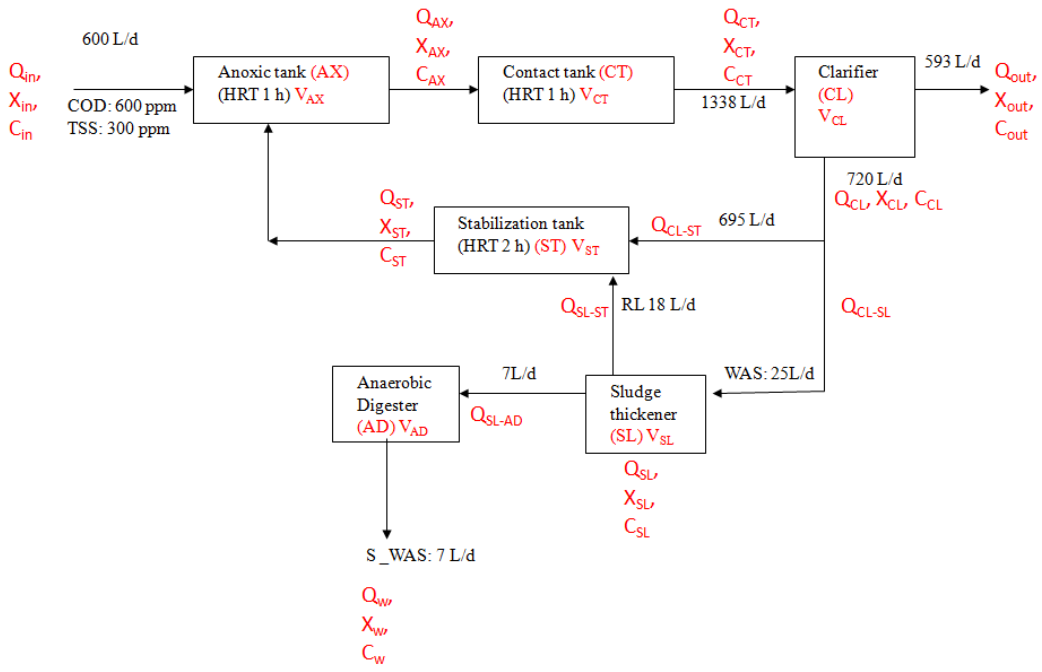

(a)

Figure 2.3. SWT's (a) conventional contact stabilization with anaerobic digestion, (b) hybrid contact stabilization with anaerobic digestion and (c) modified hybrid process with stabilization tank removed. Variable labels include Q for volumetric flow rate (L^3/t), V for tank volume (L^3), C for concentration (M/L^3), and X for biomass concentration (M/L^3).

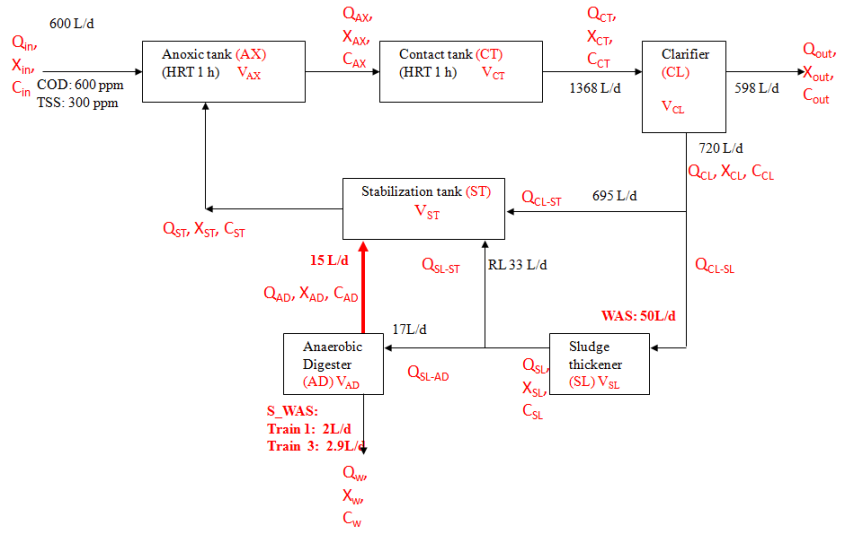

(b)

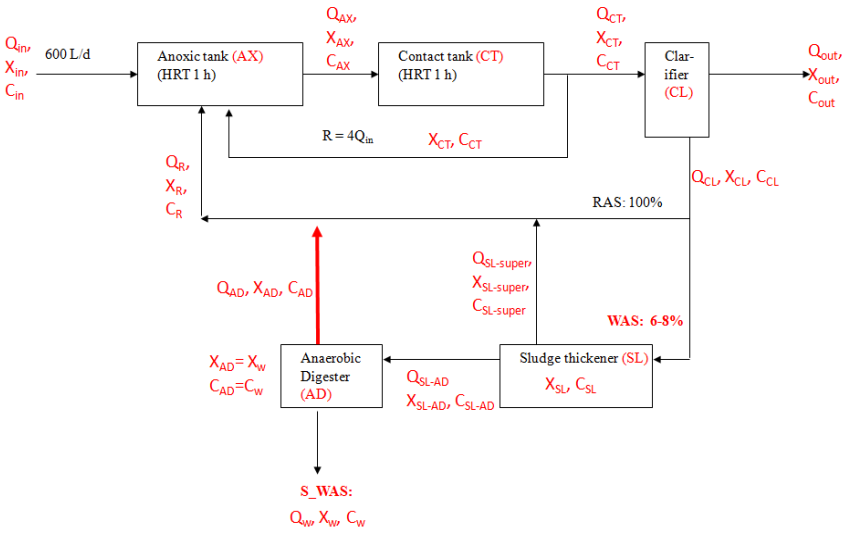

(c)

Figure 2.3 continued. SWT's (a) conventional contact stabilization with anaerobic digestion, (b) hybrid contact stabilization with anaerobic digestion and (c) modified hybrid process with stabilization tank removed. Variable labels include Q for volumetric flow rate (L^3/t), V for tank volume (L^3), C for concentration (M/L^3), and X for biomass concentration (M/L^3).

Table 2.1. Target operating parameters for the hybrid and conventional processes, as provided by SWT.

	Train 1	**Train 2**	**Train 3**
Influent flow rate	600 L/day		
RAS	100 to 120% based on the operational phase		
Wasted sludge	2 L/day	17 L/day	2 L/day
Anaerobic sludge recycle rate to the stabilization tank	15 L/day	0 L/day	15 L/day
HRT			
• Anoxic tank	1 hr		
• Contact tank	1 hr		
• Stabilization tank	2 hr		
SRT			
• Anoxic/contact/ stabilization tanks	~ 2.5 days	~ 5 days	~ 2.5 days
• Anaerobic digester	~ 30 days		
Tank volumes			
• Anoxic tank	Phases 2-11: 25 L Phase 12: 55 L	25 L	25 L
• Contact tank	Phases 2-11: 25 L Phase 12: 75 L	25 L	25 L
• Clarifier	100 L		
• Sludge thickener	100 L		
• AD	Phases 2-7: 510 L, Phases 8-12: 650 L		
• Stabilization tank	Phases 2-11: 50 L Phase 12: N/A--removed	50 L	50 L

Table 2.2. Flow, RAS, and WAS rates for each train and phase beginning with phase 6.

Parameter	Train	Phase					
		6	7	9	10	11	12
Flow from clarifier to stabilization tank (L/d)	1	720	720	726	726	605	605
	2	720	720	726	726	605	605
	3	720	720	726	726	605	605
Flow from clarifier to sludge thickener (WAS) (L/d)	1	50	50	64.8	64.8	54.7	54.7
	2	50	50	27.4	27.4	27.4	27.4
	3	50	50	64.8	64.8	54.7	54.7
Sludge thickener supernatant (L/d)	1	33	33	43.2	38.9	33	33.1
	2	33	33	5.8	1.5	5.8	5.8
	3	33	33	43.2	38.9	33	33.1
Sludge wasting rate (L/d)	1	2	2	2.9	2.9	5.9	2.9
	2	17	17	21.6	25.9	21.6	21.6
	3	2	2	2.9	2.9	5.9	5
AD sludge recycle rate (L/d)	1	15	15	18.7	23	15.8	18.7
	2	0	0	0	0	0	0
	3	15	15	18.7	23	15.8	16.6
RAS rate (% influent)	1	120	120	120	120	100	100
	2	120	120	120	120	100	100
	3	120	120	120	120	100	100
WAS rate (% sludge from clarifier)	1	6.5	6.5	8.2	8.2	8.3	8.3
	2	6.6	6.6	3.6	3.6	4.3	4.3
	3	6.5	6.5	8.2	8.2	8.3	8.3

* Target rates. Actual wasting sludge rate varied from 8 to 14 L/d during the first three weeks of the phase prior transitioned to 2.9 L/d in week 4.

In the hybrid process, biosorption is accentuated for the aerobic contact and stabilization tanks by recycling a majority of the anaerobic sludge to the stabilization tank to increase the amount of biomass available for biosorption throughout the rest of the system. Theoretically, this additional biomass can be utilized as a medium for PCOD biosorption in the contact and stabilization tanks. However, active biomass will metabolize more COD the longer it is exposed to aerobic conditions in the contact tank. As previously stated, contact tank HRTs

range from 20 minutes to one hour. A study by Jimenez et al. (2005) found that it took at least 30 minutes for 50% biosorption of PCOD in wastewater with 350 mg/L total COD (TCOD). To encourage biosorption while limiting biodegradation of PCOD in aerobic conditions, the SWT hybrid process is operated at a "longer" HRT of one hour in the contact tank and a shorter HRT of two hours in the stabilization tank to reduce the biodegradability of more complex COD. The longer HRT in the contact tank allows for adequate biosorption time, as determined by Jimenez et al. (2005), while minimizing SCOD consumption in the contact tank. The short HRT in the stabilization tank allows for some nitrification by utilizing simple SCOD substrate and biosorption of PCOD for recycle through the system. The recycled biomass eventually returns to the AD with the biosorbed particulate COD. The idea is that hydrolytic bacteria in the AD convert the PCOD to SCOD, which can be metabolized to methane through fermentation and methanogenesis. Thus, most COD removal occurs by an anaerobic, methane-producing process, not by an aerobic, oxygen-consuming process.

SWT's BioWin 3.01 model, illustrated in Figure 2.4, supports several other key claims for the hybrid process. While their model differs from the hybrid design implemented in Singapore, it retains the core concepts of sludge stabilization using stabilization tank and anaerobic digester and recycle of anaerobic sludge to the aerobic processes. However, the BioWin model assumes no sludge wasting at the anaerobic digester; all sludge removed from the

anaerobic digester is recycled back to aerobic processes. Their model supports the hypothesis that most of the COD is converted to methane in the anaerobic digester through the mechanisms described earlier. As seen in Figure 2.5, SWT's model predicts 6,100 to 11,400 kWh/day increase in energy production with 2% to 10% of RAS entering the anaerobic digester. In addition, sludge production decreases significantly, from 0.38 to 0.23 gVSS/gCBOD as the percent of RAS to the digester is increased from 2 to 20%, as seen in Figure 2.6.

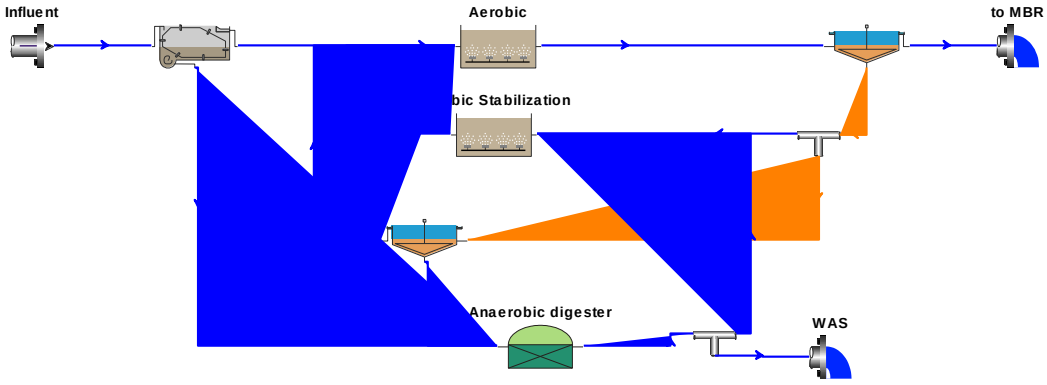

Figure 2.4. Schematic of SWT's BioWin 3.01 model of the hybrid process. Source: Liu (2008).

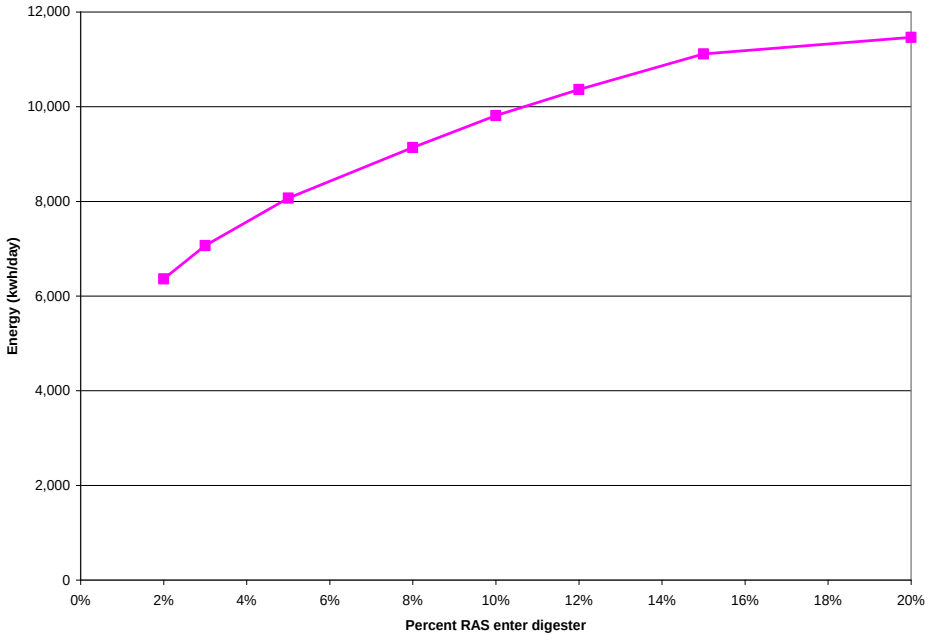

Figure 2.5. From the BioWin model, predicted energy gain from methane production due to RAS sludge being cycled to the anaerobic digester and recycled to aerobic processes. Source: Liu (2008).

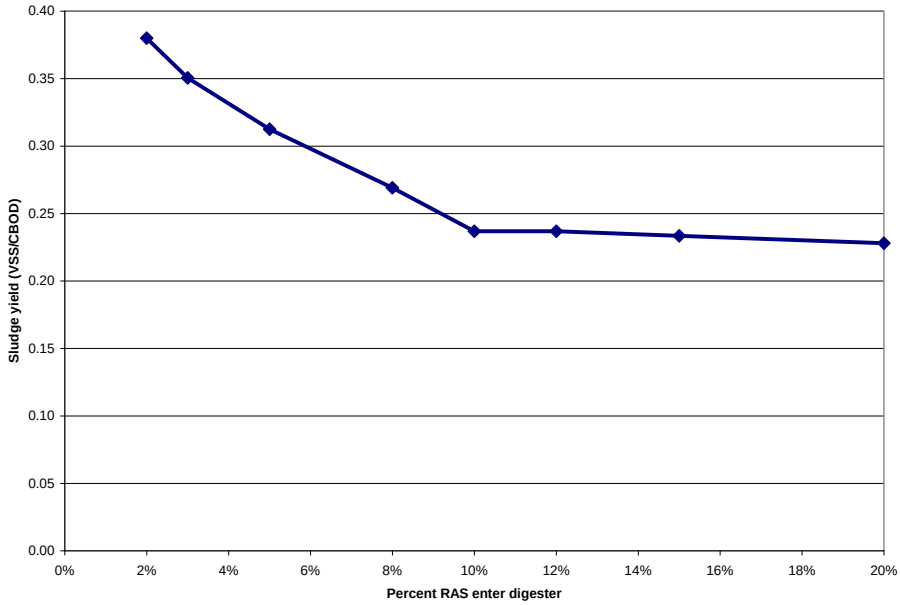

Figure 2.6. Predicted sludge yield from the BioWin model. Source: Liu (2008).

3. Analysis Methods for SWT's Processes

The SWT hybrid process presents a novel approach to wastewater treatment as a fusion of contact stabilization and anaerobic processes with additional recycle streams and an innovative biosorption mechanism. This novel process requires the application of an advanced mathematical mass balance model to facilitate interpretation of the types of physical, chemical, and biological mechanisms involved at each stage of the process. Mathematical modeling begins with identifying the key components that describe the performance of each tank and the entire process. An important aspect for this model is that the data are based on actual performance data; differentiating between distinct stages of operation is critical in contrasting the performance of each train. In addition to these complexities, different types of data are available for different phases, requiring slight variations in mass balance modeling depending upon the data available.

3.1 Operational Phases

Pilot plants are sometimes subjected to variations to determine how processes respond to upsets and to quantify operating limits. Unambiguous delineation of operational phases is critical in understanding how significant variations in SWT's operations affected the performance of each individual train. SWT's processes have functioned through 12 distinct phase variations since their startup in June 2009, when each train began operations as conventional processes to build up biomass for steady state operations and to provide baseline

performance data for typical activated sludge operating conditions. In late October 2009, two of the trains--trains 1 and 3--were converted to hybrid operations by recycling sludge from the anaerobic digester to the stabilization tank. However, the pilot plant operations experienced complications ranging from equipment sizing issues and leaks to deliberate adjustments to SRTs and flow rates. To assay the effects of these modifications, a new period was defined for each major process change affected a train's performance, as summarized in Table 3.1. These operational phases are used to compare each set of performance analyses to subsequent analyses as well as performance across trains.

The three trains were operated as conventional trains without AD sludge recycle for periods 1 through 5. Trains 1 and 3 were shifted to hybrid operations with AD sludge recycle for periods 6 and 7, while train 2 remained in conventional operation. Train 1 was briefly converted to conventional operation for phase 8 to build up sludge in anticipation of a larger AD. All trains had larger ADs installed during phase 9 of train 1 and phase 8 of trains 2 and 3. The ADs were increased from 510 L to 650 L to reduce the potential for H_2 inhibition of methane production. Train 2 was converted to hybrid operations during phase 8 to build up sludge in the larger AD. Later phases were characterized by all trains returning to their specified process configurations while variations were made to system SRTs, wasting sludge rates and anaerobic recycle rates. In efforts to improve denitrification, train 1's process was modified in phase 12 to remove the stabilization tank, enlarge the anoxic and contact tanks and add plastic packing to

the contact tank to support increased biomass retention. These variations are summarized in Table 3.1. All values in Table 3.1 are supplied by SWT.

Table 3.1a. Operational phases for (a) train 1, (b) train 2, and (c) train 3. All stated values provided by SWT. Phases highlighted in light grey are operated in hybrid mode, while phases in dark grey are operated with the modified hybrid configuration.

Train	Phase	Dates	Aerobic SRT (days)	RAS (%)	Description
1	1	6/3/09-8/12/09	2	100	Process start up
	2	8/13/09-9/01/09	2	100	Reduced HRT of contact and stabilization tanks by reducing tank volumes to 25L and 50L, respectively
	3	9/02/09-9/10/09	2	100	Aeration halted in the anoxic tank to begin denitrification.
	4	9/11/09-9/25/09	2	120	Percent RAS increased—transient phase
	5	9/26/09-10/28/09	3	120	Aerobic SRT increased
	6	10/29/09-12/21/09	3	120	Hybrid process start up
	7	12/22/09-3/11/10	3	120	Normal hybrid operations
	8	3/12/10-3/31/10	3	120	Operating as a conventional train with no AD sludge recycle
	8.5	4/1/10-4/10/10	3	120	Return to hybrid operations. New AD brought online.
	9	4/10/10-6/15/10	3	120	Normal hybrid operating conditions
	10	6/15/10-8/20/10	3	120	Decreased system SRT to 25 days
	11	8/20/10-12/20/10	3	100	Increased system SRT to 30 days and decreased RAS.
	12	12/21/10-3/15/11	3	100	To increase denitrification, the stabilization tank removed while the anoxic and contact tanks were expanded to 55L and 75L, respectively. Plastic packing was added to the contact tank to improve biomass retention.

Table 3.1b. Operational phases for (a) train 1, (b) train 2, and (c) train 3. All stated values provided by SWT. Phases highlighted in light grey are operated in hybrid mode, while phases in dark grey are operated with the modified hybrid configuration.

Train	Phase	Dates	Aerobic SRT (days)	RAS (%)	Description
2	1	6/3/09-8/12/09	3	100	Process start up with volumes of 50L in contact tank and 100L in stabilization tank
	2	8/13/09-8/20/09	3	100	Reduced HRT of contact and stabilization tanks by reducing tank volumes to 25L and 50L, respectively
	3	8/21/09-9/10/09	3	100	Aeration halted in the anoxic tank to begin denitrification.
	4	9/11/09-9/25/09	3	120	% RAS increased
	5	9/26/09-10/28/09	3	120	Normal operations
	6	10/29/09-01/11/10	3	120	Normal operations coinciding with hybrid process start up in the other trains
	7	01/12/10-3/31/10	3	120	Normal operations
	8	4/1/10-4/15/10	3	120	New AD brought online. Excess sludge is recycled to the AD, creating hybrid conditions. Recycle ratio = 8%.
	9	4/15/10-6/15/10	3	120	Returned to conventional operations
	10	6/15/10-7/30/10	3	120	Reduced system SRT of 25 days
	11	7/30/10 12/20/10	3	100	Increased SRT to 30 days
	12	12/21/10-3/15/11	3	100	New phase to correspond with phase 13 of train 1

Table 3.1c. Operational phases for (a) train 1, (b) train 2, and (c) train 3. All stated values provided by SWT. Phases highlighted in light grey are operated in hybrid mode, while phases in dark grey are operated with the modified hybrid configuration.

Train	Phase	Dates	Aerobic SRT (days)	RAS (%)	Description
3	1	6/3/09-8/12/09	4	100	Process start up with volumes of 50L in contact tank and 100L in stabilization tank
	2	8/13/09-9/01/09	3	100	Reduced HRT of contact and stabilization tanks by reducing tank volumes to 25L and 50L, respectively
	3	9/2/09-9/10/09	2	100	Aeration halted in the anoxic tank to begin denitrification.
	4	9/11/09-9/23/09	2	120	Percent RAS increased
	5	9/24/09-10/26/09	3	120	Normal operations
	6	10/27/09-1/11/10	3	120	Hybrid process start up
	7	1/12/10-3/31/10	3	120	Normal hybrid operations
	8	4/1/10-4/10/10	3	120	New AD brought online. Recycle ratio = 6%.
	9	4/10/10-6/15/10	3	120	Normal operating conditions with variations in WAS rate ranging from 0 to 2.9 L/day
	10	6/16/10-8/20/10	3	120	Reduced system SRT to 25 days
	11	8/20/10-12/20/10	3	100	Increased system SRT to 30 days and decreased RAS.
	12	12/21/10-3/15/11	3	100	New phase to correspond with phase 13 of train 1

3.2 Data Availability

SWT provided an extensive amount of data for each train over the term of the project. However, not all measurements are essential for describing the critical mechanisms occurring throughout the system. Specific physical, chemical, and biological mechanisms of interest are summarized in Table 3.2. In addition, a mass balance on the SWT system encompasses solid, soluble, and gas phases. It is particularly important to differentiate between soluble and solid components in each tank, as changes in these components serve as indicators of the mechanisms in Table 3.2. Table 3.3 summarizes the parameters measured in the SWT processes, the analytical methods used to analyze the parameters, and which facility performed the measurement.

Table 3.2. List of biological, chemical, and physical mechanisms used in mechanistic modeling

Biological, Chemical, and Physical Mechanisms
Advection in influent and effluent
Aerobic COD biodegradation
Aerobic nitrification of NH_3 to NO_3^-
Aerobic growth of heterotrophic and autotrophic biomass
Denitrification of NO_3^- to N_2 gas
Production of utilization byproducts (SMPs and EPS)
Hydrolysis of organic solids to soluble COD
Fermentation of soluble COD to acetate and H_2
Methanogenesis of acetate and H_2 to CH_4
Anaerobic growth of fermenting and methanogenic biomass
Endogenous decay of biomass
Biosorption/flocculation
Aeration

Table 3.3. List of parameters measured in the SWT processes

Parameter	Standards/Equipment	Facility Performing Test
Oxygen Demand (TCOD and SCOD)	Hach Method 8000 Dichromate Digestion Method	SWT
Suspended Solids (VSS and TSS)	Standard Methods for the Analysis of Water and Wastewater, 21st edition	SWT
TKN	APHA Pt 4500-Norg (D) Standard Method for the Determination of Water and Waste Water, 21st edition	SWT
NH_3-N	Hach Method 10023	SWT
NO_2-N	Ion Chromatography	National University of Singapore
NO_3-N	Ion Chromatography	National University of Singapore
Total Iron and Fe_{+2}	Thermo Scientific iCAP OES Spectrometer	SWT

Soluble constituents measured in the SWT processes are COD and nitrogen compounds. Changes in TCOD and SCOD are indicators of several biological processes, including biomass synthesis, hydrolysis, biosorption, and fermentation. Variations in ammonia nitrogen (NH_3-N), nitrate nitrogen (NO_3-N), and nitrite nitrogen (NO_2-N) are indicators of nitrification, denitrification, and endogenous decay.

Two key solid components measured in the SWT processes are VSS and total suspended solids (TSS). VSS concentrations are an indicator of biomass and can be converted to PCOD concentrations through the relationship

$$\frac{\text{Concentration}}{\text{of PCOD}} = \frac{\text{Concentration}}{\text{of VSS}} * \frac{1.42 \text{ mg COD}}{\text{mg VSS}} \qquad (30)$$

In biological systems, PCOD is converted SCOD through hydrolysis, and the SCOD can be utilized as substrate. VSS is also an indicator of biosorption potential, since hydrophobic SCOD can biosorbed onto biomass, when it becomes part of the PCOD (Jimenez et al., 2007). TSS is defined as the total of volatile and inert solids in the system. Variations in TSS include the amount of inert solids formed from endogenous decay in the tank, as well as inert solids entering with the influent.

Each piece of data was measured at different frequencies for each phase, depending upon the measurement complexity, labor availability, and cost of analysis. Table 3.4 highlights the data measured and average measurement frequency by phase and train for the parameters featured in this work. TCOD, SCOD, TSS, and VSS data are abundant throughout the project. These measurements are performed onsite by SWT personnel. Once the project progressed past the startup phases 2-5, TCOD and TSS were measured a minimum of two times per week through the duration of the project. SCOD and VSS were measured, respectively, 1.5 to 2.7 per week and 0.8 to 1.4 measurements per week, depending upon phase and train.

Nitrogen compounds were less frequency measured than COD and suspended solids. TKN was measured in the influent stream at a frequency of less than once per month, making TKN results too sparse to be useful. After phase 5, NH_4^+ was measured about 1.8 times per week. During the same phases, NO_2^- and NO_3^- are both measured at a frequency ranging from 0.8 to 1.1 times per week.

However, NO_2^- and NO_3^- measurements generally were omitted for effluent streams from the sludge thickener and AD with the exception of phase 9 of trains 2 and 3. The omission of NO_2^- and NO_3^- measurements in these tanks makes nitrification analysis particularly difficult, since denitrification would be possible in the sludge thickener and AD. A mass balance on the stabilization tank cannot be performed, since NO_2^- and NO_3^-concentrations are not measured for the sludge thickener supernatant.

Table 3.4a. Average frequency of data point measurement by phase across all trains for (a) train 1, (b) train 2, and (c) train 3. "ND" denotes either no data or limited data (2 or less data points) available for that phase.

Train	Data	Average Frequency by Data Point Measurement by Phase (Data Points per Week)										
		P2	P3	P4	P5	P6	P7	P8	P9	P10	P11	P12
1	TCOD	1.0	ND	0.6	2.8	4.0	3.7	4.7	3.1	1.9	2.1	1.0
	SCOD	0.6	ND	0.6	2.6	3.0	1.6	1.8	ND	1.9	2.1	0.9
	VSS	0.3	ND	0.3	1.1	1.1	0.8	ND	ND	1.1	1.0	0.5
	TSS	1.0	ND	0.9	2.8	2.9	2.0	2.9	2.3	1.8	2.1	0.9
	NH_3-N	0.2	ND	0.3	0.7	1.8	1.2	2.3	ND	1.8	2.1	2.4
	NO_2-N	0.2	ND	0.3	0.7	1.1	0.3	ND	ND	1.3	1.9	0.5
	NO_3-N	0.2	ND	0.3	0.7	0.9	0.5	ND	ND	1.5	1.8	0.5
	Total Iron	ND	ND	ND	ND	1.2	0.6	ND	ND	1.2	1.1	0.4
	Fe^{+2}	ND	ND	ND	ND	0.4	0.2	ND	ND	ND	ND	ND
	AD Biogas Concentrations (N_2/CH_4/CO_2)	0.5	ND	0.1	0.2	1.1	0.8	ND	ND	1.3	0.8	0.9

Table 3.4b. Average frequency of data point measurement by phase across all trains for (a) train 1, (b) train 2, and (c) train 3. "ND" denotes either no data or limited data (2 or less data points) available for that phase.

Train	Data	Average Frequency by Data Point Measurement by Phase (Data Points per Week)										
		P2	**P3**	**P4**	**P5**	**P6**	**P7**	**P8**	**P9**	**P10**	**P11**	**P12**
2	TCOD	3.0	2.4	ND	2.8	3.9	4.0	2.5	2.9	2.1	2.0	2.0
	SCOD	ND	ND	ND	ND	2.1	1.5	ND	2.7	2.1	1.9	1.8
	VSS	ND	1.0	1.0	1.1	1.0	0.8	ND	1.4	1.0	1.0	1.0
	TSS	3.0	2.8	3.0	3.1	2.7	2.1	2.5	2.4	2.2	2.0	1.7
	NH_3-N	ND	0.7	1.0	0.4	1.9	1.4	2.0	1.8	2.1	1.8	1.8
	NO_2-N	ND	0.7	1.0	0.4	0.7	0.6	1.5	1.1	1.9	0.9	1.2
	NO_3-N	ND	0.7	1.0	0.4	0.6	0.6	1.5	1.3	1.9	0.9	1.2
	Total Iron	ND	ND	ND	ND	0.7	0.8	ND	1.6	1.0	1.0	0.9
	Fe^{+2}	ND	ND	ND	ND	0.5	0.8	ND	ND	ND	ND	ND
	AD Biogas Concentrations (N_2/CH_4/ CO_2)	2.0	1.4	1.5	0.2	0.7	1.3	ND	2.1	1.1	0.9	0.9

Table 3.4c. Average frequency of data point measurement by phase across all trains for (a) train 1, (b) train 2, and (c) train 3. "ND" denotes either no data or limited data (2 or less data points) available for that phase.

Train	Data	Average Frequency by Data Point Measurement by Phase (Data Points per Week)										
		P2	**P3**	**P4**	**P5**	**P6**	**P7**	**P8**	**P9**	**P10**	**P11**	**P12**
3	TCOD	3.0	ND	1.8	2.8	3.7	6.4	3.1	1.9	2.0	2.0	1.3
	SCOD	ND	ND	1.8	2.8	2.6	2.5	ND	1.9	2.0	1.6	1.3
	VSS	1.0	ND	1.3	1.1	0.9	1.3	ND	1.1	1.0	1.0	0.6
	TSS	1.0	ND	3.1	2.8	2.7	3.2	2.3	1.8	2.0	1.9	1.2
	NH_3-N	0.7	ND	1.3	0.4	1.8	2.4	ND	1.8	2.0	1.7	1.2
	NO_2-N	0.7	ND	1.3	0.4	0.6	1.0	ND	1.2	1.6	0.3	0.8
	NO_3-N	0.7	ND	1.3	0.4	0.6	0.8	ND	1.5	1.6	0.5	0.5
	Total Iron	ND	ND	ND	ND	0.9	1.3	ND	1.1	1.0	1.0	0.6
	Fe^{+2}	ND	ND	ND	ND	0.5	1.3	ND	ND	ND	ND	ND
	AD Biogas Concentrations (N_2/CH_4/ CO_2)	1.7	ND	0.9	ND	0.6	2.0	ND	1.3	1.1	0.9	0.6

3.3 Mass Balance Modeling

Mass balance analysis is the fundamental approach to analyzing physical, chemical, and biological changes as mass moves through a system. Models can be developed using software such as Microsoft Excel and MATLAB. Excel was employed for this analysis, since the solution was of a set of linear mathematical equations, rather than a series of complex differential equations.

Mass balance analysis is based on the fundamental principle of conservation of mass: mass can neither be created nor destroyed, but can change phases, like liquid to gas, and form, as through chemical reactions. For engineering systems, mass balance analysis allows us to understand the rates at which specific compounds are being produced or consumed in a system. Performing mass balances on an individual tank and overall system basis allows us to quantify what is happening step by step through the process and the overall outcomes from the system.

3.3.1 Transient Mass Balance Models for SWT's Hybrid and Conventional Processes

An important characteristic of SWT's processes is that they are transient, i.e., input and output stream compositions are always changing. A non-steady state model of the law of conservation of mass can be explained using a simple worded statement:

Rate of accumulation of mass within a system	=	Rate of mass entering the system	-	Rate of mass leaving the system	+	Rate of generation of mass in the system	-	Rate of decay of mass in the system

(31)

The first term indicates that, because the system is not at steady state, mass may accumulate in any of the tanks. The second and third terms represent the movement of mass across the boundary, such a in a water or gas flow. The fourth and fifth terms are for biochemical and chemical reactions that change the form of the mass.

Assuming a completely mixed system with only liquid flows crossing the boundary and one net reaction converts the word form of Equation 30 to terms of concentrations and flow rates for soluble species

$$V\frac{dC_{effluent}}{dt} = Q_{influent}C_{influent} - Q_{effluent}C_{effluent} + R_c \qquad (32)$$

and for solid species

$$V\frac{dX_{effluent}}{dt} = Q_{influent}X_{influent} - Q_{effluent}X_{effluent} + R_X \qquad (33)$$

where V is the volume of the system (L^3), C is the concentration of a soluble species (M/L^3), X is concentration of a solid species (M/L^3), Q is the volumetric flow rate of the stream (L^3/t), R_c is the net reaction rate for the soluble species (M/t), and R_X is the net reaction rate (M/t) of the solid species.

Several assumptions were made to do the mass balance analysis of the SWT processes. First, I assumed that each tank is completely mixed, so that the concentration is uniform throughout the tank. Then, the effluent stream from the

tank is the same as the concentration inside the tank. I treated volume as a constant, which is reasonable for continuous flow reactors with fixed size. For vessels that perform solid/liquid separation, i.e. clarifier and sludge thickener, I divided their effluents divided into two separate streams: a low-solids supernatant stream removed from the top of the tank and a high-solids sludge stream removed from the bottom of the tank.

I applied mass balance equations to each tank in of SWT's processes, resulting in 7 mass balance equations per solid and soluble component for each train: one for each of the six tanks and one for the overall system. Figure 2.3 identifies which variables are associated with specific streams. For example, the influent is characterized by an influent stream volumetric flow rate, Q_{in}, and concentration, C_{in}, and the volume of the anoxic tank is V_{AX}. The individual mass balance equations are summarized in Table 3.5. The reaction rate can be calculated if all of the concentrations, flow rates, and volumes are known. For the SWT processes, the concentrations and flow rates for each stream were known at specific points of time. Therefore, the reaction rate was determined by subtracting inlet and outlet mass balance terms from the accumulation term for each tank and the overall system.

The net reaction rate of a component tank can indicate whether the expected mechanisms outlined in Table 3.2 are occurring in each vessel. Minimal consumption or production of any constituents is expected in the clarifier and sludge thickener, since advection is the dominant mechanism in these tanks.

Table 3.5. Mass balance equations for SWT's hybrid and conventional processes, including equations for the overall system and each tank.

Overall system		$V_{system}\frac{dC}{dt} = Q_{in}C_{in} - Q_{out}C_{out} - Q_wC_w + R_{system}$
Anoxic tank (AX)		$V_{AX}\frac{dC_{AX}}{dt} = Q_{in}C_{in} + Q_{ST}C_{ST} - Q_{AX}C_{AX} + R_{AX}$
Contact tank (CT)		$V_{CT}\frac{dC_{CT}}{dt} = Q_{AX}C_{AX} - Q_{CT}C_{CT} + R_{CT}$
Clarifier (CL)		$V_{CL}\frac{d(C_{CL} + C_{out})}{dt} = Q_{CT}C_{CT} - Q_{out}C_{out} - Q_{CL}C_{CL} + R_{CL}$
Sludge thickener (SL)		$V_{SL}\frac{dC_{SL}}{dt} = Q_{CL-SL}C_{CL} - Q_{SL-AD}C_{SL-AD} - Q_{SL-super}C_{SL-super} + R_{SL}$ where $C_{SL} = \frac{C_{SL-super}Q_{SL-super} + C_{SL-AD}Q_{SL-AD}}{Q_{SL-super} + Q_{SL-AD}}$
Stabilization tank (ST)	Hybrid	$V_{ST}\frac{dC_{ST}}{dt} = Q_{CL-ST}C_{CL} + Q_{SL-ST}C_{SL} + Q_{AD}C_W - Q_{ST}C_{ST} + R_{ST}$
	Conventional	$V_{ST}\frac{dC_{ST}}{dt} = Q_{CL-ST}C_{CL} + Q_{SL-ST}C_{SL} - Q_{ST}C_{ST} + R_{ST}$
Anaerobic digester (AD)	Hybrid	$V_{AD}\frac{dC_{AD}}{dt} = Q_{SL-AD}C_{SL} - C_W(Q_W + Q_{AD}) + R_{AD}$
	Conventional	$V_{AD}\frac{dC_{AD}}{dt} = Q_{SL-AD}C_{SL} - C_WQ_W + R_{AD}$

TCOD may be net consumed, but it should not be produced in any tank, because SCOD and PCOD biodegradation requires that a major portion be respired, with production of SMP or EPS being only a small fraction of SCOD loss. In addition, the biosorption theory outlined in Chapter 2 hypothesizes that the increase PCOD will be offset by loss of SCOD. Likewise the production of NO_3-N in

nitrification is accompanied by consumption of NH_3-N or NO_2-N in contact and stabilization tanks, while the consumption of NO_3-N as part of denitrification in the anoxic tank results in loss of soluble N to gaseous N_2.

3.3.2 Detailed Mass Balance of the Anaerobic Digester

In addition to the soluble and solid components mass balance performed on all tanks, the gas phase of the AD is also analyzed for the efficiency of methane production. SWT provided detailed flow rate and biogas composition data for all trains' anaerobic digesters. SWT measured the percentage of CH_4, CO_2, and N_2 present in the biogas, which then had to be converted to mass flow rates for comparison to COD consumption in the ADs.

The mass flow rate of CH_4, CO_2, and N_2 produced in an AD can be determined using the ideal gas law to calculate the density of the gas at a specified temperature and pressure. The ideal gas law is

$$PV = \frac{m}{M}RT \tag{34}$$

where P is the pressure of the gas ($ML^{-1}t^{-2}$), V is the volume (L^3), m is mass (M), M is the molecular weight of the compound (M), T is temperature (T), and R is the gas constant (expressed as 0.0821 L atm/(mol K) for the purpose of this analysis). Rearranging the equation gives the density, ρ (M/L^3):

$$\rho = \frac{m}{V} = \frac{PM}{RT} \tag{35}$$

Based on the temperature data provided for the anaerobic digester, I assumed an average biogas temperature of 30˚C for all density calculations. Thus, I

determined the mass flow rate, u_i (in M/t), of any gas i produced in the digester from

$$u_i = Q_{biogas} * c_i * \rho_i \quad (36)$$

where Q_{biogas} is the volumetric flow rate of biogas from the AD and c_i is the percent composition of gas i in the biogas.

3.4 Biomass Yield Calculations

One of SWT's objectives for the hybrid process is reduced biomass production versus conventional activated sludge processes. Biomass growth is generally quantified by measuring either VSS or PCOD (Metcalf and Eddy, 2003). VSS does not consist solely of active biomass: other constituents include adsorbed particulate substrate, EPS, and inert biomass. However, VSS is most widely applied because its measurement is simple and analysis rapid (Metcalf & Eddy, 2003).

It is important to put biomass growth in perspective by comparing the biomass growth rate to the rate of substrate consumed to maintain the microbial community. Biomass yield is used to describe this ratio of biomass growth to the amount of electron donor substrate consumed by the microbial community (Rittmann & McCarty, 2001).

As discussed in Rittmann and McCarty (2001), a variety of methods are used for determining the observed yield, Y_{obs}, of biomass in a system. Comparing VSS inventory and VSS wasting to changes in COD provide a direct relationship between the amounts of biomass generated in the system compared to substrate removed. This process is complicated by the need to take into account changes in biomass inventory when a process is not at steady state. Since the SWT processes often are non-steady state, the daily amount of VSS in the system and the amount wasted are calculated from the mass balance information. The change in VSS quantities from one data point to the next is used to determine how

VSS changes with time. The average change in VSS mass per day was then divided by the average change in COD mass per day for each phase. This can be represented mathematically as

$$\text{Yield } Y_{obs} = \frac{\frac{\text{Average } \Delta VSS_{inventory}}{\Delta t} + \frac{\text{Average } \Delta VSS_{wasting}}{\Delta t}}{\frac{\text{Average } \Delta COD}{\Delta t}} \quad (37)$$

Each change in inventory calculation must be weighted appropriately when the average change for the phase is calculated. Therefore, the average yield calculations by phase are weighted using the equation

$$\text{Weighted Yield } Y_w = \frac{\frac{\sum \Delta VSS_{inventory}}{\text{Phase duration}} + \frac{\text{Average } \Delta VSS_{wasting}}{\Delta t}}{\frac{\text{Average } \Delta COD}{\Delta t}} \quad (38)$$

For comparison, SWT requested that yield also be calculated using TSS by the same approach as applied with the same weighting method for VSS data.

3.5 Solids Retention Time Calculations

3.5.1 SWT's Methods for Calculating SRTs

SRTs are critical parameter in optimizing AD due to the slow growth rates of methanogens. Rittmann and McCarty (2001) define SRT as

$$\text{SRT} = \frac{\text{Amount of active biomass in system}}{\text{Production rate of active biomass}} \tag{39}$$

SRT is also defined as the reciprocal of the net specific growth rate of the microorganisms in the system. However, there are various interpretations of how to quantitatively describe SRT for a given system.

For example, SWT defines SRT several different ways in this project. SWT defines aerobic SRT as the nominal retention time of solids in the aerobic section of the process, which assumes biomass losses in the clarified effluent are negligible. A schematic of the system boundaries used to calculate aerobic SRT is presented in Figure 3.1. SWT's aerobic SRT definition is

$$\text{Aerobic SRT} = \frac{V_{AX}TSS_{AX} + V_{CT}TSS_{CT} + V_{CL}TSS_{CL} + V_{ST}TSS_{ST}}{Q_{CL-SL} * TSS_{CL-SL}} \tag{40}$$

where the subscripts represent streams labeled in Figure 3.1. For SWT's system, the denominator reflects only the mass flow rate of TSS in the WAS stream. This contradicts Rittmann and McCarty's definition in three ways. First, the loss rate also involved biomass lost in the clarifier effluent. Leaving out the effluent loss rate makes the denominator too small, which translates into a too-large SRT. Second, the denominator only addresses solids removal from the system—not reintroduction of solids in sludge thickener supernatant or AD sludge recycle.

Production rate is really the difference between output rate and input rate of active biomass. Ignoring the input of active biomass makes the denominator too large, which translates into a too-small SRT. Third, TSS is comprised of active and inactive solids, but the concentration of active biomass in each stream is not known. If the different streams were to have different ratios of active biomass to TSS, then the relative values in the denominator or numerator could be too high or too low. The issue probably is more important for the denominator than the numerator. Taken together, the three contradictions could, in principle, mean that the SRT computation is too large or too small. If the biomass returned from the anaerobic system has significant active biomass, then its impact would be the largest, and the SWT-computed SRT would be too small.

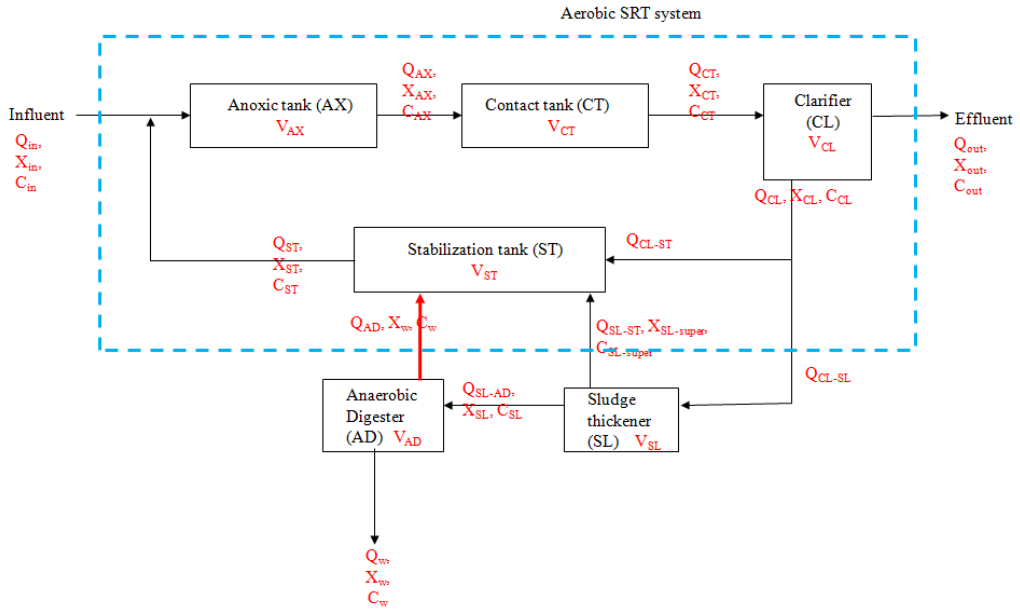

Figure 3.1. Schematic of the system boundary (bordered in the dashed blue line) used for aerobic SRT calculations. The conventional system is represented without the AD recycle stream (represented in red).

SWT considers the anaerobic digester SRT differently than stated in Eqn. 40. SWT treats the AD as a chemostat, as highlighted in Figure 3.2, resulting in the hydraulic and solids retention times being equivalent:

$$\text{AD SRT} = V_{AD}/(Q_{AD} + Q_W) \tag{41}$$

This also may be misleading for the ADs in the hybrid process, since the sludge recycled to the stabilization tank eventually reenters the AD. If some of the anaerobic biomass retains its activity and is returned to the AD, then its SRT would be larger than that computed by Eqn. 41.

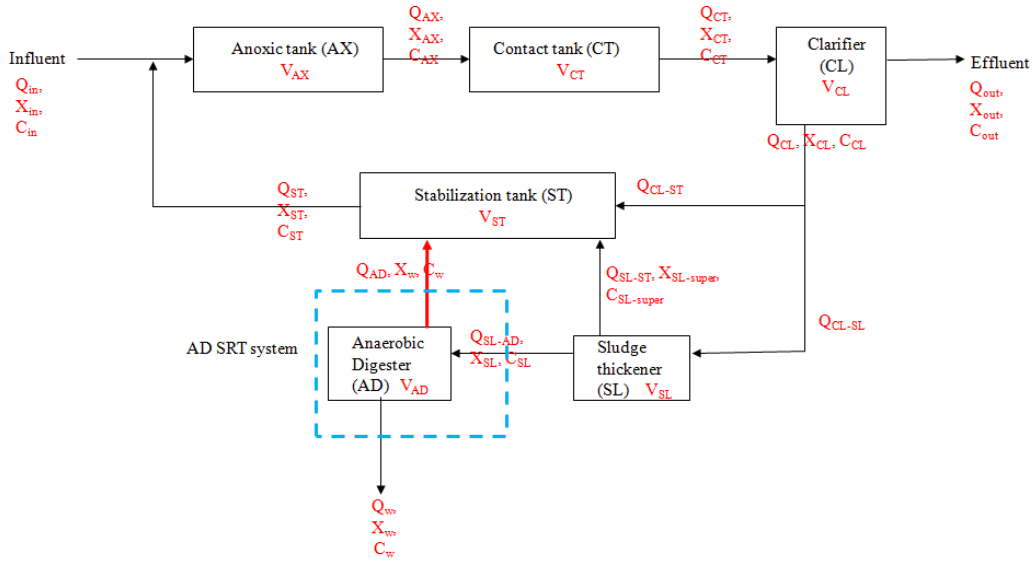

Figure 3.2. Schematic of the system boundary (bordered in the dashed blue line) used for AD SRT calculations. The conventional system is represented without the AD recycle stream (represented in red).

The variations in flow rates due to changes in anaerobic SRTs and RAS rates can significantly affect SRT calculations. With the decrease in anaerobic SRT between phases 9 and 10, the flow rate of WAS did not change, but the flow

rate of sludge from the sludge thickener to the AD increased from 21.6 to 25.9 L/d, while the AD recycle rate increased in the hybrid trains from 18.7 to 23.0 L/d. As the trains transitioned between phases 10 and 11, the RAS was decreased from 120% to 100% of the influent flow rate. This resulted in the WAS flow rate decreasing in the hybrid trains from 64.8 to 54.7 in the hybrid trains, while the conventional train maintained a WAS flow rate of 27.4 L/d.

3.5.2 Aerobic SRTs

While the definition of SRT always is the reciprocal of the growth rate, the methods by which SRTs are calculated can vary significantly depending on the operation and complexity of the process. One method of aerobic SRT calculation takes the approach that the AD recycle should be included, as it can contain a substantial amount of biomass that is active in the aerobic system.. Expanding upon Eqn. 40, the AD recycle is included the denominator by

$$\text{Aerobic SRT} = \frac{V_{AX}TSS_{AX} + V_{CT}TSS_{CT} + V_{CL}TSS_{CL} + V_{ST}TSS_{ST}}{Q_{CL-SL}TSS_{CL-SL} - Q_{AD}TSS_{AD}} \quad (42)$$

Eqn. 42 assumes minimal contribution of solids and active biomass from the sludge thickener supernatant and clarifier effluent.

Eqn. 42 can be expanded to take into account for solids leaving in the clarifier effluent and entering in the thickener supernatant.

$$\text{Aerobic SRT} = \frac{V_{AX}TSS_{AX} + V_{CT}TSS_{CT} + V_{CL}TSS_{CL} + V_{ST}TSS_{ST}}{Q_{out}TSS_{out} + Q_{CL-SL}TSS_{CL-SL} - (Q_{AD}TSS_{AD} + Q_{SL-AD}TSS_{SL-AD})} \quad (43)$$

3.5.2 Anaerobic Digester SRTs

As reviewed in Eqn. 41, SWT treats the AD as a chemostat to obtain a definition of SRT. However, this method ignores that some of the biomass recycled to the stabilization tank may eventually returns to the AD. In the extreme case that all the active biomass from the AD returns to it, the AD SRT becomes:

$$\text{AD SRT} = V_{AD}/Q_W \quad (44)$$

Eqn. 44 should give the maximum boundary of the AD SRT.

The one parameter that makes any AD calculation difficult is that the liquid/solid fill level of the AD is not well known. Most likely the actual liquid volume was less than the nominal volume, which would cause an overestimation the actual AD SRTs. However, the relative trends should be consistent and relatively comparable.

3.5.3 Total System SRTs

SWT does not define a total-system SRT. Since TSS concentrations are known in all tanks and streams, a total-system SRT can be calculated using

$$\text{Total System SRT} = \sum_{\text{i=all tanks}} V_i * TSS_i \, Q_{out} TSS_{out} + Q_W TSS_W \quad (45)$$

which assumes that the process influent does not contain any active biomass. Eqn. 46 can be simplified to exclude solids in the clarifier effluent:

$$\text{Total System SRT} = \frac{\sum_{\text{i=all tanks}} V_i * TSS_i}{Q_W TSS_W} \quad (46)$$

Ultimately, the true system SRT will be lie somewhere in the range of the values calculated here.

4. Results and Discussion

To assist with understanding the hybrid process performance, the conventional and hybrid trains are compared to each other for a variety of criteria for overall system performance and tank-by-tank performance. These criteria are aligned with the goals of the project, including effluent quality, COD and nitrogen compound removals, methane production, and biomass yields. Baseline effluent quality standards for TSS, 5-day biological oxygen demand (BOD_5), and pH are taken from the U.S. EPA's National Pollutant Discharge Elimination System (NPDES) Permit Writers' Manual (2010) standards for secondary wastewater treatment, which are summarized in Table 4.1. The EPA allows for COD to be substituted for BOD_5 measurements in a user's permit when a long-term BOD_5-to-COD correlation can be demonstrated. While BOD_5 standards are not directly applicable to COD, the general minimum removal standards can be expanded for application to COD. Also discussed in the Writers' Manual, the EPA allows states to set their own nutrient removal limits, including nitrogen and phosphorus. For example, Arizona's total nitrogen discharge limits range from 1.2 to 2 mg N/L depending upon body of water discharged to (Arizona Department of Environmental Quality, 2009).

This chapter explores various performance parameters to quantify differences between the two processes. The first section explores the SRTs of the system. The second section discusses COD removal as a function of process type for the overall system, as well as individual tanks. The third section examines the

removal of three key nitrogen compounds: NH_3-N, NO_2-N, and NO_3-N. The fourth section is an in-depth analysis of AD performance. The fifth section discusses biomass yields. The sixth section reviews microbial community analysis (MCA) results. Each of these sections focuses specifically on data from phases 9 through 12, when the trains operated consistently.

Table 4.1. U.S. EPA's secondary wastewater treatment effluent quality standards. Source: U.S. EPA's NPDES Permit Writers' Manual Chapter 5 (2010).

Parameter	**30-day average**	**7-day average**
BOD_5	30 mg/L	45 mg/L
TSS	30 mg/L	45 mg/L
BOD_5 and TSS % removal (concentration basis)	Minimum 85% removal	
pH	6.0 to 9.0	

4.1 System SRTs

4.1.1 Aerobic SRTs

Using actual performance data, aerobic SRTs were calculated for all trains and phases using Eqns. 40, 42, and 43. The results of calculating aerobic SRT by these three methods are summarized in Table 4.2. Calculations of train 1 SRTs in phase 12 neglect biofilm biomass, since it could not be quantified; this causes a systematic underestimation of SRT. Using SWT's method (Eqn. 40), the hybrid trains consistently had a lower SRT than the conventional train and lower than the stated target of 3 days. Train 1's SRTs ranged from 1.7 to 2.6 days, while train 3's SRTs ranged from 1.9 to 2.4 days. Train 2's SRT generally exceeded the stated target of 3 days, ranging from 2.3 days prior to the AD enlargement to 4.6 days in phase 12. It is expected that the conventional train would generally have higher SRTs than the hybrid trains in phases 9 through 12, as the hybrid trains' WAS flow rates were at least two times more than the conventional train's WAS flow rate.

When the SRTs are calculated using Eqn. 42 (which includes the maximum impact of solids input from the AD), the range of operating SRTs in the hybrid trains expanded and were generally larger than for the conventional train. Train 1's SRTs ranged from 2.6 to 7.1 days, while train 3's SRTs ranged from 3.5 to 6.4 days. The conventional train 2 has the same SRTs as calculated from Eqn. 40, since no AD sludge was recycled. When comparing phases 9 and 10 in the hybrid trains, the aerobic SRT increased with the decrease in AD SRT, because

the AD sludge recycle rate increased to the stabilization tank. This increase in AD sludge recycle rate outweighed the effect of any change in TSS concentration in the AD, resulting in lower denominator values in the SRT calculation. The RAS rate decreased from 120 to 100% of the influent flow rate between phases 9 and 11 resulted in a lower absolute WAS flow rate and a decrease in AD sludge recycle rate in all trains. The WAS flow rate decrease was the controlling factor in the SRT calculation for the hybrid trains, resulting in increased SRTs between phases 9 and 11.

Table 4.2. Aerobic SRTs by train and phase

Calculation method	Phase	Stated SRT (d)	Calculated SRT (d)		
			Train 1	Train 2	Train 3
Eqn. 40: SWT's method	9	3	1.7	4.4	1.9
	10	3	2.0	4.3	1.9
	11	3	2.4	3.8	2.4
	12	3	2.6	4.6	2.4
Eqn. 42: Includes AD recycle stream	9	3	2.6	4.4	3.5
	10	3	7.1	4.3	5.0
	11	3	5.2	3.8	6.4
	12	3	4.3	4.6	4.3
Eqn. 43: Includes AD recycle and all effluents	9	3	2.5	4.0	3.2
	10	3	6.2	4.1	4.8
	11	3	4.9	3.6	6.0
	12	3	3.8	4.2	5.8

When calculated using Eqn. 43 (which include AD solids recycle and the loss of solids in the clarifier effluent), the SRT values fall between those obtained by the other two equations. This is as expected, because the denominator must have a value between that of the other two equations.

In summary, the different ways to compute aerobic SRT give distinctly different interpretations. Whereas the SWT approach says that train 2 had the highest SRT, the other methods say that train 2 has the lowest aerobic SRT. However, all of the computed SRTs are relatively low, which suggests that nitrification ought to be minimal, since the slow-growing nitrifiers should be largely washed out.

4.1.2 AD SRTs

Table 4.3 presents the AD SRTs by the different computing methods. When calculated using SWT's method in Eqn. 41, the AD SRTs match the SWT's stated values for each train and phase, with exception of train 1. Calculating SRT using Eqn. 41 represents the lowest potential SRT in the anaerobic digester, as it represents the largest flow rates through the system. However, this calculation method may be underestimating the actual anaerobic SRT since anaerobic biomass that is recycled to the stabilization tank is eventually returned to the AD.

When calculated using Eqn. 44, the conventional train 2's SRTs remain unchanged, because no AD sludge was recycled. Calculation of SRT using Eqn. 44 represents the longest potential anaerobic SRT since it does not include biomass recycled back to the AD as in Eqn. 41. However, AD SRTs increased significantly for the hybrid trains and are well above the SWT's stated SRTs. The differences in the hybrid trains' SRTs follow changes in the wasting sludge rates: the AD SRTs increased with decreases in the wasting sludge rate. The hybrid SRTs were much higher than the stated SRT of 25 or 30 days, depending upon the

phase. The reason for the lack of change using Eqn. 44 is that the wasting sludge rate was constant at 2.9 L/d during the two phases. With the RAS decrease in phase 11, the amount of wasting sludge produced from the hybrid trains doubles and, consequently, in the AD SRTs decrease by about half.

The most significance trend from the AD SRT calculations is that the hybrid trains probably retained solids much longer than the conventional train. The longer SRTs should favor increased hydrolysis of complex organic compounds, and this should lead to more methane generation. Thus, the hybrid trains should demonstrate increased CH_4 production in the phases with the larger SRTs. In addition, these results support the concept that the actual anaerobic SRT experienced by the processes lies somewhere between the values obtained by the two different calculation methods.

Table 4.3. AD SRTs by train and phase

Calculation method	Phase	Stated SRT (d)	Calculated SRT (d)		
			Train 1	Train 2	Train 3
Eqn. 41: All effluent streams	9	30	30	30	30
	10	25	25	25	25
	11	30	30	30	30
	12	30	47	30	30
Eqn. 44: Only wasting sludge in denominator	9	30	220	30	220
	10	25	220	25	220
	11	30	110	30	110
	12	30	110	30	130

4.1.3 Total System SRTs

The total-system SRTs are summarized in Table 4.4. The hybrid trains exhibited longer total-system SRTs, which corresponds with their longer AD

SRTs. This trend should lead to increased methane production and system COD removal. Its impact on N removal is not obvious, as the aerobic SRTs were too low to allow reliable nitrification.

As calculated using Eqn. 45 and 46, train 3 has the longest SRTs, ranging from 130 to 210 days using Eqn. 45 and 150 to 270 days using Eqn. 46. Train 1's SRTs generally were slightly lower than train 3's, ranging from 100 to 190 days using Eqn. 45 and 130 to 270 days using Eqn. 46. Since all of these SRTs are long and dominated by the AD SRT, trains 1 and 3 should have had generally similar performance. However, train 2's SRTs were significantly lower, ranging from 34 to 39 days using Eqn. 45 and 36 to 42 days using Eqn. 46. This much-smaller SRT was dominated by the small SRT for the AD and may be reflected in reduced overall methane production and total COD removal.

Table 4.4. Total system SRTs by train and phase

Calculation method	Phase	Calculated SRT (d)		
		Train 1	Train 2	Train 3
Eqn. 45: All liquid effluent streams	9	190	37	160
	10	190	34	210
	11	110	39	210
	12	100	36	130
Eqn. 46: Wasting sludge stream only	9	270	42	270
	10	250	36	260
	11	130	42	260
	12	130	41	150

4.2 COD Removal

4.2.1 Effluent Quality and Overall System Removal

Average effluent TCOD concentrations (in mg COD/L) are summarized in Figure 4.1 for all trains and phases. No consistent trend between train configuration and effluent concentration is obvious, although the highest effluent COD concentrations are associated with conventional train 2, particularly in phases 9 and 12. As expected, the effluent COD values exceeded the BOD_5 discharge standards by a factor of roughly 2 to 3. However train 1 had an especially low effluent COD in phase 12, which coincided with biofilm media being added to the contact tank.

Table 4.5 summarizes the overall mass changes of COD and overall TCOD removal efficiency in all periods and for all trains. TCOD removal refers to the amount of soluble or solid COD removed from the overall system and is calculated from

$$\%\ \text{TCOD Removal} = \frac{Q_{in}TCOD_{in} - Q_{out}TCOD_{out} - Q_{w}TCOD_{w}}{Q_{in}TCOD_{in}} * 100\% \quad (47)$$

It is important to note that this table accounts for COD removal from the liquid and solid phases from the clarifier and AD effluents. The table lists the influent and effluent mass loading rates in grams per day for TCOD, SCOD, PCOD, and error COD. Input and output TCOD and VSS loading values were generally available from measurements at the pilot plant. Complete system SCOD measurements were unavailable for all phases; for these situations, SCOD was

calculated from the difference in TCOD and PCOD values. PCOD was calculated by multiplying the VSS loading rate by a conversion factor, 1.42 g COD/g VSS (Rittmann & McCarty, 2001). Unlike SCOD, which was back calculated from TCOD and VSS for some phases, and PCOD, which was based on a conversion factor, TCOD was directly measured, which means that it is not subject to errors from assumptions or conversion factors.

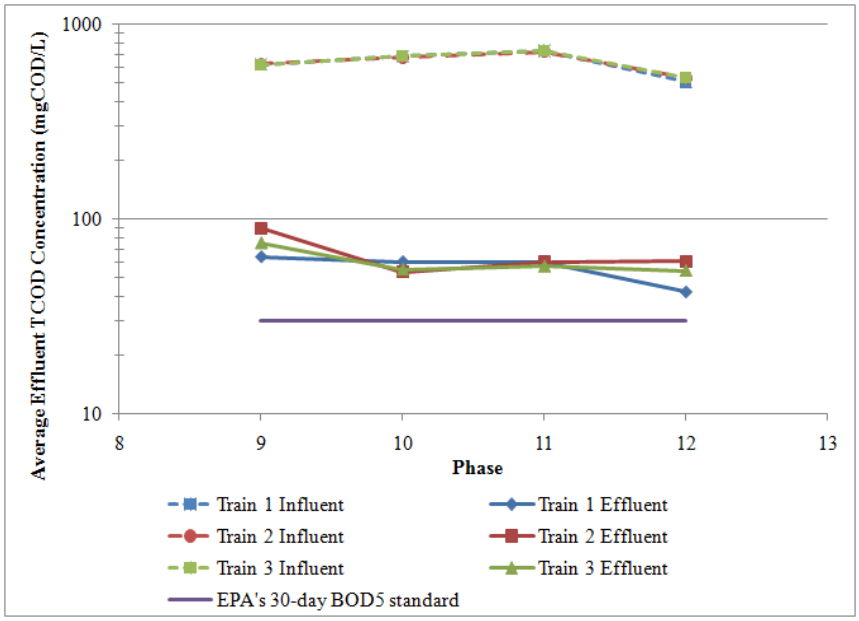

Figure 4.1. Influent and effluent TCOD concentrations in mg COD/L for all trains and phases, excluding phases with three or fewer data points. EPA BOD_5 standard source: U.S. Environmental Protection Agency NPDES Writers' Permit 2010.

The hybrid trains consistently removed a higher percentage of TCOD than the conventional train. Since transitioning to hybrid operation, the hybrid trains' TCOD removals ranged from 71-88% for train 1 and 72-86% for train 3 in phases 7 through 11. During that same time frame, train 2's TCOD removals ranged

from 49-60%. These trends suggest that anaerobic sludge recycling in the hybrid systems benefited COD removal, since TCOD and PCOD removals increased in absolute terms and as percentages. The reason for train 2's markedly poor performance cannot be determined from the overall mass balances alone.

The hybrid trains demonstrated little change in performance with variations in SRT and RAS, as demonstrated in Figure 4.2. During phases 9 and 10, the AD SRTs (as supplied by SWT) decreased from 30 to 25 days by diverting 4.3 L/d more sludge from the sludge thickener to the AD. The WAS rate remained constant between phases. With the SRT decrease, the hybrid trains demonstrated little change in the TCOD removal from the effluent streams: train 1's TCOD removal increased from 81 to 83%, and train 3's TCOD removal decreased from 83 to 82%. Conventional train 2's TCOD removal increased from 48 to 52%.

A comparison of phases 9 and 11 demonstrates the effects of a decrease in percent RAS from 120 to 100% of the influent flow rate. With this decrease, the WAS rate was maintained at 8.2% in the hybrid trains, but increased to 3.6 to 4.3% in the conventional train. The flow rate from the sludge thickener to the AD remained constant at 21.6 L/d in all trains. Variations in RAS affect the amount of dilution in the RAS and WAS streams (Rittmann & McCarty, 2001): increasing the RAS flow rate lowered the solids concentration of the RAS and WAS. This trend is supported by conventional train 2's TCOD removal from the liquid and solid phases, which increased from 49 to 60% with the decrease in

RAS. The decrease in RAS resulted in a more concentrated WAS stream being transported to the AD and increased conversion of influent COD to methane (detailed in an upcoming section). With the decrease in RAS rate, hybrid trains 1 and 3 experienced a decrease in TCOD removal in the solid and liquid phases from 81 to 74% and 83 to 72%, respectively. This decrease in removal was a combined effect of increased sludge wasting (from 2.9 to 5.9 L/d) from the AD and a decrease (from 18.7 to 15.8 L/d) in the AD sludge recycle to the stabilization tank.

Phase 12 demonstrated decreased COD removal efficiency from all trains from phase 11. However, the type of hybrid train configuration did not significantly affect TCOD removal. The modified hybrid layout in train 1 demonstrated the highest TCOD removal, 71% of the influent TCOD removed from the effluent streams. Hybrid train 3 removed 68% of the influent TCOD. Conventional train 2 had significantly lower TCOD removal than the hybrid trains at 52%. The key lesson from this phase is that the modification to train 1 to improve denitrification did not affect the efficacy of overall TCOD removal when compared to the other hybrid train.

Table 4.5. Overall mass flows (g/d) and percent removals of COD components in the liquid and solid phases throughout the three trains. Highlighted light gray phase are the hybrid operation, dark gray is modified hybrid operations, and all others are conventional operation.

		Input loading (g/day)				Output loading (g/day)			Removal ratio (%)
	Period	TCOD[I]	SCOD[II]	PCOD[III]	Error[IV]	TCOD[V]	SCOD+Error[VI]	PCOD[VII]	TCOD[VIII]
Train 1	2	310	70	210	26	91	27	64	71
	4	360	96	260	13	87	16	71	76
	5	420	87	270	61	80	18	62	81
	6	390	59	280	50	58	12	46	86
	7	430	98	310	19	58	14	43	88
	9	390	64	380	-50	74	27	150	81
	10	420	47	360	11	71	26	52	83
	11	440	49	370	29	120	22	57	74
	12	370	42	330	-2	110	19	71	71
Train 2	2	210	110	100	1	200	-	-	46
	3	380	63	270	-44	120	48	71	68
	4	340	94	250	3	79	21	58	77
	5	420	87	270	-61	88	20	68	79
	6	430	61	290	-75	220	-44	260	49
	7	400	97	310	-8	200	32	170	50
	9	370	63	390	-77	190	29	283	49
	10	410	47	350	9	200	27	174	52
	11	440	49	380	15	170	23	151	60
	12	370	43	320	8	180	21	160	52

- I, II, V and VII are directly calculated with experimental data. III=1.42×VSS, IV=I-(II+III), VI=V-VII, VIII=(I-V)/I×100

Table 4.5 continued. Overall mass flows (g/d) and percent removals of COD components in the liquid and solid phases throughout the three trains. Highlighted light gray phase are the hybrid operation, dark gray is modified hybrid operations, and all others are conventional operation.

		Input loading (g/day)				Output loading (g/day)			Removal ratio (%)
	Period	$TCOD^{I}$	$SCOD^{II}$	$PCOD^{III}$	Error	$TCOD^{V}$	SCOD+Error	$PCOD^{VII}$	$TCOD^{VIII}$
Train 3	2	310	61	210	36	120	40	79	62
	4	380	91	260	30	86	24	62	77
	5	350	110	270	-23	100	30	75	70
	6	440	59	290	90	61	24	37	86
	7	410	100	320	-21	70	22	48	83
	9	380	64	270	46	66	30	46	83
	10	420	47	360	11	76	26	57	82
	11	440	49	340	58	120	23	57	72
	12	370	43	320	8	120	20	87	68

- I, II, V and VII are directly calculated with experimental data. III=1.42×VSS, IV=I-(II+III), VI=V-VII, VIII=(I-V)/I×100

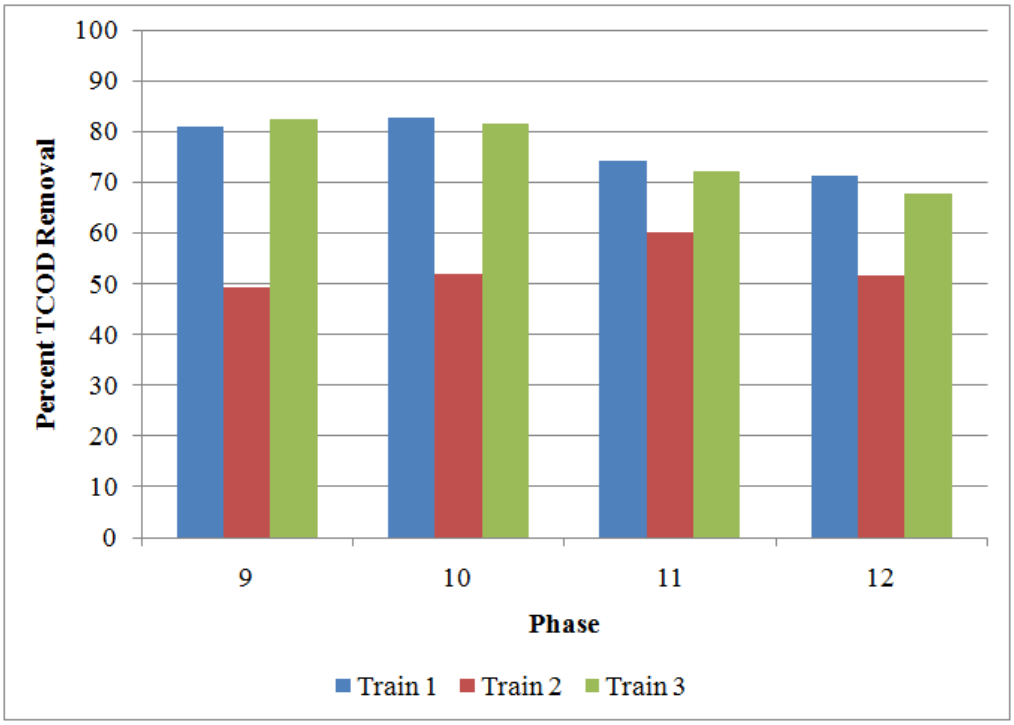

Figure 4.2. Percent overall system TCOD removal in the liquid and solid phases by phase beginning with phase 9 (excluding methane production).

4.2.2 COD Removal Trends by Tank

Table 4.6 summarizes COD removal by tank beginning with phase 9 for all trains. Positive values representing COD consumption, while negative values represent production.

As a confirmation of measurement and flow-rate consistency across the system, the individual mass consumptions are compared by tank to the total liquid/solid phase COD removed from each train. When the individual tank consumptions are added together for a train, the total should be equivalent to the TCOD removed from the entire system. The amount of COD consumed per tank is summarized in Table 4.6, as well as the amount of COD converted to methane

(which is covered in the AD section). An "accuracy" ratio was computed from the following equation:

$$\text{Accuracy ratio} = \frac{\sum \text{COD consumption from all tanks} + \text{COD converted to methane}}{\text{Overall system TCOD consumption}} \quad (48)$$

with the ideal being a value of one. The accuracy ratio can exceed one if the total of each tank's consumption exceeds the total COD removed from the system. This might be possible if COD were produced somewhere in the system. One way to have this occur is through autotrophic reactions, such as nitrification.

As illustrated in Figure 4.3, the individual tank measurements deviate significantly from the overall COD removal from the system. Measurements from the hybrid trains generally overestimate the amount of COD removed internally: train 1's accuracy ratios ranged from 1.0 to 1.6, while train 3's were 1.1 to 2.1. Train 2's ratios spanned from 0.7 to 1.4. Further inspection finds a systematic trend to the deviations throughout the process. In the aerobic sections of the process, i.e., the anoxic tank, contact tank, stabilization tank, and clarifier, the variations were likely associated with the internal flow rate inconsistencies in the reported RAS flow rate. The anaerobic tank also experienced inconsistencies that probably are rooted in assumptions of the tank's volume. Without accurate level controls, it is impossible to quantify the volume of sludge in the AD, leading to the assumption that the tank volume was full of sludge.

Table 4.6a. COD removals by tank and component for (a) train 1, (b) train 2, and (c) train 3 and phases 7 through 11. Negative values represent production while positive values represent consumption. The "SCOD+Error" column is calculated from TCOD-PCOD. Other SCOD values are from experimental data. The highlighted values were calculated by subtracting PCOD values from TCOD values.

	Units: g/d		Anoxic Tank (AX)	Contact Tank (CT)	Clarifier (CL)	Stabilization Tank (ST)	Sludge Thickener (SL)	Anaerobic Digester (AD)
Train 1	Phase 7	TCOD	110				160	20
		SCOD+Error	60	10	110		-50	-110
		PCOD	0	-510	-930	1370	210	90
	Phase 9	TCOD	-60	-180	-590	870	160	230
		SCOD	30	10	-10	10	0	0
		PCOD	-110	-260	-500	850	170	50
	Phase 10	TCOD	-17	-230	200	270	36	16
		SCOD	20	9	-4	1	-1	-2
		PCOD	300	-430	590	-250	-3	80
	Phase 11	TCOD	-510	-220	44	880	42	81
		SCOD	20	-6	8	6	-1	0
		PCOD	-1100	-290	1060	470	45	79
	Phase 12	TCOD	-1800	1510	530	NA	-30	30
		SCOD	18	11	-6	NA	0	-1
		PCOD	-1440	1040	540	NA	10	140

Table 4.6b continued. COD removals by tank and component for (a) train 1, (b) train 2, and (c) train 3 and phases 7 through 11. Negative values represent production while positive values represent consumption. The "SCOD+Error" column is calculated from TCOD-PCOD. Other SCOD values are from experimental data. The highlighted values were calculated by subtracting PCOD values from TCOD values.

	Units: g/d		Anoxic Tank (AX)	Contact Tank (CT)	Clarifier (CL)	Stabilization Tank (ST)	Sludge Thickener (SL)	Anaerobic Digester (AD)
Train 2	Phase 7	TCOD	-50				350	150
		SCOD+Error	40	20	-100		50	50
		PCOD	450	-790	-270	600	300	100
	Phase 9	TCOD	-280	320	-670	720	-70	130
		SCOD	20	20	-10	10	0	0
		PCOD	-690	940	-780	540	-60	130
	Phase 10	TCOD	-646	175	-144	793	-124	154
		SCOD	17	5	-8	8	-1	0
		PCOD	-1299	581	399	502	-105	119
	Phase 11	TCOD	-254	-226	-135	849	-81	21
		SCOD	18	4	0	5	-1	0
		PCOD	-98	-465	877	-129	-41	65
	Phase 12	TCOD	140	-346	510	-140	-42	90
		SCOD	15	-2	2	3	0	0
		PCOD	560	-1030	870	-255	-88	130

Table 4.6c continued. COD removals by tank and component for (a) train 1, (b) train 2, and (c) train 3 and phases 7 through 11. Negative values represent production while positive values represent consumption. The "SCOD+Error" column is calculated from TCOD-PCOD. Other SCOD values are from experimental data. The highlighted values were calculated by subtracting PCOD values from TCOD values.

	Units: g/d		Anoxic Tank (AX)	Contact Tank (CT)	Clarifier (CL)	Stabilization Tank (ST)	Sludge Thickener (SL)	Anaerobic Digester (AD)
Train 3	Phase 7	TCOD	120				130	210
		SCOD+Error	60	10	-10		10	60
		PCOD	-600	-60	100	610	150	140
	Phase 9	TCOD	20	-200	-460	720	320	180
		SCOD	30	0	0	10	0	0
		PCOD	-1770	1550	-280	530	60	90
	Phase 10	TCOD	-1059	437	-99	876	108	36
		SCOD	22	6	-6	3	-1	-4
		PCOD	-2561	1306	670	692	102	58
	Phase 11	TCOD	-641	80	61	730	25	66
		SCOD	22	3	-1	5	-1	0
		PCOD	-1125	-196	1456	44	-11	114
	Phase 12	TCOD	-860	270	1170	-420	-3	64
		SCOD	18	2	1	3	1	-3
		PCOD	-1260	110	1850	-560	-40	70

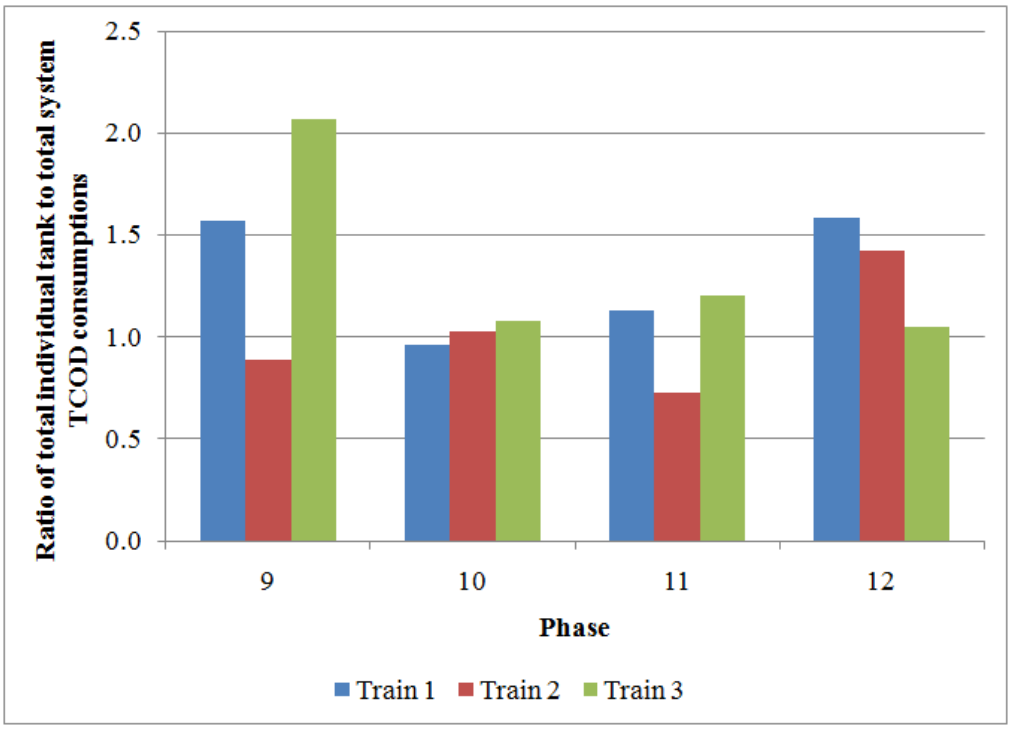

Figure 4.3: Ratio of the sum of the TCOD consumed in all individual tanks versus the overall consumption based on system influent and effluents.

Figure 4.4 illustrates TCOD and PCOD consumption rates by tank and phase. Again, positive values represent COD consumption in the tank, while negative values represent COD production. An unusual trend is that the anoxic tank, contact tank, clarifier, and stabilization tank have COD consumption or production rates that exceed the overall amount of COD consumed in the system. The law of conservation of mass states that the COD consumed cannot exceed the COD than being transported into the system at steady state. This discrepancy further supports the concept that some reported internal flow rates were not accurate. The smaller inconsistencies for the entire system (Fig. 4.3), compared

with inconsistencies for the single tanks, support the concept that the mass-balance problems probably were due to inaccuracies in internal flow rates for the aerobic part and assumptions around the AD's volume. While these inconsistencies mean that the absolute values for individual tanks cannot be taken as correct, trends among tanks and phases probably are representative.

In the anoxic tank, all three trains demonstrated some SCOD consumption, but TCOD and PCOD production rates were high. The higher levels of PCOD production than TCOD production support that biomass growth and biosorption were occurring in the anoxic tank. The strongest case for biosorption in the anoxic tank is displayed during phase 9 of train 3. An indicator of biosorption is a low rate of TCOD consumption or production in a tank associated with substantial PCOD production. This PCOD production should be the result of SCOD being transferred to the solid phase by biosorption. During phase 9, train 3 demonstrated a low ratio of 0.04 grams TCOD per day consumed to grams influent TCOD per day, while 4.3 times more PCOD were formed versus influent TCOD.

TCOD and PCOD consumptions dramatically changed in the anoxic tank with the reconfiguration of train 1 in phase 12. This was the first phase in which TCOD production outpaced PCOD production in the anoxic tank. For comparison, train 3 produced 1.5 times more PCOD than TCOD in this same phase. Thus, train 3's hybrid configuration appears to favor PCOD formation more than train 1's modified hybrid configuration.

Contact tank trends, illustrated in Figure 4.4b, were less consistent than those demonstrated in the anoxic tank, but train 1 displayed evidence of biosorption by consistently producing PCOD. However, trains 2 and 3 did not exhibit consistent PCOD and TCOD consumption or production. TCOD and PCOD consumptions in phases 10 and 11 can be indicators of two different phenomena: biosorbed COD in the anoxic tank being utilized as substrate in the contact tank or further evidence of internal flow rate inconsistencies in the aerobic section of the processes. To the degree that the first phenomena was true, COD oxidation was defeating the purpose of biosorption. However, TCOD and PCOD consumptions in phases 10 and 11 were about the same as the amount of TCOD production in the anoxic tank during these same phases. This further supports that inaccuracies in the internal flow rates resulted in mass balance inaccuracies between the anoxic and contact tanks.

During phase 12, train 1 demonstrated higher TCOD consumption than in any other phase or train. This is a strong indicator of aerobic biodegradation of COD when nitrification is accentuated in the contact tank. Train 3 also consumed PCOD, but at a ratio 11% of that in train 1. These data support the concept that train 1's modified hybrid configuration was much less favorable for net biosorption than for aerobic biodegradation.

Settlers are often modeled as having minimal substrate utilization (Rittmann & McCarty, 2001; Metcalf & Eddy, 2003). However, the clarifier performance in all trains, illustrated in Figure 4.4c, demonstrates either large

production or consumption of TCOD and PCOD. COD trends in the later phases seem to indicate that cellular maintenance was the dominant mechanism in the clarifier. However, such large levels of production or consumption are not consistent with behaviors generally exhibited in industry (Metcalf & Eddy, 2003). Thus, the extremes exhibited in the levels of COD production and consumption are additional support for the concept of internal flow rate inaccuracies.

As seen in Figure 4.4d, the stabilization tank consistently demonstrated the highest levels of COD consumption for all trains and phases. This trend indicates that aerobic biodegradation was the dominant mechanism in the stabilization tank. Furthermore, the hybrid trains exhibited higher levels of TCOD and PCOD consumption than the conventional train. This seems to indicate that a large fraction of the COD was consumed aerobically in the stabilization tank, rather than being converted to methane or being consumed during denitrification. The methane trend is confirmed in a later section.

COD trends are unusual in the sludge thickener. Again, theory regards the thickener as a settler with little COD reactivity. While the hybrid trains demonstrated low levels of COD consumption across all phases, the conventional train demonstrated noticeable TCOD and PCOD production in phases 9-11. This suggests errors in flow rate or concentrations around the train 2 thickener.

While a more detailed analysis of AD performance is performed in a later section, it is important to note here that TCOD and PCOD consumptions were higher in hybrid trains 1 and 3 than in conventional train 2, as illustrated in Figure

4.4f. The overall consumption of COD in the anaerobic digester was far less than the amount of COD entering in the influent. More importantly, Figure 4.5 illustrates that the amount of COD consumed in the AD was much lower than the amount consumed in the stabilization tank for each phases and train. This supports that most of the COD was being oxidized aerobically, which defeated the goal of stabilizing as much COD as possible via methane generation. Decreasing system SRT generally resulted in increasing COD consumption, while decreasing RAS had mixed results between all trains.

(a)

(b)

Figure 4.4. COD consumption or production by tank and phase. (a) Anoxic tank, (b) contact tank, (c) clarifier, (d) stabilization tank, (e) sludge thickener, and (f) AD. Positive values represent consumption, while negative values represent production.

(c)

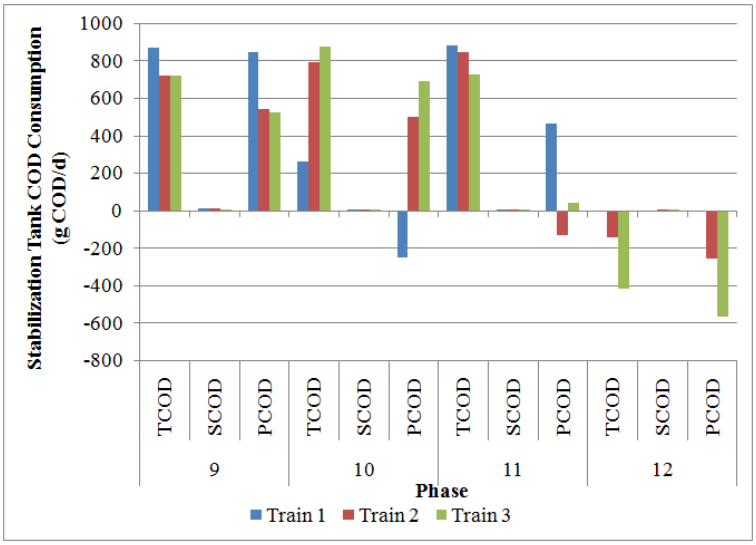

(d)

Figure 4.4 continued. COD consumption or production by tank and phase. (a) Anoxic tank, (b) contact tank, (c) clarifier, (d) stabilization tank, (e) sludge thickener, and (f) AD. Positive values represent consumption, while negative values represent production.

(e)

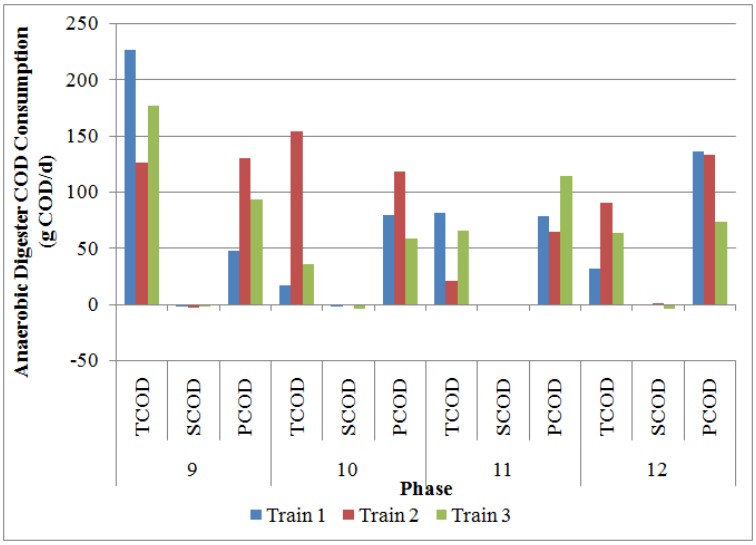

(f)

Figure 4.4 continued. COD consumption or production by tank and phase. (a) Anoxic tank, (b) contact tank, (c) clarifier, (d) stabilization tank, (e) sludge thickener, and (f) AD. Positive values represent consumption, while negative values represent production.

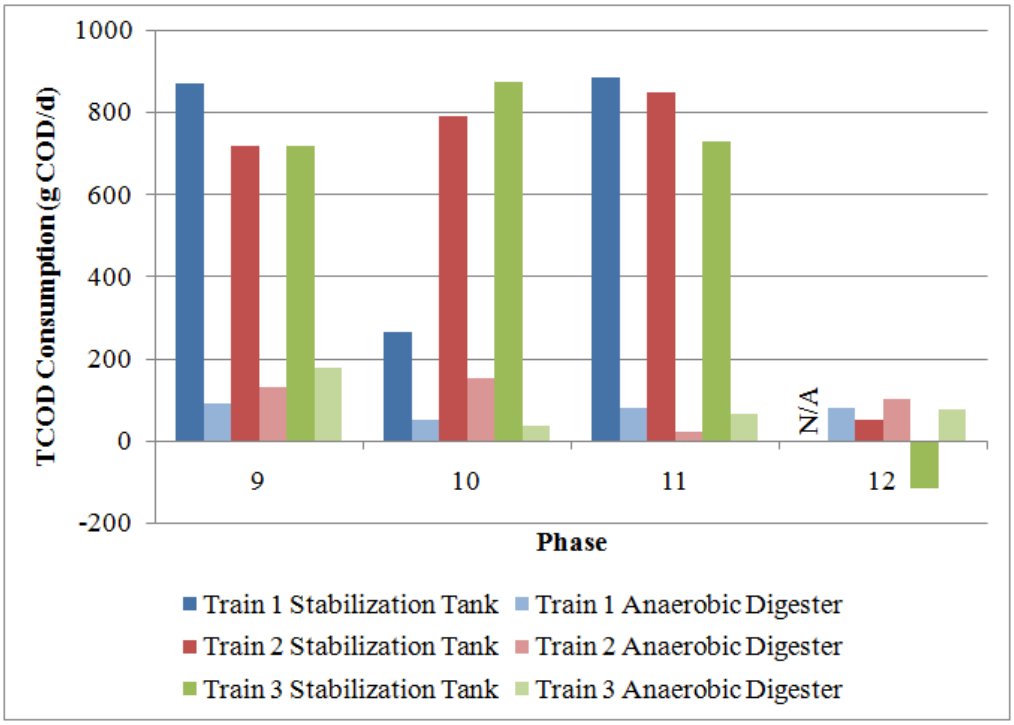

Figure 4.5. Comparison of stabilization tank and AD TCOD consumptions. Positive values represent consumption, while negative values represent production.

4.2.3 COD Removal Summary Highlights

The hybrid trains exhibited higher total-system COD removals than the conventional train. The production of PCOD and TCOD in the anoxic tank suggests that anoxic conditions were suitable for biosorption. On the other hand, the contact tank did not consistently exhibit PCOD removals that support biosorption; instead, microorganisms in the contact tank appeared to utilize COD biosorbed in the anoxic tank. The highest levels of COD consumption occurred in the stabilization tank, which limited the amount of COD that could be transferred to the AD for methane generation. While a more-detailed analysis of AD

performance will be performed in a later section, TCOD and PCOD removals show that more COD was being removed in the hybrid versus conventional ADs. This supports the concept that more COD was transferred to the AD with the hybrid strategy. However, COD removal in the AD consistently was much less than in the stabilization tank.

4.3 Inorganic Nitrogen Removal

4.3.1 Effluent Quality and Overall System Removal

Table 4.7 illustrates the overall mass changes of inorganic nitrogen compounds for phases 9 through 12 for all trains. Train 1's process configuration was modified in phase 12 with the purpose of increasing nitrification and denitrification. Figure 4.6 illustrates effluent concentrations of the inorganic-nitrogen species and total nitrogen. The table lists the input and output loading rates for NH_3-N, NO_2-N, and NO_3-N in grams per day, as well as the removal efficiency for each compound and total nitrogen, when possible to calculate. It is impossible to complete an overall mass balance on NO_3-N and NO_2-N, since data are unavailable for all sludge streams after phase 6. Because of this lack of data, it also is impossible to determine total nitrogen removal from the trains. Furthermore, TKN has been omitted from this analysis, since data were not consistently available during the course of this project. Even though each train received the same influent, the influent loading rates varied slightly from train to train due to small variations in phase duration.

As presented in Table 4.7, a majority of influent nitrogen was present as NH_3-N, with the concentrations ranging from 14.7 to 17.5 mg NH_3-N/L. Trace amounts of NO_3-N (0.1 mg NO_3-N/L) were measured throughout the project. NO_2-N was not detected in the influent.

NH_3-N dominated the effluent nitrogen loading, but NO_3-N and NO_2-N were present in the effluent at higher concentrations than they are present in the

influent. During phases 6 to 11, all trains exhibited a reduction in the NH_3-N between the influent and effluent, while the NO_2-N and NO_3-N concentrations increased. Train 1's effluent concentrations ranged from 9.0 to 17.2 mg NH_3-N/L, 0.6 to 1.1 mg NO_2-N/L, and 1.4 to 2.9 mg NO_3-N/L. During that same timeframe, train 2's effluent nitrogen concentrations ranged from 8.1 to 13.2 mg NH_3-N/L, 0.2 to 1.0 mg NO_2-N/L. and 0.9 to 2.8 mg NO_3-N/L. Train 3's effluent nitrogen concentrations range from 9.7 to 19.6 mg NH_3-N/L, 0.4 to 1.0 mg NO_2-N/L, and 1.0 to 4.2 mg NO_3-N/L. The presence of NO_3^- and NO_2^- in the effluent indicates that some nitrification was occurring. However, the extent of the nitrification clearly was limited, since the effluent still contained a high concentration of NH_3. Poor nitrification is consistent with the relatively low values of aerobic SRT (Table 4.2).

Nitrogen discharge rates improved significantly with the change in train 1's configuration in phase 12. When train 1 transitioned to the modified hybrid configuration, the NH_3-N effluent concentration decreased to 3.1 mg NH_3-N/L, while trains 2 and 3 maintained higher effluent concentrations of 9.2 and 19.6 mg NH_3-N/L, respectively. NO_2-N and NO_3-N data are unavailable for this phase. The clear increase in nitrification supports that adding biofilm carrier improved retention of nitrifying bacteria by increasing the aerobic SRT, as was discussed in section 4.1.1. However, additional NO_2-N and NO_3-N data are required to truly quantify the benefits of adding the biofilm carrier.

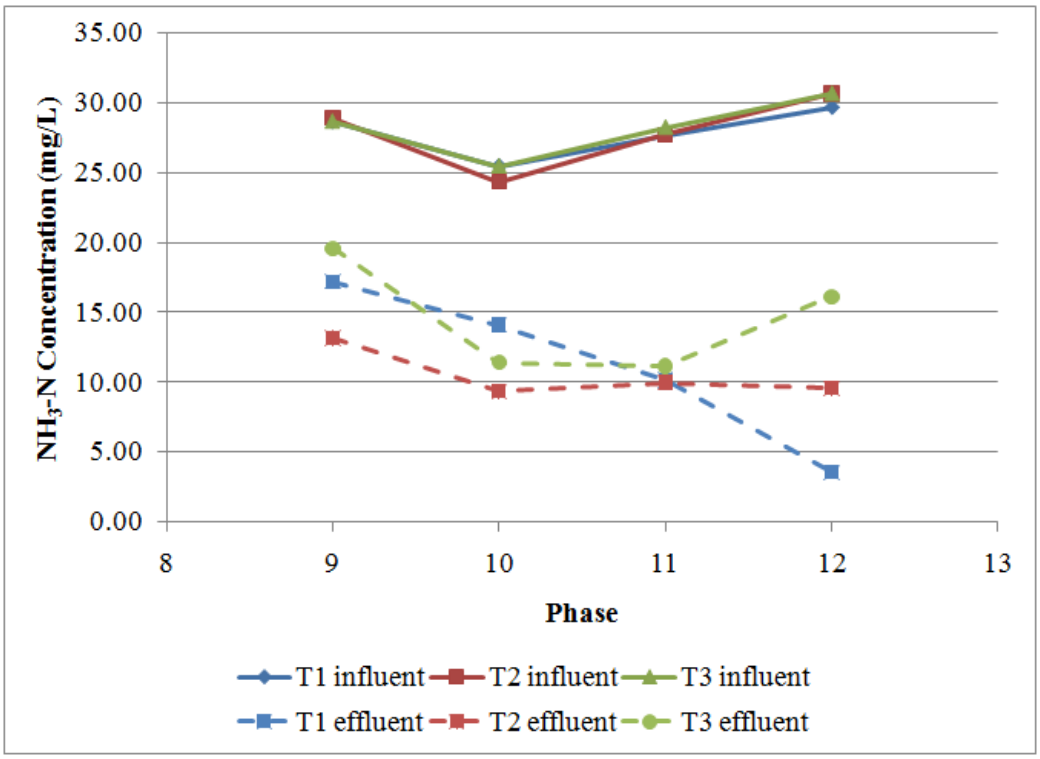

Figure 4.6. Effluent nitrogen concentrations by phase and train.

Table 4.7. Overall mass flows in g/d and percent removals of nitrogen components in the liquid phase throughout the three trains. Highlighted gray phase represents the transition to the modified hybrid process.

	Period	Input loading (g/d)				Output loading (g/d)				Removal ratio (%)	
		NH_3-N	NO_2-N	NO_3-N	TN	NH_3-N	NO_2-N	NO_3-N	TN	NH_3-N	TN
Train 1	9	17.3	0.0	NA	17.3	10.9	NA	NA	-	37	-
	10	15.4	0.0	0.1	15.5	9.2	NA	NA	-	40	-
	11	16.7	0.0	0.1	16.8	6.6	NA	NA	-	61	-
	12	17.9	0.0	0.2	18.1	4.3	NA	NA	-	86	
Train 2	9	17.3	0.0	0.1	17.4	11.3	0.2	1.0	12.4	35	29
	10	14.7	0.0	0.1	14.8	9.7	NA	NA	NA	34	-
	11	16.8	0.0	0.1	16.9	9.1	NA	NA	NA	46	-
	12	18.5	0.0	0.2	18.7	9.1	NA	NA	NA	51	-
Train 3	9	17.2	0.0	0.1	17.3	12.5	0.3	0.8	13.6	28	20
	10	15.4	0.0	0.1	15.5	7.5	NA	NA	-	52	-
	11	17.1	0.0	0.1	17.2	7.5	NA	NA	-	56	-
	12	18.5	0.0	0.2	18.7	10.6	NA	NA	-	43	-

The effluent concentration results for N offer a few insights into process performance. First, none of the trains performed efficient nitrification, as the effluent contained large concentrations of NH_3-N. This is probably due to AOB and NOB being washed out as a result of the low aerobic SRTs, as illustrated in Table 4.2. Second, the lack of good nitrification adversely affected denitrification, since denitrification demands that NO_3^- or NO_2^- be available from the aerobic processes. Third, the conventional train 2 maintained the lowest average nitrogen concentrations -- 10.1 mg NH_3-N/L, 0.4 mg NO_2-N/L, 1.7 mg NO_3-N/L, and 12.2 mgTN/L. Hybrid train 3 discharged lower average concentrations than train 1, with concentrations of 12.7 versus 13.1 mg NH_3-N/L, 0.7 versus 0.8 mg NO_2-N/L, 1.8 versus 2.2 mg NO_3-N/L, and 15.2 versus 16.1 mgTN/L. The better TN removal by the conventional process may have been caused by its higher sludge-wasting rate, as the wasted sludge contains nitrogen. However, the lack of TKN data severely hampers making definitive conclusions about the fate of N.

During phase 12, the modified train 1 achieved the highest levels of NH_3-N removal during the project: 86%, compared to 61% removal in phase 11. Trains 2 and 3 removed 43 to 51% of NH_3-N, respectively, in phase 12. These two trains experienced a decrease in NH_3-N removal efficiency from phase 11, which removed 46% and 56%, respectively. The apparently poor nitrification in train 3 seems inconsistent with the observed increase in COD consumption in the

contact tank (Table 4.6). Again, the lack of TKN data prevents a definitive interpretation.

4.3.2 Inorganic Nitrogen Removal Trends by Tank

As established with the COD data, it is important to determine if there were indicators of flow rate inconsistencies in the nitrogen data. With the limited amount of data available, this analysis could only be performed for nitrogen by comparing the individual mass consumptions by tank to the total NH_3-N removed from each train. When the individual tank consumptions (as reported in Table 4.8) are added together for a train, the total should be equivalent to the total NH_3-N removed from the entire system. Like COD, an "accuracy" ratio for NH_3-N was calculated from the following equation:

$$\text{Accuracy ratio} = \frac{\sum \text{NH}_3 - \text{N consumption from all tanks}}{\text{Overall system NH}_3 - \text{N consumption}} \tag{49}$$

with the ideal being a value of one. The accuracy ratio can exceed one if the total of each tank's consumption exceeds the total NH_3-N removed from the system.

As summarized in Figure 4.7, individual tank NH_3-N consumptions deviated significantly from the overall system NH_3-N removals. Measurements form the hybrid trains generally underestimated the amount of NH_3-N removed internally: train 1's accuracy ratios ranged from 0.7 to 1.1, while train 3's were 0.6 to 1.6. Train 2's ratios overestimated the internal removals, as indicated with ratios ranging from 1.6 to 2.8. Again, further inspection finds a systematic trend to the deviations throughout the process. Like the TCOD results, the sum of the aerobic sections of the process (i.e., the anoxic tank, contact tank, stabilization

tank, and clarifier) represented the largest deviations in accuracy. This further supports that the variations were likely associated with the internal flow rate inconsistencies in the reported RAS flow rate.

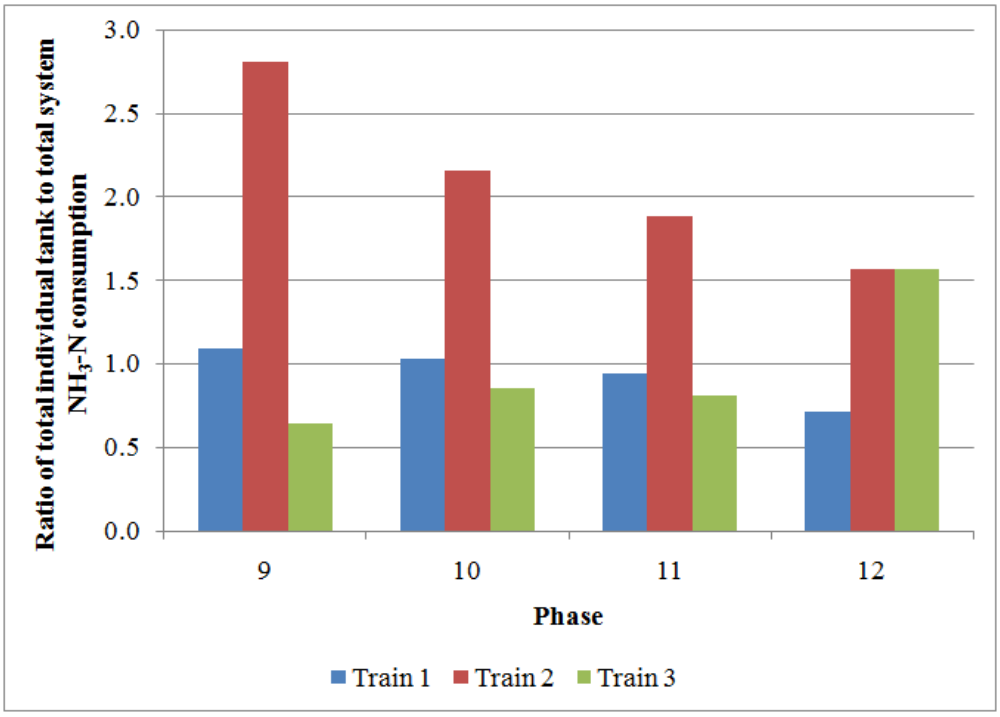

Figure 4.7: Ratio of the sum of the NH_3-N consumed in all individual tanks versus the overall consumption based on system influent and effluents.

Table 4.8 summarizes the removal of nitrogen components (NH_3-N, NO_2-N and NO_3-N) in tanks/components beginning with phase 9 for all trains. Positive values represent nitrogen being consumed, while negative values represent nitrogen production by adsorption or synthesis. While NH_3-N information is available for all tanks, NO_2-N and NO_3-N data were not obtained consistently for sludge streams. This makes it impossible to quantify overall consumption of nitrogen in the stabilization tank, sludge thickener, and AD. All trains perform as

expected from the individual tanks in an activated sludge processes: consumption of NO_2-N and NO_3-N in the anoxic tank; consumption of NH_3-N and production of NO_2-N and NO_3-N in the contact and stabilization tanks, and production of NH_3-N due to biomass decay in the AD.

In the anoxic tank, all trains demonstrated typical denitrification trends, including consumption of NO_2-N and NO_3-N, although NH_3-N also was consumed. During phases 9 to 11, N consumption was higher in the hybrid trains 1 and 3 than in the conventional train 2, indicating that denitrification occurred in the hybrid trains at a higher absolute level than the conventional train. In addition, low residual levels of N were consistent with the intermediate NO_2-N being almost fully utilized to produce nitrogen gas. Without NO_2-N and NO_3-N data available in phase 12, it is difficult to provide conclusive denitrification results between the three process configurations. However, the hybrid trains consumed about the same amount of NH_3-N in their anoxic tanks, while conventional train 2 consumed three times more than the hybrid trains. Phase 12's measurements imply that the removal of the stabilization tank in the modified hybrid process may not have a large effect on the operation of the anoxic tank.

All trains exhibited NH_3-N consumption and NO_2-N and NO_3-N production in the contact tank, as expected in aerobic nitrification processes. Prior to phase 12, no one train presented better nitrification than the others, and no obvious trends were established with variations in SRT and RAS. Train 3, which

had the most consistent hybrid performance, experienced lower absolute values of NH_3-N consumption and NO_2-N and NO_3-N production than the other trains. This indicates that the hybrid process was either not as effective at nitrification as the conventional process or more highly effected by the internal flow rate inconsistencies. Since the efficiency of ammonia removal in the CT of all trains was low, oxygen was likely being diverted to COD oxidation, including COD that had been biosorbed in the AX tank.

Nitrification performance in train 1's contact tank changed dramatically with the train reconfiguration in phase 12, and it was consistent with the overall system performance during that phase. Train 1 exhibited five times more NH_3-N consumption than train 3 and nine times more than train 2. In addition, train 1's NO_3-N production was 25 times higher than train 2's and 100 times higher than train 3's. While flow rate inconsistencies may be a contributing factor, it is likely that the addition of packaging media in train 1's contact tank resulted in improved retention of AOB and NOB in the contact tank and, therefore, increased oxidation of NH_3-N to NO_3-N. Another benefit of this reconfiguration is that this NO_3-N was being recycled directly back to the anoxic tank for denitrification. However, an observed consequence of increased nitrification in the contact tank is that the conditions appeared to divert biosorbed COD to aerobic oxidation. This is supported by increased COD utilization in the contact tank of train 1, as illustrated in Table 4.3. These results underscore a crucial tradeoff between the desires for nitrification and biosorption.

Clarifier trends are inconsistent with phenomena known to occur in the clarifier: the potential for denitrification as the sludge become anoxic and the release of NH_3 due to biomass decay. During phases 9-11, however, the conventional train experienced higher removals of NH_3-N than the hybrid trains: train 2 removed 4.3 to 7.9 g/d of NH_3-N compared with 0.6 to 2.2 g/d in train 1 and -1.5 to 1.0 in train 3. These inconsistencies further support the concept of deviations in internal flow rates, as clarifiers rarely exhibit such high activity (Metcalf & Eddy, 2003). No discernable trends were established with variations in RAS and SRT.

Prior to phase 12, the stabilization tanks of all trains demonstrated 2 to 4 times more NH_3-N consumption than the contact tanks. The better overall nitrogen removal in the hybrid trains appears to have been due to the stabilization tanks in the hybrid trains performing more nitrification than in the conventional train. This behavior also is consistent with higher COD consumption in the stabilization tanks in the hybrid trains versus the conventional train. This further supports the inherent conflict between good nitrification and COD transport to the AD for methanogenesis.

The sludge thickeners and AD of all trains exhibited low levels of NH_3-N production, which was consistent with endogenous decay. While the absolute numbers are low, the AD produced 2-4 times more NH_3-N than the sludge thickener as a result of the longer SRT and increased decay in the tank prior to phase 12. The hybrid trains had 1 to 2 times higher NH_3-N production in the AD

than the conventional train. This may have been caused by the longer AD SRT values with the hybrid trains.

Table 4.8. Nitrogen removals by tank and component for all trains since phase 9. Positive values represent consumption, while negative values represent production.

Units: g/d			Anoxic Tank (AX)	Contact Tank (CT)	Clarifier (CL)	Stabilization Tank (ST)	Sludge Thickener (SL)	Anaerobic Digester (AD)
Train 1	Phase 9	NH_3-N	-1.1	0.5	2.2	10.0	-1.0	-3.7
		NO_2-N	1.4	-0.3	-0.2	-1.3	0.0	N/A
		NO_3-N	3.4	1.7	-0.9	-5.2	0.1	0.0
	Phase 10	NH_3-N	1.4	2.4	0.6	6.7	-0.8	-3.9
		NO_2-N	0.9	-0.5	0.5	N/A	N/A	N/A
		NO_3-N	4.1	-0.1	0.7	N/A	N/A	N/A
	Phase 11	NH_3-N	2.3	3.0	1.1	7.4	-0.6	-4.0
		NO_2-N	0.9	-0.5	0.1	N/A	N/A	N/A
		NO_3-N	5.5	-2.1	1.6	N/A	N/A	N/A
	Phase 12	NH_3-N	1.3	15.7	0.7	N/A (Tank Removed)	-0.6	-7.3
		NO_2-N	N/A	-0.3	0.0		N/A	N/A
		NO_3-N	N/A	-25.9	3.3		N/A	N/A

Table 4.8 continued. Nitrogen removals by tank and component for all trains since phase 9. Positive values represent consumption, while negative values represent production.

Units: g/d			Anoxic Tank (AX)	Contact Tank (CT)	Clarifier (CL)	Stabilization Tank (ST)	Sludge Thickener (SL)	Anaerobic Digester (AD)
Train 2	Phase 9	NH_3-N	-1.7	5.4	7.9	7.9	-0.4	-1.3
		NO_2-N	0.1	-0.3	-0.1	-0.2	0.0	0.0
		NO_3-N	2.7	-0.1	0.9	-4.1	0.0	0.0
	Phase 10	NH_3-N	1.5	3.0	4.3	6.0	-0.3	-3.3
		NO_2-N	0.4	-0.3	-0.3	N/A	N/A	N/A
		NO_3-N	6.3	-1.7	1.5	N/A	N/A	N/A
	Phase 11	NH_3-N	3.4	2.4	7.0	4.9	-0.2	-3.1
		NO_2-N	0.4	-0.1	-0.4	N/A	N/A	N/A
		NO_3-N	4.7	-0.9	0.5	N/A	N/A	N/A
	Phase 12	NH_3-N	4.5	1.7	7.1	4.4	-0.2	-2.7
		NO_2-N	0.2	-0.3	-0.3	N/A	N/A	N/A
		NO_3-N	5.6	-1.2	0.2	N/A	N/A	N/A

Table 4.8 continued. Nitrogen removals by tank and component for all trains since phase 9. Positive values represent consumption, while negative values represent production.

Units: g/d			Anoxic Tank (AX)	Contact Tank (CT)	Clarifier (CL)	Stabilization Tank (ST)	Sludge Thickener (SL)	Anaerobic Digester (AD)
Train 3	Phase 9	NH_3-N	-2.1	2.3	1.0	8.5	-3.4	-3.1
		NO_2-N	0.6	-0.2	0.2	-0.9	0.0	0.0
		NO_3-N	2.1	-0.5	0.2	-2.5	0.1	0.0
	Phase 10	NH_3-N	0.7	3.4	0.8	8.6	-2.3	-4.3
		NO_2-N	1.0	-0.6	0.3	N/A	N/A	N/A
		NO_3-N	6.1	N/A	N/A	N/A	N/A	N/A
	Phase 11	NH_3-N	2.4	2.9	-1.5	9.7	-2.5	-3.6
		NO_2-N	1.1	-0.5	0.2	N/A	N/A	N/A
		NO_3-N	4.4	-0.9	1.0	N/A	N/A	N/A
	Phase 12	NH_3-N	1.3	3.1	1.3	7.1	-1.9	-3.9
		NO_2-N	1.8	-0.5	0.4	N/A	N/A	N/A
		NO_3-N	2.9	0.0	-0.8	N/A	N/A	N/A

4.3.3 Nitrogen Removal Summary Highlights

Prior to phase 11, the hybrid trains exhibited higher levels of nitrogen removal, particularly NH_3-N, than the conventional train. However, all trains exhibited low levels of absolute nitrogen removal in the overall systems. Hybrid trains generally showed greater denitrification in the anoxic tank, nitrification in the aerobic tanks, and NH_3-N production in the AD. The stabilization tank drove the removal of NH_3-N from each train, and the hybrid trains exhibited the higher nitrogen removals versus the conventional train. However, the trend of increased removal in the stabilization tank also coincided with the undesired effect of the increased COD consumption in the stabilization tank of the hybrid trains. In addition, the observed trends are likely affected by variations in internal flow rates in the aerobic section of the trains.

NH_3-N removal increased in train 1 versus the other trains when that train was reconfigured in phase 12. While nitrification appeared to increase, it is impossible to quantify which modification to the train had the largest impact on the performance, since NO_2^-, NO_3^-, and TKN data are missing. In addition, increases in nitrification and COD consumption in train 1's contact tank indicate that COD was being diverted away from biosorption and transfer to the AD.

4.4 Anaerobic Digester Performance

Figure 4.8 summarizes the composition of methane in the biogas from the anaerobic digesters in all trains. All trains produced biogas with about the same percentage of methane, 62 to 67%. This percentage is typical for AD systems and is favorable for efficient conversion of methane to electricity using combustion engines or microturbines (Eastern Research Group, Inc. and Energy and Environmental Analysis, Inc., 2007; U.S. Environmental Protection Agency Combined Heat and Power Partnership, 2008). However, the hybrid trains produced more biogas volume than the conventional train. Consequently, a dramatically higher amount of methane was produced in the hybrid trains than in the conventional train for comparable phases, as illustrated in Figure 4.9. Methane production in hybrid trains range from 47to 72 g COD/d, while the conventional train produces 10 to 21 g COD/d. This equates to the hybrid trains producing 1.5 to 5.5 more methane than the conventional train.

As demonstrated in Table 4.3, the hybrid trains had significantly higher anaerobic digester SRTs than the conventional trains, which should favor increased concentrations of methanogens and increased hydrolysis of complex organic compounds, both of which lead to more methane. Figure 4.10 confirms this trend: SRTs obtained from Eqn. 44 (based on only the effluent flow of wasting sludge from the AD and not sludge recycled to the stabilization tank) generally demonstrated increased methane production with increased AD SRT.

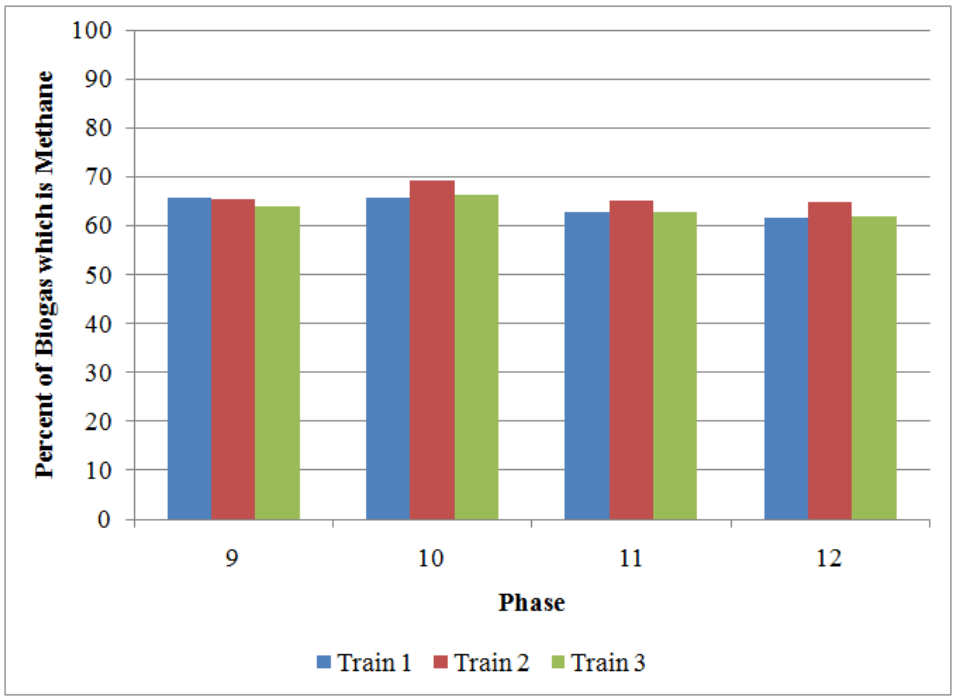

Figure 4.8. Methane composition in biogas by phase and train.

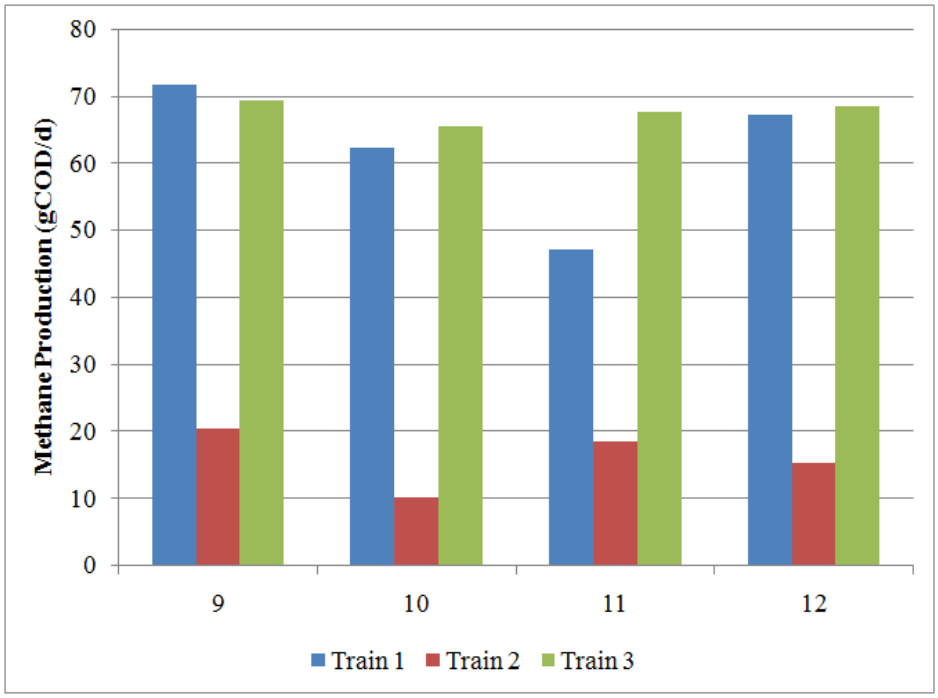

Figure 4.9. Methane production by phase and train.

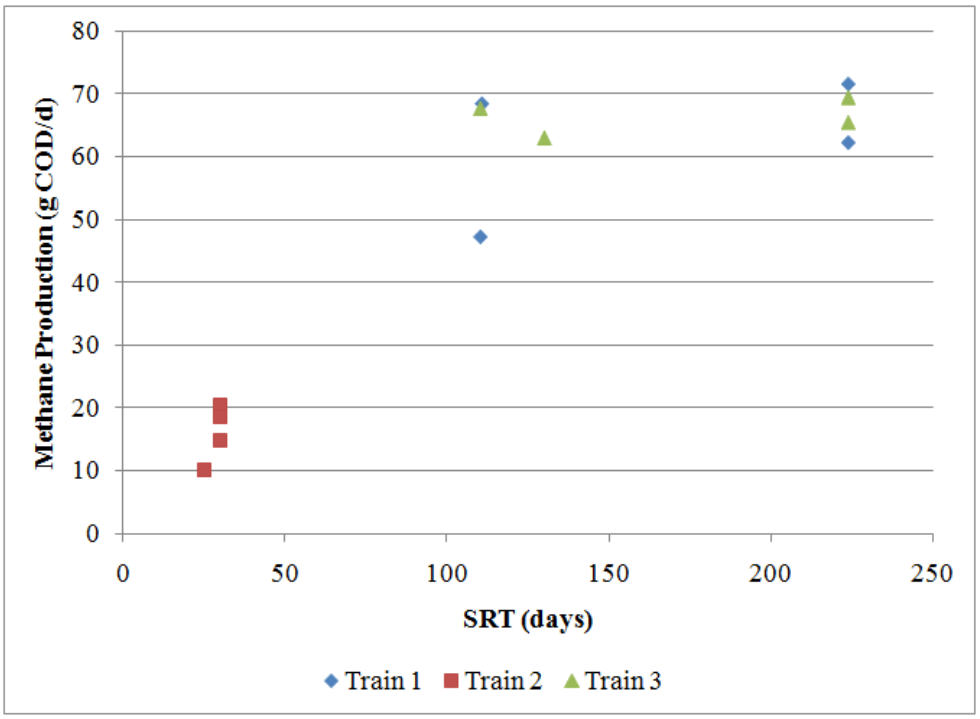

Figure 4.10. Methane production as a function of AD SRT by train for phases 9 through 12. AD SRT was determined using Eqn. 44, in which the production rate takes into account waste sludge from the AD only and does not include sludge recycled to the stabilization tank.

During phase 12, the modified train configuration produced slightly more methane than the other hybrid train 3: train 1's production was 69 g COD/d, while train 3's was 63 g COD/d. This may seem unexpected, as train 1 had lower AD and total system SRTs than train 3, but all SRT values were large. The hybrid trains outperformed the conventional train's methane production, 15 g COD/d in methane. While the modified configuration appears to have improved nitrification, it did not negatively affect the absolute amount of methane produced in the system over the duration of phase 12 (57 days).

One of the objectives of the hybrid system is to transport COD in the influent to the AD for conversion to methane. Figure 4.11 shows the percentage of influent TCOD converted to methane for all trains. The hybrid processes converted 12 to 22% of the influent COD to methane since phase 9. Train 2 converted between 5 and 12% of influent COD to methane. Again, these data support the concept of increased influent COD consumption with increased system and AD SRTs. While the absolute amount of methane produced was not very different, train 1's conversion of influent COD to methane increased dramatically in phase 12, to 41% of the influent COD. This increase supports that more COD was diverted to the AD and not being oxidized in aerobic processes, particularly the stabilization tank, since the stabilization was removed.

While the hybrid train outperformed the conventional train, both process configurations failed to meet the performance estimates in the original project proposal. The original project proposal estimates that 60-65% of the influent TCOD would be utilized in the AD at WAS rates of 6 to 8% of the RAS rate. One reason the original project proposal estimated higher methane production is that proposal's design included one-third of the primary sludge being diverted directly to the AD, as illustrated in Figure 2.4. As discussed earlier, the aeration processes diverted COD away from the AD and reduced the potential conversion of COD to methane.

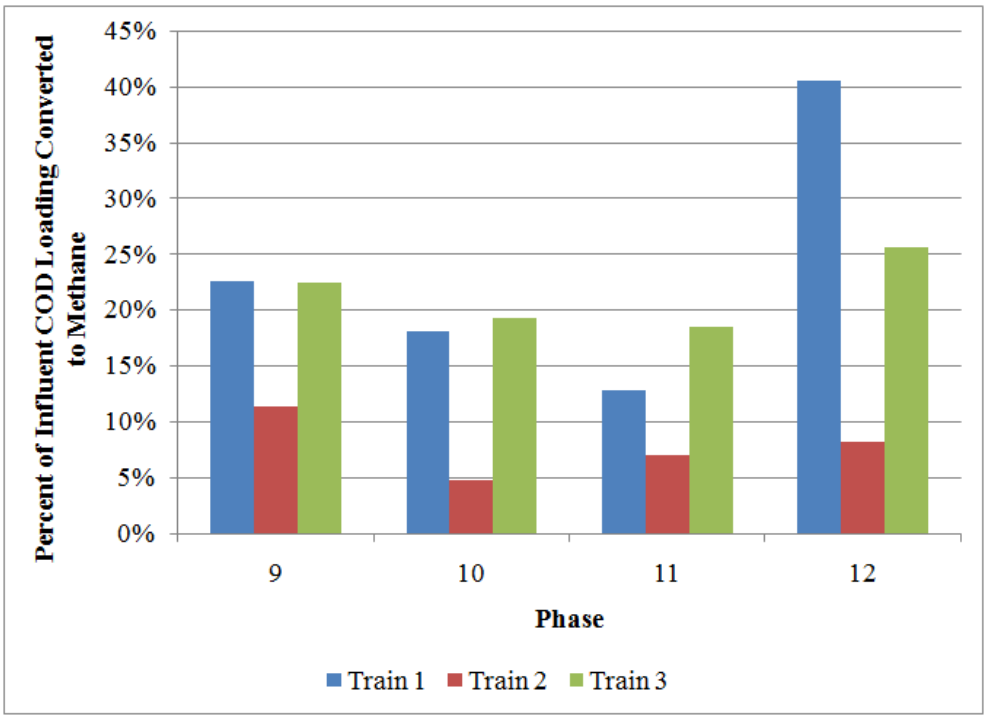

Figure 4.11. Percentage of influent COD converted to methane by train and phase.

4.5 Yield Analysis

Figure 4.12 illustrates the average weighted biomass yields based on VSS measurements by train and phase, as well as the average weighted biomass yield since phase 9. The hybrid trains consistently had lower biomass yield than the conventional train. Train 1's biomass yields ranged from 0.04 to 0.17 g VSS/g COD, and train 3's yields ranged from 0.02 to 0.36 g VSS/g COD. By comparison, train 2's yields ranged from 0.35 to 0.69 g VSS/g COD. The yields in the hybrid trains are consistently lower than the conventional train for two reasons. The hybrid trains experienced longer AD and total system SRTs, which reflects a lower net biomass production rate. Also, the hybrid trains consistently demonstrated higher TCOD removal, which affected the yield calculation by effectively increasing the denominator the hybrid trains versus the conventional train.

Biomass yields also adequately describe how the performance of the trains changes with variations in SRT and RAS. As illustrated in Figures 4.13 and 4.14, biomass yields generally decreased with increasing AD SRT and total system SRT. Increasing AD SRT allowed increased PCOD hydrolysis, which decreased the amount of waste sludge produced by the system. This same conclusion can also be applied with increasing total system SRT, which was largely controlled by the higher retention time in the AD. Decreases in RAS between phases 9 and 11 gave an increase in biomass yield. Again, this directly reflects trends in SRT, since the AD SRTs were essential halved with the decreasing RAS rate.

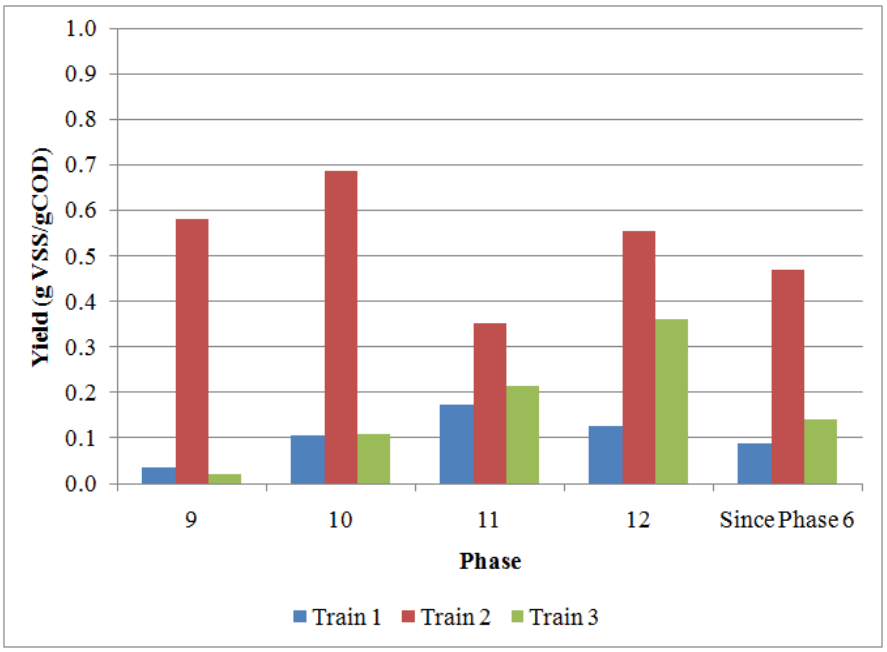

Figure 4.12. Average weighted biomass yields by phase and train since phase 9.

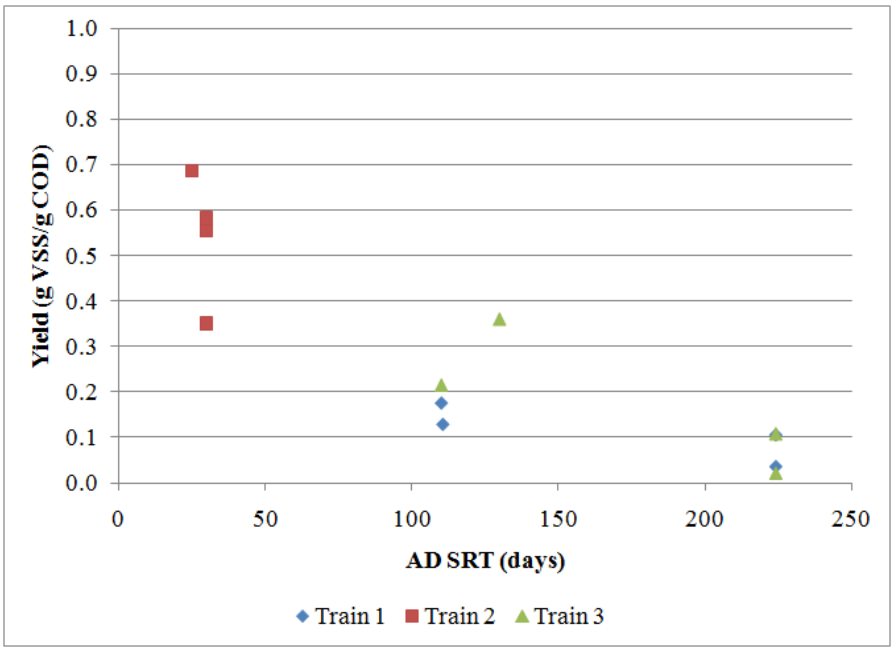

Figure 4.13. Biomass yield as a function of AD SRT. AD SRT was determined using Eqn. 44, in which the production rate takes into account waste sludge from the AD only and does not include sludge recycled to the stabilization tank.

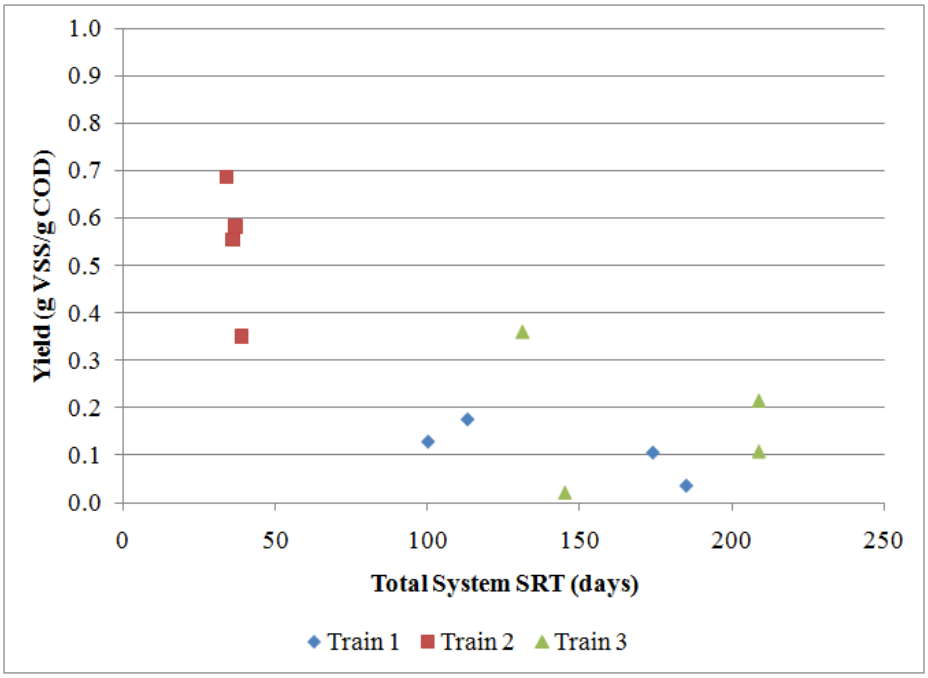

Figure 4.14. Biomass yield as a function of total-system SRT determined using Eqn. 45, in which the production rate biomass removed from the system in the effluent and wasting sludge streams.

4.6 Microbial Community Analysis

4.6.1 Overview of MCA and Sampling Procedures

One of the critical questions in this analysis was to determine the fate of methanogens, AOB, and NOB throughout the hybrid and conventional processes. AD sludge was recycled to the stabilization tank in the hybrid process, where *Archaea* were exposed to aerobic conditions. *Archaea* are considered strictly anaerobic microorganisms, and oxygen exposure may be toxic. If important, O_2 exposure would have dramatically reduced the amount of active *Archaea* eventually cycled back to the AD. A similar issue arises for AOB and NOB: when AOB and NOB were exposed to totally anaerobic conditions in the AD, they definitely were metabolically inactive, and they also may have been killed. In the latter case, active AOB and NOB were not returned to the aerobic system by recycle of AD sludge. Thus, one of ASU's objectives was to determine the fate of *Archaea*, AOB, and NOB in the hybrid and conventional processes using Quantitative Real Time Polymerase Chain Reaction (qPCR) and Terminal Restriction Fragment Length Polymorphism (T-RFLP).

Prior to any sampling, detection methods had to be identified for all *Archaea* and nitrifiers. ASU had extensive experience with detecting and quantifying the different types of methanogens. However, detection and quantifications methods for AOB and NOB had to be developed and tested for this project. Based on literature reviews, we targeted the 16S rRNA gene and distinctive functional genes in AOB and NOB. Using T-RFLP, we were able to

identify the genes targeted for detection: 16S rDNA for *Nitrosomonas* and amoA, which is the functional gene for ammonia oxidation by AOB; and 16S rDNA for *Nitrobacter* and *Nitrospira* and nxrB, which is the functional gene for NOB nitrite oxidation by NOB. Table 4.9 summarizes the qPCR primer targets applied for detection of these genes.

Table 4.9. qPCR primers used to detect targeted AOB and NOB genes.

Target Organism	**Target Gene**	**Primer**	**Sequence**
Nitrosomonas (AOB)	16 rRNA gene	CTO 189fA/B CTO 189fC RT1r	GGAGRAAAGCAGGGGATCG GGAGGAAAGTAGGGGATCG CGTCCTCTCAGACCARCTACTG
	amoA	amoA-1F amoA-2R	GGGGTTTCTACTGGTGGT CCCCTCKGSAAAGCCTTCTTC
Nitrobacter (NOB)	16 rRNA gene	FGPS1269 FGPS872	TTTTTTGAGATTTGCTAG CTAAAACTCAAAGGAATTGA
	nxrB	NxrB 1F NxrB 1R	ACGTGGAGACCAAGCCGGG CCGTGCTGTTGAYCTCGTTGA
Nitrospira (NOB)	16S rRNA gene	NSR1113f NSR1264r	CCTGCTTTCAGTTGCTACCG GTTTGCAGCGCTTTGTACCG

With ASU's guidance, SWT selected six sampling points in each hybrid and conventional train. These sampling points are summarized in Table 4.10. Four sets of biomass samples were sent by SWT to ASU for microbial community analysis (MCA). All samples were shipped in liquid using dry ice to minimize sample deterioration. The first set of samples was obtained in May 2010, which coincides with phase 9 for all trains. The purpose of this set of samples was to determine what obstacles might derive from shipping to the United States from Singapore and to validate the procedures to assay for the different microorganisms. The May samples were delayed in United States Customs,

resulting in the samples thawing and potentially deteriorating prior to arrival at ASU.

The last three sets of samples were obtained on 1 November, 25 November, and 16 December 2010. All of these dates fall within phase 11. The 16 December 2010 had no train 3 samples. The last three sets of samples were successfully shipped to the United States without delays in Customs and arrived frozen in dry ice.

Table 4.10. Summary of MCA sampling points

MCA Sampling Points
Influent stream
Flow out of the anoxic tank
Flow out of the contact tank
Flow from clarifier to stabilization tank
Flow from the stabilization tank to the anoxic tank
Flow out of the anaerobic digester

Nitrobacter is omitted from the results figures, as its concentrations were 100 times less than *Nitrospira*. This is interesting, since *Nitrobacter* is often cited as the important genus of NOB (Mara & Horan, 2003; Gray, 1989). However, recent research has determined *Nitrospira* is often the dominant NOB in activated sludge (e.g., Siripong & Rittmann, 2007).

4.6.2 qPCR Results

Figure 4.15 illustrates the average concentration of *Archaea*, general Bacteria, AOB and *Nitrospira* (NOB) in the anoxic tank, contact tank, stabilization tank, and AD at each sampling date. Concentrations for *Nitrobacter* were so low that they are not displayable on these charts. The concentrations are

in mgVS/L and were determined by using conversion factors based on the number of gene copies per cell and cell volume. Literature-obtained conversion factors were 2 16S rDNA copies per cell for *Archaea* (Yu et al., 2005) and 3.5 rDNA copies per cell for general bacteria (Xu et al., 2009). The average cell volumes were 2.14 μm^3 for *Archaea* (Zellner, et al., 1998) and 2 μm^3 for bacteria, including AOB and NOB (Madigan & Martinko, 2006). Due to inconsistencies introduced during sampling and transport of the DNA, the concentration values should only be used to provide general guidance about the presence of the different groups of microorganisms, not strict values of biomass concentration.

Figure 4.15a shows that *Archaea* were present throughout each system. When comparing 1 November results across all trains, hybrid train 1 generally had higher *Archaea* concentrations that conventional train 2, which had higher concentrations that hybrid train 3. For the 25 November and 16 December samples, train 2 had higher concentrations of *Archaea* than trains 1 and 3, except for the stabilization tank in train 3. One expected trend is observed: the hybrid trains have higher concentrations of *Archaea* in the stabilization tank than the conventional train due to the recycle of AD sludge to the stabilization tank.

As seen in Figure 4.15b, general *Bacteria* presented no strong trends. General *Bacteria* concentrations were in the same order of magnitude or one order of magnitude smaller than *Archaea*, regardless of train or phase. This is unexpected, since heterotrophs ought to be the dominant microorganism in all

systems due to their relatively higher yields, more plentiful supply of substrate (BOD), and ability to survive in aerobic, anoxic, and anaerobic conditions.

The AOB and *Nitrospira* data in Figures 4.15c and d, respectively, illustrates the presence of these microbes in all tanks. AOB and NOB were present in concentrations that are approximately one-tenth to one-hundredth that of general *Bacteria*, but they were present throughout the processes. Train 2 had generally higher concentrations of AOB and *Nitrospira*, which is most visible in the stabilization tank and AD data; however, nitrification was minimal in all trains, and N removal was dominated by sludge wasting.

Figure 4.16 illustrates the ratio of total microorganism concentration (*Archaea* +general *Bacteria*) to VSS concentration for each train. Again focusing on relative trends, conventional train 2 consistently demonstrated the higher ratios than the hybrid trains. The hybrid train had higher total system and AD SRTs, resulting in higher concentrations of inert biomass being retained in the hybrid trains. Consequently, the hybrid trains exhibited a lower ratio of microorganisms to VSS.

To summarize, the MCA data support the hypothesis that *Archaea* and nitrifiers can survive throughout the system, whether the environment is aerobic, anoxic, or anaerobic. Although the MCA data cannot be used to quantify absolute concentrations of any of the biomass types, the presence of all types of biomass around the system supports that the recycling biomass between the aerobic and AD part of the hybrid process was increasing the AD and total-system SRT.

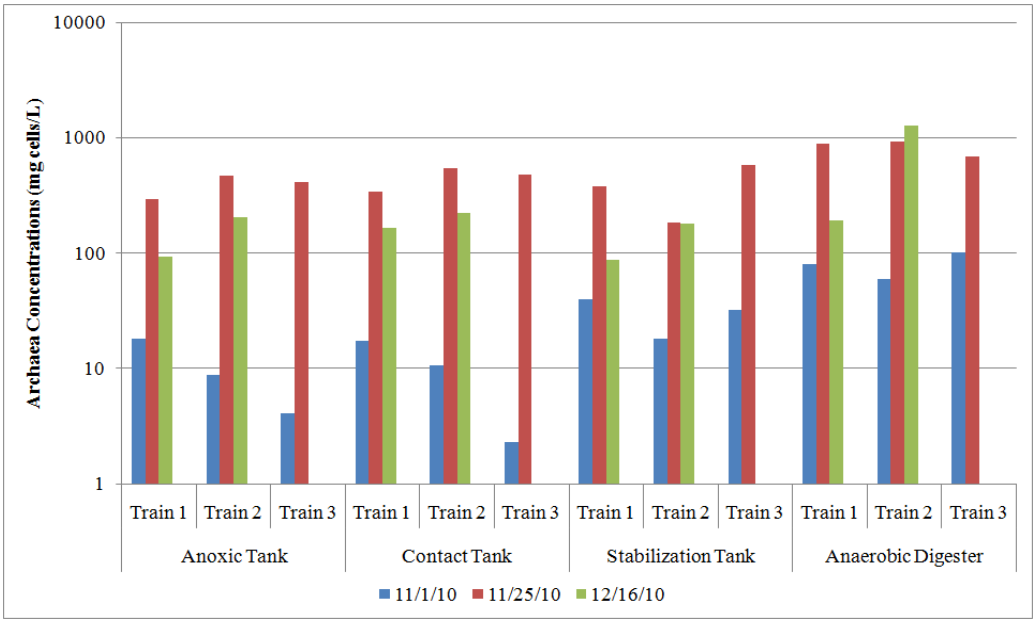

(a)

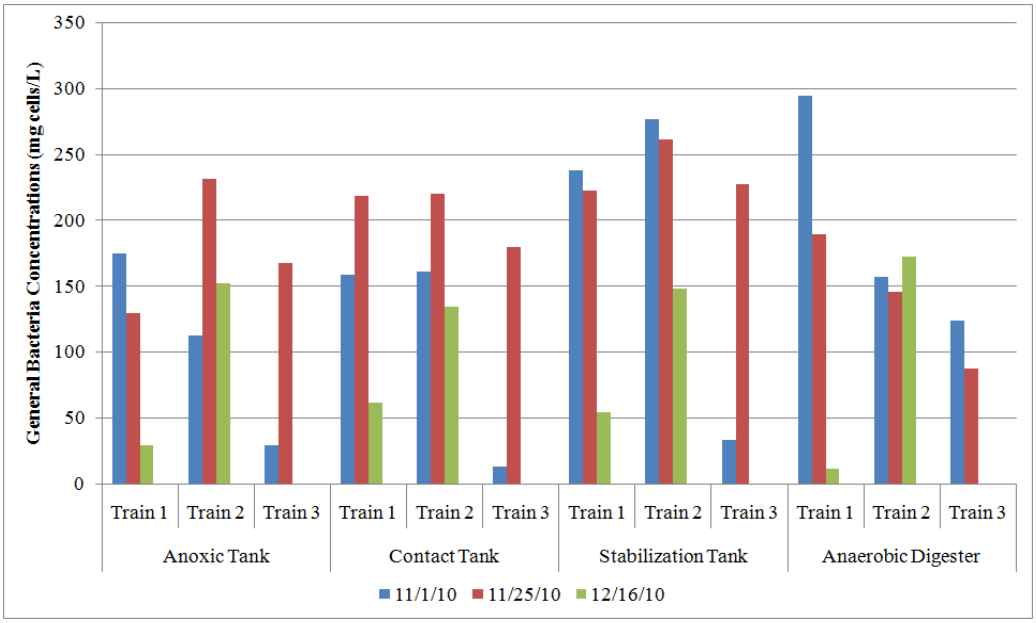

(b)

Figure 4.15. Average concentration of microorganism by phase, tank, and train. (a) *Archaea*, (b) General *Bacteria*, (c) AOB, and (d) *Nitrospira*.

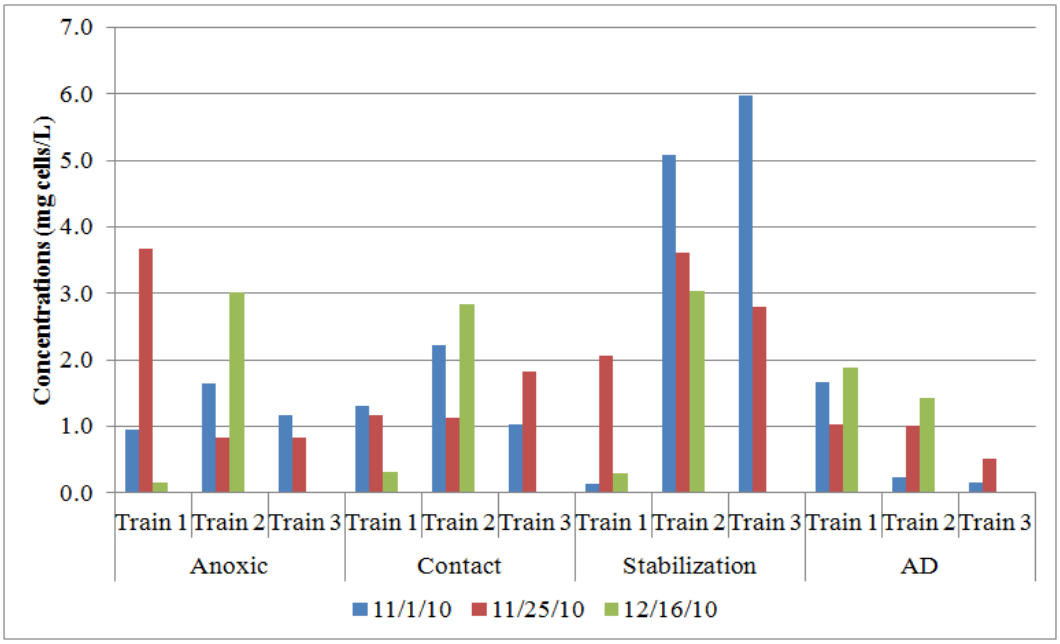

(c)

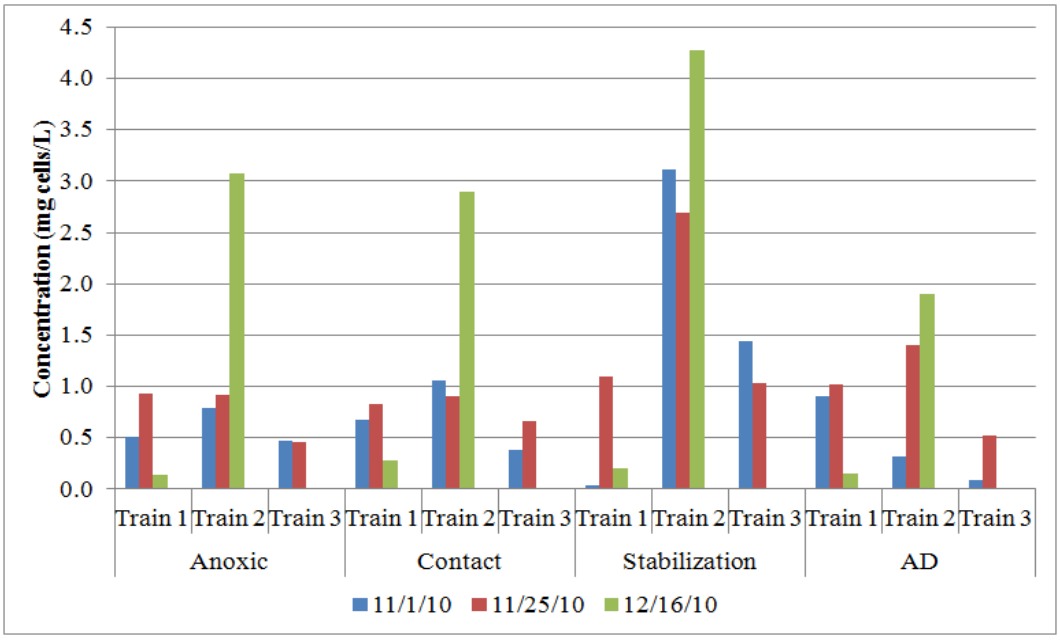

(d)

Figure 4.15 continued. Average concentration of microorganism by phase, tank, and train. (a) *Archaea*, (b) General *Bacteria*, (c) AOB, and (d) *Nitrospira*.

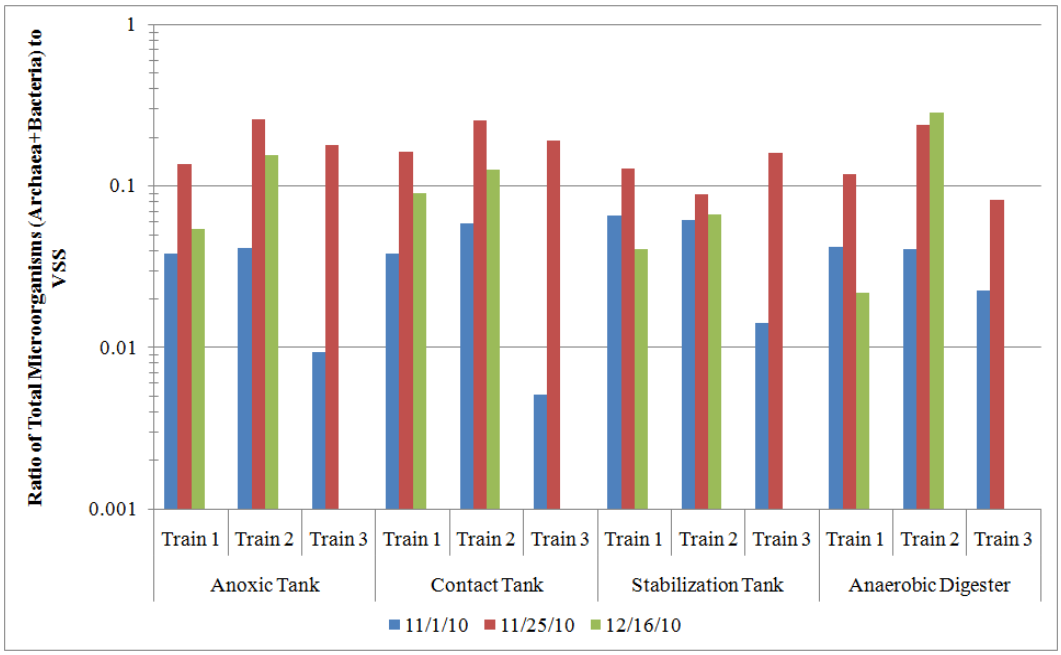

Figure 4.16. Ratio of total microorganisms (*Archaea* + *Bacteria*) to VSS per tank and train.

4.7 Conclusions

The SWT process demonstrated true potential to provide a more sustainable wastewater treatment process by lowering waste sludge production. COD data demonstrated that the hybrid processes consistently reduced net sludge production to ~15% of the sludge produced by the conventional system. The hybrid trains also discharged less COD as waste sludge: the hybrid trains consistently removed about 80% of COD from the discharge waste streams (effluent+wasting sludge), compared with 60% in the conventional train. While the hybrid system generated at least three times more methane than the conventional train, the percentage of influent COD transferred to methane remained low (12-22%).

As they were operated in this project, the hybrid systems achieved the low sludge yield mainly by oxidizing the COD in the aerobic portion of the process: particularly in the stabilization tank and to a lesser extent in the contact tank. PCOD analysis supports that biosorption occurred in the anoxic tank and that sludge recycled from the AD to the aerobic system increased biosorption there. However, subsequent aerobic oxidation of the biosorbed COD subverted the goals of transferring most of the TCOD and PCOD to the AD to generate methane. This is the reason for the low conversion of influent COD to methane

An SRT analysis suggests that the SRT of the AD was much greater than the nominal value computed by flow rates (Eqn. 43). When the recycling of active anaerobic biomass was taken into account to compute the AD SRT (Eqn.

44), the AD SRT was at least 50 days and perhaps greater than 200 days in the hybrid systems. This is much higher than the conventional SRT of 25 to 30 days, and may have been responsible for the 3-fold greater methane production rate in the hybrid trains. Microbial community analysis found *Archaea* throughout the trains, which supports that biomass recycle increased the AD SRT in the hybrid systems.

None of the trains was effective at nitrification and denitrification, although a small amount of nitrification occurred. The individual tanks exhibited expected nitrogen trends: denitrification in the anoxic tank, nitrification in the contact and stabilization tanks, and NH_3-N production in the AD. However, poor nitrification was evidenced by high concentrations of effluent NH_3-H (9 to 19 mgN/L prior to phase 12). However, a small degree of nitrification has to have occurred, because some NO_2^- and NO_3^- were produced in all systems, and AOB and NOB were detected throughout the trains. With poor nitrification occurring, denitrification also was minimal. Poor nitrification probably was the result of having a low aerobic SRT, ranging between 2 and 7 days for all trains

When hybrid train 1 was modified to remove the stabilization tank in phase 12, the level of nitrification increased, since AOB and NOB probably were retained in higher numbers in the contact tank due to the biofilm media; in this case, more nitrate was directly recycled to the anoxic tank from the contact tank for denitrification. Additionally, train 1's methane generation was slightly higher than train 3's, probably due to less COD being utilized in aerobic processes,

particularly the stabilization tank, which was removed. However, additional NO_2, NO_3^-, and TKN data are required to quantify the performance improvement.

5. Mathematical Modeling of the Hybrid System

The performance data analyzed in previous chapters illustrate the potential for the hybrid system to provide better performance than a conventional system. However, the pilot data alone cannot be used to predict potential performance over a myriad of operating conditions. For successful commercialization, it is essential to understand the effects of all mechanisms on tank and overall system performance, as well as over a wider, more extensive list of conditions which cannot be produced on a pilot scale.

Mathematical models have been applied to a variety of biological water and wastewater systems to gain understanding of system performance. However, existing software and models fail to account for all of the potential mechanisms involved in SWT's hybrid process, particularly PCOD biosorption and the exchange of biomass among the different tanks in the hybrid system. For example, the well-known activated-sludge models (ASM) established by the International Water Association (IWA) assume rapid adsorption and slower hydrolysis of PCOD in floc, but neglect the effects of flocculation on PCOD entrapment (Jimenez et al., 2005). Likewise, Jimenez et al. (2005) applied jar tests to establish an empirical model to describe the effects of floc entrapment based on first-order kinetics and COD concentration, but their model does not include PCOD adsorption kinetics. Other commonly used software, including BioWIN, fail to incorporate PCOD floc entrapment and adsorption mechanisms (Jimenez et al., 2007).

For SWT's hybrid process, mathematical modeling can provide additional understanding of the hybrid process's performance and the role of key mechanisms, including biosorption and sludge recycle. Using MATLAB, I produced a dynamic, multispecies mathematical model that incorporates all critical components and mechanisms, including aerobic and anoxic reactions, anaerobic digestion, and settling. I also developed a sub-model for PCOD flocculation and adsorption kinetics. I combined all of these features into a series of non-steady-state, differential mass-balance equations that comprehensively describe the performance of the system.

My approach consisted of four steps. First, I established the foundation for the mathematical model by identifying the modeling system (illustrated in Figure 2.3b), critical mechanisms, and mass balance equations for SWT's system. I defined the physical, chemical, and biological mechanisms present in each tank, as summarized in Table 3.2. This process was facilitated by a literature review of anaerobic, activated sludge, and biosorption mechanisms and through the analysis of performance data provided by SWT. The common physical mechanism is advective mass transfer from tank to tank. The most novel mechanism modeled included in the model is a combined approach to PCOD biosorption using flocculation and adsorption kinetics. Another unique concept is the exchange of different types of biomass between the aerobic and anaerobic parts of the hybrid process. With the mechanisms defined, I was able to establish which chemical

components, reactions, and kinetics are required to model the system. The chemical components are summarized in Table 5.1.

The second step involved formulation of a MATLAB model of a chemostat with all of the established mechanisms. I tested and refined the model until mass balance closure was achieved for all COD and N components. I then employed the chemostat model for the conditions present in each tank in the system.

The third step was to expand the chemostat model to represent the entire system without biosorption. This required applying the equations in Table 3.5 to all components listed in Table 5.1. The model without biosorption provides baseline of system performance using established mechanisms and kinetic parameters. The results of this model can be compared to actual performance to determine if the model accurately models SWT's trains without including biosorption. Note that I model all influent nitrogen as NH_3 and not as TKN, as limited data were available for TKN.

Table 5.1. Components to be included in the conceptual model.

Solid Components		**Soluble Components**	**Gaseous Components**
		Substrate	
Heterotrophs	$PCOD_a$	NH_4^+	N_2
AOB	$PCOD_f$	NO_2^-	CH_4
NOB	$PCOD_s$	$NO3^-$	
Fermenters	Inert biomass	Dissolved oxygen (DO)	
Methanogens	EPS	Acetate	
		Biomass associated products (BAP)	
		Utilization associated products (UAP)	

The final step was including biosorption mechanisms. My model considers the PCOD biosorption mechanisms described in Section 5.2. Based on this model, I established several new kinetic parameters from data provided by SWT and NUS, and through model sensitivity analysis. I then ran the model under a variety of operating conditions, including variations in RAS rate, WAS rate, and SRT.

In this chapter, I develop the mechanistic model for the SWT hybrid process and discuss the model formulation and assumptions. I introduce novel concepts applied in the model, including development of a combined theory of biosorption through floc entrapment and adsorption and the application of switch factors. The results of the modeling are presented in Chapter 6. All modeling equations are summarized in Appendix A.

5.1 Model Formulation and Assumptions

This model requires non-steady-state mass balance equations of each component (listed in Table 5.1) for each tank and the overall system. For model development, I had to make several assumptions:

(1) Each tank is a completely mixed reactor, with the exception of the settlers (i.e., clarifier and sludge thickener).

(2) Each settler is composed of two distinct layers: a supernatant and a sludge layer. While the same concentration of soluble components exists in each layer, the efficiency of solids partitioning depends upon settler efficiency. For example,

with 99% settling efficiency, 99% of solids by mass are in the sludge layer and 1% is in the supernatant.

(3) To simplify MATLAB modeling, I treated all mechanisms as though they can occur in each tank; however, any mechanism can be minimized or neglected entirely through the application of switch factors (discussed below).

(4) Each tank is well buffered so that inhibition from extreme pH is not relevant.

(5) Unless otherwise stated, hydrolysis of any form of PCOD can occur in any environment, and it is modeled as an active mechanism in all tanks. This assumption will later be loosened for certain models of overall system performance.

All biomass undergoes three common processes: production of new active biomass from substrate utilization, endogenous decay of active biomass, and production of EPS and SMP. Accordant with Bae and Rittmann (1996), biomass consumes substrate via multiplicative, dual-limitation Monod kinetics based on the concentrations of the electron donor and acceptor. Microorganism decay is first-order in active biomass concentration (Rittmann & McCarty, 2001). I apply the unified theory of EPS and SMP utilization presented by Laspidou and Rittmann (2002a) with small modifications. Consistent with Laspidou and Rittmann (2002b), all biomass produce EPS and UAP, and BAP is produced from EPS hydrolysis. Heterotrophs and fermenters are the only microorganisms capable of reutilizing UAP and BAP as substrate. Laspidou and Rittmann (2002b) assumed that utilization of SMPs and EPS does not result in additional

production of SMP and EPS. However, I assume that utilization of EPS and UAP can result in the formation of additional SMPs and EPS.

Aquino's and Stuckey's (2008) model of anaerobic digestion provided the basis of my anaerobic digestion model, and I make several key assumptions regarding the anaerobic digestion process. Like Aquino and Stuckey, my model simplifies the mass balance by focusing on one set of bacteria that ferment complex and particulate organics to acetate, which is later converted to CH_4 via methanogenesis. However, Aquino and Stuckey do not define the composition of substrate available for fermentation, which can include SCOD, PCOD, and inactive biomass such as heterotrophs, AOB, and NOB. I assume that all forms PCOD, heterotrophs, AOB, and NOB may undergo hydrolysis for use as substrate by fermenters. This assumption is based on the fact that aerobic biomass becomes inactive in the AD and is essentially particulate substrate. Unlike Aquino and Stuckey, I employ Laspidou and Rittmann's (2002a) unified theory for SMP and EPS. Rather than assuming which step is rate-limiting, the model includes hydrolysis, fermentation, and methanogenesis mechanisms individually. Other assumptions include that the anaerobic process is mesophilic, the rate of hydrolysis follows a first-order relationship, and CH_4's solubility of in water is negligible so that all CH_4 produced is captured as biogas.

For the anoxic systems, I assume no intermediates between the reduction of NO_3^- (or NO_2^-) and formation of N_2 gas. In other words, the consumption of

NO_3^- as an electron acceptor produces N_2 gas directly without producing NO_2^- or any other intermediate.

Finally, I use $C_5H_7O_2N$ as the chemical formula for all biomass, which is standard based on Rittmann and McCarty (2001) and Metcalf & Eddy (2003).

5.2 A Combined Theory of Biosorption and Flocculation

When particles of $PCOD_s$ enter a tank, they can undergo three processes illustrated in Figure 5.1. First, $PCOD_s$ can be hydrolyzed to SCOD by active biomass. Second, PCOD can be trapped by the floc (denoted $PCOD_f$) and eventually hydrolyzed to SCOD. Finally, $PCOD_s$ can be absorbed by biomass (including inerts) (denoted $PCOD_a$), where it eventually can be hydrolyzed to SCOD. Additional $PCOD_s$ can be formed through floc breakup.

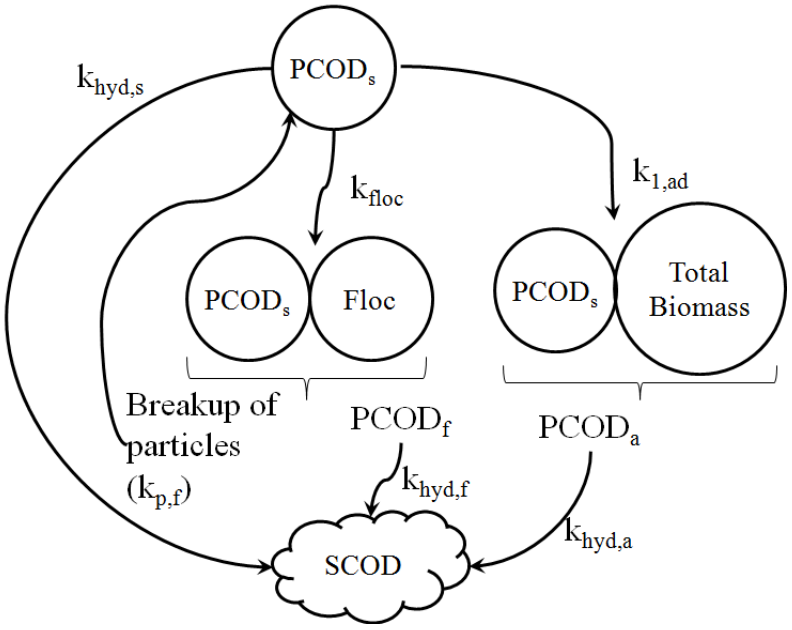

Figure 5.1. Potential paths for PCOD in the model.

The total amount of PCOD ($PCOD_T$) is

$$PCOD_T = PCOD_s + PCOD_f + PCOD_a \quad (50)$$

Mass balances for $PCOD_s$, $PCOD_f$ and $PCOD_a$ are developed for a CSTR with complete mixing.

As reviewed in Section 2.3, flocculation mechanisms are described using Eqn. 27 (Henze et al., 1995).

$$r_f = \frac{dC_{PCOD}}{dt} = K_f(PCOD_s/M_{PCOD})\Phi G \quad (27)$$

Floc break up is described using Eqn. 28 (Henze et al., 1995).

$$r_p = K_p PCOD_f \Phi G^p \quad (28)$$

Adsorption mechanisms are described using Eqn. 15 (Aksu, 2005).

$$r_{hyd} = -k_{hyd} PCOD_a \quad (15)$$

Figure 5.2 illustrates the basic format for developing a mass balance: a chemostat with one influent stream and one effluent stream. Based on the format, the net rate of $PCOD_f$ accumulation in a chemostat is

$$\frac{dPCOD_f}{dt} = k_{floc} PCOD_s \Phi G - k_{p,f} \Phi G^{p-1} PCOD_f - k_{hyd,f} PCOD_f + \frac{Q}{V}(PCOD_f^0 - PCOD_f) \quad (51)$$

where the first term on the right hand side describes the flocculation of $PCOD_s$ single particles together, the second term describes the floc breakup, the third term describes the hydrolysis of $PCOD_f$ to SCOD, and the final term describes the mass flow into and out of the system.

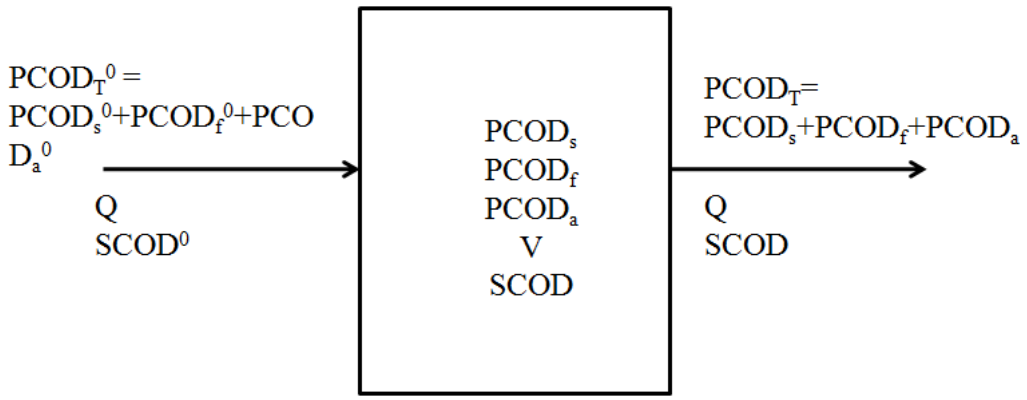

Figure 5.2: Format for developing a PCOD mass balance.

The mass balance for $PCOD_a$ is

$$\frac{dPCOD_a}{dt} = k_{1,ad}(q - q_{eq}) - k_{hyd,a}PCOD_a + \frac{Q}{V}(PCOD_s^0 - PCOD_s) \tag{52}$$

where the first term on the right hand side describes the adsorption of $PCOD_s$ single particles, the second term describes the hydrolysis of $PCOD_a$ to SCOD, and the final term describes the mass flow into and out of the system.

The mass balance for $PCOD_s$ is

$$\frac{dPCOD_s}{dt} = -k_{floc}PCOD_s\Phi G + k_{p,f}\Phi G^{p-1}PCOD_f - k_{1,ad}(q - q_{eq}) - k_{hyd,s}PCOD_s + \frac{Q}{V}(PCOD_s^0 - PCOD_s) \tag{53}$$

where terms 1 and 2 describe the change in $PCOD_s$ concentration due to flocculation, term 3 describes loss of $PCOD_s$ to adsorption, term 4 describes hydrolysis of $PCOD_s$ to SCOD, and the final term describes the mass flow into and out of the system.

The biosorption capacity is described by the Freundlich equation,

$$q_{eq}\ (\text{or } q) = k_1 C_{eq}^{1/n}\ (\text{or } C^{1/n}) \tag{54}$$

where k_1 and n are Freundlich coefficients related to adsorption capacity and adsorption intensity, respectively; typically, they are determined experimentally. These constants can be obtained from linearizing the logarithmic form of Eqn. 54 using the concentrations of absorbed sorbate and sorbate in solution obtained from adsorption experiments. This relationship can be directly substituted into Eqn. 52 and 53.

5.3 Switch Factors

As stated previously, to simply modeling in MATLAB, I assumed that any mechanism can act in any tank. However, a mechanism's level of activity can be turned off through the application of a switch factor (de Silva & Rittmann, 2000). For example, the switch factor for DO, DO^{switch}, is

$$DO^{switch} = \frac{K_{DO}^{switch}}{K_{DO}^{switch} + DO} \tag{55}$$

where DO is the DO concentration in solution (M/L^3) and K_{DO}^{switch} is the half-maximum rate concentration for DO (M/L^3). When the DO concentration is low, DO^{switch} approaches 1, and the process is turned on. When the DO concentration is high (compared to K_{DO}^{switch}), DO^{switch} goes to 0, and the process is turned off. For example, DO^{switch} is applied to anoxic and anaerobic mechanisms to deactivate these mechanisms when significant DO is present.

Similarly, switch factors are applied to NO_2^- and NO_3^- to activate strictly anaerobic mechanisms:

$$NO_x^{switch} = NO_2^{switch} + NO_3^{switch} = \frac{K_{NO_2}^{switch}}{K_{NO_2}^{switch} + NO_2} + \frac{K_{NO_3}^{switch}}{K_{NO_3}^{switch} + NO_3} \tag{56}$$

where $K_{NO_2}^{switch}$ is the half-maximum rate concentration for NO_2^-, $K_{NO_3}^{switch}$ is the half-maximum rate concentration for NO_3^-, and NO_2 and NO_3 are the concentrations of NO_2^- and NO_3^- in the tank, respectively.

5.4 Operating and Kinetic Parameters

5.4.1 Basic Operating Parameters

Values for model parameters must represent typical hybrid operating conditions. Parameters for operating conditions (e.g., flow rates, influent concentrations, and vessel volumes) were selected based on typical hybrid operations during the course of the pilot plant trials and are summarized in Table 5.2. The chosen model parameters represent the performance of train 3 during phase 9, and are also summarized in Table 5.2.

I chose to simulate train 3 during phase 9 for three reasons. Train 3's performance was the most consistent of all trains. Its RAS ratio of 1.2 was applied to all trains through phase 10 and, therefore, the most commonly used RAS ratio during the project. A WAS rate of 6% was typical for train 3 throughout its operations.

Table 5.2. Operating parameters for modeling based on phase 9 of train 3's performance at 120% RAS and 6% WAS of influent flow rate.

		Model Parameters	Actual Influent Values
Flow Rates			
Influent	L/d	605	605
Effluent	L/d	600	602
Wasting Sludge from AD	L/d	5	3
Concentrations			
TCOD	mgCOD/L	582	620
SCOD	mgCOD/L	150	110
Total VSS	mgVSS/L	205	310
PCOD	mgCOD/L	250	440
TSS	mgTSS/L	305	440
NH_4^+-N	mgN/L	100	30
NO_2^--N	mgN/L	0	0.0
NO_3^--N	mgN/L	0.2	0.2
Heterotrophs	mgVSS/L	25	NA
AOB	mgVSS/L	1	NA
NOB	mgVSS/L	1	NA
Fermenters	mgVSS/L	1	NA
Methanogens	mgVSS/L	0.5	NA
DO	mgDO/L	2	NA
Tank Volumes			
Anoxic tank	L	25	25
Contact tank	L	12	12
Clarifier	L	100	100
Stabilization tank	L	50	50
Sludge thickener	L	100	100
Anaerobic digester	L	Based on AD SRT	650
Settler Efficiency	%	99.9	--
Fraction of sludge thickener flow rate to the supernatant	--	2/3	2/3
% WAS (of RAS flow rate)	%	6	6
% RAS (of influent flow rate)	%	120	120
AD SRT (based on Eqn. 41)	d	30	30
DO Saturation Concentration	mgDO/L	9.1	--
K_La		3030	--
Contact Tank DO Concentration	mgDO/L	2	--
Stabilization Tank DO Concentration	mgDO/L	4	--

5.4.2 Kinetics for Microorganisms

I based the kinetic parameters on typical values found in an extensive literature review of aerobic, anaerobic, and anoxic processes; they are summarized in Table 5.3. Heterotrophic biomass, AOB, and NOB kinetics are well documented in Rittmann and McCarty (2001) and Rittmann and Park (2008), and these values are consistent with IWA's ASM model (Henze et al., 2000). The values for fermenter and methanogens kinetics are a compromise between stated values in Rittmann and McCarty (2001) and in Aquino and Stuckey (2008), who also utilized the simplification that acetate is the only intermediate produced from fermentation.

Table 5.3. Kinetic parameters for the microorganisms.

Kinetic Parameters		Symbol	Units	Heterotrophs	AOB	NOB	Fermenters	Methanogens
True Yield Coefficient	Substrate	Y	mgVSS/mgCOD	0.45	0.33	0.083	0.2	0.077
	SMP	Y_p	mgVSS/mgCOD	0.5	0.5	0.5	0.5	0.5
Maximum utilization rate	Substrate	$\hat{q}$	mgCOD/mgVSS-d	10	3.1	13	10	--
	UAP	$\hat{q}_{UAP}$	mgCOD/mgVSS-d	1.8	--	--	1.8	--
	BAP	$\hat{q}_{BAP}$	mgCOD/mgVSS-d	0.5	--	--	0.5	--
	Acetate	$\hat{q}_{Ace}$	mgAce/mgVSS-d	8.1	--	--	--	7
Half-maximum rate concentration	Substrate	K_S	mgCOD/L	10	1.5	2.7	10	--
	Acetate	K_{Ace}	mgAce/L	168	--	--	--	30
	DO	K_{DO}	mgDO/L	0.2	0.5	0.68	--	--
	UAP	K_{UAP}	mgCOD/L	100	--	--	100	--
	BAP	K_{BAP}	mgCOD/L	85	--	--	85	--
	NO_2^- or NO_3^-	K_n	mgN/L	0.2	1.5	2.7	--	--
Formation rate of UAP		k_{UAP}	mgCOD/mgCOD	0.05				
Formation rate of EPS		k_{EPS}	mgCOD/mgCOD	0.18				
Hydrolysis rate	EPS	k_{hyd}	1/d	0.17				
	PCOD	k_{PCOD}	1/d	0.22				
Decay rate		b	1/d	0.3	0.15	0.15	0.04	0.03
Fraction of biodegradable biomass		f_d	-	0.8				

5.4.3 Biosorption Parameters

Determining the biosorption parameters presents the greatest obstacle for implementing the model, since no existing data address the biosorption kinetics proposed in this model. Several works provide adsorption parameters for metals or phosphorus (Henze et al., (1995); Aksu, 2005; Gadd, 2009). Jimenez et al. (2005, 2007) and La Motta et al. (2007) empirically address bioflocculation and adsorption as one kinetic parameter. However, my model separates the two mechanisms.

To run the biosorption model, I had to make several assumptions. (1) Biosorption can occur in any tank in the system. (2) The adsorption capacity of the biomass and associated parameters $k_{1,ad}$, n, and k_f are constant throughout the system. (3) Because the magnitude of mixing vary by tank, the values of G and Φ change. The values of these constants are summarized in Table 5.4. I assumed that G is zero in the clarifier and sludge thickener, since active mixing is absent in the tanks. I assumed twice as much mixing energy in the stabilization tank when compared with the contact tank and half the amount of mixing energy in the anoxic tank and AD due to the lack of aeration. Because of the low retention times in the anoxic and contact tanks, I assumed that Φ was 0.1 L^3_{floc}/ L^3_{water}. At the other end, I assumed that the AD and sludge thickener had much higher Φ at 0.9 and 0.7 L^3_{floc}/ L^3_{water}, respectively. This number was slightly lower in the sludge thickener, since it has some supernatant. I assumed that the clarifier's Φ was slightly lower than the sludge thickener at 0.5 L^3_{floc}/ L^3_{water}, since it is the

first separations process. Finally, I assumed that the stabilization tank had an Φ of 0.3 L^3_{floc}/ L^3_{water}, since it received a fair amount of clarifier sludge and supernatant, but pilot plant performance indicated little biomass growth from nitrifiers or heterotrophs.

I estimated the adsorption constants from limited biosorption data provided by NUS batch experiments 35 through 37. The constants k_1, $k_{1,ad}$, and n were fit to NUS's data using the linearized form of Eqn. 54. Because technical data are unavailable for the propellers in the tanks, I estimated a value of G equal to 3000 1/d in the contact based on a website that describes the work performed by a propeller at assumed diameters between 8 and 12 inches (Propeller Turbine Mixer Design Calculator, http://www.ajdesigner.com/phpmixing/propeller_mixing_power_turbulent.php).

I established the flocculation constants through a sensitivity analysis reviewed in Section 6.3.

Table 5.4. Biosorption parameters by tank.

Parameter	Variable	Units	Anoxic tank	Contact tank	AD	Stabilization tank	Clarifier	Sludge thickener
Adsorption coefficient	$k_{1,ad}$	1/d	144					
Freundlich constant for adsorption capacity	k_1	--	0.079					
Freundlich constant for adsorption intensity	n	--	1.34					
RMS velocity	G	1/d	1500	3000	0	6000	0	0
Floc volume ratio	Φ	L^3_{floc}/ L^3_{water}	0.1	0.1	0.9	0.3	0.5	0.7
Floc shearing constant	p	--	2					
Adsorbed PCOD equilibrium concentration	$PCOD_{eq}$	mgCOD/L	55					

6. Mathematical Modeling Results

Mathematical modeling is a powerful tool used to facilitate understanding of system performance trends. My approach is to use the model as a tool for identifying and interpreting system trends. In this chapter, I review the results of mathematical modeling, analyze model trends, and provide general recommendations for optimized hybrid performance.

6.1 Observations from Single-Tank (Chemostat) Mass-Balance Analyses

The mathematical model analysis began by testing for mass balance at steady state for each individual tank. This involved analyzing each tank as a single chemostat with influent concentrations into each tank equal to the concentrations stated in Table 5.2. With this approach, I verified that mass balance was achieved for nitrogen and COD components in each individual tank. An example of the chemostat mass balance is presented in Appendix B.

An important observation from the single-tank trials is that washout of all biomass occurred when the influent concentrations to the contact tank were set equal to the system influents presented in Table 5.2. This was the only vessel in which washout of all biomass occurred, and it further supports the experimentally observed trend of no nitrification occurring in the contact tank (Section 4.3.2) and the improvement in performance once packing was added to the contact tank of train 1 in phase 12.

6.2 Observations from Full-System Mass-Balance Analyses

Once mass balance was achieved for each individual tank, I activated all mechanisms for all tanks and executed the model to determine if each individual tank and the overall system (e.g., the system influent and all effluents) achieved mass balance closure. I was able to obtain mass balance closure with all COD and nitrogen compounds simultaneously within 1% tolerance. This variation in tolerance is related to the fact that the systems did not necessarily achieve full steady state operations within 1500 days of simulated time. Inert biomass continued to accumulate at a rate less than 1% over one month in the sludge thickener and AD. An example of the chemostat mass balance is presented in Appendix B.

6.3 Modeling Excluding Biosorption Kinetics

I evaluated the full model without biosorption for four scenarios with the conventional and hybrid configurations: varying RAS rate at a constant WAS rate of 6% of influent flow rate and varying WAS at a RAS rate of 120% of influent flow rate. For each of these scenarios, I assumed that the nominal AD SRT (as calculated by Eqn. 41) is 30 days and that hydrolysis of $PCOD_s$ occurs under all operating conditions.

As illustrated in Figure 6.1a and b, the hybrid process consistently produces more CH_4 than the conventional process, with significant increases in CH_4 with increases in WAS and RAS. As RAS increases, the hybrid process produces twice as much CH_4 at 50% RAS and 8 times more at 210% RAS. As WAS increases, the hybrid process produces twice as much CH_4 at 2.5% WAS and 20 times more at 20% WAS. Larger percent WAS and RAS ratios result in a larger actual AD SRTs (calculated from Eqn. 44) in the hybrid configuration (Figure 6.2) and, consequently, increased methane production.

The trends are opposite for the conventional configuration: it experiences declines in CH_4 with increasing RAS and WAS rates, which do not alter the AD SRT. With increases in RAS, the concentrations of COD throughout the system become more diluted, and this dilution carries over to the AD, where less CH_4 is produced. A similar trend occurs with increasing WAS: as WAS increases, the flow rate of supernatant also increases at a rate that is twice the flow to the AD. Therefore, more soluble substrate is being diverted to the stabilization tank and not being converted to methane in the AD.

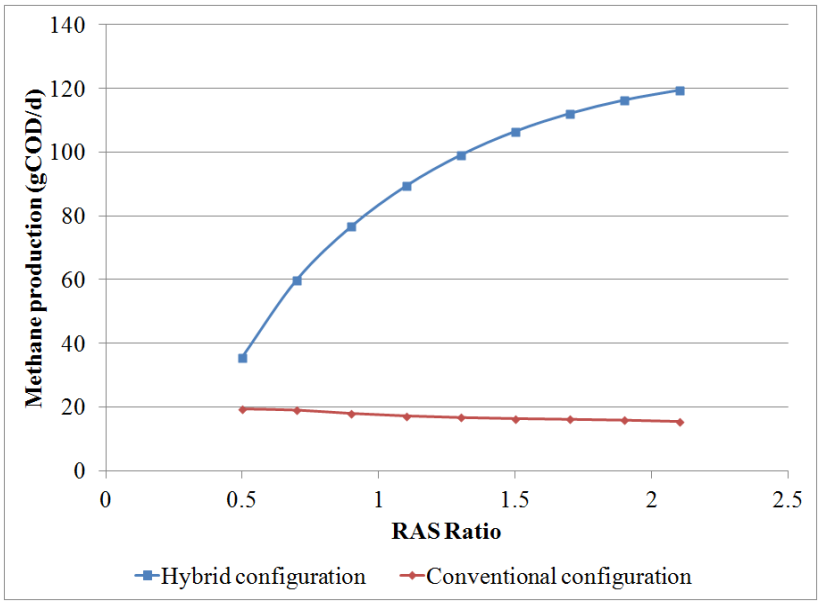

(a)

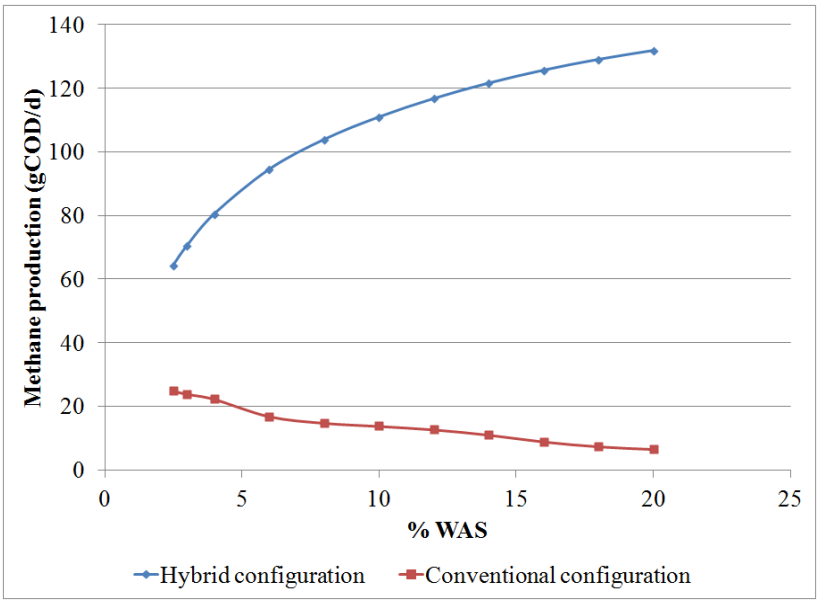

(b)

Figure 6.1. CH_4 production in the AD with the hybrid and conventional configurations as a function of (a) RAS ratio at a constant WAS rate of 6% and (b) WAS rate at a constant RAS ratio of 1.2.

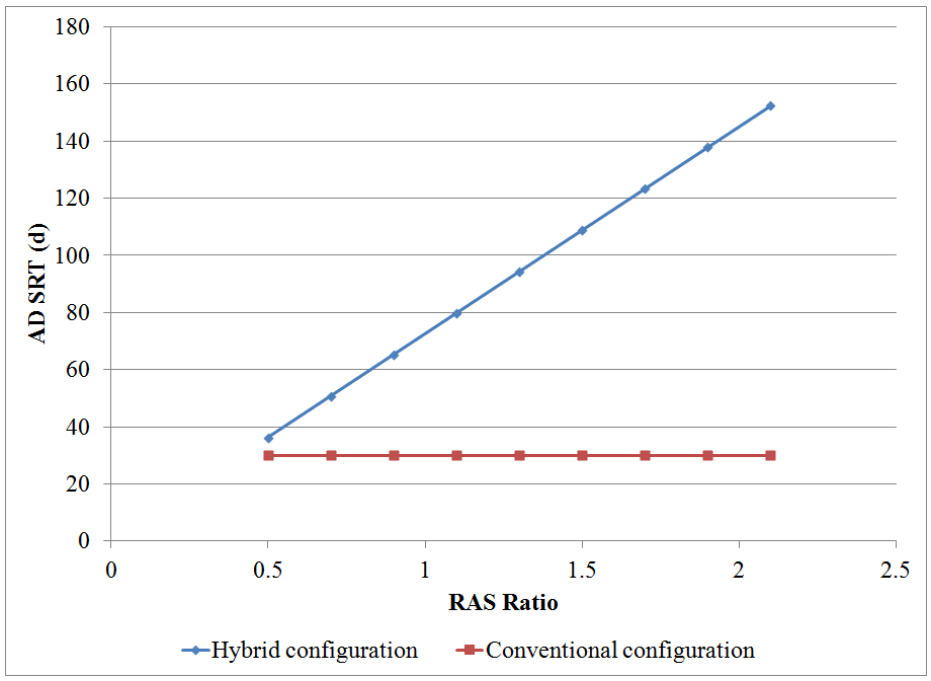

(a)

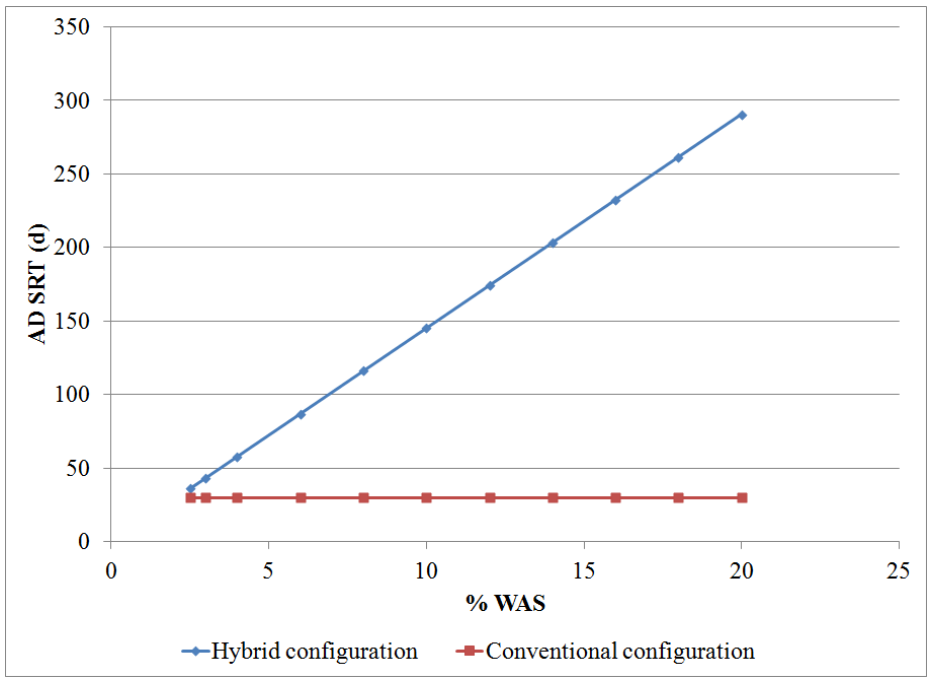

(b)

Figure 6.2. AD SRT as a function of (a) RAS ratio and (b) percent WAS.

What is just as interesting is the trend exhibited in Figure 6.3: a significant amount of CH_4 is produced in the clarifier, particularly for a low RAS or WAS ratio. (Note: All other tanks are excluded from the figures due to their negligible levels of CH_4 production.) CH_4 production in the clarifier is promoted by two mechanisms: (1) the recycling of AD sludge rich with fermenters and methanogens to the stabilization tank results in transport of these microorganisms to the anoxic and contact tanks; and (2) low DO, NO_2^-, and NO_3^- concentrations in the anoxic tank and clarifier produce anaerobic conditions in these tanks. While the anoxic tank and clarifier have essentially the same concentrations of methanogens and fermenters, the larger volume in the clarifier allows for more CH_4 production there. The significance of this trend is that CH_4 produced in the anoxic tank and clarifier is not captured for conversion to energy; instead, it is being released to the atmosphere, where it has 20 times more potency than CO_2 as a greenhouse gas (U.S. Energy Information Administration, 2010).

The model predicts almost no nitrification or denitrification in the system, which is consistent with the experimental results in Chapter 4.3. Effluent NH_3 concentration increases with increasing RAS and WAS flow rate regardless of configuration, as demonstrated in Figures 6.4a and b. NO_2^- and NO_3^- are negligible in the system effluent for either system configuration. Regardless of configuration, AOB and NOB concentrations are consistent between the anoxic and contact tank and very low. Thus, AOB or NOB do not have positive growth in the contact tank and are washed out of the contact tank.

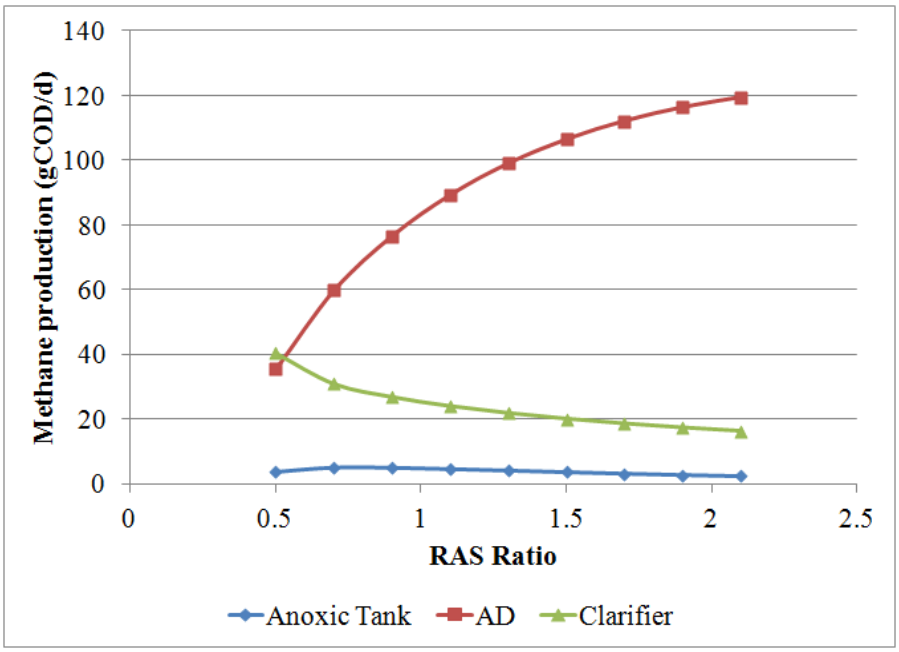

(a)

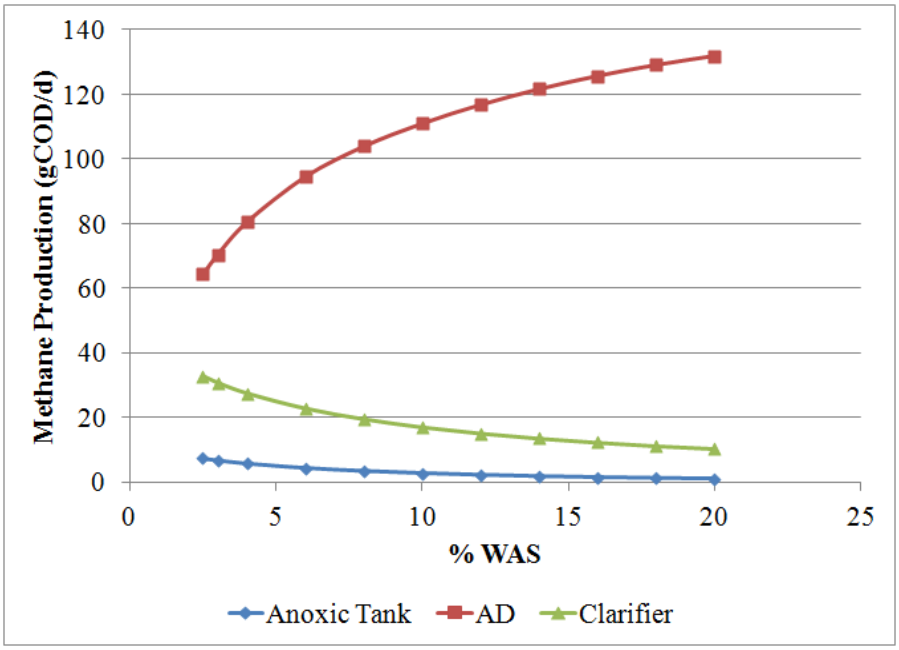

(b)

Figure 6.3. CH_4 production in the anaerobic digester, anoxic tank and clarifier with AD sludge recycle as a function of (a) RAS ratio at a constant WAS rate of 6% and (b) WAS rate at a constant RAS ratio of 1.2.

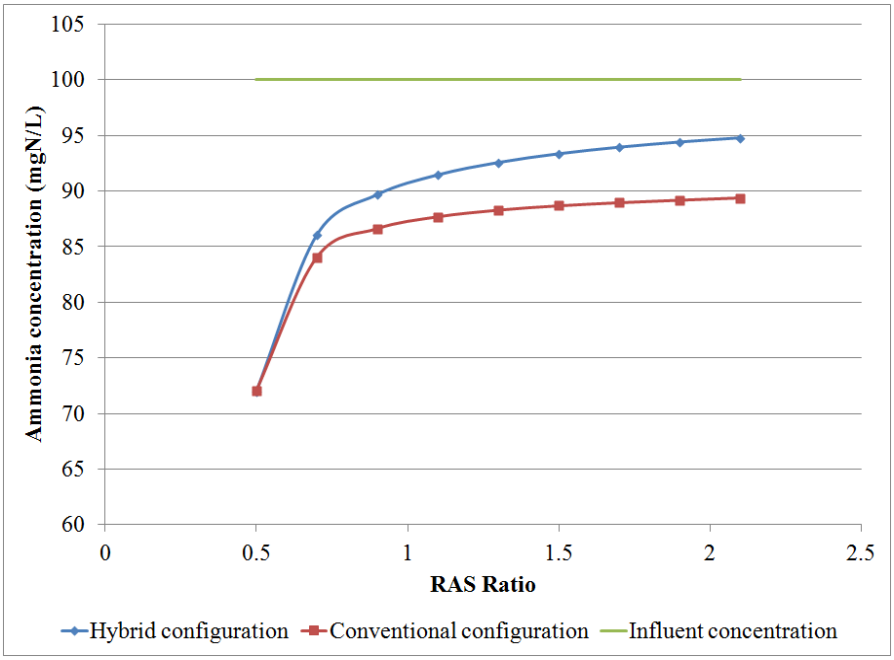

(a)

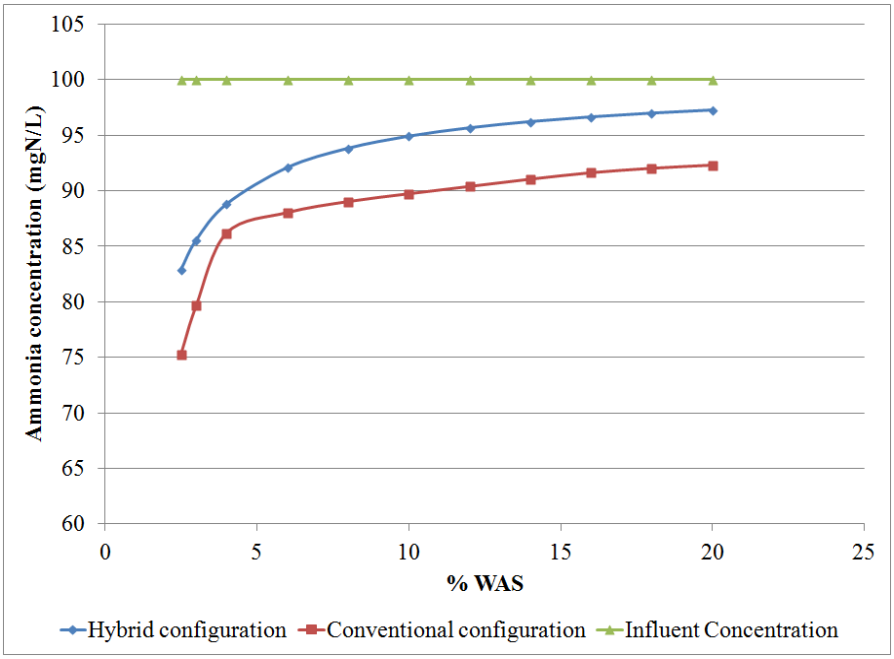

(b)

Figure 6.4. Effluent ammonia concentration as a function of (a) RAS ratio and (b) percent WAS.

The hybrid configuration removes less NH_3 (representing all TKN in the model) from the overall system than the conventional configuration. With the hybrid configuration, the longer SRTs result in more biomass decay and less net NH_3 uptake into wasted biomass. Because the stabilization tank is ineffective at nitrification, as seen in Figures 6.5a and b, the concentration of NH_3 is higher in the hybrid mode. The modeling also supports that nitrification is more effective at lower RAS rates, as there is higher rates of NO_2^- and NO_3^- production in the stabilization tank. This increase in nitrification is a direct result of longer SRTs in the stabilization tank at lower RAS rates. The same trend is also observed with WAS in lower magnitudes.

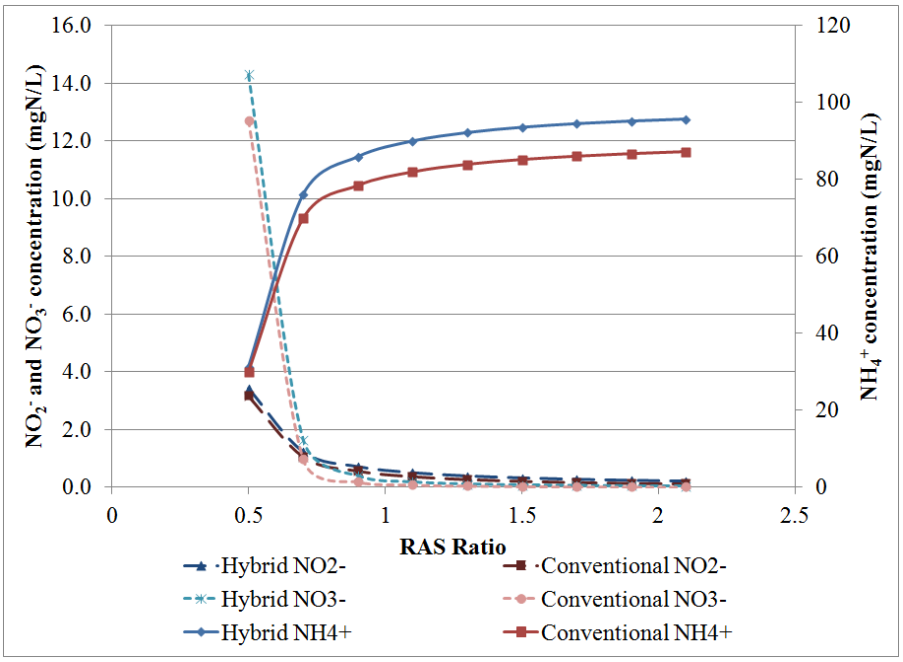

(a)

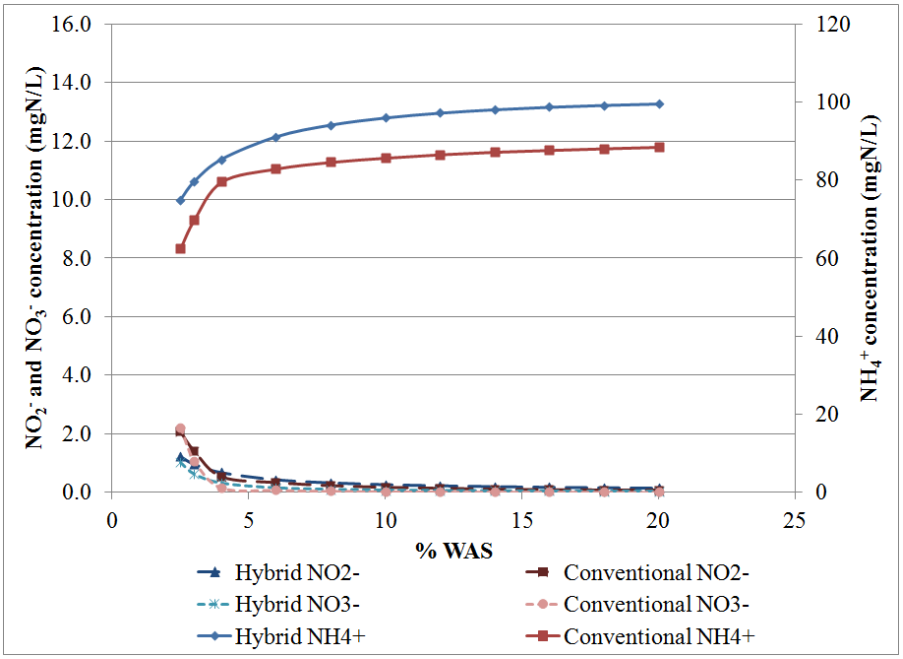

(b)

Figure 6.5. Stabilization tank inorganic nitrogen concentrations as a function of (a) RAS ratio and (b) percent WAS.

6.4 Establishing the Biosorption Parameters k_{floc} and $k_{p,f}$

I first executed the model using a range of values for k_{floc} and $k_{p,f}$ at the influent rates in Table 5.2 and with RAS of 120% and WAS of 6%. I assumed that a healthy activated sludge system would have a predominance of floc production versus shearing; therefore, I set k_{floc} greater than $k_{p,f}$. When the model was run with k_{floc} and $k_{p,f}$ active throughout the system, the model results were the same as without biosorption. This makes sense — if all PCOD hydrolyzes at the same rate throughout the system, it does not matter what form (flocculated, adsorbed or single particles) it is in.

With a second set of trials, I assumed that hydrolysis occurs in anaerobic conditions only by adding DO and NO_x switch factors to the $PCOD_f$ and $PCOD_a$ hydrolysis terms of Eqn. 51 and 52, resulting in equations 57 and 58:

$$\frac{dPCOD_f}{dt} = k_f PCOD_s \Phi G - k_{p,f} \Phi G^{p-1} PCOD_f - \left(\frac{K_{DO}^{switch}}{K_{DO}^{switch} + DO}\right)\left(\frac{K_{NO_2}^{switch}}{K_{NO_2}^{switch} + NO_2} + \frac{K_{NO_3}^{switch}}{K_{NO_3}^{switch} + NO_3}\right) k_{hyd,f} PCOD_f + \frac{Q}{V}(PCOD_f^0 - PCOD_f) \quad (57)$$

and

$$\frac{dPCOD_a}{dt} = k_{1,ad}(q - q_{eq}) - \left(\frac{K_{DO}^{switch}}{K_{DO}^{switch} + DO}\right)\left(\frac{K_{NO_2}^{switch}}{K_{NO_2}^{switch} + NO_2} + \frac{K_{NO_3}^{switch}}{K_{NO_3}^{switch} + NO_3}\right) k_{hyd,a} PCOD_a + \frac{Q}{V}(PCOD_s^0 - PCOD_s) \quad (58)$$

As reported in Table 6.1, the absolute values of k_{floc} and $k_{p,f}$ are not as important as the ratio of k_{floc} to $k_{p,f}$. Absolute values of k_{floc} and $k_{p,f}$ give reasonable results between 0.01 to 100 L^3 water/L^3 floc, but neither literature nor NUS data are available to confirm this independently. A higher the ratio of k_{floc} to $k_{p,f}$ generally leads to a larger formation of $PCOD_f$, which consumes the $PCOD_s$ available for adsorption. However, this increase in $PCOD_f$ only has a minor effect on the formation of CH_4 in the AD, and this leads to a more important point. In my model, the fractionation of $PCOD_f$ to $PCOD_a$ is less important than the process of removing $PCOD_s$ from solution. Adsorption kinetics state that any PCOD not captured by floc will be biosorbed by biomass until an equilibrium concentration of $PCOD_s$ is achieved between the solution and the biomass. Since equilibrium is reached, approximately the same total amounts of $PCOD_f$ and $PCOD_a$ flow through the system unhydrolyzed until they reache the AD, where all PCOD is hydrolyzed at the same rate. Therefore, it is more important that the PCOD is transferred to a form of biosorbed PCOD rather than a specific type of biosorbed PCOD.

The model with biosorption supports concepts put forward by the IWA ASM and by Jimenez et al. (2005 and 2007). Both sources agree that biosorption is important, even though they do not agree on whether adsorption or flocculation is the controlling mechanism in biosorption. My model concludes both are important, depending upon the operating conditions. As seen in Table 6.1, significant concentrations of $PCOD_f$ are produced when the k_{floc} to $k_{p,f}$ ratio exceeds 1000, as Jimenez et al. (2005 and 2007)'s research supports. Below that

ratio, most biosorbed PCOD occurs in $PCOD_a$ form, which is how it is modeled by IWA.

Model outputs suggest maximum and minimum values for k_{floc} to $k_{p,f}$ and the ratio of k_{floc} to $k_{p,f}$. k_{floc} and $k_{p,f}$ values lower than 10^{-7} L^3 water/L^3 floc provide no $PCOD_f$ formation, and all PCOD is absorbed by biomass. The ratio of k_{floc} to $k_{p,f}$ must range between 1000 and 5000 for floc formation and adsorption to be in equilibrium. While the model converges at larger values of k_{floc} and $k_{p,f}$, value of k_{floc} and $k_{p,f}$ exceeded 10^6 L^3 water/L^3 floc end up producing negative values of $PCOD_a$. This is specifically related to the fact that first-order adsorption kinetics does not allow for bulk solution concentrations to have values lower than the equilibrium concentration. Similarly, when the ratio of k_{floc} to $k_{p,f}$ exceeds 5000 L^3 water/L^3 floc, $PCOD_a$ concentrations becomes negative due to higher levels of $PCOD_s$ being diverted to $PCOD_f$, resulting in the wastewater being undersaturated with $PCOD_s$. This is a result of the time step between iterations being 8 hrs. When the ratio of k_{floc} to $k_{p,f}$ is equal to one, floc formation and shearing values are the same, essentially nullifying the flocculation mechanism. When the ratio of k_{floc} to $k_{p,f}$ is less than one, shearing is more important then floc entrapment. This adds additional PCODs that is then adsorbed to PCODa until the equilibrium concentration of PCODs is reached in the bulk solution.

While not elaborated in this report, variations in k_{floc} and $k_{p,f}$ had no noticeable effect on nitrogen compounds. This is related to overall system performance, and will be discussed in the next sections of this chapter.

Table 6.1. PCOD concentrations (in mgCOD/L) by tank as a function of k_{floc} and $k_{p,f}$ as well as CH_4 production in the AD. The model has a WAS of 6% of RAS flow rate and RAS of 120% of influent flow rate.

k_{floc} (floc formation) (L^3 water/L^3 floc)	**$k_{p,f}$ (floc shearing)** (L^3 water/L^3 floc)	**Ratio of k_{floc} to $k_{p,f}$**	**Concentrations (mgCOD/L)**									
			Anoxic Tank			**Contact Tank**			**Anaerobic Digester**			
			$PCOD_f$	$PCOD_a$	$PCOD_s$	$PCOD_f$	$PCOD_a$	$PCOD_s$	$PCOD_f$	$PCOD_a$	$PCOD_s$	CH_4 Production (gCOD/d)
0.001	0.0005	2	0	680	310	0	680	300	0	190	60	130
100	50	2	0	680	310	0	680	300	0	190	60	130
10000	5000	2	0	680	310	0	680	300	0	190	60	130
10	1	10	0	680	310	0	680	300	0	190	60	130
100	10	10	0	680	310	0	680	300	0	190	60	130
1000	100	10	0	680	310	0	680	300	0	190	50	130
10000	1000	10	0	680	310	0	680	300	0	190	50	130
1000	50	20	0	670	310	0	680	300	0	190	50	130
100	1	100	20	660	300	10	670	310	0	180	50	130
0.0001	0.000001	100	0	680	310	0	680	300	0	190	50	130
10	0.01	1000	160	560	250	100	560	300	40	150	50	130
100	0.1	1000	170	560	250	100	560	300	40	150	50	130
5000	1	5000	460	370	140	370	370	220	160	30	50	130

Table 6.1 continued. PCOD concentrations (in mgCOD/L) by tank as a function of k_{floc} and $k_{p,f}$ as well as CH_4 production in the AD. The model has WAS of 6% of RAS flow rate and RAS of 120% of influent flow rate.

k_{floc} (floc formation) (L^3 water/L^3 floc)	**$k_{p,f}$ (floc shearing)** (L^3 water/L^3 floc)	**Ratio of k_{floc} to $k_{p,f}$**	**Concentration (mgCOD/L)**								
			Stabilization Tank			**Clarifier**			**Sludge Thickener**		
			$PCOD_f$	**$PCOD_a$**	**$PCOD_s$**	**$PCOD_f$**	**$PCOD_a$**	**$PCOD_s$**	**$PCOD_f$**	**$PCOD_a$**	**$PCOD_s$**
0.001	0.0005	2	0	1190	380	0	700	260	0	910	130
100	50	2	0	1190	380	0	700	260	0	910	130
10000	5000	2	0	1190	380	0	700	260	0	910	130
10	1	10	0	1180	380	0	700	260	0	910	130
100	10	10	0	1180	380	0	700	260	0	910	130
1000	100	10	0	1180	380	0	700	260	0	910	120
10000	1000	10	0	1180	380	0	700	260	0	910	130
1000	50	20	0	1180	380	10	700	260	0	910	120
100	1	100	10	1150	400	40	680	240	20	890	120
0.0001	0.000001	100	10	1180	380	0	700	260	10	900	120
10	0.01	1000	80	970	480	240	560	140	180	730	110
100	0.1	1000	80	970	470	240	560	140	180	730	110
5000	1	5000	400	640	470	510	360	60	530	400	60

6.5 Modeling Results Including Biosorption Parameters k_{floc} and $k_{p,f}$

To execute the model with biosorption, I assumed k_{floc} and $k_{p,f}$ values of 100 and 0.1 L^3 water/L^3 floc, respectively, or a ratio of 1000. I evaluated the model for three different scenarios varying the following parameters: WAS between 2.5 and 20%, RAS between 50 and 210%, and SRT between 25 to 210 days. For the scenarios with varying RAS and WAS, I also evaluated the model with the conventional configuration as a baseline.

6.5.1 Variations on Percent RAS

I began by analyzing the performance of the different configurations at RAS values between 50 to 210% of influent flow rate and at a constant 6% WAS and $PCOD_0$ concentration of 250 mg VSS/L. As expected, hybrid systems consistently remove more total COD from the solid and liquid phases (including the effluent and AD wasted sludge), as seen in Figure 6.6. This is consistent with the recycle systems consistently wasting less sludge and creating a larger AD SRTs based on Eqn. 44

$$\text{AD SRT} = V_{AD}/Q_W \tag{44}$$

and demonstrated in Figure 6.7.

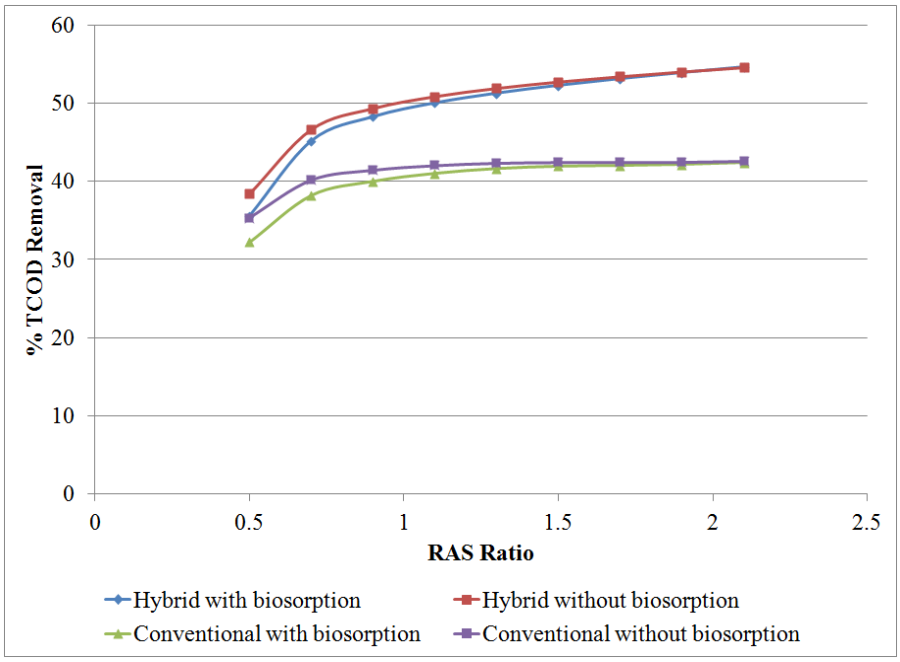

Figure 6.6. Percent total COD removal from the liquid and solids phases as a function of the RAS ratio. Total COD removal includes COD removed from the effluent and AD wasted sludge.

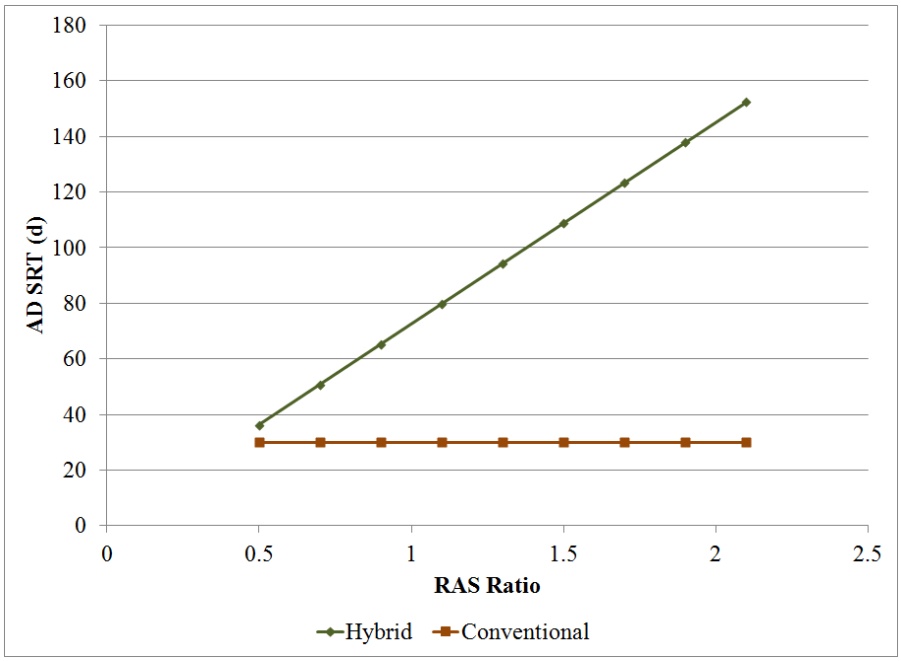

Figure 6.7. AD SRTs as a function of RAS ratio.

What may be counter-intuitive is that the model runs for the hybrid configuration excluding biosorption consistently discharges higher concentrations of TCOD in the effluent than the model including biosorption. This trend results from having consistently higher heterotrophic biomass concentrations and SRTs in the anoxic, contact, and stabilization tanks when biosorption occurs throughout the system. In the model, $PCOD_s$ is being hydrolyzed throughout the system, supplying additional substrate for biomass growth in these tanks. Therefore, the anoxic and aerobic sections of the system remove more T COD.

The hybrid trains clearly outperform the conventional trains in CH_4 production. The hybrid trains produce an average of 85 to 650% more CH_4 than the conventional trains, and the difference becomes larger with increasing RAS. A second clear trend is that including biosorption kinetics in either configuration results in increased CH_4 production, as illustrated in Figure 6.8. The hybrid model with biosorption kinetics projects 6 to 17% more CH_4 production than the same model without biosorption. With the conventional model, 11 to 16% more CH_4 is produced with biosorption in the model than without.

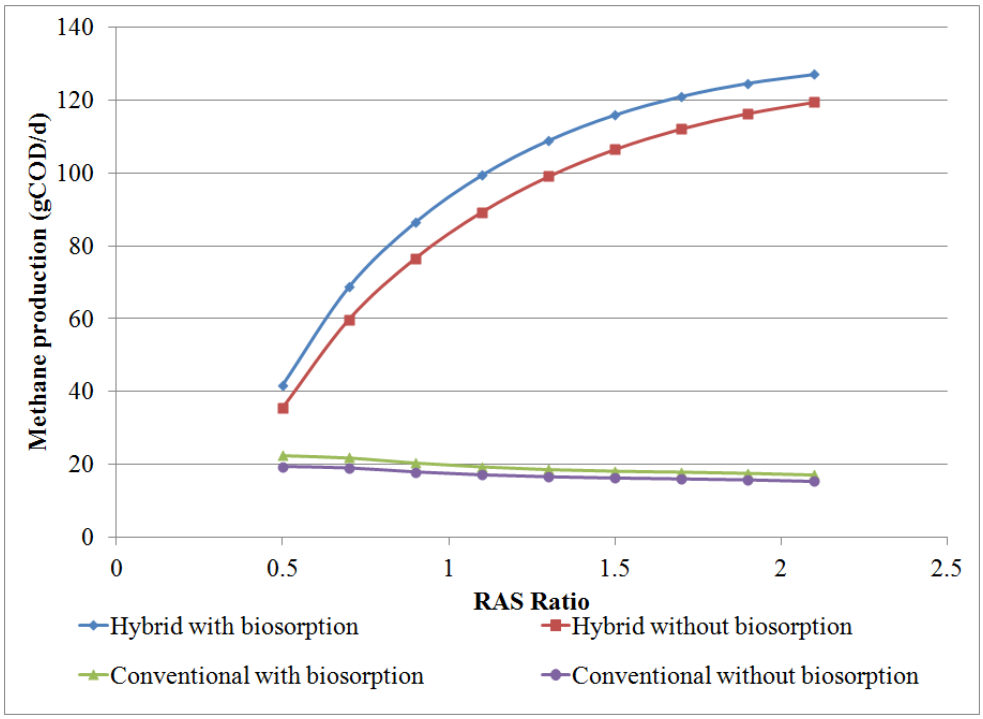

Figure 6.8. CH_4 production as a function of RAS ratio.

These same trends are observed in the amount of influent TCOD converted to CH_4, Figure 6.9. Again, the hybrid process converts more influent TCOD to CH_4 than the conventional process. With the inclusion of biosorption in the model, the hybrid system's conversion of influent TCOD increases with increasing RAS from 24 to 41%, compared with a decrease from 17 to 9% in the conventional system. For the models without biosorption, the hybrid process converts 22 to 39% of influent TCOD to CH_4 with increasing RAS, while the conventional process utilization decreases from 17 to 8%. The increases in CH_4 production are directly coupled to the assumption that hydrolysis of biosorbed PCOD can only occur in the AD and the longer AD SRTs in the hybrid process. The hybrid system also converts 7 to 33% more influent TCOD to CH_4 with

increasing RAS than the conventional system with biosorption, and 6 to 31% higher conversion without biosorption. This trend is critical--the hybrid systems achieved its goal of COD diversion to the AD, although it is driven more by AD sludge recycle than the inclusion of biosorption.

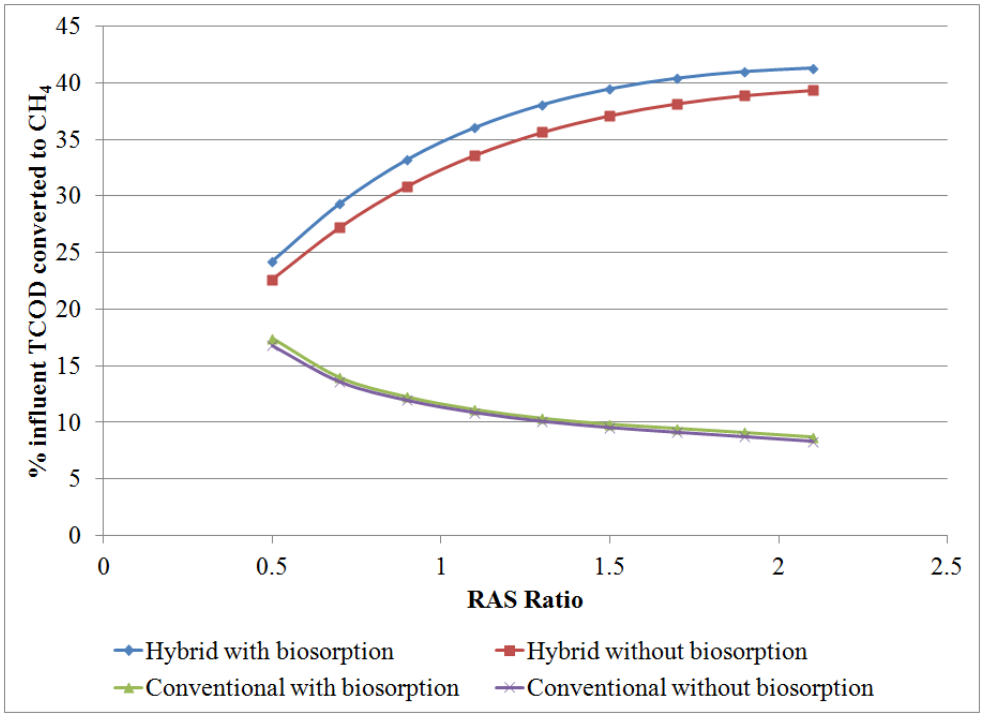

Figure 6.9. Percent of influent TCOD converted to CH_4 as a function of RAS ratio.

Sludge yields decrease with increasing RAS rate, as demonstrated in Figure 6.10, and the hybrid configuration produces less sludge than the conventional train. These differences correspond with longer AD SRTs in the hybrid configuration compared to the conventional, which is demonstrated in Figure 6.10. For the hybrid configuration, yields vary between 0.08 at 210% RAS and 0.40 at 50% RAS. For comparison, the conventional configuration yields

vary between 0.40 at 210% RAS and 0.48 at 50% RAS. Net sludge yields less than 0.15 mgVSS/mgCOD are achieved with the hybrid system only when it is operated at a RAS of 130% or greater. Net sludge yields below 0.10 mgVSS/mgCOD are only achieved at a RAS of 190% or greater in the hybrid system.

Another important trend from Figure 6.10 is that the yields are approximately the same regardless of whether the model was executed with biosorption kinetics or not. Yields vary less than 3% when comparing models with and without biosorption for the hybrid and conventional systems, respectively.

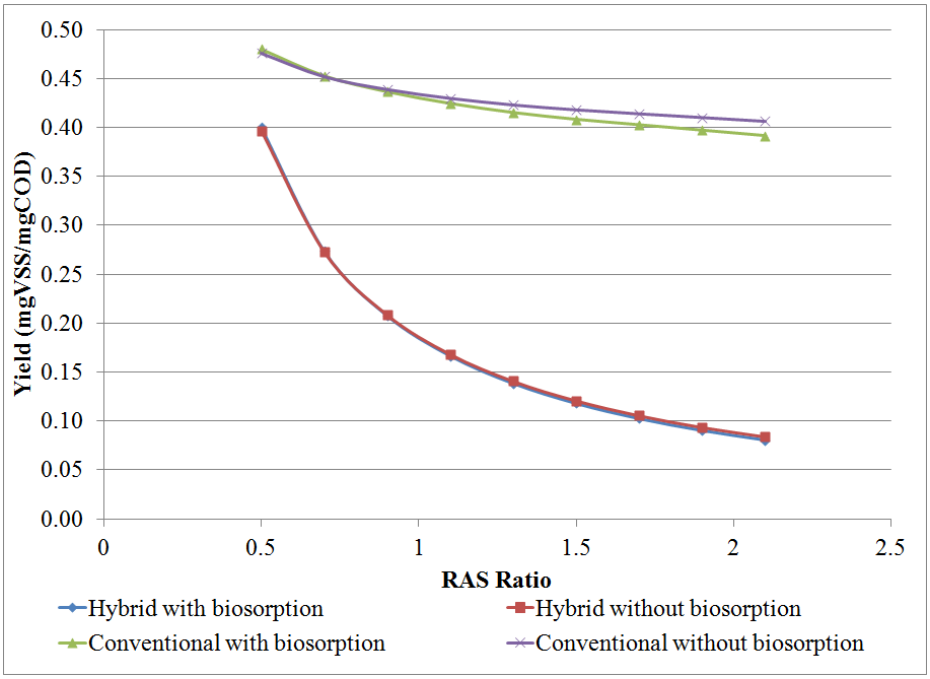

Figure 6.10. Sludge yield as a function of RAS ratio.

In conclusion, the application of sludge recycle in the hybrid system has a much more significant effect on sludge yields than the inclusion of biosorption

kinetics in the model. This supports the concept that still larger CH_4 and yield benefits could be achieved by minimizing aerobic metabolism, such as by eliminating the contact stabilization process and retaining an anoxic contactor

The lack of nitrogen NH_3 utilization in the overall system indicates that most NH_3 is being used for cell synthesis rather than nitrification. The conventional system with no biosorption has the best NH_3-removal performance, as demonstrated in Figure 6.11. At RAS ratios of 0.7 or higher, the system with no AD sludge recycle or biosorption removed 11 to 16% of influent NH_3. For comparison, the other systems all perform similarly and remove 5 to 11% of influent NH_3. In addition, NO_2^- and NO_3^- are omitted from Figure 6.11 due to their effluent concentrations being less than 0.05 mgN/L. The lack of NO_2^- and NO_3^- in the effluent also supports the concept that NH_3 is being used for cell synthesis rather than nitrification.

The stabilization tank exhibits some nitrification, because NO_2^- and NO_3^- are produced in the tank, but at low levels (< 1.0 and 3.4 mgN/L, respectively). The stabilization tank exhibits SRTs between 1.3 and 5.3 hrs for all models except the model with no AD sludge recycle or biosorption kinetics, which exhibits SRTs between 3.6 and 5.5 hrs, as demonstrated in Figure 6.12. AOB and NOB wash out at these low SRTs rather than accumulating. However, the stabilization tank was designed for low SRTs to keep anaerobic biomass inactive, but alive, and to minimize PCOD utilization. Based on this information, increased

nitrification conflicts with the goal of biosorption and, ultimately, increased CH_4 production.

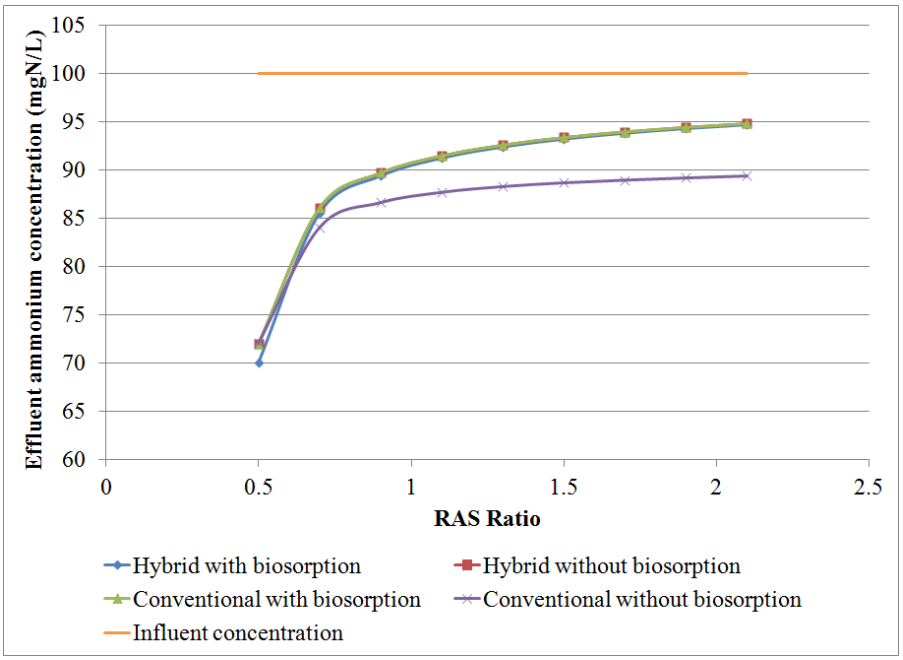

Figure 6.11. Effluent NH_3 concentration as a function of RAS ratio.

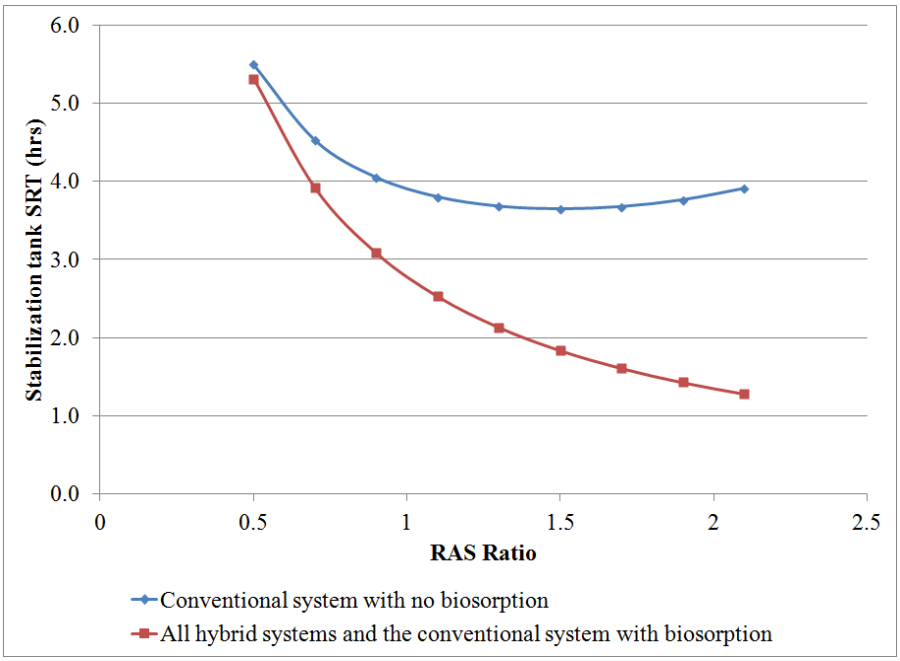

Figure 6.12. Stabilization tank SRTs with variation in RAS.

For configurations with AD recycle, additional NH_3 is transported to the stabilization tank from the AD as a result of biomass decay. The recycle causes additional NH_3 loading, which the stabilization tank does not nitrify.

While both configurations experience minimal levels of denitrification (due to minimal nitrification), minimal N_2 production and loss of total nitrogen in the system further indicate that a majority of N consumed is being diverted to cell synthesis. The conventional system is slightly more effective at denitrification than the hybrid system. In addition, increasing the RAS ratio results in decreasing denitrification efficacy, especially in the anoxic tank. As the retention time in the stabilization tank decreases, the potential for washout of AOB and NOB increases, and, therefore, the quantity of nitrification products decreases. Thus, the increasing RAS ratio results in less production of NO_2^- and NO_3^- and less denitrification under anoxic conditions in the anoxic tank or sludge thickener.

One indicator of denitrification is the loss of total nitrogen from all effluents from the system, as long as that nitrogen is not diverted entirely to cell synthesis. All trains experience a loss in total nitrogen between the influent and effluent streams, which is exhibited in Figure 6.13. While total nitrogen drops from influent to effluent, a cursory inspection cannot indicate whether this loss is due to denitrification or cell synthesis.

The model explicitly includes production of N_2 from denitrification reactions. Figure 6.14 illustrates that, like total nitrogen, N_2 production decreases with increasing RAS rate, while additional nitrogen is being removed from the

system in the wasting sludge. The models without biosorption generally result in modestly higher levels of N_2 production, and the conventional system performs more denitrification than the hybrid system under the same conditions. Similar to total nitrogen, N_2 production declines as the RAS rate goes from 50% and 70%.

What is most important in Figure 6.14 is that substantially more nitrogen is removed via AD sludge wasting than by denitrification to N_2. More nitrogen is removed as wasted sludge from the conventional system opposed to the hybrid trains. This corresponds with more nitrogen is being diverted to cell synthesis in the hybrid system versus the conventional.

A surprising trend is that a majority of denitrification does not necessarily take place in the anoxic tank, as seen in Figure 6.15. For RAS greater than 50%, a majority of N_2 is actually produced in the sludge thickener.

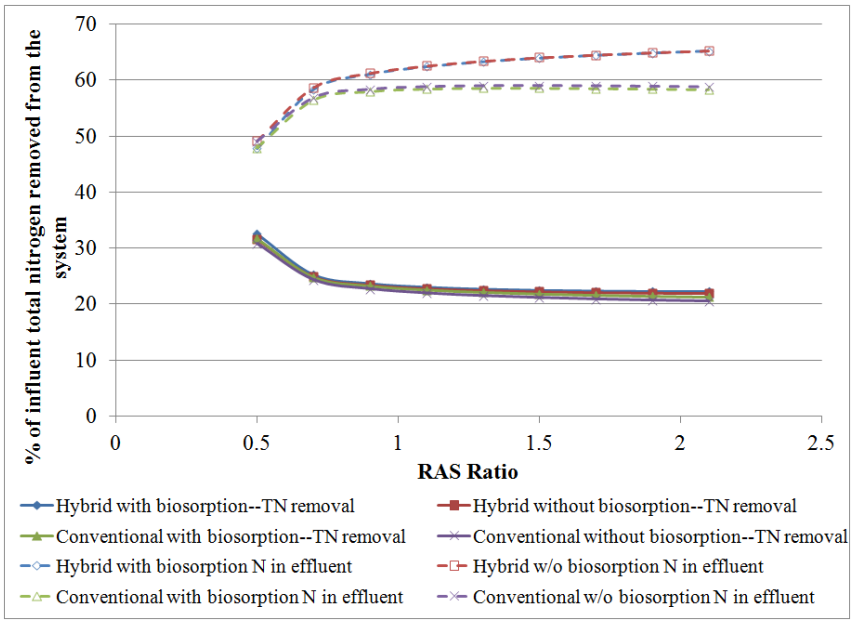

Figure 6.13. Percentage of total nitrogen removal from each system and percentage of total nitrogen discharged in the effluent from the clarifier as a function of RAS ratio.

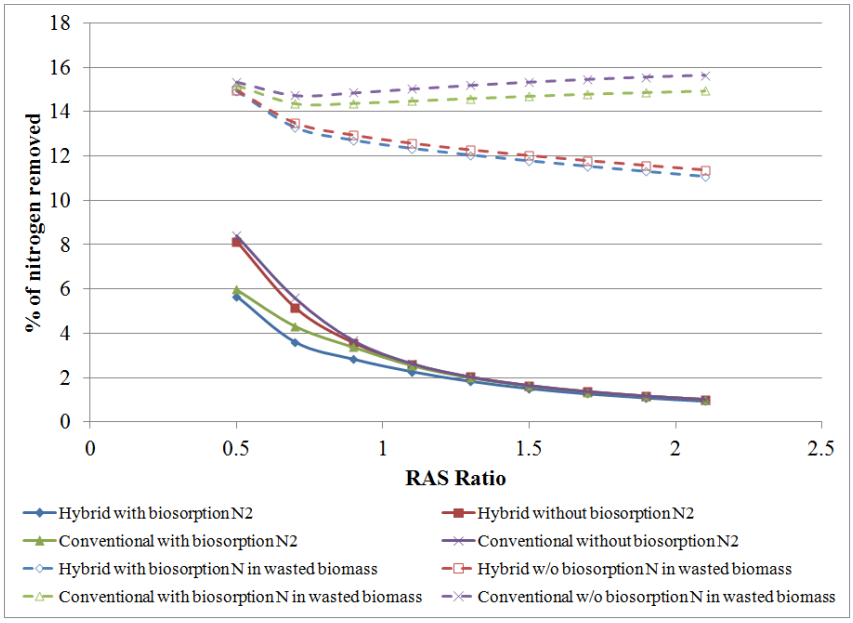

Figure 6.14. Percentage of total nitrogen that is converted to N_2 and wasted as AD sludge as a function of RAS ratio.

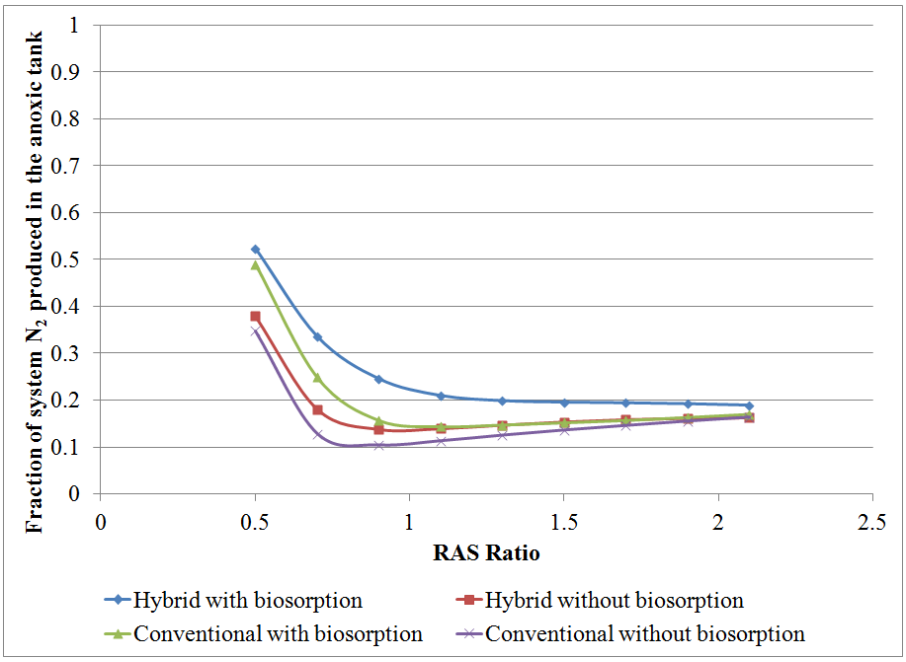

(a)

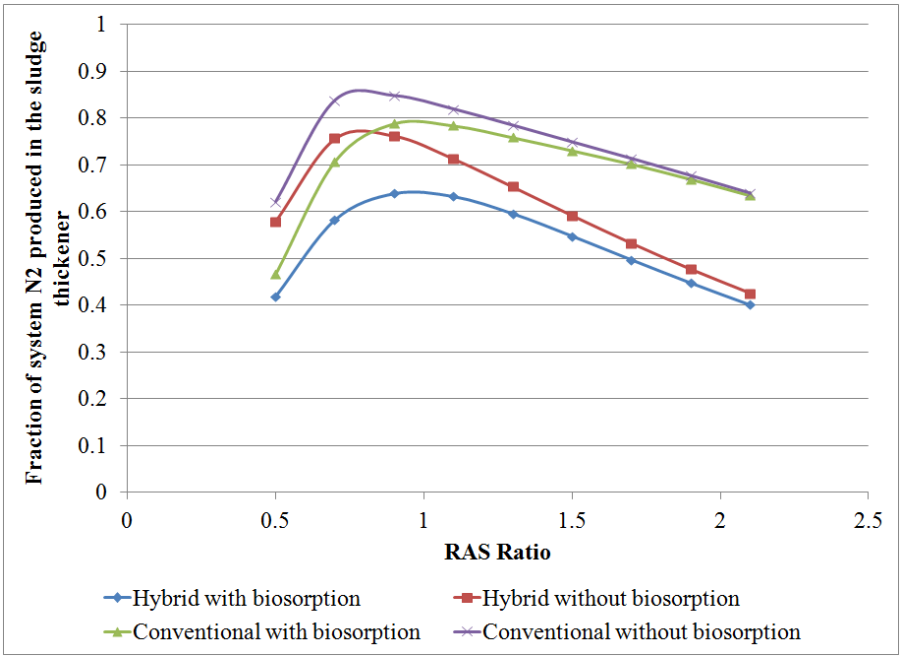

(b)

Figure 6.15. Fraction of total N_2 produced in (a) the anoxic tank and (b) sludge thickener.

To determine basic biomass trends, Figures 6.16 a through g illustrate biomass concentrations by tank for each scenario at a RAS of 90% for all active biomass, EPS, and inerts. I choose to focus on trends rather than specific numbers, since the data represent only one set of data points; specific concentrations or change percentages are not equivalent at different RAS ratios.

One trend in the biomass analysis further supports that biosorption has less effect than sludge recycle on system performance. Biosorption does not have a significant effect on any biomass concentrations in any tank. Conversely, sludge recycle with the hybrid process presents a marked increase in the concentrations of fermenters and methanogens throughout the hybrid trains.

Regardless of configuration, the anoxic tank, contact tank, and clarifier have biomass concentrations that are about one-half of that in the stabilization tank. This is caused by the concentration of solids in the underflow of the settler, which is the feed to the stabilization tank.

The hybrid configuration has higher concentrations of all active biomass than the conventional configurations except for heterotrophs, which are present in slightly higher concentrations in the conventional system. This occurs because more BOD is consumed aerobically in the conventional system, with more converted to methane in the hybrid system. As expected with AD sludge recycle and more methane production, the hybrid train has at least significantly more fermenters and methanogens than in the conventional train.

As expected, methanogens and fermenters concentrations are highest in the AD, but they also are present in the sludge thickener at concentrations at one-half to one-third of those in the AD. Although it is operating under anoxic conditions, the sludge thickener's small volume and shorter SRT prevent methanogens from performing effective CH_4 production. Importantly, methanogens and fermenters are present in significant levels in all tanks of the hybrid system. This is cause by AD sludge recycle and is consistent with the experimental findings in Chapter 4.

The concentrations of AOB and NOB are similar in all tanks and all configurations except for the AD and the ST. The concentrations are high in the ST due to solids concentration in the settler underflow. The concentrations of AOB and NOB drop significantly in the AD due to hydrolysis of inactive biomass.

Trends in inert biomass generally track those of methanogens, while EPS generally has a unique pattern. EPS is high in the ST, SL, and AD, and this related to high solids concentrations in those tanks.

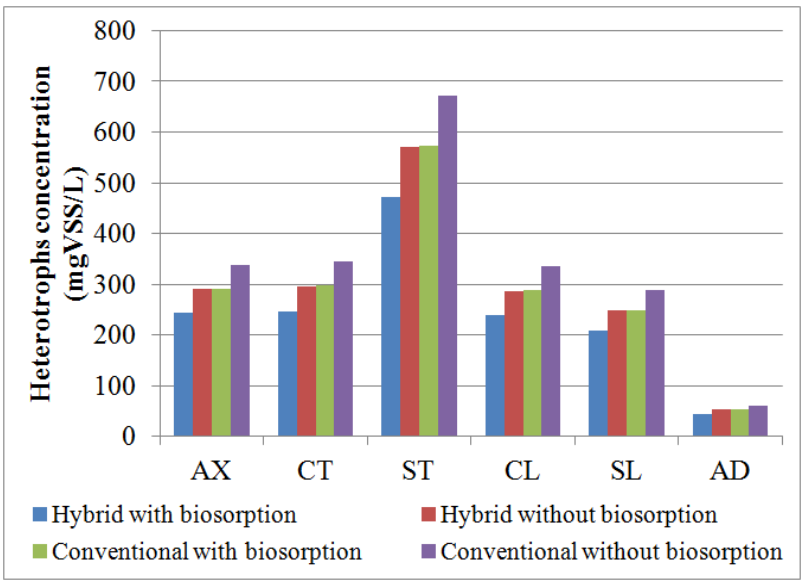

(a)

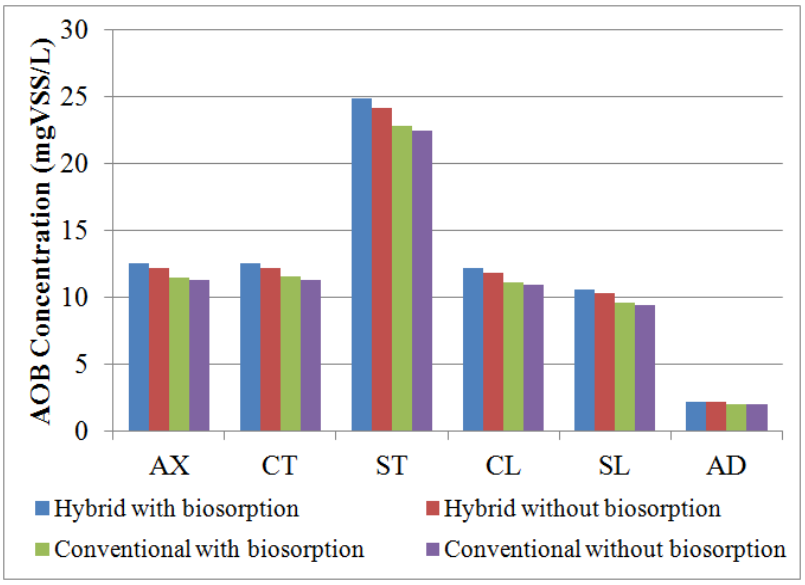

(b)

Figure 6.16. Biomass concentrations by tank for the hybrid and conventional trains with and without biosorption at 90% RAS. (a) Heterotrophs, (b) AOB, (c) NOB, (d) fermenters, (e) methanogens, (f) EPS, and (g) inert biomass.

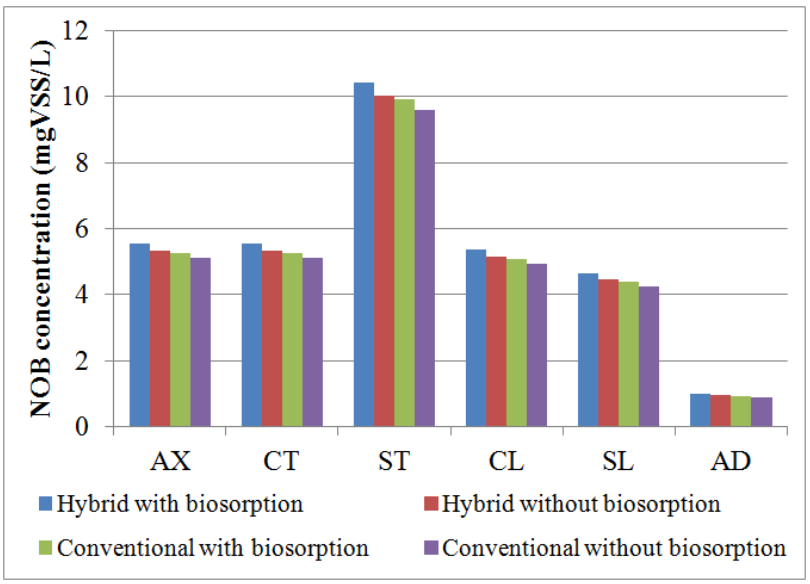

(c)

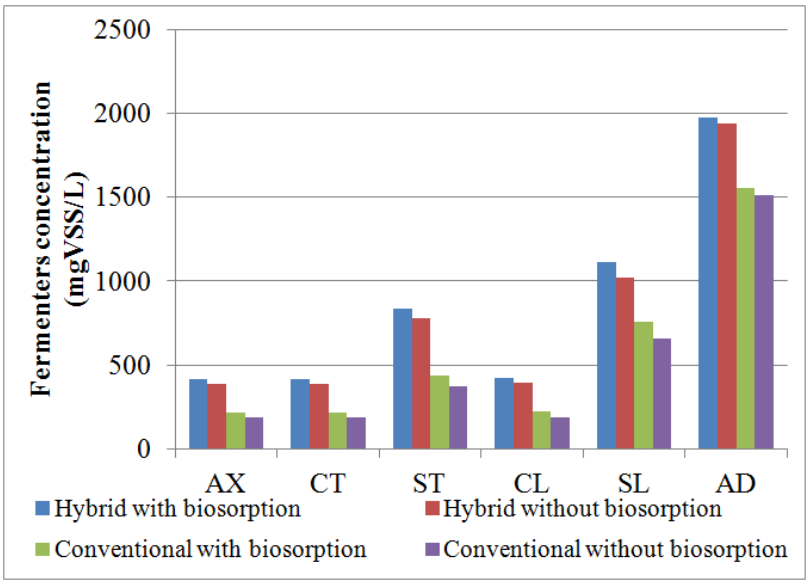

(d)

Figure 6.16 continued. Biomass concentrations by tank for the hybrid and conventional trains with and without biosorption at 90% RAS. (a) Heterotrophs, (b) AOB, (c) NOB, (d) fermenters, (e) methanogens, (f) EPS, and (g) inert biomass.

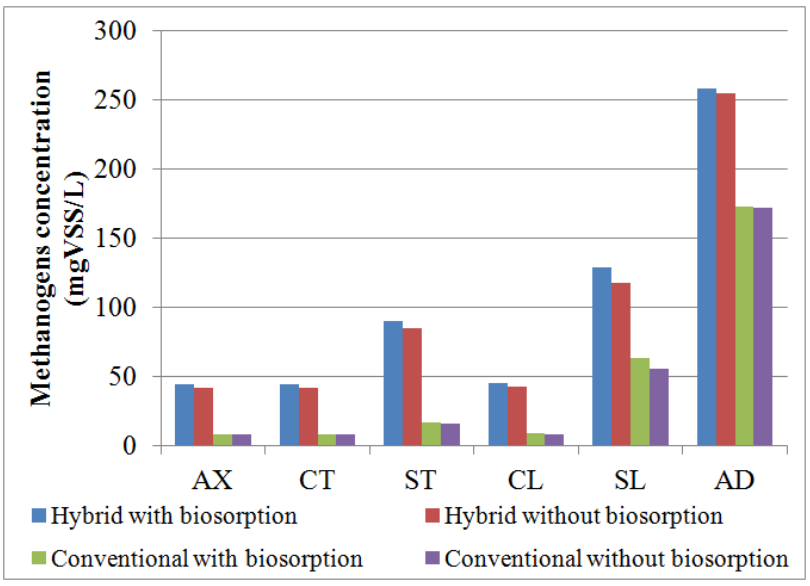

(e)

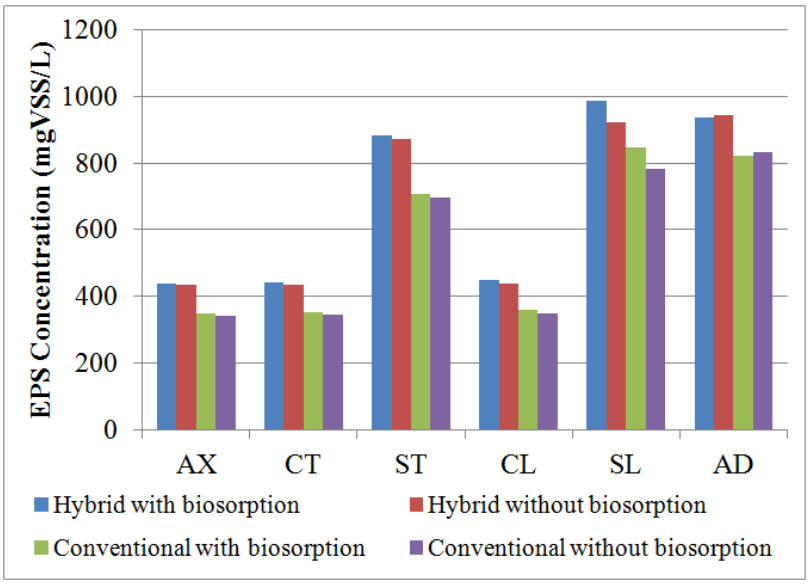

(f)

Figure 6.16 continued. Biomass concentrations by tank for the hybrid and conventional trains with and without biosorption at 90% RAS. (a) Heterotrophs, (b) AOB, (c) NOB, (d) fermenters, (e) methanogens, (f) EPS, and (g) inert biomass.

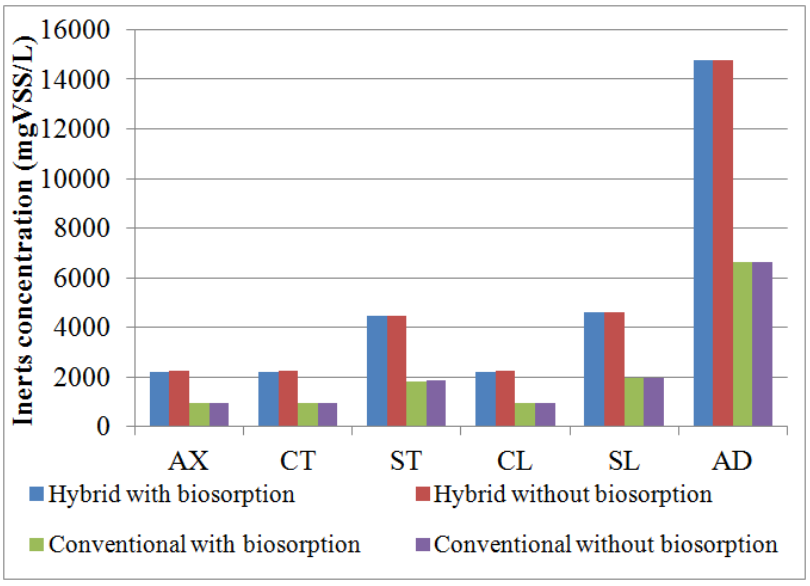

(g)

Figure 6.16 continued. Biomass concentrations by tank for the hybrid and conventional trains with and without biosorption at 90% RAS. (a) Heterotrophs, (b) AOB, (c) NOB, (d) fermenters, (e) methanogens, (f) EPS, and (g) inert biomass.

Consistent with the trend in actual AD SRTs, process configuration plays a critical role in the time required for the systems to reach steady-state operation, with increases in RAS resulting in the hybrid trains taking 33 to 158% more time to reach steady state than the conventional trains. I define operational steady state as less than 1% change in all concentrations in all tanks over a two-week period. As seen in Figure 6.17, biosorption does not have an effect on the time to reach steady state. All systems take approximately 260 to 270 days (0.75 yrs) to reach steady state at a RAS of 50%, and culminate in 546 days (1.5 yrs) for the hybrid

and 211 (0.58 yrs) days for the conventional train to reach steady state at a RAS of 210%. This is directly influenced by the effect of increasing AD SRT in the hybrid trains with increasing RAS. This may be a substantial consideration when commercializing the hybrid process, since it takes so long to reach steady state and achieve the maximum returns on sludge yields, CH_4 production and TCOD removal.

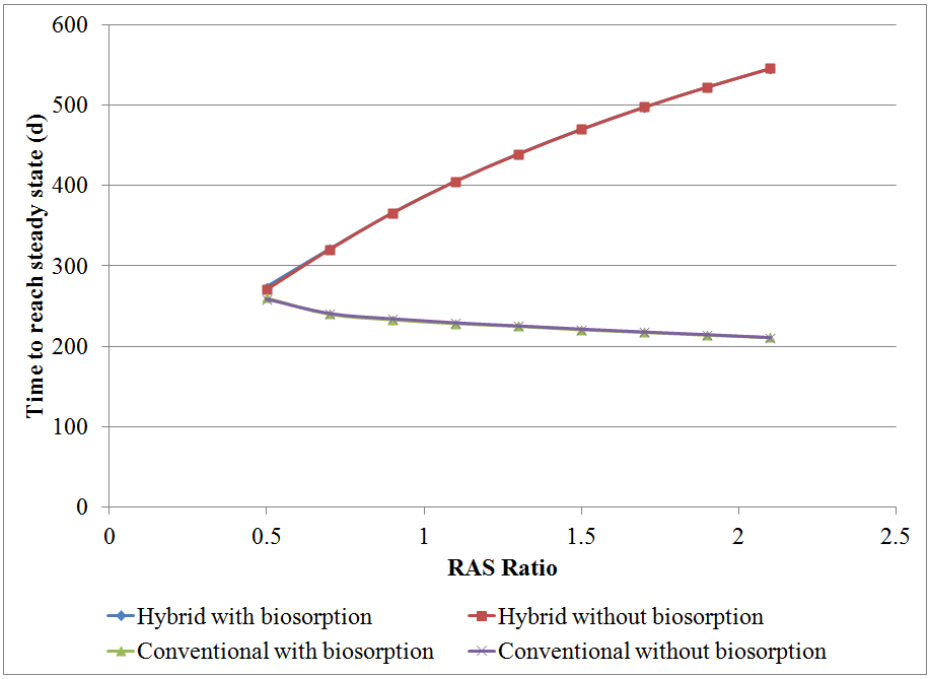

Figure 6.17. The time required for the system to reach steady state operations as a function of RAS ratio.

In summary, with increasing RAS rate, the hybrid systems removes marginally more total COD from the liquid phase, but has significantly higher CH_4 production and lower sludge yields than the conventional configuration. With increasing RAS ratio, the hybrid train produces 83 to 680% more CH_4 than the conventional train with biosorption and 86 to 640% more CH_4 without

biosorption. In addition, the hybrid train converts 7 to 33% more influent TCOD to CH_4 than the conventional train when biosorption kinetics are present in the model. The hybrid models without biosorption result in a conversion from 6 to 31% when compared with the conventional model. Regardless of the presence of biosorption kinetics, the hybrid train generates 17 to 79% less sludge than the conventional train, with the difference larger with increasing RAS ratio.

Regardless of configuration, the system exhibits poor nitrification due to the short SRTs in the stabilization and contact tanks. Short SRTs are necessary to encourage PCOD adsorption and transport of TCOD to the AD for conversion to CH_4. Effluent NH_3-N is higher with the hybrid configuration due to the influx of additional NH_3 from the AD. The lack of NO_2^- and NO_3^- production due to poor nitrification means that denitrification performance is poor. While denitrification is minimal, N_2 production decreases as RAS ratio increases, and the conventional train outperforms the hybrid system at the same operating conditions.

Biosorption does not have a significant impact on most aspects of process performance, except that CH_4 production increases by 10 to 15% with AD sludge recycle. More important than biosorption is recycling AD solids to the aerobic part of the hybrid system, as it significantly increases the overall SRT and allows for increased methanogens and fermenters concentrations throughout the hybrid system. Consequently, AD sludge recycle improves CH_4 production and decreases sludge yields.

6.5.2 Variations on Percent WAS

WAS flow rate was varied between 2.5 and 20% of RAS flow rate with constant RAS of 120% of the influent flow rate, AD SRT of 30 days, and $PCOD_0$ concentration of 250 mg VSS/L. For variations in WAS rate, I focus my analysis specifically on the differences in performance between the configurations with (hybrid) and without (conventional) AD sludge recycle.

Like with variations in RAS, the hybrid system shows greater total COD removal than the conventional configuration, and the hybrid system's performance improves with increasing WAS rate. As seen in Figure 6.18, the hybrid model demonstrates 6 to 10% more COD removal from the overall system in the liquid phases (including the effluent and AD wasted sludge). Also like with variations of RAS, the hybrid system wastes less overall sludge from the AD. However, Figure 6.19 demonstrates that increasing the WAS rate results in much higher AD SRTs (as calculated from Eqn. 44) than demonstrated with increasing RAS rate. This indicates that changing WAS (while holding RAS constant) can have a much greater effect on total COD reduction than changing RAS (with WAS at a fixed ratio of RAS).

The hybrid configuration produces more CH_4 than the conventional train, and its methane production improves with increasing WAS. The hybrid configuration produces 2 to 40 times more CH_4 than the conventional configuration (Figure 6.20). Conversely, the conventional configuration actually experiences a decrease in CH_4 production with increasing WAS rate. As demonstrated in Figure 6.21, this trend significantly affects the conversion of

influent TCOD to CH_4, which favors the hybrid train by 15 to 38% with increasing WAS. This demonstrates that the increased AD SRT in the hybrid trains and the retention of AD sludge throughout the hybrid system is a prominent driver in increased CH_4 production.

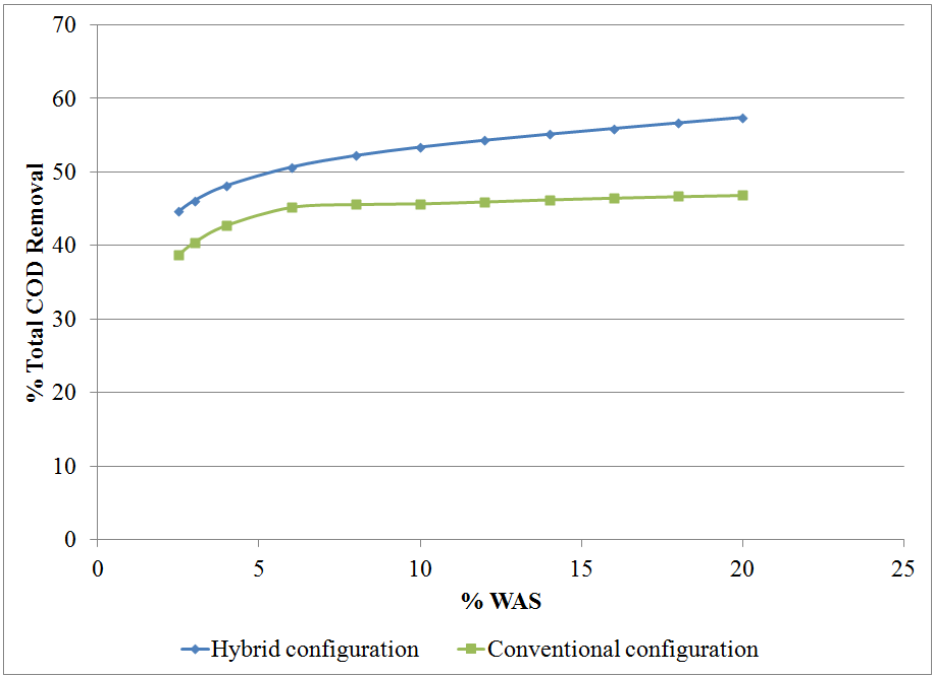

Figure 6.18. Percent of total COD removal from the liquid phases as a function of percent WAS. Total COD removal includes COD removed from the effluent and AD wasted sludge.

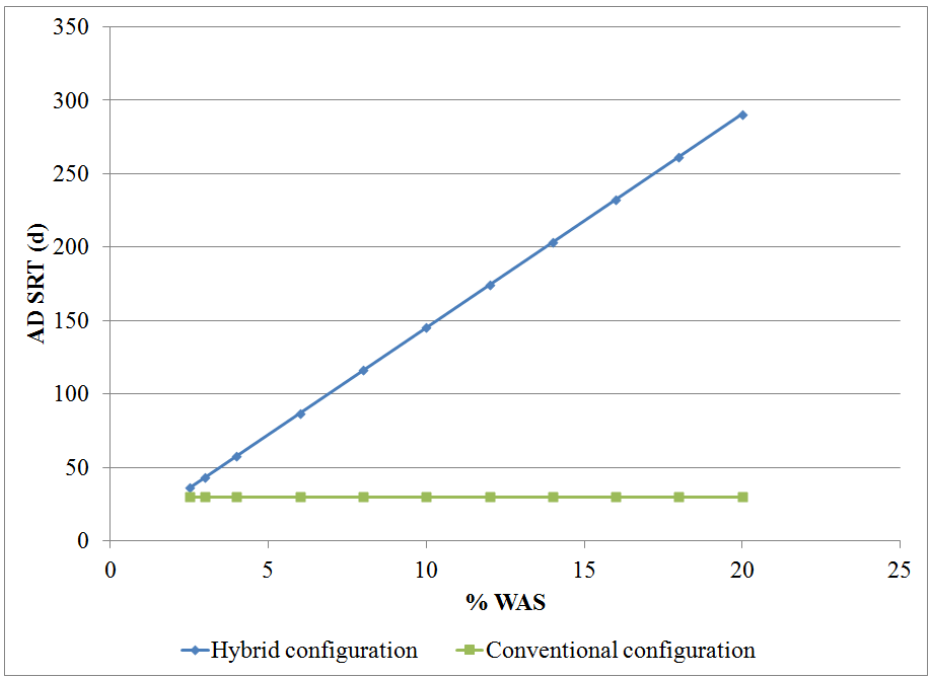

Figure 6.19. Variation in AD SRTs with changes in WAS flow rate.

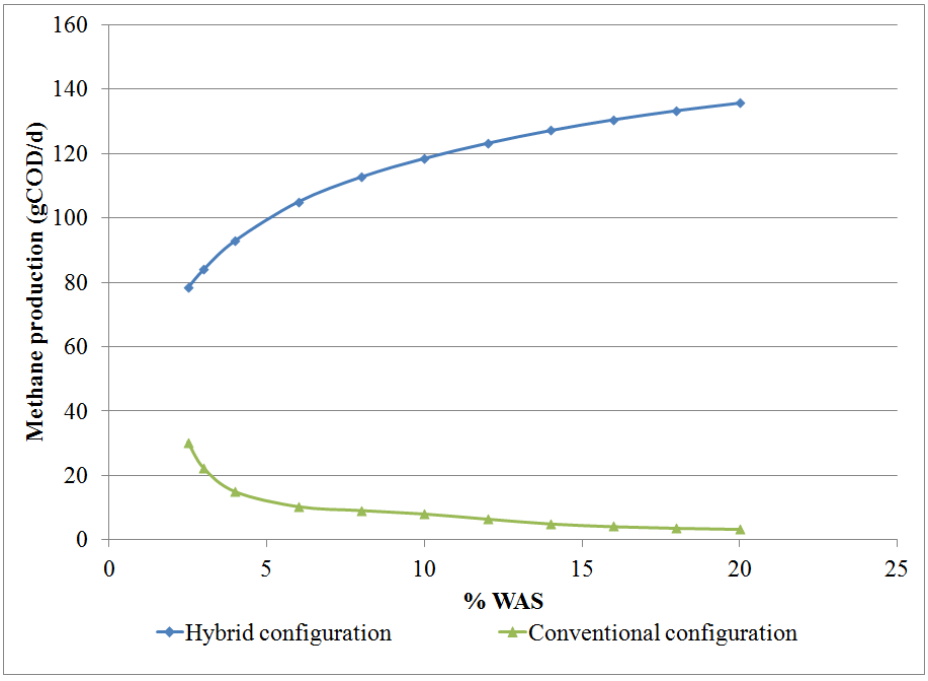

Figure 6.20. Changes in AD CH_4 production with increasing WAS flow rate.

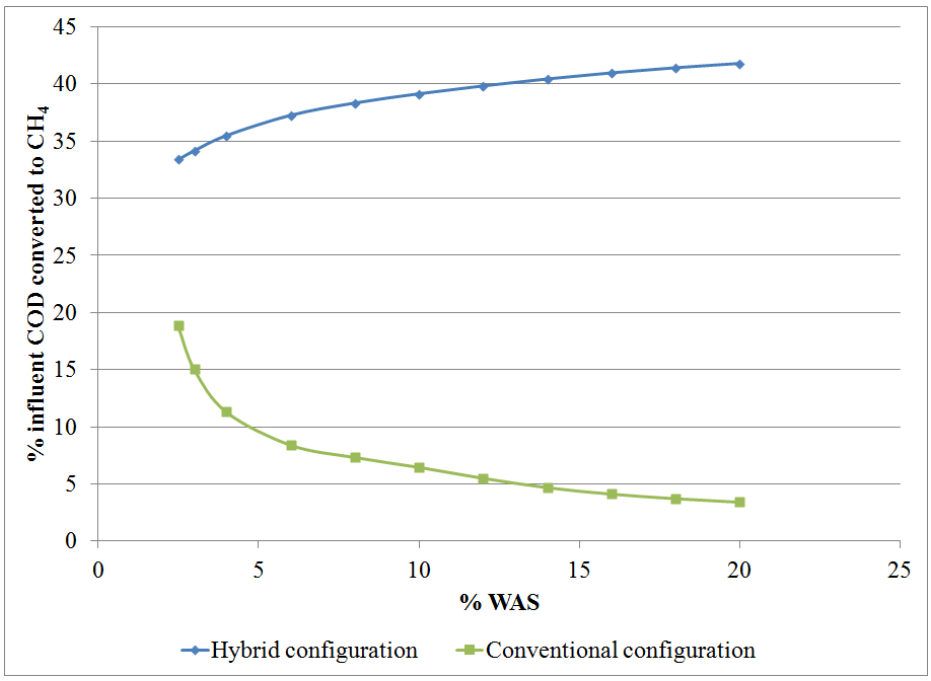

Figure 6.21. Percent of influent TCOD converted to CH_4 as a function of RAS ratio.

The hybrid system demonstrates a significant performance advantage over the conventional system through significantly lower sludge yields, as illustrated in Figure 6.22. For both systems, yields decrease with increasing WAS rate. The hybrid configuration produces 11% to 83% less sludge than the conventional train with increasing WAS. Again, this is SRT controlled: as SRT increases in the AD, sludge yields decrease due to biomass decay. Like RAS, significantly low sludge yields are only obtained by the hybrid train. Unlike RAS, these low sludge rates can be produced at relatively low WAS rates: net sludge yields below 0.15 mgVSS/mgCOD can be achieved at a WAS rate of 6% or higher, and yields below 0.10 can be obtained at WAS rates of 10% or more. In addition, the lower sludge yields in the hybrid trains indicate a lower solids concentration in the AD.

This lower solids concentration is ultimately supports that COD is being anaerobically, which is not consistent with improved biosorption.

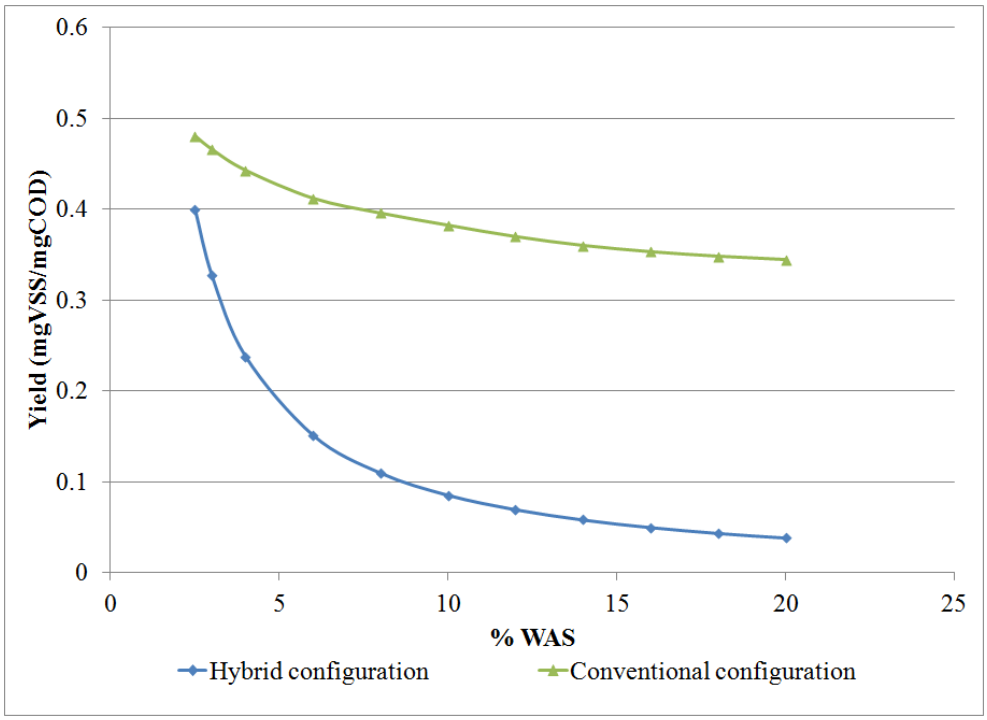

Figure 6.22. Sludge yield as a function of WAS flow rate.

Nitrification trends with increasing WAS are the similar to those with increasing RAS: both configurations present poor NH_3 removal, but the conventional system reduces effluent NH_3 concentration more than the hybrid system, as illustrated in Figure 6.23. The hybrid process reduces NH_3 in the effluent by 3 to 18%, while the conventional process reduces NH_3 by 10 to 26%. Like RAS trends, the hybrid process experiences less nitrification for several reasons: washout in the contact tank, shorter SRTs in the stabilization tank (Figure 6.24), and the transport of additional NH_3 to the stabilization tank from biomass decay in the AD.

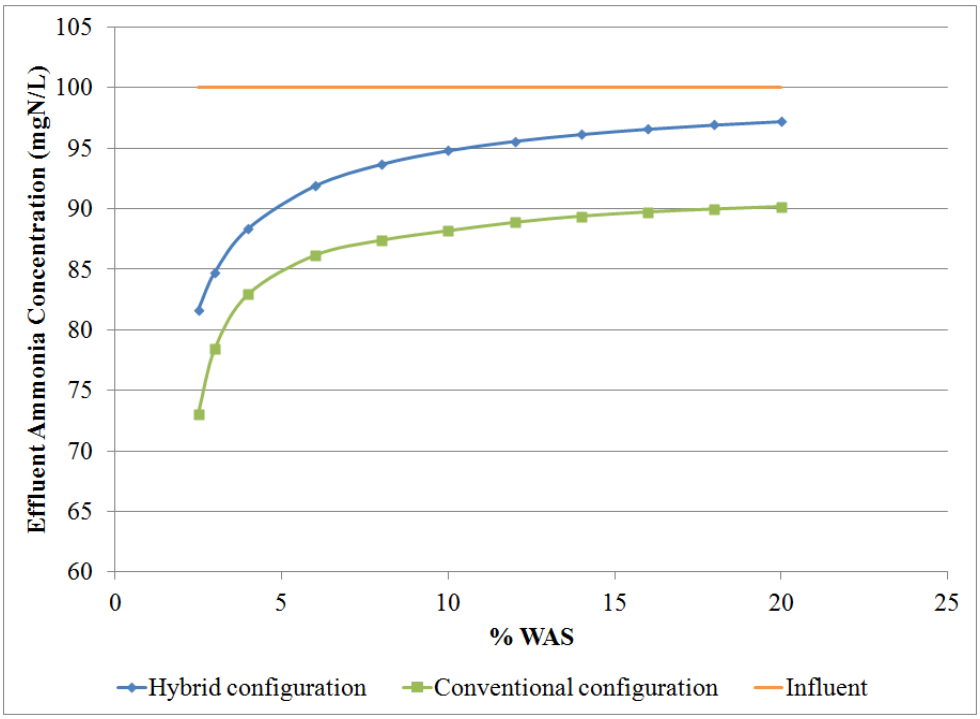

Figure 6.23. Effluent ammonia concentration as a function of WAS rate.

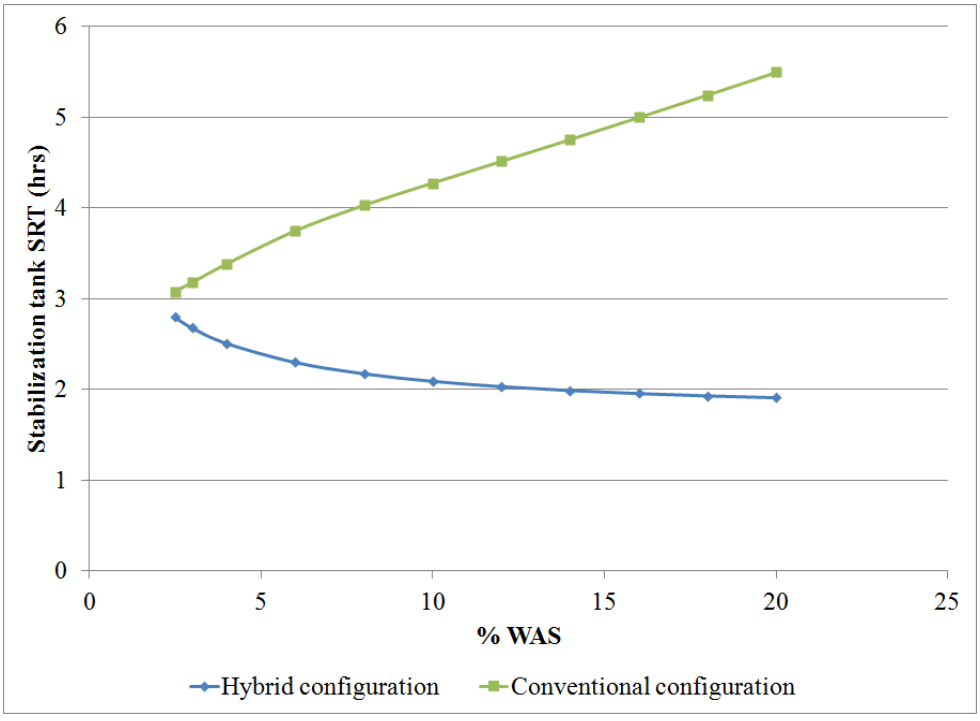

Figure 6.24. Stabilization tank SRT as a function of WAS rate.

While both systems exhibit lackluster denitrification, the conventional train is consistently removes more total nitrogen than the hybrid train. Like RAS, increasing WAS ratio results in decreasing denitrification efficacy. As exhibited in Figure 6.25, all trains experience a reduction in total nitrogen between the influent and effluent streams. At the same time, more nitrogen was being diverted to wasting sludge. The highest levels of removal occur at 2.5% WAS, and drop by half at a WAS of 6%.

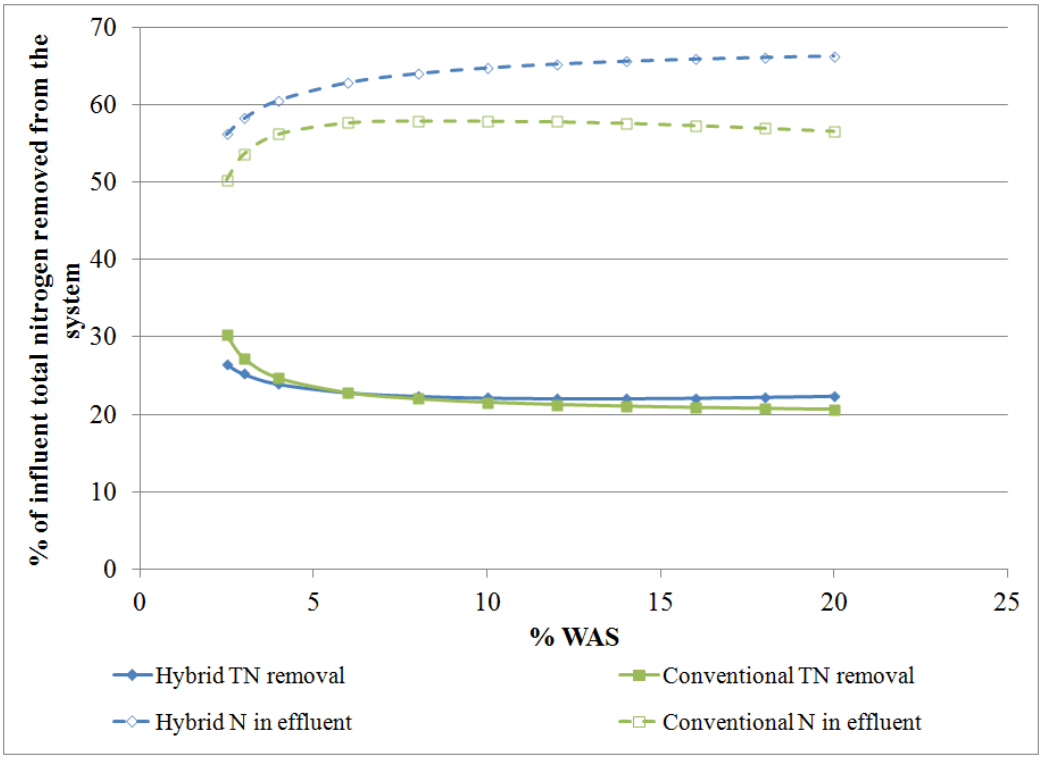

Figure 6.25. Percentage of total nitrogen removed from system and the percentage of total nitrogen discharged in the clarifier effluent as a function of WAS ratio.

Figure 6.26 illustrates a decrease in N_2 production with increasing WAS rate, with the conventional system performing more denitrification than the hybrid

system. At a WAS of 2.5%, the conventional train converts 6% of influent TN to N_2, while the hybrid process produces 4%. As WAS increases, both trains produce less N_2, with the lowest production at 0.5% at 20% WAS. This reiterates how sensitive N_2 removal is to small increases in RAS rate.

Nitrogen removal in wasted AD sludge is much greater than denitrification in all cases. The conventional train wastes 1 to 5% more TN in its wasting sludge opposed to the hybrid train, since the net biomass yield is higher.

Following the same trend as RAS, a majority of N_2 is actually produced in the sludge thickener, not in the anoxic tank (not shown).

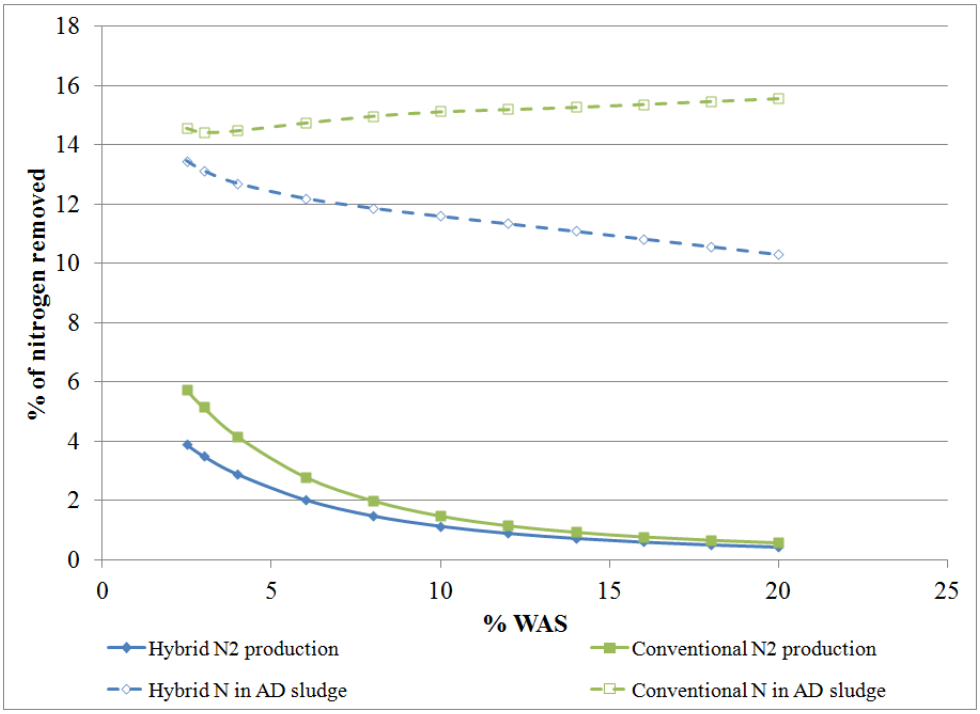

Figure 6.26. Percentage of total nitrogen that is converted to N_2 and discharged as wasted sludge as a function of % WAS.

Figures 6.27 a through g demonstrate biomass concentrations in each tank for each configuration at a WAS of 6%. The biomass concentrations in the WAS model demonstrate similar trends to the concentrations demonstrated at a RAS of 90%. Like RAS, concentrations are almost identical between the anoxic tank, contact tank, and clarifier portions, with the little anaerobic biomass in these tanks being supplied by the AD sludge recycle via the stabilization tank. Again, the longer AD SRTs encourage larger concentrations of fermenters and methanogens in the AD and sludge thickener of the hybrid system as opposed to the conventional system. The AD exhibits hydrolysis of heterotrophs, AOB, and NOB. The stabilization tank's biomass concentrations integrate improved aerobic conditions with the increased concentration of anaerobic biomass from the AD sludge recycle.

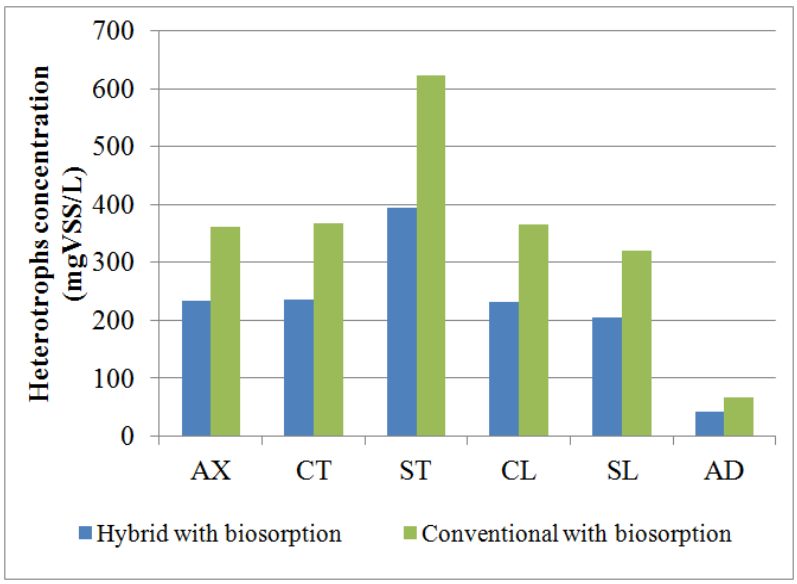

(a)

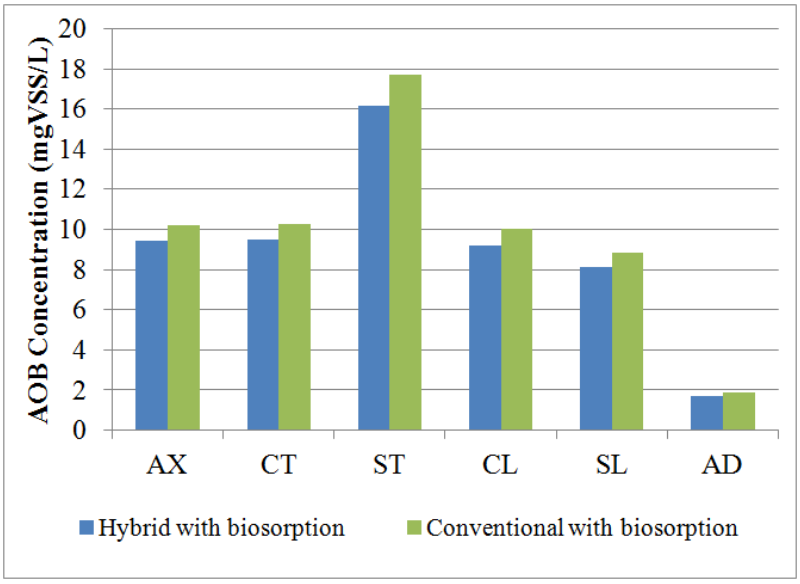

(b)

Figure 6.27. Biomass concentrations by tank for the hybrid and conventional trains with and without biosorption at 6% WAS. (a) Heterotrophs, (b) AOB, (c) NOB, (d) fermenters, (e) methanogens, (f) EPS, and (g) inert biomass.

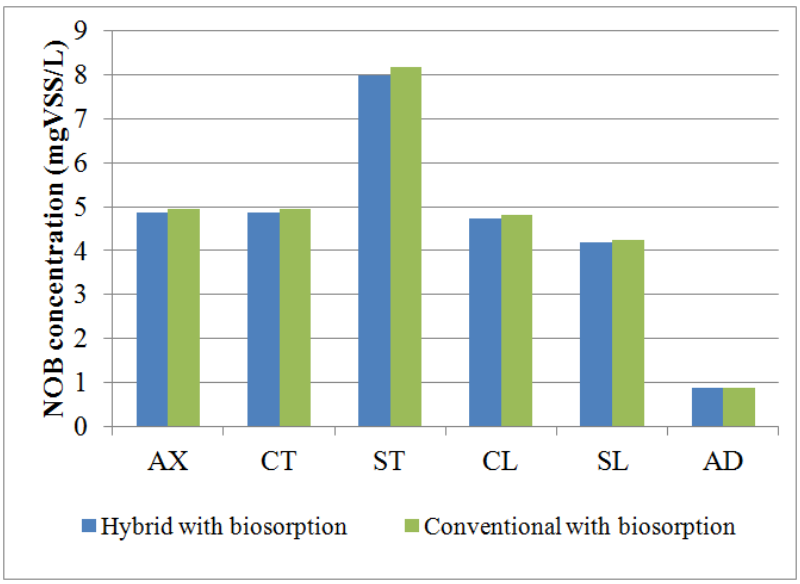

(c)

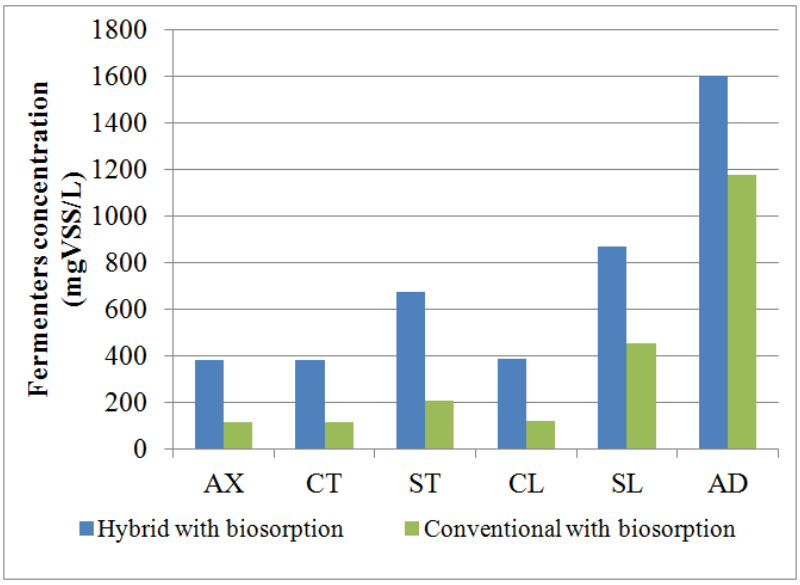

(d)

Figure 6.27 continued. Biomass concentrations by tank for the hybrid and conventional trains with and without biosorption at 6% WAS. (a) Heterotrophs, (b) AOB, (c) NOB, (d) fermenters, (e) methanogens, (f) EPS, and (g) inert biomass.

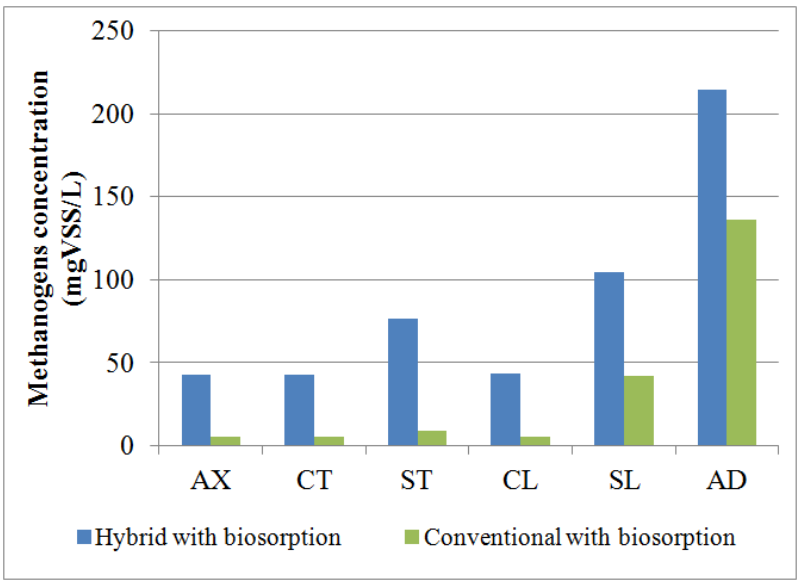

(e)

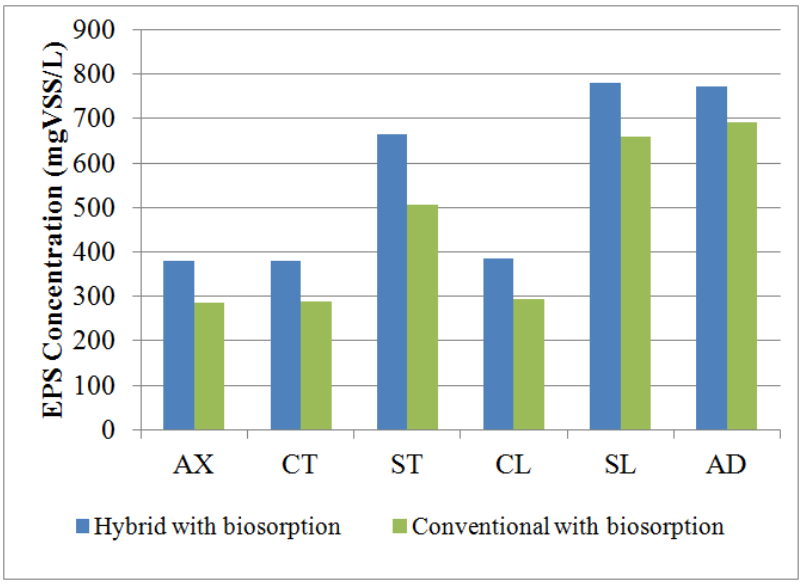

(f)

Figure 6.27 continued. Biomass concentrations by tank for the hybrid and conventional trains with and without biosorption at 6% WAS. (a) Heterotrophs, (b) AOB, (c) NOB, (d) fermenters, (e) methanogens, (f) EPS, and (g) inert biomass.

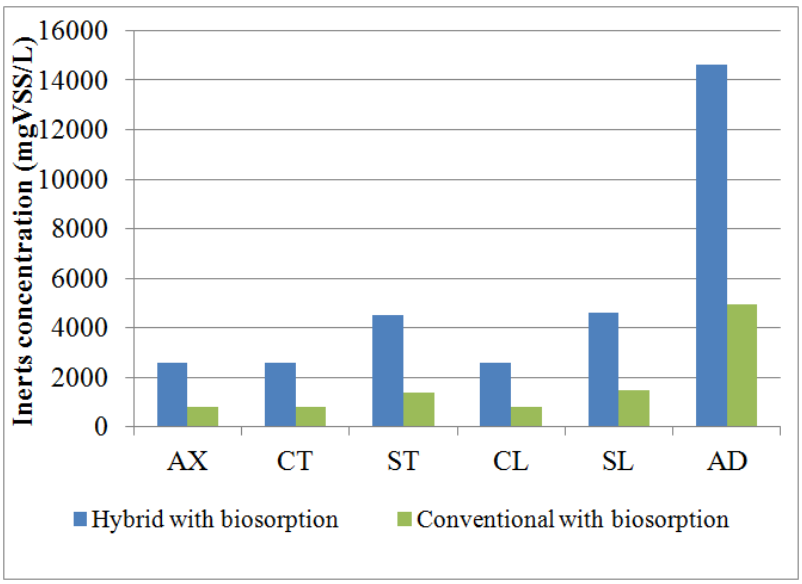

(g)

Figure 6.27 continued. Biomass concentrations by tank for the hybrid and conventional trains with and without biosorption at 6% WAS. (a) Heterotrophs, (b) AOB, (c) NOB, (d) fermenters, (e) methanogens, (f) EPS, and (g) inert biomass.

Like the trend in RAS, the hybrid system takes much longer to reach steady state operations when compared with the conventional train, which is illustrated in Figure 6.28. At a WAS of 2.5%, the time to steady state is approximately 265 days (0.73 years) for each configuration. With increasing WAS, the time it takes the hybrid train to reach steady state increases to 723 days (1.98 years) by 20% WAS. Conversely, the conventional train's time to steady state decreases with increasing WAS to 201 days at 20% WAS. Again, the hybrid system takes longer to reach steady state due to actual AD SRT increasing from 36 to 290 days with increasing WAS. For comparison, the hybrid train takes 546

days to reach steady state at a RAS of 20%. Therefore, WAS has a more significant effect on time to steady state than RAS.

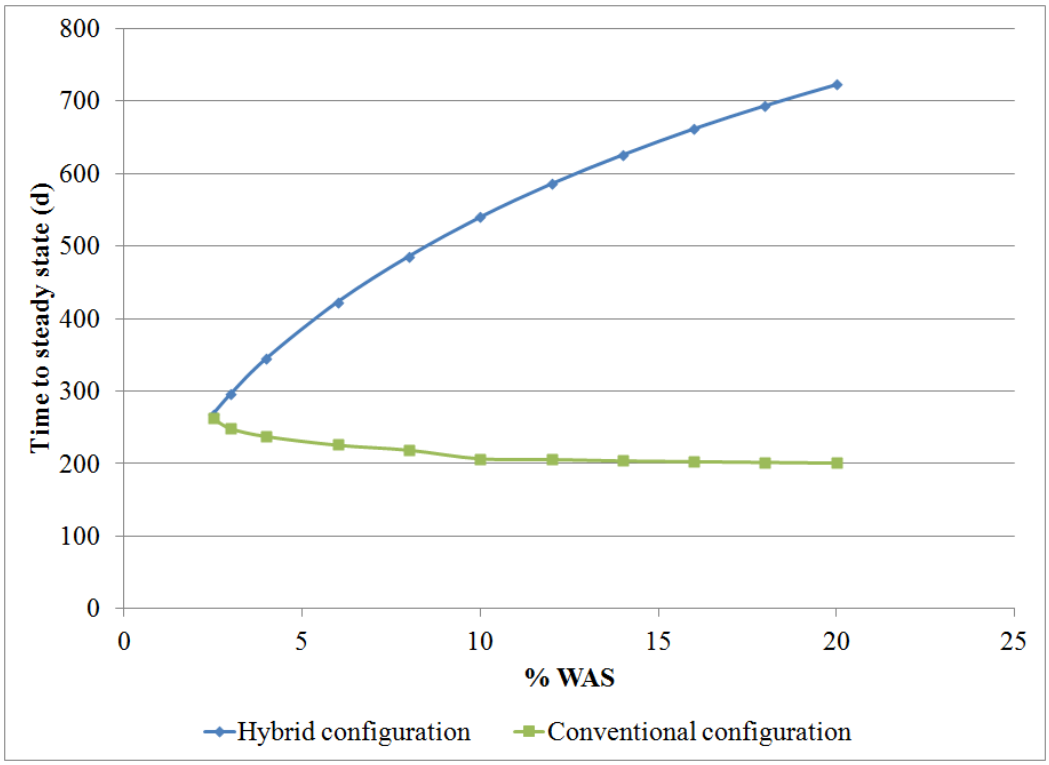

Figure 6.28. The time required for each system to reach operational steady state as a function of percent WAS.

To summarize, the trends in system performance are similar between variations in WAS and RAS: the hybrid configuration removes marginally more total COD from the liquid stream, produces significantly more methane, and produces considerably less sludge than the conventional train. The hybrid system produces 2 to 40 times more CH_4 and converts 15 to 38% more influent TCOD to CH_4 in comparison with the conventional system. The hybrid process produces 11% to 83% less sludge than the conventional process with increasing WAS. These parameters improve with increasing WAS rate. Again, this is directly

related to AD SRTs being larger in the hybrid train. With increasing WAS, the hybrid train experiences longer SRTs and, consequently, more CH_4 production and less sludge than the same configuration with increasing RAS. Thus, it is slightly more beneficial to maximize WAS when compared with RAS.

6.5.3 Variations in SRT

For the analysis of effects of AD SRT, I specifically focused on the effects on the hybrid system, since it has consistently outperformed the conventional system in CH_4 production and sludge yield reduction. Nominal AD SRTs were varied between 25 and 210 days, based on Eqn. 41:

$$\text{AD SRT} = V_{AD}/(Q_{AD} + Q_W)$$

Actual AD SRTs can be substantially larger. For comparison, I also calculated an "actual" SRT based on Eqn 44:

$$\text{AD SRT} = V_{AD}/Q_W$$

The model was executed assuming values of 100 for k_{floc} and 0.1 L^3 water/L^3 floc for $k_{p,f}$, or a ratio of 1000.

Illustrated in Figures 6.29 and Figure 6.30, TCOD removal and CH_4 production increase with increasing AD SRT, in part due to hydrolysis being the limiting kinetic mechanism. For the operating conditions used, the actual SRT is about 3-fold larger than the nominal SRT.

Figure 6.30 appears to have an inflection point around 60 days nominal SRT. This is further elaborated by the net production rate of acetate in Figure 6.31, where the rate of increase in net acetate production decreases after about 50

days. This begins to make the methanogens severely acetate limited, which corresponds to a very low net growth rate methanogens, as illustrated in Figure 6.32.

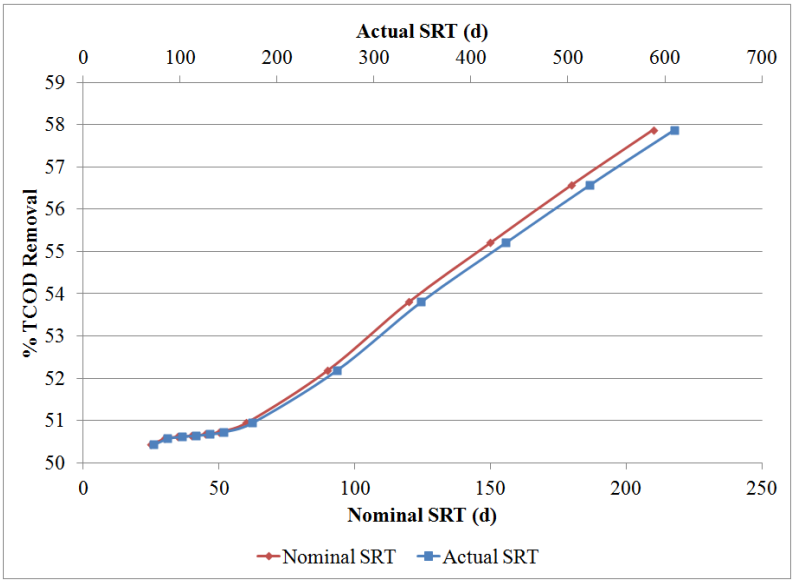

Figure 6.29. Percent TCOD removed from the system with increasing SRT, expressed with nominal and actual SRT.

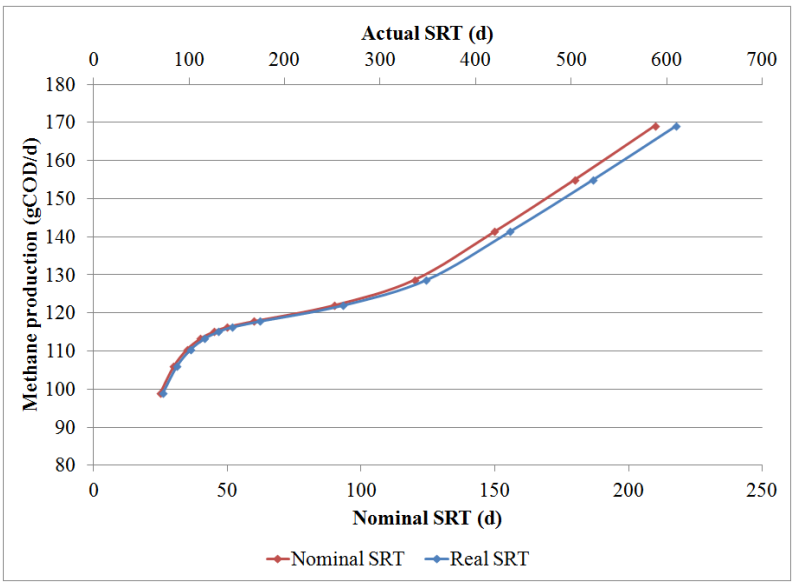

Figure 6.30. CH_4 production as a function of nominal and actual SRT.

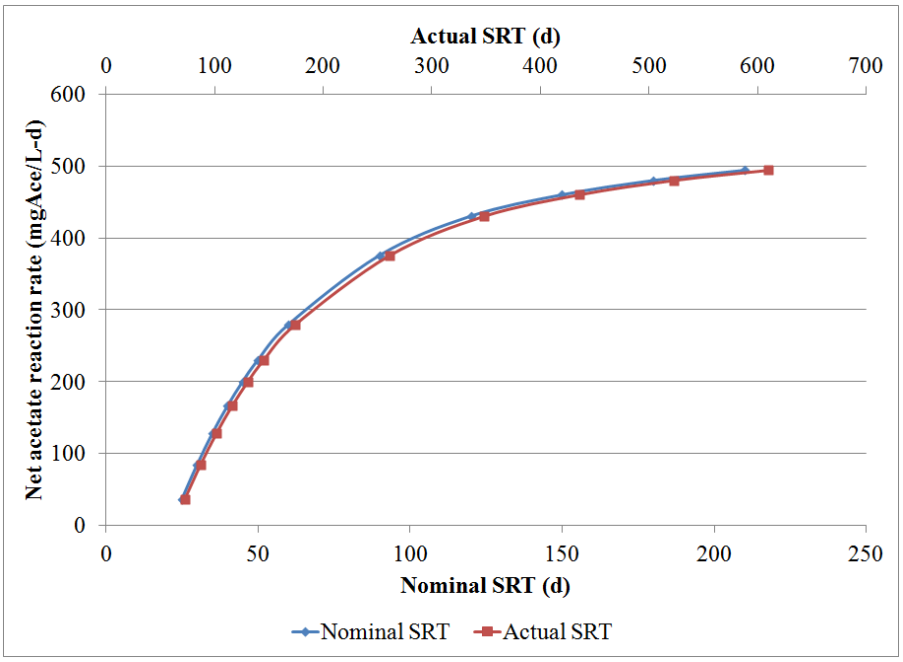

Figure 6.31. Net rate of acetate production throughout the AD as a function of nominal and actual SRT.

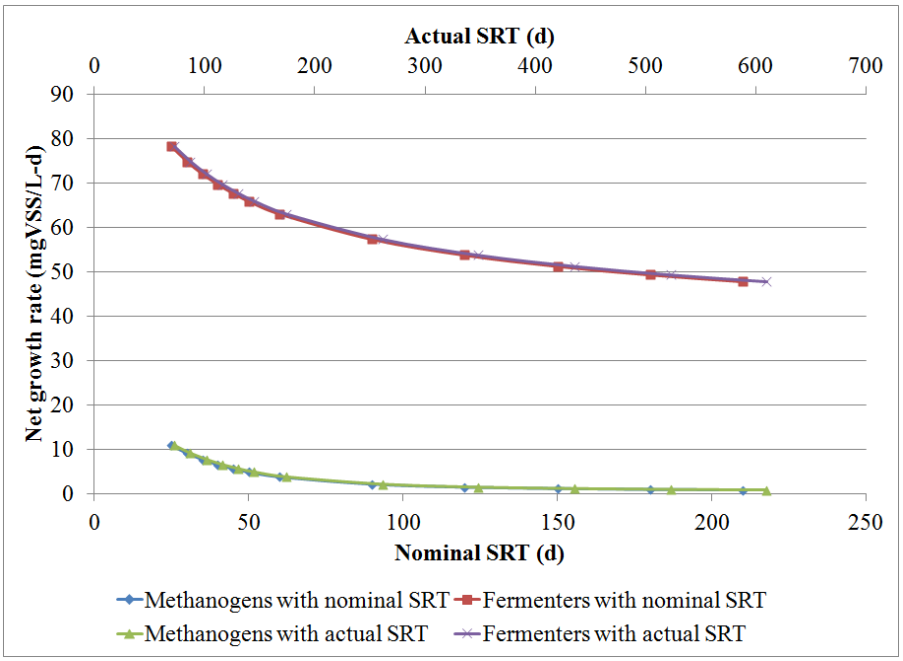

Figure 6.32. Net growth rate of methanogens and fermenters as a function of nominal and actual AD SRT.

Figure 6.30 shows a second inflection point, where the methane production rate increases significantly with increasing AD SRT. The cause of this second inflection point is subtle, but discernible from the model. Its cause is rooted in the fact that methanogens and heterotrophs compete for acetate. As the AD SRT becomes very large, the concentration of heterotrophs becomes negligible, and methanogens have little competition for acetate. In fact, around 120 days, the concentration of heterotrophs essentially levels out to 12 mgVSS/L, as seen in Figure 6.33. Thus, methanogens increase the total amount of methane produced after 120 days, as the competition from heterotrophs dwindles.

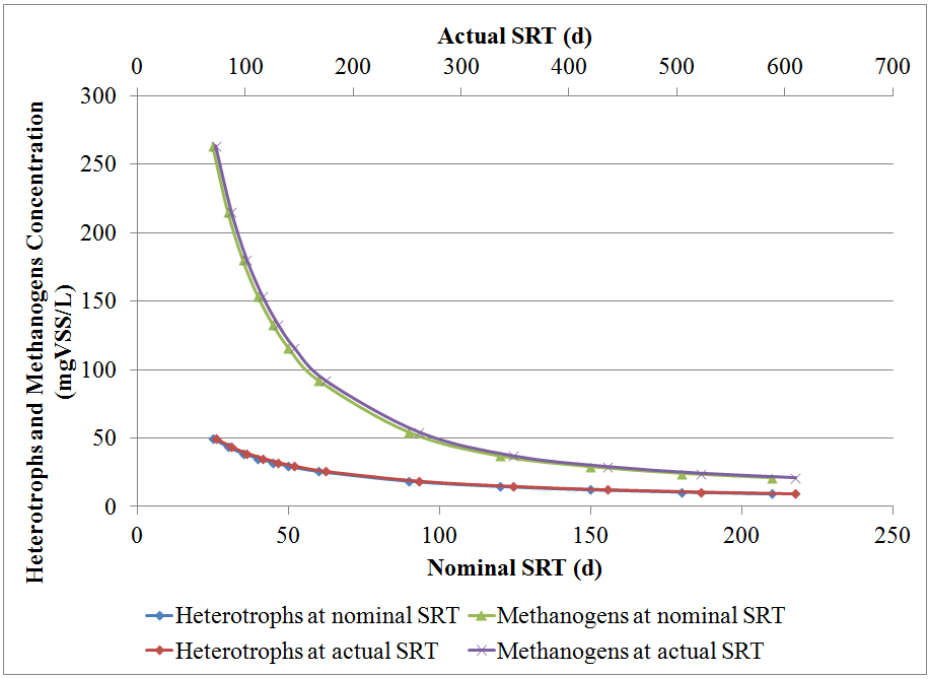

Figure 6.33. The concentration of methanogens and heterotrophs as a function of nominal and actual SRT.

Sludge yields decrease with increasing nominal AD SRT. As illustrated in Figure 6.34, the most prominent drop in yields occurs between 25 and 60 days,

where the yields decrease from 0.18 to 0.07 mg VSS/mg COD. Yields eventually settle to around 0.02 mg VSS/mg COD at 150 days. This result is not surprising – an SRT that is so long would encourage complete hydrolysis of heterotrophs, AOB, and NOB in the AD.

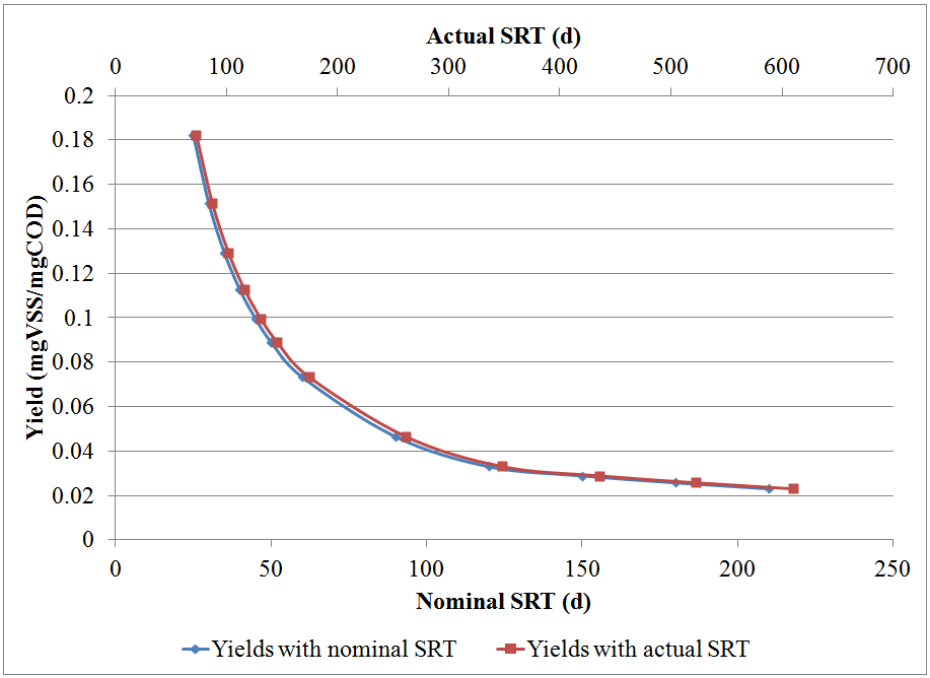

Figure 6.34. Sludge yield as a function of nominal and actual AD SRT.

Increasing AD SRT does not lead to increased nitrification in the system. As seen in Figure 6.35, increasing SRT causes a slight increase from 91 to 94 mgN/L in effluent NH_3 concentration. The linear nature would indicate that AD hydrolysis, a first-order mechanism, is the controlling factor in system nitrification. One reason for minimal nitrification is that washout still occurs in the contact tank. Unlike the trends with RAS and WAS, the system performance is not necessarily linked to shorter stabilization tank SRTs: the SRTs stay fairly constant between 5.5 and 5.7 hours (Figure 6.36). This further supports the

theory that the NH_3 produced from biomass decay in the AD has a significant effect on reducing nitrification in the stabilization tank.

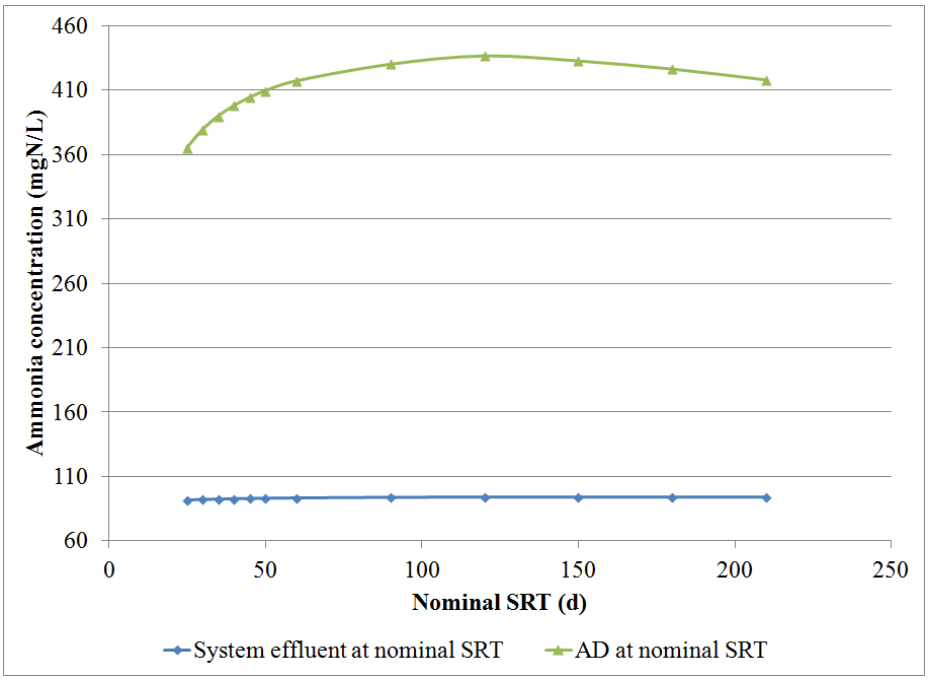

Figure 6.35. Effluent and AD ammonia concentration as a function of nominal AD SRT.

Increases in nominal AD SRT provide the worst denitrification performance of all models tested. As seen in Figure 6.37, less than 3.5% of influent total inorganic nitrogen is converted to N_2. Again, this performance is indirectly related to lackluster nitrification in the aerobic tanks and the additional NH_3 loading in the stabilization tank with increased biomass decay at longer AD SRTs.

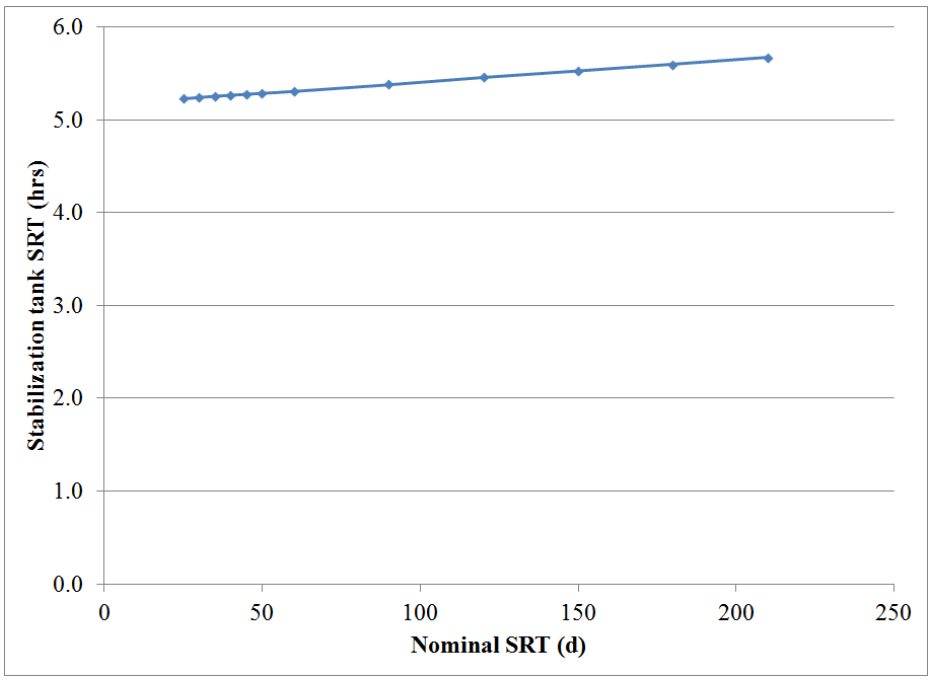

Figure 6.36. Stabilization tank SRT as a function of nominal AD SRT.

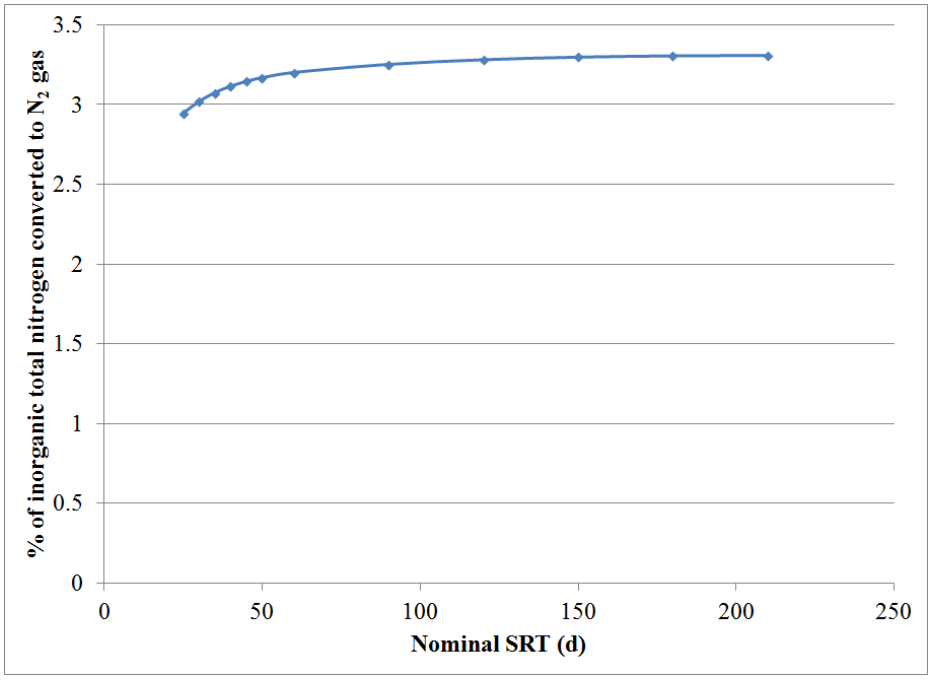

Figure 6.37. Percent of influent total inorganic nitrogen converted to N_2.

As expected, the time required to attain steady state to increases with increasing SRT. It takes the hybrid system 387 days (1.06 years) at a 25-day nominal SRT and 939 days (2.57 years) at a 210-day nominal SRT to achieve steady state (Figure 6.38). Following the trends of the previous models, this is directly related to the increase in SRT and is something to consider during commercialization.

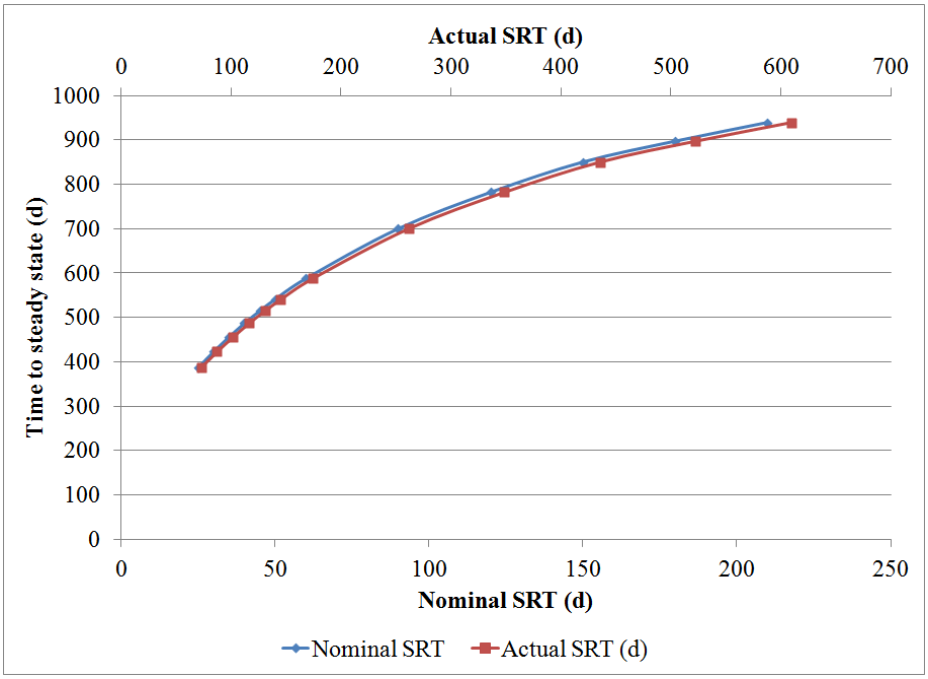

Figure 6.38. The time required to reach steady state operations as a function of nominal and actual AD SRT.

To summarize, CH_4 production increases and sludge production decreases with increasing SRT. CH_4 production increases from 99 to 169 gCOD/L when the nominal AD SRT was increased from 25 to 210 days. Sludge yields decrease from 0.18 at a 25-day to 0.02 at a 210-day nominal SRT. The rate of improvement in these parameters slows considerably for SRT over 60 days.

6.5 Modeling Conclusions

A multispecies, dynamic mathematical model was developed to predict the performance of the hybrid and conventional trains and to determine what effect biosorption kinetics may have on system performance. Mass balance analyses on each individual tank and the overall system resulted in complete mass balance closure. An analysis of contact tank performance determined that the contact tank experiences washout at its current operating conditions.

A sensitivity analysis was performed to determine a range of values for the biosorption floc kinetic parameters k_{floc} and $k_{p,f}$. What is interesting about these parameters is that the specific value of the parameters is less important than the ratio of k_{floc} to $k_{p,f}$. The analysis determined that the model is most sensitive to a k_{floc} to $k_{p,f}$ ratio between 10 and 5000, with the larger ratio producing larger amounts of $PCOD_f$. When the ratio is lower than 1000, adsorption is the dominant mechanism in biosorption. When the ratio is 1000 or greater, floc entrapment is the dominant mechanism. The model operated well when the k_{floc} and $k_{p,f}$ values range between 0.01 and 1000. The presence of biosorption kinetics in the model improves CH_4 production and decreases sludge yield. The hydrolysis of $PCOD_f$ and $PCOD_a$ produced up to 16% more CH_4 while decreasing sludge production up to 25% versus a conventional configuration.

Based on total system modeling, the hybrid system outperforms the conventional system for several key parameters. The hybrid model consistently produces more CH_4 and produces less sludge than the conventional train. This

performance is heavily influenced by the significantly higher SRTs in the hybrid trains. Biosorption kinetics play only a minor role in the model performance, with CH_4 being the only parameter to demonstrate any noticeable changes. However, neither configuration effectively performs nitrification or denitrification. The stabilization and contact tanks demonstrate low SRTs, essentially eliminating the production of nitrification products. Since these products are not produced, denitrification does not happen at significant levels in the systems. All systems demonstrate the same biomass concentrations trends by tank regardless of the inclusion of biosorption kinetics. However, the hybrid system has much higher fermenter and methanogen concentrations in the aerobic and anoxic tanks.

In contrast to the trends with a conventional system, CH_4 production, sludge yield, and total COD consumption consistently improve with increasing RAS, WAS, and AD SRTs in the hybrid system. The hybrid process increases CH_4 production by 6 to 17% while producing 20 to 80% less sludge. This improved performance is heavily influenced by the increase in AD SRT that is attained when sludge is recycled back through the system. There are significant increases in CH_4 production with AD SRT increases up to 50 to 60 days. After 60 days, there are significant decreases in sludge yield, but less CH_4 produced. Ultimately, an AD SRT between 50 to 60 days seems to provide a suitable balance between CH_4 production and sludge reduction.

The hybrid and conventional systems provide minimal nitrification and denitrification. The conventional train shows marginally better performance in these areas versus the hybrid system, but neither system converts more that 13% this inorganic nitrogen to nitrogen gas. Total nitrogen removal is never more than 33%, and most of that is from biomass wasting. The lackluster performance is a result of low SRTs in the contact and stabilization tanks, which effectively washout AOB and NOB from these tanks. When RAS, WAS, or AD SRT are increased, nitrification is further marginalized in the stabilization tank, as the recycled sludge from the AD undergoes consistently increases in NH_3 concentration as a result of increased biomass decay. The overloading of the contact and stabilization tank prevents effective production of the nitrification products of NO_2^- and NO_3^-, further inhibiting denitrification performance.

Based on the modeling data, the hybrid train's impressive methane and sludge-yield performances give it significant sustainability advantages over a conventional train. Furthermore, these advantages increase with larger RAS, WAS, and AD SRT. The enhancements are directly related to the increased real AD SRTs that are produced through AD sludge recycle. While substantially less significant, biosorption also improves performance improvements in these critical areas.

It is important to understand that fulfilling the sustainability goals for methane production and sludge yield leads to the hybrid train being unable to

perform significant nitrification and denitrification. Nitrification and denitrification are better addressed outside the hybrid system.

7. Summary and Recommendations

Since an overall summary of the hybrid train's performance is included at the end of Chapters 4 and 6, the summary below focuses on large overall trends. In addition, I provide recommendations as to how to improve the hybrid process to further meet and exceed SWT's goals.

7.1 Summary

SWT has proposed a hybrid process as a "green" alternative for wastewater treatment that can easily be retrofit into existing medium and large WWTPs. The hybrid process utilizes recycling of anaerobic digestion sludge to the activated sludge processes to improve methane production and reduce sludge production versus conventional WWTP systems. SWT's process differs from conventional WWTP systems in three key ways: biosorption of PCOD in the anoxic and contact tanks for transfer to the anaerobic digester; anaerobic digestion of this PCOD in the AD to enhance methane production; and recycle of AD sludge to the beginning of the process to act as additional sorbent for PCOD. As a result of the recycling of sludge and longer overall system sludge retention time, SWT has proposed that the increase in anaerobic digestion will decrease sludge yield from the overall system. It is SWT's expectations that the hybrid process will produce effluent that meets existing U.S. EPA effluent discharge standards.

I performed an extensive mass balance analysis and performance analysis for the conventional and hybrid pilot trains. The performance analysis began with a detailed discussion of SRTs in the aerobic system (i.e., all tanks except the AD

and sludge thickener), anaerobic, and the overall systems. I performed a mass balance analysis for COD, suspended solids, nitrogen compounds, and methane for all trains and "steady-state" phases. I presented an in-depth examination of the AD performance for each train and phase, including methane production and sludge yields. I provided analysis of MCA sampling results sent to the ASU team. I developed a biosorption theory to describe PCOD entrapment in floc and biosorption to biomass. Applying this theory, I developed and executed a mathematical model that modeled 20 components and 9 mechanisms in the each individual tank and the overall system.

The SRT analyses of each train established inconsistencies between the stated SWT SRTs and the calculated SRTs. Based on my calculations of the SRT, which represents the inverse of the specific growth rate of biomass in the system, the overall system SRTs in the hybrid trains were longer, at 100 to 210 days, than the conventional train, which ranged from 36 to 42 days. This was heavily influenced by the significantly longer AD SRTs in the hybrid trains (110 to 225 days) versus the conventional train (25-30 days). This disparity provided a significant benefit for the hybrid trains for improved methane and reduced sludge productions.

Several conclusions were obtained from the COD analyses of each train. One of the most important trends is mass balance closure between different sections of the trains, i.e., aerobic, anaerobic, and total system, is incomplete. While this can be the result of measurement error, the lack of mass balance

closure along with the trends in SRT indicate inaccurate recording of internal flow rates. The hybrid trains exhibited significantly higher total COD removals versus the conventional train with similar TCOD effluent concentrations: the hybrid trains' removed 71-88% of influent COD, compared with 49-60% in the conventional train. The hybrid trains' ADs consistently exhibited higher COD consumption than the conventional trains, resulting in 1.5 to 5.5 times more methane production in the hybrid trains. While the anoxic tank's production of PCOD and TCOD suggested that its conditions are viable for biosorption, the contact tank demonstrated biomass consumption of COD rather than exhibiting behaviors consistent with biosorption. However, the highest levels of COD consumption occurred in the stabilization tank, which diverts COD from the ADs, which can be converted to methane.

Prior to train 1's reconfiguration in phase 12, the hybrid trains exhibited higher levels of nitrogen removal, particularly NH_3-N, than the conventional train. However, inorganic nitrogen removal performance for all trains was lackluster, ranging between 25 to 61% for all trains. With train 1's reconfiguration, inorganic nitrogen removal significantly improved to 86% versus 51% in train 1 and 43% in train 2. Hybrid trains demonstrated higher levels of denitrification and nitrification, as well as more NH_3-N production in the AD, with the stabilization tank driving overall NH_3-N removal from all trains. However, this increase in nitrification in the stabilization tank corresponded with the unwanted consequence of increased COD consumption in the stabilization tank. These

results suggest that washout of AOB and NOB may be taking place in the smaller vessels, including the contact tank, which prevents effective nitrification from occurring.

During each phase, the hybrid trains consistently achieved lower biomass yields than the conventional train. Whereas hybrid train 1's biomass yields ranged from 0.04 to 0.17 g VSS/g COD and train 3's yields ranged from 0.02 to 0.36 g VSS/g COD, conventional train 2's biomass yields ranged from 0.35 to 0.69 g VSS/g COD. Hybrid train yields are lower due to AD performance: the longer AD SRTs allow for increased PCOD hydrolysis and increased COD removal leads to greater conversion of COD to methane.

MCA analysis of each train detected AOB, NOB, and *Archaea* throughout each system, suggesting that these microorganisms can survive throughout the trains. *Archaea* copy numbers were not significantly different between the two types of trains.

A multispecies, dynamic mathematical model was developed to predict the performance of the hybrid and conventional trains with and without biosorption kinetics and to determine what effect biosorption kinetics may have on system performance. Mass balance analyses on each individual tank and the overall system resulted in complete mass balance closure. Modeling of the contact tank confirmed the observed pilot plant performance of washout of AOB and NOB in the tank.

While most biosorption kinetics parameters were determined experimentally by NUS, a sensitivity analysis had to be performed to determine a range of values for the flocculation formation constant, k_{floc}, and floc shearing constant, $k_{p,f}$. Sensitivity analysis established that the individual values of k_{floc} to $k_{p,f}$ were less important than the ratio of these two flocculation constants, which is most sensitive between 10 and 5000. When the ratio is lower than 1000, adsorption is the dominant mechanism in biosorption. When the ratio is 1000 or greater, floc entrapment is the dominant mechanism. The hydrolysis of $PCOD_f$ and $PCOD_a$ produced up to 16% more CH_4 while decreasing sludge production up to 25% versus a conventional configuration.

Consistent with observed pilot plant trends, total system modeling confirms the hybrid system outperforms the conventional system on several key parameters. In the hybrid system, CH_4 production, sludge yield, and total COD consumption consistently improve with increasing RAS, WAS, and AD SRTs. This improved performance is heavily influenced by the increase in AD SRT that is attained when sludge is recycled back through the system and less influenced by the inclusion of biosorption kinetics. An AD SRT between 50 to 60 days seems to provide a suitable balance between CH_4 production and sludge reduction.

Also consistent with pilot plant performance, the hybrid and conventional systems provide minimal nitrification and denitrification. Neither system removes more than 25% of the influent nitrogen or converts more that 13% this

inorganic nitrogen to nitrogen gas. The lackluster performance is a result of two phenomena: (1) low SRTs in the contact and stabilization tanks, which effectively washout AOB and NOB from these tanks and (2) additional NH_3 from biomass decay is present in the AD sludge recycle line causing overloading in an already undersized stabilization tank. However, increasing the size of the aerobic tanks would divert more COD away from the AD. Thus, fulfilling the goals of increased CH_4 production and decreased sludge yields has resulted in the hybrid train being unable to perform adequate nitrification and denitrification.

In conclusion, the pilot plant data support that the hybrid configuration is a more sustainable wastewater treatment process than the conventional configuration. While the overall performance of all trains was less efficient that typical wastewater treatment processes, the hybrid trains consistently removed more COD, produced more methane, and exhibited lower sludge yields versus the conventional train. *Archaea*, AOB, and NOB were present throughout each process configuration. However, nitrification and denitrification were inhibited by washout in the contact tank, producing effluent that may not meet discharge guidelines for nitrogen compounds. In addition, the pilot plant performance was confirmed by mathematical modeling. Mathematical modeling determined that AD sludge recycle plays a more significant role in the hybrid train performance than inclusion of biosorption kinetics.

7.2 Recommendations

SWT's hybrid process shows great potential for increasing methane production in existing wastewater treatment plants. However, its current limitations, particularly effluent quality, must be addressed prior to large-scale commercialization. In this section, I provide several recommendations for modifications to the process to improve methane production and effluent quality. I also provide suggestions on how to modify sampling protocols to provide a more thorough analysis of the process. My recommendations are divided into three sections: process recommendations, sampling protocol/ methods recommendations, and other miscellaneous recommendations.

7.2.1 Process Recommendations

Process modification can be made to enhance the performance of the hybrid process for a myriad of criteria. SWT is in the process of implementing several suggestions presented by the ASU team, with some of the suggestions reviewed in this document. However, other changes will require significant consideration prior to implementation. Like any process, modifications may result in tradeoffs between desired results, so prioritization of goals in essential in deciding which changes to implement.

One suggestion already implemented by SWT is the elimination of the stabilization tank. As discussed in Chapter 4, the greatest consumption of COD in all trains occurs in the stabilization tank at a rate of 2 to 4 times higher than the influent COD rate. SWT has implemented this suggestion as part of the

modifications of train 1 in phase 12, and it appears to result in greater influent COD conversion to methane in the AD. In addition, the usefulness of the contact tank is questionable and can also be removed. Both of these modifications can easily be modeled with the MATLAB program by setting their tank volume to a very low number (e.g., 10^{-9}).

There are other potential drawbacks to keeping the aerobic tanks in the hybrid process. A significant amount of the O_2 supplied in the aerobic tanks is potentially being used to oxidize sulfide from the AD. In colder climates, the heat required for anaerobic digestion will quickly dissipate as the sludge is cycled to the aerobic tanks. This will require more of the methane produced in anaerobic digestion be utilized for process heating to maintain mesophilic temperatures in the AD.

If methane production is the primary goal, one method for increasing methane production is to divert influent solids directly to the AD, as was modeled in the original project description by Liu (2008). This exposes more influent substrate directly to the fermenters for conversion to volatile fatty acids, which are precursors to methane during methanogenesis. However, methanogens typically require a minimum 15-day SRTs due to their very slow growth (Metcalf & Eddy, 2003). If the HRT is the same as the SRT, as is common for most ADs, the reactor volumes quickly become unrealistic. HRT can be decoupled from SRT and, therefore, reduce reactor volumes with the application of various new technologies. My recommendation is to divert a modest flow rate of influent (up

to 50%) to the AD. This range can be narrowed through mathematical modeling of the process by modifying the existing MATLAB model, or by using existing software like BioWin, which may be faster than a creating a custom program but does not account for biosorption.

The model results determined that there is a fair amount of methane being produced in the clarifier and sludge thickener due to the presence of methanogens in the influent (as reviewed as part of the MCA results in Chapter 4.6.2). However, this methane is not currently being captured. Not only is this methane is being produced which is not being captured, but the methane is being vented to the atmosphere as a greenhouse gas that is 20 times more potent than CO_2 (U.S. Energy Information Administration, 2010). It may be more beneficial to treat the entire system as a potential anaerobic digester, and capture the methane produced in the AD, clarifier, and sludge thickener.

Methanogens are fastidious microorganisms that are sensitive to temperature and pH. SWT has plans to place to determine how the hybrid process may be affected by different operating temperatures. However, pH is equally as important, as methanogens are known to prefer pH in the range of 6.5 to 7.6 (Parkin & Owen, 1986). SWT should consider further research on the effects of consistent pH control on increased methane production.

Changes to the anoxic and aeration tanks have multiple effects and tradeoffs on the intertwined concepts of biomass growth, COD removal, and nitrogen removal. Longer SRTs in aeration tanks promote the growth of slow-

growing AOB and NOB, but increased energy consumption from aeration. AOB and NOB are critical for the formation of NO_3^-, which is converted to N_2 gas in anoxic conditions. However, extended SRTs in the aerobic tank generally favor increased heterotrophic growth, which utilize simple soluble COD as substrate and will not be biosorbed and transferred to the AD. The process of denitrification of NO_3^- to N_2 gas utilizes soluble COD as an electron donor. This interdependence requires that a tradeoff must be considered between CH_4 production and decreased sludge yields and nitrification and denitrification.

To address this tradeoff, I suggest that that nitrogen removal be implemented for the effluent from the clarifier, as illustrated in Figure 7.1. The process retains the elements of a contact tank with mixing to promote biosorption and reducing wasting sludge production by recycling AD sludge to function as additional COD sorbent in the contact tank. As demonstrated in all trains, the contact tank may not require aeration to accomplish biosorption. The anoxic tank and the stabilization tank are eliminated from the process prior to the clarifier. This is done for two reasons. First, nitrification and denitrification had limited effectiveness in the existing processes. Second, the stabilization tank currently requires additional energy for aeration while utilizing COD that would be converted to methane in the AD. The clarifier influent will be treated with a post-oxic/anoxic reactor configuration with effluent recycle from the aeration tank to the anoxic tank for optimal nitrogen removal. These modifications have several benefits. Like the current configurations, post treatment will allow for any NH_3-N

produced in the AD to be removed from the effluent. Post treatment would require only a minimal amount of COD be diverted to the anoxic and aeration tanks. The COD can be supplied by diverting flow from the influent to the system. This will also reduce the reactor sizes and aeration requirements for denitrification and nitrification. Finally, if washout of AOB and NOB is still an issue in the aeration tank, packing material can be added without the potential of interfering with the formation of a suspended sludge blanket for COD capture and biosorption.

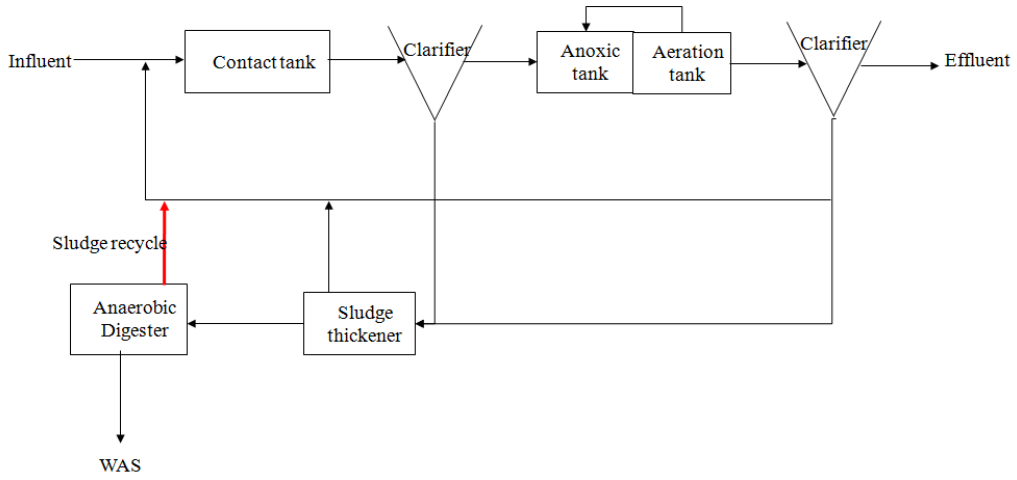

Figure 7.1. Suggested modifications to hybrid system, including post-nitrification+denitrification.

Another concern is whether the stated HRTs in the anoxic and contact tanks are optimal for biosorption. The current 1-hour HRT in the contact and anoxic tanks is longer than the 30 minutes required for biosorption, as established by Jimenez et al. (2007). Because the retention time is longer than suggested, additional soluble COD is probably being utilized by microorganisms rather than being biosorbed. I recommend that the HRT in each of the anoxic and contact

tanks be reduced in steps to 45 and 30 minutes to determine the effects of these reduce HRTs on biosorption while reducing the potential for substrate utilization by heterotrophs. SWT is currently in the process of reducing these HRTs to improve biosorption.

If research continues using the current configurations continues, further research is needed to determine which mechanisms are producing increased nitrification and denitrification in the modified hybrid configuration. As demonstrated with train 1 in phase 12, I am unable to determine which of the process modifications has had the largest effect on increased nitrification and denitrification, because several changes were performed at once. My recommendation is to modify train 3 in steps starting with the removal of the stabilization tank and progress through the rest of the changes until the primary drivers can be determined.

7.2.2 Sampling Protocol/Methods Recommendations

Sampling protocols and frequency are subject to trade offs for any experimental process. The goal of sampling, which is to provide enough information to characterize the system, must be balanced with the costs and manpower required to perform these tests. While several significant conclusions were obtained from the data provided, knowledge gained from the last year underscores the need for thorough planning and execution of sampling in future phases of the project. Sampling frequencies for TCOD, SCOD, VSS, TSS, and NH_3-N were generally adequate to provide insight into mechanisms involved with

these constituents in all tanks. However, additional data from sludge streams would benefit comprehensive mass balances of other components in the systems.

A major opportunity is closing the gaps in the nitrogen balance. TKN measurements were obtained on a monthly basis from the influent. For all trains, NO_2-N and NO_3-N measurement frequencies were less than twice per week. In addition, NO_2-N and NO_3-N measurements are unavailable for sludge streams, making it difficult to obtain a comprehensive analysis of nitrification and denitrification in the trains. I recommend a testing frequency of at least twice per week for all streams, including sludge streams. One of the reasons sludge stream concentrations were not obtained is that the existing methods for NO_2-N and NO_3-N are more applicable to liquid streams, and turbidity can cause performance issues with instrumentation. To facilitate the measurement of NO_2-N and NO_3-N in sludge samples while maintaining the operations of the instrument, researchers have centrifuged sludge samples and decanted and filtered the supernatant (Kelly & Love, 2007; Percheron et al., 1998). It is recommended that centrifuging and measurement be applied immediately after sampling to preserve NO_2-N and NO_3-N concentrations in the sample (APHA, AWWA, WEF, 2006). This process can be applied for samples being analyzed with ion chromatography or ultraviolet spectrophotometry.

MCA data determined the presence of *Archaea*, AOB, and NOB, but additional MCA information could provide further insights into the performance of the system. MCA samples were not obtained from the stream between the

sludge thickener and anaerobic digester. If MCA samples are obtained from this line, we can determine microorganism concentrations and specific solid retention times for these microorganisms in each of the tanks. This analysis could provide additional information to improve AOB and NOB retention in the aeration tank(s).

One major obstacle in modeling was the lack of data available to describe biosorption flocculation constants. Additional biosorption testing could provide more accurate values for PCOD floc constants k_{floc} and $k_{p,f}$. La Motta et al. (2004) designed continuously-mixed reactor experiments to quantify COD entrapment though biofloccuation as a function of various RMS gradients, vessel volumes, HRTs, and SRTs. La Motta's experiment can provide the basis for flocculation experiments to determine an appropriate ratio of k_{floc} to $k_{p,f}$.

7.2.3 Miscellaneous Recommendations

From Jimenez et al. (2005 and 2007), EPS plays a crucial role in the formation and transfer of biosorbed COD throughout the system. The fusion of COD mass balance information provided in this thesis with the EPS data (measured by NUS) has the potential to provide significant insights into the biosorption mechanisms and confirmation of biosorption in the anoxic and contact tanks.

One element neglected in this analysis is phosphorus, a critical element for cellular growth and maintenance. Wastewaters with high phosphorus levels are prone to promote eutrophication in surface waters. Therefore, WWTPs often

engage in phosphorus removal as part of their overall biological nutrient removal goals. Therefore, mass balance analysis should be extended to include phosphorus or phosphate ions.

Other reasons support analyzing phosphorus removal performance. From a sustainability standpoint, phosphorus is increasingly considered a scarce resource (Cordell et al, 2011). Technologies that SWT has considered for phosphorus removal include sequencing batch reactors, membrane biofilm reactors and various precipitation methods (Siemens Water Technologies). The coupling of the hybrid process with phosphorus removal has the potential to be both a holistic approach to wastewater treatment and environmental preservation while providing a two revenue streams for municipalities.

Future train modifications should be implemented in steps to truly quantify the impact of the modifications. This recommendation is a result of train 1's performance in phase 12. With the myriad of changes made to this train, I am unable to determine which of the process modifications had the largest effect on increased nitrification and denitrification. By implementing changes in phases, the most effective modifications will be identified and reduce overall implementation and capital costs.

WORKS CITED

AJ Design Software. (2011). *Propeller Turbine Mixer Design Calculator--Wastewater Treatment - Mixing*. Retrieved March 2011, from AJ Design Software: http://www.ajdesigner.com/phpmixing/propeller_mixing_power_turbulent.php

Aksu, Z. (2005). Application of Biosorption for the Removal of Organic Pollutants: A Review. *Process Biochemistry , 40*, 997-1026.

Aksu, Z., & Tezer, S. (2005). Biosorption of reactive dyes on the green alga Chlorella vulgaris. *Process Biochemistry , 40*, 1347-1361.

APHA, AWWA, WEF. (2006). Standard Methods for the Examination of Water and Wastewater. *21st*. American Water Works Association.

Aquino, S. F., & Stuckey, D. C. (2008). Integrated model of the production of soluble microbial products (SMP) and extracellular polymeric substances (EPS) in anaerobic chemostats during transient conditions. *Biochemical Engineering Journal , 38* (2), 138-146.

Arizona Department of Environmental Quality. (2009). *2009 Surface Water Quality Standards.* Unofficial Copy of Final Rules, Arizona Department of Environmental Quality.

Bae, W., & Rittmann, B. E. (1996). A Structured Model of Dual-Limitation Kinetics. *Biotechnology and Bioengineering , 49* (6), 683-689.

Benefield, L. D., & Randall, C. W. (1976). Design procedure for a contact stabilization activated sludge process. *Water Environment Federation , 48* (1), 147-152.

Bitton, G. (2005). *Wastewater Microbiology* (Vol. 3rd). Hoboken, New Jersey: John Wiley & Sons, Inc.

Buswell, A. M. (1928). The Biology of Activated Sludge--A Historical Review. *American Chemical Society Monograph , 38*, 352.

Camp, T., & Stein, P. (1943). Velocity gradients and internal work in fluid motion. *Journal of the Boston Society of Civil Engineering , 85*, pp. 219-37.

Carns, K. (2005). *Bringing Energy Efficiency to the Water and Wastewater Industry: How Do We Get There?* Washington University in St. Louis, EPRI Community Environmental Center. Oakhurst, CA: EPRI Solutions, Inc.

Center for Sustainable Systems, University of Michigan. (2009). U.S. Wastewater Treatment Fact Sheet.

Cordell, D., Rosemarin, A., Schröder, J. J., & Smit, A. L. (2011). Towards global phosphorus security: A systems framework for phosphorus recovery and reuse options. *Chemosphere , 84* (6), 747-758.

Dermissi, N. (1991). Contact Stabilization--an Economic Alternative for Water Pollution Abatement in Developing Countries. *Journal for Water and Wastewater Research , 24* (5), 207-211.

Eastern Research Group, Inc. and Energy and Environmental Analysis, Inc. (2007). *Opportunities for and Benefits of Combined Heat and Power at Wastewater Treatment Facilities.* United States Environmental Protection Agency.

Gadd, G. M. (2009). Biosorption: Critical Review of Scientific Rationale, Environmental Importance and Significance for Pollution Treatment. *Journal of Chemical Technology and Biotechnology , 84* (1), 13-28.

Gray, N. F. (1989). *Biology of Wastewater Treatment.* Oxford: Oxford University Press.

Henze, M., Gujer, W., Mino, T., & van Loosdrecht, M. (2000). *Activated Sludge Models ASM1, ASM2, ASM2d and ASM3.* London: International Water Association Publishing.

Henze, M., Harremoes, P., Jansen, J. L., & Arvin, E. (1995). *Wastewater Treatment: Biological and Chemical Processes.* Berlin, Germany: Springer-Verlag.

Jimenez, J. A., La Motta, E. J., & Parker, D. S. (2007). Effect of Operational Parameters on the Removal of Particulate Chemical Oxygen Demand in the Activated Sludge Process. *Water Environment Research , 79* (9), pp. 984-990.

Jimenez, J. A., La Motta, E. J., & Parker, D. S. (2005). Kinetics of Removal of Particulate Chemical Oxygen Demand in the Activated-Sludge Process. *Water Environment Research , 77* (5), pp. 437-446.

Keiding, K., & Nielsen, P. (1997). Desorption of organic macromolecules from activated sludge: Effect of ionic composition. *Water Research , 31* (7), 1665-1672.

Kelly, R. T., & Love, N. G. (2007). Ultraviolet Spectrophotometric Determination of Nitrate: Detecting Nitrification Rates and Inhibition. *Water Environment Research , 79* (7), 808-812.

La Motta, E. J., Jimenez, J. A., Josse, J. C., & Manrique, A. (2004). Role of Bioflocculation on Chemical Oxygen Demand Removal in Solids Contact Chamber of Trickling Filter Solids Contact Process. *Journal of Environmental Engineering , 130* (7), 726-735.

La Motta, E. J., McCorquodale, J. A., & Rojas, J. A. (2007, January). Using the Kinetics of Biological Flocculation and the Limiting Flux Theory for the Preliminary Design of Activated Sludge Systems. I: Model Development. *Journal of Environmental Engineering , 133* (1), pp. 104-110.

Lagergren, S. (1898). Zur theorie der sogenannten adsorption gelöster stoffe. *Kungliga Svenska Vetenskapsakademiens , 24* (4), 1-39.

Laspidou, C. S., & Rittmann, B. E. (2002a). A Unified Theory for Extracellular Polymeric Substances, Soluble Microbial Products, and Active and Inert Biomass. *Water Research* , 2711-2720.

Laspidou, C. S., & Rittmann, B. E. (2002b). Non-steady State Modeling of Extracellular Polymeric Substances, Soluble Microbial Products, and Active and Inert Biomass. *Water Research* , 1983-1992.

Liu, W. (2008). Minimizing Energy Usage by Applying a Bio-sorption and Anaerobic Digestion Hybrid Process for Water Reclamation.

Madigan, M. T., & Martinko, J. M. (2006). *Brock Biology of Microorganisms* (11th ed.). Upper Saddle River, New Jersey: Pearson Prentice Hall.

Majone, M., Massanisso, P., & Ramadori, R. (1998). Comparison of carbon storage under aerobic and anoxic conditions. *Water Science and Technology , 38* (8-9), 77-84.

Mara, D., & Horan, N. (Eds.). (2003). *Handbook of Water and Wastwater Microbiology.* London: Academic Press.

Masters, G. M., & Ela, W. P. (2008). *Introduction to Environmental Engineering and Science* (3rd ed.). Upper Saddle River, New Jersey: Pearce Education, Inc.

McCarty, P. L. (2001). The development of anaerobic treatment and its future. *Water Science and Technology , 44* (8), 149-156.

McCarty, P. L., & Smith, D. P. (1986). Anaerobic wastewater treatment. *Environmental Science & Technology , 20* (12), 1200-1206.

Metcalf & Eddy, Inc. (2003). *Wastewater Engineering: Treatment and Reuse* (4th ed.). (I. Metcalf & Eddy, Ed.) New York: McGraw-Hill.

O'Callaghan, P. (2009, September). *Water and Energy: A Presentation for the Water Innovations Alliance*. (O2 Environmental) Retrieved August 26, 2010, from O2 Environmental: http://www.o2env.com/documents/WaterandEnergyPaper_Chicago09.pdf

Parkin, G. F., & Owen, W. F. (1986). Fundamentals of Anaerobic Digestion of Wastewater Sludge. *Journal of Environmental Engineering , 112* (5), 867-920.

Pavoni, J. L., Tenney, M. W., & Echelberger, W. F. (1972). Bacterial exocellular polymers and biological flocculation. *Journal (Water Pollution Control Federation) , 44* (3), 414-431.

Percheron, G., Michaud, S., Bernet, N., & Moletta, R. (1998). Nitrate and Nitrite Reduction of a Sulphide-Rich Environment. *Journal of Chemical Technology and Biotechnology , 72* (3), 213-220.

Rittmann, B. E., & McCarty, P. L. (2001). *Environmental Biotechnology: Principles and Applications* (1st ed.). New York: McGraw-Hill.

Rittmann, B. E., & Park, S. (2008). *Development of Compact Advanced Treatment Technology for Concentrated Food Wastewaters: Modeling of the Bacillus-Based, Comact Wastewater Treatment System.* Center for Environmental Biotechnology, Biodesign Institute at Arizona State University.

Sahagun, L. (2010, June 7). *City of L.A., Kern County battle over human waste disposal.* Retrieved August 21, 2010, from Greenspace: http://latimesblogs.latimes.com/greenspace/2010/06/city-of-la-kern-county-at-loggerheads-over-human-waste-disposal.html

Siemens Water Technologies. (n.d.). *Enhanced Nutrient Removal Solutions*. Retrieved March 14, 2011, from Siemens Water Technologies:

http://www.water.siemens.com/en/municipal/Wastewater/Pages/Municipal-Enhanced-Nutrient-Removal.aspx

Siripong, S., & Rittmann, B. E. (2007). Diversity study of nitrifying bacteria in full-scale municipal wastewater treatment plants. *Water Research* , 1110-1120.

Smoluchowski, M. (1917). Versuch einer Mathematischen Theorie der Koagulationskinetik Kolloider LoÈ sungen. *Zeitschrift für physikalische Chemie , 92*, pp. 129-168.

Thomas, D., Judd, S., & Fawcett, N. (1999). Flocculation Modelling: A Review. *Water Research , 33* (7), pp. 1579-1592.

U. S. Environmental Protection Agency. (2008). *Clean Watershed Needs Survey 2008: Report to Congress.*

U.S. Energy Information Administration. (2010, May 11). *Economic Growth Case Comparisons*. Retrieved August 26, 2010, from Annual Energy Outlook 2010: http://www.eia.doe.gov/oiaf/aeo/pdf/appb.pdf

U.S. Environmental Protection Agency. (2010, September). *Chapter 5: Technology-Based Effluent Limits*. Retrieved October 16, 2010, from NPDES Permit Writers' Manual: http://www.epa.gov/npdes/pubs/chapt_05.pdf

U.S. Environmental Protection Agency Combined Heat and Power Partnership. (2008). *Catalog of CHP Technologies.* U.S. Environmental Protection Agency.

Wilen, B.-M., Jin, B., & Lant, P. (2003a). Relationship between flocculation of activated sludge and composition of extracellular polymeric substances. *Water Science and Technology , 47* (12), 95-103.

Wilen, B.-M., Jin, B., & Lant, P. (2003b). The influence of key chemical constituents in activated sludge on surface and flocculating properties. *Water Research , 37*, 2127–2139.

Xu, K., Liu, H., Du, D., & Chen, J. (2009). Real-time PCR assays targeting formyltetrahydrofolate synthetase gene to enumerate acetogens in natural and engineered environments. *Anaerobe , 15* (5), 204-213.

Yu, Y., Lee, C., Kim, J., & Hwang, S. (2005). Group-specific primer and probe sets to detect methanogenic communities using quantitative real-time polymerase chain reaction. *Biotechnology and Bioengineering , 89* (6), 670-679.

Zellner, G., Messner, P., Winter, J., & Stackebrandt, E. (1998). E. Methanoculleus palmolei sp. nov., an irregularly coccoid methanogen from an anaerobic digester treating wastewater of a palm oil plant in North-Sumatra, Indonesia. *International Journal of Systematic Bacteriology , 48*, 1111-1117.

APPENDIX A.

MATHEMATICAL MODELING EQUATIONS APPLIED IN MATLAB

A.1 Nomenclature

Symbols	Description	Units (if needed)
Qi	Volumetric flow rate	L/d
Cx	Concentration of species x	mgCOD/L or mgN/L
Xx	Biomass concentration of species x	mgVSS/L
Vi	Volume	L
R	Reaction rate	mg/d
Subscripts		
Ace	Acetate	
AD	Anaerobic digester	
Amm	Ammonium	
AOB	Ammonium oxidizing bacteria	
AX	Anoxic tank	
BAP	Biomass associated products	
CL	Clarifier	
CL-SL	Effluent from clarifier to the sludge thickener	
CL-ST	Effluent from clarifier to the stabilization tank	
COD	Chemical oxygen demand	
CT	Contact tank	
DO	Dissolved oxygen	
EPS	Extracellular polymeric substances	
f1	Acetogen fermenters	
het	Heterotrophs	
hyd	Hydrolysis	
in	Influent to the system	
m	Methanogens	
NaN or Nan	Nitrate	
NiN or Nin	Nitrite	
NOB	Nitrite oxidizing bacteria	
out	Effluent from the system	
$PCOD_a$	Absorbed PCOD	
$PCOD_f$	PCOD captured in floc	
$PCOD_s$	Single particles of PCOD	
SL	Sludge thickener	
SL-AD	Effluent from sludge thickener to anaerobic digester	
SL-ST or SL-super	Effluent from sludge thickener to stabilization tank	

Subscripts		
ST	Stabilization tank	
sys	Overall system	
UAP	Utilization associated products	
W	Wasting sludge from anaerobic digester	

A.2 Modeling system and components

System Overview Diagram:

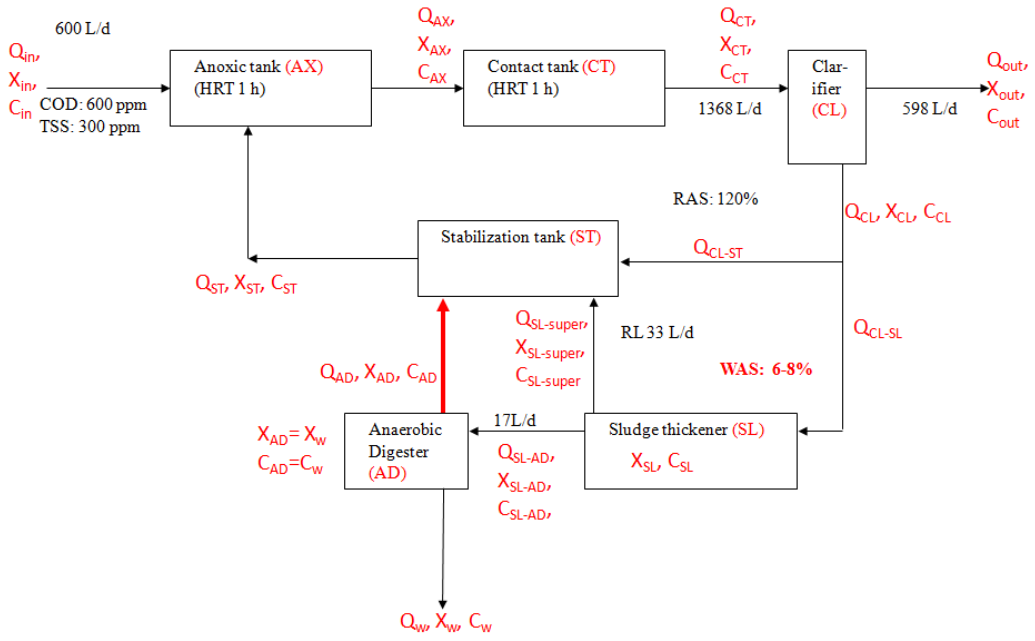

Components modeled

Variable	Description	Index in MATLAB Coding
Xhet	Facultative heterotrophs	1
XAOB	AOB	2
XNOB	NOB	3
Xf1	Fermenters	4
Xm	Methanogens	6
X EPS	EPS	7
Xinerts	Inerts	8
S	Substrate	9
UAP	UAP	10
BAP	BAP	11
Ace	Acetate	12
PCODf	Floc PCOD	15
PCODa	Biosorbed PCOD	16
PCODs	Single cell PCOD	17
NiN or NO2	Nitrite	18
NaN or NO3	Nitrate	19
Amm or NH4	Ammonia	20
DO	Dissolved oxygen	21
CH_4	Methane	22
N_2	Nitrogen gas	23

A.3 Preliminary reaction rate and mass balance equations for MATLAB modeling

A.3.1 Switch Equations and Constants

Nitrite switch:

$$NO_2^{switch} = \frac{K_{NO_2}^{switch}}{K_{NO_2}^{switch} + NO_2}$$

Nitrate switch:

$$NO_3^{switch} = \frac{K_{NO_3}^{switch}}{K_{NO_3}^{switch} + NO_3}$$

NO_x switch:

$$NO_x^{switch} = NO_2^{switch} + NO_3^{switch}$$

DO switch:

$$DO^{switch} = \frac{K_{DO}^{switch}}{K_{DO}^{switch} + DO}$$

$$\gamma_O = 160/113$$
$$\gamma_N = 14/113$$

All γ constants based on a biomass molecular formula of $C_5H_7O_2N$.

A.3.2. Utilization Rates for Soluble Components

1. Original Substrate (S):

- Utilization by heterotrophs:

$$r_{ut,het,S} = \left(\frac{\hat{q}_S\, S}{K_{S,het} + S}\right)\left(\frac{DO}{K_{DO,het} + DO}\right) X_{het} \qquad \left(\text{units: } \frac{mgCOD}{L\, d}\right)$$

- Production of substrate through hydrolysis of inactive biomass (during anaerobic digestion):

$$r_{hyd} = k_{hyd}\left(DO^{switch}\right)\left(NO_x^{switch}\right)(X_{het} + X_{AOB} + X_{NOB}) \qquad \left(\text{units: } \frac{mgVSS}{L\, d}\right)$$

- Utilization by fermenters (f1) (fermentation during anaerobic digestion):

$$r_{ut,f1,S} = \left(\frac{\hat{q}_{S,f1} S}{K_{S,f1} + S}\right) DO^{switch} NO_x^{switch} X_{f1} \quad \left(\text{units: } \frac{mgCOD}{L\, d}\right)$$

2. Nitrite (NiN):

- Utilization by heterotrophs (in anoxic conditions):

$$r^i_{ut,het,NiN} = \left(\frac{\hat{q}_{Nin} S_i}{K_S + S_i}\right)\left(DO^{switch}\right)\left(\frac{NiN}{K_{NiN,het} + NiN}\right) X_{het} \qquad \left(\text{units: } \frac{mgCOD}{L\, d}\right)$$

where i is the types of SCOD utilized when NO_2^- is the electron acceptor: 1=S substrate, 2=UAP, 3=BAP, and 4= acetate.

- Utilization by NOB (in aerobic conditions):

$$r_{ut,NOB} = -\left(\frac{\hat{q}_{NOB} NiN}{K_{Nin,NOB} + NiN}\right)\left(\frac{DO}{K_{DO,NOB} + DO}\right) X_{NOB} \quad \left(\text{units: } \frac{mgNO_2^- - N}{L\, d}\right)$$

3. Nitrate (NaN):

- Utilization by heterotrophs

$$r^i_{ut,het,NaN} = \left(\frac{\hat{q}_{Nan} S_i}{K_S + S_i}\right)\left(DO^{switch}\right)\left(\frac{NaN}{K_{NaN,het} + NaN}\right) X_{het} \qquad \left(\text{units: } \frac{mgCOD}{L\, d}\right)$$

where i is the types of SCOD utilized when NO_3^- is the electron acceptor: 1=S substrate, 2=UAP, 3=BAP, and 4= acetate.

4. Ammonia (Amm):

- Utilization by AOB to produce NiN:

$$r_{ut,AOB} = -\left(\frac{\hat{q}_{AOB}Amm}{K_{Amm,AOB} + Amm}\right)\left(\frac{DO}{K_{DO,AOB} + DO}\right)X_{AOB}$$

$$\left(\text{units: } \frac{mgNH_4^+ - N}{L\ d}\right)$$

- Production of Amm through endogenous decay:

$$r_{prod,Amm,total} = \sum_{a=1}^{3} f_d b_a \left(\frac{DO}{K_{DO,a}+DO}\right)X_a + f_d b_{het}\left(\frac{NiN}{K_{NiN,het}+NiN}\right. +$$

NaNKNaN,het+NaNDOswitchXhet+a=45DOswitchNOxswitchf

dbaXa

$$\left(\text{Units: } \frac{mgNH_4^+ - N}{L\ d}\right)$$

where a is the index indicating the type of biomass decaying: 1=facultative heterotrophs, 2=AOB, 3=NOB, 4=acetogens (f1), and 5=methanogens

5. Acetate (Ace):

- Utilization by facultative heterotrophs in aerobic conditions:

$$r_{ut,Ace,het} = \left(\frac{\hat{q}_{Ace}Ace}{K_{Ace,het} + Ace}\right)\left(\frac{DO}{K_{DO,het} + DO}\right)X_{het} \quad \left(\text{units: } \frac{mgCOD}{L\ d}\right)$$

- Production by fermenters (f1):

$$r_{prod,Ace,f1} = \left(\frac{\hat{q}_{S,f1}S}{K_{S,f1} + S}\right)DO^{switch}NO_x^{switch}X_{f1} \quad \left(\text{units: } \frac{mgCOD}{L\ d}\right)$$

- Utilization by methanogens (m):

$$r_{ut,m} = \left(\frac{\hat{q}_{Ace,m}Ace}{K_{Ace,m} + Ace}\right)DO^{switch}NO_x^{switch}X_m \quad \left(\text{units: } \frac{mgCOD}{L\ d}\right)$$

6. UAP:

All units are

$$\frac{mgCOD}{L\ d}$$

- Production by
  - Heterotrophs:

$$r_{UAP,het} = k_{UAP}\big(r_{ut,het,S} + r^{S}_{ut,het,NiN} + r^{Ace}_{ut,het,NiN} + r^{S}_{ut,het,NaN} +$$

rut,het,NaNAce+rut,Ace,het

  - AOB and NOB:

$$r_{UAP,AOB} = -k_{UAP}r_{ut,AOB} \quad \text{and} \quad r_{UAP,NOB} = -k_{UAP}r_{ut,NOB}$$

- Fermenters (f1):

$$r_{UAP,f1} = k_{UAP} r_{ut,f1,S})$$

- Methanogens (m):

$$r_{UAP,m} = k_{UAP} r_{ut,m}$$

- Consumption by
  - Heterotrophs in aerobic conditions:

$$r_{degUAP,het} = \left(\frac{\hat{q}_{UAP,het} UAP}{UAP + K_{UAP}}\right)\left(\frac{DO}{K_{DO} + DO}\right) X_{het} \quad \left(\text{units: } \frac{mgCOD}{L\,d}\right)$$

Heterotrophs during denitrification of NO_3^- and NO_2^- are represented in Eqn. 1 and 2:

$$r_{degUAP,het,NiN} = \left(\frac{\hat{q}_{UAP,het} UAP}{UAP + K_{UAP}}\right)\left(\frac{NiN}{K_{NiN} + NiN}\right) X_{het} \quad \left(\text{units: } \frac{mgCOD}{L\,d}\right)$$

$$r_{degUAP,het,NaN} = \left(\frac{\hat{q}_{UAP,het} UAP}{UAP + K_{UAP}}\right)\left(\frac{NaN}{K_{NaN} + NaN}\right) X_{het} \quad \left(\text{units: } \frac{mgCOD}{L\,d}\right)$$

  - Fermenters (f1):

$$r_{degUAP,f1} = \left(\frac{\hat{q}_{UAP,f1} UAP}{UAP + K_{UAP}}\right)\left(NO_x^{switch}\right)\left(DO^{switch}\right) X_{f1} \quad \left(\text{units: } \frac{mgCOD}{L\,d}\right)$$

7. BAP:

- Production:

$$r_{BAP} = k_{hyd} EPS \quad \left(\text{units: } \frac{mgVSS}{L\,d}\right)$$

- Consumption by
  - Heterotrophs in aerobic conditions:

$$r_{degBAP,het} = \left(\frac{\hat{q}_{BAP,het} BAP}{BAP + K_{BAP}}\right)\left(\frac{DO}{K_{DO} + DO}\right) X_{het} \quad \left(\text{units: } \frac{mgCOD}{L\,d}\right)$$

  - Fermenters (f1):

$$r_{degBAP,f1} = \left(\frac{\hat{q}_{BAP,f1} BAP}{BAP + K_{BAP}}\right) NO_x^{switch} DO^{switch} X_{f1} \quad \left(\text{units: } \frac{mgCOD}{L\,d}\right)$$

8. Biosorption/Flocculation:

All units are

$$\frac{mgVSS}{L\,d}$$

- Flocculent PCOD ($PCOD_f$):

$$r_{PCODf} = \Phi k_{floc} PCOD_s G - k_{p,f} \Phi G^p PCOD_f - k_{hyd,f} PCOD_f$$

or with hydrolysis in anaerobic conditions only

$$r_{PCODf} = \Phi k_{floc} PCOD_s G - k_{p,f} \Phi G^p PCOD_f - DO^{switch} NO_x^{switch} k_{hyd,f} PCOD_f$$

Where Φ=floc unit volume (L floc/L unit volume), G=RMS velocity gradient, p=dimensionless constant=1

- Absorbed PCOD ($PCOD_a$):

$$r_{PCODa} = k_{1,ad}(q - q_{eq}) - k_{hyd,a} PCOD_a$$

or with hydrolysis in anaerobic conditions only

$$r_{PCODa} = k_{1,ad}(q - q_{eq}) - DO^{switch} NO_x^{switch} k_{hyd,a} PCOD_a$$

Where $q_{eq} = k_F PCOD_{eq}^{1/n}$ and $q = k_F {PCOD_s}^{1/n}$

- Single (free-form) PCOD particles ($PCOD_s$):

$$r_{PCODs} = -\Phi k_{floc} PCOD_s G + k_{p,f} G^p PCOD_f - k_{hyd,s} PCOD_s - [k_{1,ad}(q - q_{eq})]$$

A.3.3. Net reaction rates for all components

Substrate (S1):

$$R_{COD} = R_{S1} = -(r_{ut,S} + r_{ut,het,NiN}^S + r_{ut,het,NaN}^S + r_{prod,Ace,f1}) + \gamma_O r_{hyd} + k_{hyd,s} PCOD_s + DO^{switch} NO_x^{switch} (k_{hyd,a} PCOD_a + k_{hyd,f} PCOD_f)$$

$$\left(\text{units: } \frac{\text{mgCOD}}{\text{L d}}\right)$$

UAP (S2):

$$\begin{aligned} R_{UAP} = R_{S2} &= (r_{UAP,Het} + r_{UAP,f1} + r_{UAP,m}) \\ &+ \frac{\gamma_O}{\gamma_N}(r_{UAP,AOB} + r_{UAP,NOB}) \\ &- (1 - k_{UAP})(r_{degUAP,Het} + r_{ut,het,NiN}^{UAP} + r_{ut,het,NaN}^{UAP} \\ &+ r_{degUAP,f1}) + k_{UAP}(r_{degBAP,Het} + r_{ut,het,NiN}^{BAP} + r_{ut,het,NaN}^{BAP} \\ &+ r_{degBAP,f1}+) \end{aligned}$$

$$\left(\text{units: } \frac{\text{mgCOD}}{\text{L d}}\right)$$

BAP (S3):

$$R_{BAP} = R_{S3} = \gamma_O r_{BAP} - \left(r_{degBAP,Het} + r_{ut,het,NiN}^{BAP} + r_{ut,het,NaN}^{BAP} + \right.$$
rdegBAP,f1

$$\left(\text{units: } \frac{\text{mgCOD}}{\text{L d}}\right)$$

DO (S4):

$$\begin{aligned} R_{DO} = R_{S4} \\ &= -\alpha_{Het}\left(r_{ut,het,S} + r_{ut,Ace,het}\right) \\ &- \alpha_{Het,p}\left(r_{degUAP,Het} + r_{degBAP,Het}\right) - \alpha_{AOB} r_{ut,AOB} \\ &- \alpha_{NOB} r_{ut,NOB} \\ &- \gamma_O \sum_{i=1}^{3}\left[\left(\frac{DO}{DO + K_{DO,i}}\right) b_i f_d X_i\right] \quad \left(\text{units: } \frac{\text{mgO}_2}{\text{L d}}\right) \end{aligned}$$

where i represents type of biomass 1=facultative heterotrophs, 2=AOB, and 3=NOB and

$$\alpha_{Het} = 1 - k_{UAP,Het} - k_{EPS,Het} - \left(1 - k_{UAP,Het} - k_{EPS,Het}\right) Y_{Het}\gamma_O$$
$$\alpha_{Het,p} = 1 - k_{UAP,Het} - k_{EPS,Het} - \left(1 - k_{UAP,Het} - k_{EPS,Het}\right) Y_p\gamma_O$$
$$\alpha_{AOB} = 3.43 - k_{EPS,AOB} - \left[Y_{AOB}\left(\gamma_O + 3.43\gamma_N - k_{EPS,AOB}\right)\right]$$
$$\alpha_{NOB} = 1.14 - Y_{NOB}\gamma_O - 1.14 Y_{NOB}\gamma_N$$

Ammonia (Amm) (S5):

$$R_{AmN} = R_{S5} = \gamma_N\left(r_{BAP} + r_{prod,Amm,total}\right) + (1 - k_{UAP})r_{ut,AOB} - k_{UAP}r_{ut,NOB} + (\gamma_N/\gamma_O)r_{hyd} - \gamma_N\left[(1 - k_{UAP} - k_{EPS})Y_{het}\left(r_{ut,S} + \right.\right.$$
rut,het,NiNS+rut,het,NaNS+rut,het,NiNAce+rut,het,NaNAce+r
ut,het,Ace+YP1−kUAP−kEPSrdegUAP,het+rut,het,NiNUAP+r
ut,het,NaNUAP+rdegUAP,f1+YP1−kUAP−kEPSrdegBAP,Het+
rut,het,NiNBAP+rut,het,NaNBAP+rdegBAP,f1+1−kUAP−kEPS
rut,mYm+Yf1rut,S,f1−γNγOkEPSrut,S+i=14rut,Het,NiN+i=14
rut,Het,NaN+rut,Ace,het++rdegUAP,Het+rdegUAP,f1+rdegBA
P,Het+rdegBAP,f1+rut,m+rut,S,f1

$$\left(\text{units: } \frac{\text{mgNH}_4^+ - \text{N}}{\text{L d}}\right)$$

Nitrite (NiN) (S6):

$$R_{NiN} = R_{S6} = r_{ut,NOB} - \gamma_{NiN}\left[\sum_{i=1}^{4} r_{ut,Het,NiN} - \gamma_O f_d b_{het}\left(\frac{NiN}{K_{NiN,het} + NiN}\right) DO^{switch} X_{het}\right] - r_{ut,AOB}(1 - k_{UAP} - k_{EPS})(1 - \gamma_N Y_{AOB})$$

$$\left(\text{units: } \frac{mgNO_2^- - N}{L\ d}\right)$$

Nitrate (NaN) (S7):

$$R_{NaN} = R_{S7} = (1 - k_{UAP} - k_{EPS})(1 - \gamma_N Y_{NOB}) r_{ut,NOB} - \gamma_{NaN}\left[\sum_{i=1}^{4} r_{ut,Het,NaN} + \gamma_O f_d b_{het}\left(\frac{NaN}{K_{NaN,het} + NaN}\right) DO^{switch} X_{het}\right]$$

$$\left(\text{units: } \frac{mgNO_3^- - N}{L\ d}\right)$$

Acetate (Ace) (S8):

$$R_{Ace} = R_{S8} = (1 - k_{UAP} - k_{EPS})(1 - \gamma_O Y_{f1}) r_{prod,Ace,f1} + (1 - k_{UAP} - k_{EPS})\left(1 - \gamma_O Y_p\right)\left(r_{degUAP,f1} + r_{degBAP,f1}\right) - r_{ut,m} - r_{ut,Ace,het} - r_{ut,het,Nan}^{Ace} - r_{ut,het,Nin}^{Ace} + \gamma_O DO^{switch} NO_x^{switch} f_d b_{f1} X_{f1}$$

$$\left(\text{units: } \frac{mgCOD}{L\ d}\right)$$

$PCOD_f$ (S9):

$$R_{PCODf} = R_{S9} = r_{PCODf} \quad \left(\text{units: } \frac{mgVSS}{L\ d}\right)$$

$PCOD_s$ (S10):

$$R_{PCODs} = R_{S10} = r_{PCODs} \quad \left(\text{units: } \frac{mgVSS}{L\ d}\right)$$

$PCOD_a$ (S11):

$$R_{PCODa} = R_{S11} = r_{PCODa} \quad \left(\text{units: } \frac{\text{mgVSS}}{\text{L d}}\right)$$

Nitrogen Gas (N_2) (S12):

$$\begin{aligned} R_{N2} = R_{S12} = {} & (1 - k_{UAP} - k_{EPS})(1 - \gamma_O Y_{het})\left(r^{S}_{ut,het,NiN} + r^{S}_{ut,het,NaN}\right. \\ & \left. + r^{Ace}_{ut,het,NiN} + r^{Ace}_{ut,het,NaN} + r_{ut,het,Ace}\right) \\ & + (1 - k_{UAP} - k_{EPS})\left(1 - \gamma_O Y_p\right)\left(r^{UAP}_{ut,het,NiN} + r^{UAP}_{ut,het,NaN}\right. \\ & \left. + r^{BAP}_{ut,het,NiN} + r^{BAP}_{ut,het,NaN} +\right) \\ & + \gamma_O f_d b_{het}\left(\frac{NaN}{K_{NaN,het} + NaN}\right) DO^{switch} X_{het} \\ & + \gamma_O f_d b_{het}\left(\frac{NiN}{K_{NiN,het} + NiN}\right) DO^{switch} X_{het} \end{aligned}$$

$$\left(\text{units: } \frac{\text{mgN}}{\text{L d}}\right)$$

Facultative heterotrophs (X1):

$$\begin{aligned} R_{het} = R_{X1} = {} & Y_{Het}(1 - k_{UAP} - k_{EPS})\left(r_{ut,S} + r^{S}_{ut,het,NiN} + r^{S}_{ut,het,NaN} + r^{Ace}_{ut,het,NiN}\right. \\ & \left. + r^{Ace}_{ut,het,NaN} + r_{ut,Ace,het}\right) \\ & + Y_p(1 - k_{UAP} - k_{EPS})\left(r_{degBAP,Het} + r_{degUAP,Het} + r^{UAP}_{ut,het,NiN}\right. \\ & \left. + r^{UAP}_{ut,het,NaN} + r^{BAP}_{ut,het,NiN} + r^{BAP}_{ut,het,NaN}\right) \\ & - b_{Het} X_{Het}\left[\frac{DO}{K_{DO,het} + DO}\right. \\ & \left. + DO^{switch}\left(\frac{NiN}{K_{NiN,het} + NiN} + \frac{NaN}{K_{NaN,het} + NaN}\right)\right] \\ & - k_{hyd} X_{Het} DO^{switch} NO_x^{switch} \end{aligned}$$

AOB (X2):

$$\begin{aligned} R_{AOB} = R_{X2} = {} & -Y_{AOB}(1 - k_{UAP} - k_{EPS}) r_{ut,AOB} - b_{AOB} X_{AOB}\left(\frac{DO}{K_{DO,het} + DO}\right) \\ & - k_{hyd} X_{AOB} DO^{switch} NO_x^{switch} \end{aligned}$$

NOB (X3):

$$\begin{aligned} R_{NOB} = R_{X3} = {} & -Y_{NOB}(1 - k_{UAP} - k_{EPS}) r_{ut,NOB} - b_{NOB} X_{NOB}\left(\frac{DO}{K_{DO,het} + DO}\right) \\ & - k_{hyd} X_{NOB} DO^{switch} NO_x^{switch} \end{aligned}$$

Fermenters (X4):

$$R_{f1} = R_{X4} = Y_{f1}(1 - k_{UAP} - k_{EPS})(r_{prod,Ace,f1}) + Y_p(1 - k_{UAP} - k_{EPS})(r_{degBAP,f1} + r_{degUAP,f1}) - b_{f1}X_{f1}DO^{switch}NO_x^{switch}$$

Methanogens (X5):

$$R_m = R_{X5} = Y_m(1 - k_{UAP} - k_{EPS})r_{ut,m} - b_m X_m DO^{switch} NO_x^{switch}$$

EPS (X6):

$$R_{EPS} = R_{X6} = \frac{k_{EPS}}{\gamma_O}\left(r_{ut,S} + \sum_{i=1}^{4} r_{ut,Het,NaN} + \sum_{i=1}^{4} r_{ut,Het,NiN} + r_{degUAP,Het} + r_{degBAP,Het} + r_{ut,Ace,het} + r_{prod,Ace,f1} + r_{degUAP,f1} + r_{degBAP,f1} + r_{ut,m} - k_{EPS}\gamma_{nrut,AOB} + r_{ut,NOB} - r_{BAP}\right.$$

Inert Biomass (X7):

$$R_{inert} = R_{X7} = (1 - f_d)\left[(b_{Het}X_{Het} + b_{AOB}X_{AOB} + b_{NOB}X_{NOB})\left(\frac{DO}{K_{DO,het} + DO}\right) + b_{Het}X_{Het}DO^{switch}\left(\frac{NiN}{K_{NiN,het} + NiN} + \frac{NaN}{K_{NaN,het} + NaN}\right) + (b_{f1}X_{f1} + b_m X_m)DO^{switch}NO_x^{switch}\right]$$

A.3.4. Mass balance reactions

- Anoxic Tank

$$\frac{dS_i^{AX}}{dt} = \frac{1}{V^{AX}}\left(Q^{in}S_i^{in} + Q^{ST}S_i^{ST} - Q^{AX}S_i^{AX} + R_{Si}^{AX}V^{AX}\right)$$

where i=8-21 (for all soluble materials present)

$$\frac{dX_i^{AX}}{dt} = \frac{1}{V^{AX}}\left(Q^{in}X_i^{in} + Q^{ST}X_i^{ST} - Q^{AX}X_i^{AX} + R_{Xi}^{AX}V^{AX}\right)$$

where i=1-7 (for all biomass/solid materials present)

- Contact Tank

$$\frac{dS_i^{CT}}{dt} = \frac{1}{V^{CT}}\left(Q^{AX}S_i^{AX} - Q^{CT}S_i^{CT} + R_{Si}^{CT}V^{CT}\right)$$

For DO,

$$\frac{dS_i^{CT}}{dt} = \frac{1}{V^{CT}}\left[Q^{AX}S_i^{AX} - Q^{CT}S_i^{CT} + R_{Si}^{CT}V^{CT} + K_La(DO^{sat} - S_i^{CT})\right]$$

where the last term describes the oxygen added to the contact tank through aeration.

$$\frac{dX_i^{CT}}{dt} = \frac{1}{V^{CT}}\left(Q^{AX}X_i^{AX} - Q^{CT}X_i^{CT} + R_{Xi}^{CT}V^{CT}\right)$$

- Clarifier

The clarifier uses an average of the effluent (C_{out}) and clarifier sludge (C_{CL_SL}) concentrations which is called C_{CL} for the calculations.

$$\frac{dS_i^{CL}}{dt} = \frac{1}{V^{CL}}\left(Q^{CT}S_i^{CT} - (Q^{out} + Q^{CL}) * S_i^{CL} + R_{Si}^{CL}V^{CL}\right)$$

where

$$S^{CL} = \frac{Q^{out}S^{out} + Q^{CL}S^{CL-SL}}{Q^{out} + Q^{CL}} \Rightarrow S^{out} = \frac{(Q^{out} + Q^{CL})S^{CL} - Q^{CL}S^{CL-SL}}{Q^{out}}$$

$$\frac{dX_i^{CL}}{dt} = \frac{1}{V^{CL}}\left(Q^{CT}X_i^{CT} - (Q^{CL} + Q^{out})X_i^{CL} + R_{Xi}^{SL}V^{CL}\right)$$

- Stabilization Tank

$$\frac{dS_i^{CT}}{dt} = \frac{1}{V^{ST}}\left(Q^{CL-ST}S_i^{CL} + Q^{SL-ST}S_i^{SL-super} + Q^{AD}S_i^{AD} - Q^{ST}S_i^{ST} + R_{Si}^{ST}V^{ST}\right)$$

$$\frac{dX_i^{CT}}{dt} = \frac{1}{V^{ST}}\left(Q^{CL-ST}X_i^{CL} + Q^{SL-ST}X_i^{SL-super} + Q^{AD}X_i^{AD} - Q^{ST}X_i^{ST} + R_{Xi}^{ST}V^{ST}\right)$$

- Sludge Thickener

$$\frac{dS_i^{SL}}{dt} = \frac{1}{V^{SL}}\left[Q^{CL-SL}S_i^{CL} - (Q^{SL-ST} + Q^{SL-AD})S_i^{SL} + R_{Si}^{SL}V^{SL}\right]$$

where

$$S^{SL} = \frac{Q^{SL-super}S^{SL-super} + Q^{SL-AD}S^{SL-AD}}{Q^{SL-super} + Q^{SL-AD}}$$

$$\Rightarrow S^{SL-super} = \frac{(Q^{SL-super} + Q^{SL-AD})S^{SL} - Q^{SL-AD}S^{SL-AD}}{Q^{SL-super}}$$

$$\frac{dX_i^{SL}}{dt} = \frac{1}{V^{SL}}\left[Q^{CL-SL}X_i^{CL} - (Q^{SL-ST} + Q^{SL-AD})X_i^{SL} + R_{Xi}^{SL}V^{SL}\right]$$

- Anaerobic Digester

$$\frac{dS_i^{AD}}{dt} = \frac{1}{V^{AD}}\left(Q^{SL-AD}S_i^{SL} - (Q^{W} + Q^{AD})S_i^{AD} + R_{Si}^{AD}V^{AD}\right)$$

$$\frac{dX_i^{AD}}{dt} = \frac{1}{V^{AD}}\left(Q^{SL-AD}X_i^{SL} - (Q^{W} + Q^{AD})X_i^{AD} + R_{Xi}^{AD}V^{AD}\right)$$

APPENDIX B.

SAMPLES OF CHEMOSTAT AND OVERALL SYSTEM MASS BALANCE CLOSURE CONFIRMATION

B.1 An example of mass balance analysis on the contact tank

COD Balance			COD Influent				COD Effluent				
	In	Out	Total SCOD	Total PCOD	Total VSS*1.42	Total	Total SCOD	Total PCOD	Total VSS*1.42	CH4	Total
Flow rate (L/d)	1471	1471	95354	857206	6113235	7065796	99489	856382	6121860	0	7077731
Volume	12	12							Difference:		0.17%
Heterotrophs (mgVSS/L)	140	142			291073				296714		
AOB (mgVSS/L)	3	3			7009				7036		
NOB (mgVSS/L)	2	2			4761				4755		
Fermenters f1 (mgVSS/L)	126	126			262438				262683		
Methanogens (mgVSS/L)	17	17			36034				36036		
EPS (mgVSS/L)	112	113			233754				236351		
Inerts (mgVSS/L)	2534	2534			5278166				5278286		
Substrate (mgVSS/L)	41	33	60930				47844				
UAP (mgCOD/L)	4	5	6549				7207				
BAP (mgCOD/L)	7	8	10787				11040				
Acetate (mgCOD/L)	10	10	15955				16392				
PCODf (mgVSS/L)	2	1		2554				1259			
PCODa (mgVSS/L)	321	324		471609				477366			
PCODs (mg2/L)	260	257		383044				377756			
NO2-N(mgN/L)	0.0	0.0									
NO3-N(mgN/L)	0.0	0.0									
NH4-N(mgN/L)	98.6	98.0									
DO (mgO2/Ld)	0.8	8.7	1133				17005				
CH4 (mgCOD/Ld)	0.0									0	
N2 (mgN/Ld)	0.0									0	

Nitrogen Balance			Nitrogen Influent				Nitrogen Effluent				
	In	Out	N soluble	N solid	N compounds	Total	N soluble	N solid	N compounds	CH4	Total
Flow rate (L/d)	1471	1471	0	534908	145064	679972	0	535663	144227	0	679889
Volume	12	12							Difference:		-0.01%
Heterotrophs (mgVSS/L)	140	142		25469				25962			
AOB (mgVSS/L)	3	3		613				616			
NOB (mgVSS/L)	2	2		417				416			
Fermenters f1 (mgVSS/L)	126	126		22963				22985			
Methanogens (mgVSS/L)	17	17		3153				3153			
EPS (mgVSS/L)	112	113		20453				20681			
Inerts (mgVSS/L)	2534	2534		461840				461850			
Substrate (mgVSS/L)	41	33									
UAP (mgCOD/L)	4	5									
BAP (mgCOD/L)	7	8									
Acetate (mgCOD/L)	10	10									
PCODf (mgVSS/L)	2	1									
PCODa (mgVSS/L)	321	324									
PCODs (mg2/L)	260	257									
NO2-N(mgN/L)	0.0	0.0			27				30		
NO3-N(mgN/L)	0.0	0.0			21				9		
NH4-N(mgN/L)	98.6	98.0			145017				144188		
DO (mgO2/Ld)	0.8	8.7									
CH4 (mgCOD/Ld)	0.0										
N2 (mgN/Ld)	0.0								0		

B.2 An example of mass balance analysis on the overall system

COD Balance	Concentrations						
	In	AX	CT	CL total	ST total	SL total	AD total
Flow rate (L/d)	605.0	1369.6	1369.6	1369.6	764.6	43.6	14.5
Volume		25	12	100	50	100	650
Total							
Heterotrophs (mgVSS/L)	25	180	183	179	295	188	39
AOB (mgVSS/L)	0	0	0	0	0	0	0
NOB (mgVSS/L)	0	0	0	0	0	0	0
Fermenters (mgVSS/L)	1	299	299	303	520	637	1207
Methanogens (mgVSS/L)	0.5	38	38	38	66	84	172
EPS (mgVSS/L)	0	246	247	253	423	567	577
Inerts (mgVSS/L)	100	4267	4267	4276	7453	7697	22686
Substrate (mgVSS/L)	150	19	10	3	0	0	0
UAP (mgCOD/L)	0	5	5	5	5	3	1
BAP (mgCOD/L)	0	11	11	13	18	21	11
Acetate (mgCOD/L)	0	34	34	39	20	19	3
PCODf (mgVSS/L)	0	456	368	511	395	527	155
PCODa (mgVSS/L)	0	364	367	359	640	399	28
PCODs (mg2/L)	250	137	221	61	473	63	47
NO2-N(mgN/L)	0	0	0	0	0	0	0
NO3-N(mgN/L)	0.2	0	0	0	0	0	0
NH4-N(mgN/L)	100	96	96	88	92	87	268
DO (mgO2/L)	0.5	-168	-362	0	0	-214	-27
CH4 (mgCOD/L)	0.0	136	19	171	339	13	198
N2 (mgN/L)	0.0	4	0	0	0	0	0

	Mass rate by line or tank (mgCOD/d)								
	In	AX	CT	CL total	Qout	Qcl	CL check	WAS	Qcl-st
Flow rate (L/d)	605	1393	1393	1393	602	791		65	726
Volume		25	12	100					
Heterotrophs (mgVSS/L	21416	354715	360242	352990	353	352637	352990	28896	323741
AOB (mgVSS/L)	0	0	0	0	0	0	0	0	0
NOB (mgVSS/L)	0	0	0	0	0	0	0	0	0
Fermenters (mgVSS/L)	857	588869	589288	597432	597	596834	597432	48906	547928
Methanogens (mgVSS/L	428	74409	74421	75466	75	75391	75466	6178	69213
EPS (mgVSS/L)	0	485422	487749	498980	499	498481	498980	40847	457634
Inerts (mgVSS/L)	85664	8415581	8415581	8433332	8433	8424898	8433332	690356	7734542
Substrate (mgVSS/L)	90750	26358	14111	4179	1806	2372	4179	194	2178
UAP (mgCOD/L)	0	6944	7544	7391	3195	4196	7391	344	3852
BAP (mgCOD/L)	0	15005	15566	18037	7797	10240	18037	839	9401
Acetate (mgCOD/L)	0	47899	46940	54468	23544	30923	54468	2534	28389
PCODf (mgVSS/L)	0	635063	512423	711772	712	711060	711772	58266	652794
PCODa (mgVSS/L)	0	507022	511826	500116	500	499616	500116	40940	458676
PCODs (mg2/L)	151250	190543	307444	85415	85	85329	85415	6992	78337
NO2-N(mgN/L)	0								
NO3-N(mgN/L)	121								
NH4-N(mgN/L)	60500								
DO (mgO2/L)	303	4206	4350	0					
CH4 (mgCOD/L)	0	3393	230	17147					
N2 (mgN/L)	0	103	2	0					

	Mass rate by line or tank (mgCOD/d)							Mass Balance (mgCOD/d)			
	ST total	SL total	Slad	Slsuper	AD total	Qw	Qad	Into AX	Out of AX	Into CT	Out of CT
Flow rate (L/d)	788	65	22	43	22	3	19				
Volume	50	100			650						
Total	11009217	931162	905675	2737	906552	102054	658075	11342640	11355532	11347830	11347487
Heterotrophs (mgVSS/L	329169	17212	17194	17	1207	162	1045	350585	354715	354715	360242
AOB (mgVSS/L)	0	0	0	0	0	0	0	0	0	0	0
NOB (mgVSS/L)	0	0	0	0	0	0	0	0	0	0	0
Fermenters (mgVSS/L)	580168	58410	58352	58	36915	4956	31958	581025	588869	588869	589288
Methanogens (mgVSS/L	73805	7721	7713	8	5258	706	4552	74233	74409	74409	74421
EPS (mgVSS/L)	472199	52024	51971	52	17638	2368	15270	472199	485422	485422	487749
Inerts (mgVSS/L)	8314646	706217	705511	706	693830	93153	600677	8400310	8415581	8415581	8415581
Substrate (mgVSS/L)	360	29	10	19	1	0	1	91110	26358	26358	14111
UAP (mgCOD/L)	3813	177	59	118	13	2	11	3813	6944	6944	7544
BAP (mgCOD/L)	14152	1336	445	891	239	32	207	14152	15005	15005	15566
Acetate (mgCOD/L)	16086	1206	402	804	65	9	57	16086	47899	47899	46940
PCODf (mgVSS/L)	310841	34123	34089	34	3354	450	2903	310841	635063	635063	512423
PCODa (mgVSS/L)	504027	25864	25838	26	603	81	522	504027	507022	507022	511826
PCODs (mg2/L)	373009	4095	4091	4	1006	135	871	524259	190543	190543	307444
NO2-N(mgN/L)											
NO3-N(mgN/L)											
NH4-N(mgN/L)											
DO (mgO2/L)	1	21408			17821				4206		4350
CH4 (mgCOD/L)	16941	1343			128593				3393		0
N2 (mgN/L)	0	0			9				103		2
% Difference									**-0.11%**		**0.00%**

	Mass Balance (mgCOD/d)									
	Into CL	Out of CL	Into SL	Out of SL	Into AD	Out of AD	Into ST	Out of ST	Into System	Out of System
Total	11343135	11356723	925291	931162	905675	906552	11027499	10992276	350667	348027
Heterotrophs (mgVSS/L)	360242	352990	28896	17212	17194	1207	324803	329169	21416	515
AOB (mgVSS/L)	0	0	0	0	0	0	0	0	0	0
NOB (mgVSS/L)	0	0	0	0	0	0	0	0	0	0
Fermenters (mgVSS/L)	589288	597432	48906	58410	58352	36915	579945	580168	857	5554
Methanogens (mgVSS/L)	74421	75466	6178	7721	7713	5258	73773	73805	428	781
EPS (mgVSS/L)	487749	498980	40847	52024	51971	17638	472956	472199	0	2867
Inerts (mgVSS/L)	8415581	8433332	690356	706217	705511	693830	8335926	8314646	85664	101586
Substrate (mgVSS/L)	14111	4179	194	29	10	1	2198	360	90750	1806
UAP (mgCOD/L)	7544	7391	344	177	59	13	3981	3813	0	3196
BAP (mgCOD/L)	15566	18037	839	1336	445	239	10499	14152	0	7829
Acetate (mgCOD/L)	46940	54468	2534	1206	402	65	29250	16086	0	23553
PCODf (mgVSS/L)	512423	711772	58266	34123	34089	3354	655732	310841	0	1162
PCODa (mgVSS/L)	511826	500116	40940	25864	25838	603	459224	504027	0	581
PCODs (mg2/L)	307444	85415	6992	4095	4091	1006	79212	373009	151250	220
NO2-N(mgN/L)										
NO3-N(mgN/L)										
NH4-N(mgN/L)										
DO (mgO2/L)		0		21408		17821		1	303	47785
CH4 (mgCOD/L)		17147		1343		128593		0	0	150476
N2 (mgN/L)		0		0		9		0	0	114
% Difference		**-0.12%**		**-0.63%**		**-0.10%**		**0.32%**		**0.76%**

	Mass rate by line or tank (mgN/d)												
	In	AX	CT	CL total	Qout	Qcl	WAS	Qcl-st	ST total	SL total	Slad	Slsuper	AD total
Flow rate (L/d)	605	1370	1370	1370	600	770	44	726	765	44	15	29	15
Volume		25	12	100					50	100			650
Total	70103	984860	985561	977263	53657	923606	52280	871327	899889	53291	50715	2576	48293
Heterotrophs (mgVSS/L)	1874	30518	30993	30369	30	30339	1717	28621	27949	1012	1011	1	71
AOB (mgVSS/L)	0	0	0	0	0	0	0	0	0	0	0	0	0
NOB (mgVSS/L)	0	0	0	0	0	0	0	0	0	0	0	0	0
Fermenters (mgVSS/L)	75	50663	50699	51399	51	51348	2906	48441	49261	3436	3432	3	2171
Methanogens (mgVSS/L)	37	6402	6403	6493	6	6486	367	6119	6267	454	454	0	309
EPS (mgVSS/L)	0	41763	41963	42929	43	42886	2428	40459	40093	3060	3057	3	1037
Inerts (mgVSS/L)	7496	724025	724025	725552	726	724826	41028	683798	705980	41539	41498	42	40811
Substrate (mgVSS/L)	0	0	0	0	0	0	0	0	0	0	0	0	0
UAP (mgCOD/L)	0	0	0	0	0	0	0	0	0	0	0	0	0
BAP (mgCOD/L)	0	0	0	0	0	0	0	0	0	0	0	0	0
Acetate (mgCOD/L)	0	0	0	0	0	0	0	0	0	0	0	0	0
PCODf (mgVSS/L)	0	0	0	0	0	0	0	0	0	0	0	0	0
PCODa (mgVSS/L)	0	0	0	0	0	0	0	0	0	0	0	0	0
PCODs (mg2/L)	0	0	0	0	0	0	0	0	0	0	0	0	0
NO2-N(mgN/L)	0	0	0	0	0	0	0	0	0	0	0	0	0
NO3-N(mgN/L)	121	4	1	0	0	0	0	0	0	0	0	0	1
NH4-N(mgN/L)	60500	131478	131478	120521	52800	67721	3833	63888	70340	3790	1263	2526	3891
N2 (mgN/Ld)	0	9	0	0					0	0			1

	Mass rate by line or tank (mgN/d)			Mass rate (mgN/d)					
	AD total	Qw	Qad	Into AX	Out of AX	Into CT	Out of CT	Into CL	Out of CL
Flow rate (L/d)	15	5	10						
Volume	650								
Total	48293	16630	31663	969992	984860	984851	985561	985561	977263
Heterotrophs (mgVSS/L)	71	24	47	29823	30518	30518	30993	30993	30369
AOB (mgVSS/L)	0	0	0	0	0	0	0	0	0
NOB (mgVSS/L)	0	0	0	0	0	0	0	0	0
Fermenters (mgVSS/L)	2171	748	1424	49336	50663	50663	50699	50699	51399
Methanogens (mgVSS/L)	309	107	203	6304	6402	6402	6403	6403	6493
EPS (mgVSS/L)	1037	357	680	40093	41763	41763	41963	41963	42929
Inerts (mgVSS/L)	40811	14053	26757	713475	724025	724025	724025	724025	725552
Substrate (mgVSS/L)	0	0	0	0	0	0	0	0	0
UAP (mgCOD/L)	0	0	0	0	0	0	0	0	0
BAP (mgCOD/L)	0	0	0	0	0	0	0	0	0
Acetate (mgCOD/L)	0	0	0	0	0	0	0	0	0
PCODf (mgVSS/L)	0	0	0	0	0	0	0	0	0
PCODa (mgVSS/L)	0	0	0	0	0	0	0	0	0
PCODs (mg2/L)	0	0	0	0	0	0	0	0	0
NO2-N(mgN/L)	0	0	0	0	0	0	0	0	0
NO3-N(mgN/L)	1	1	1	121	4	4	1	1	0
NH4-N(mgN/L)	3891	1340	2551	130840	131478	131478	131478	131478	120521
N2 (mgN/Ld)	1				9		0		0
% Difference					1.53%		0.07%		-0.84%

	Mass rate (mgN/d)							
	Into SL	Out of SL	Into AD	Out of AD	Into ST	Out of ST	Into System	Out of System
Flow rate (L/d)								
Volume								
Total	52280	53291	50715	48293	905566	899889	70103	70296
Heterotrophs (mgVSS/L)	1717	1012	1011	71	28669	27949	1874	55
AOB (mgVSS/L)	0	0	0	0	0	0	0	0
NOB (mgVSS/L)	0	0	0	0	0	0	0	0
Fermenters (mgVSS/L)	2906	3436	3432	2171	49868	49261	75	799
Methanogens (mgVSS/L)	367	454	454	309	6322	6267	37	113
EPS (mgVSS/L)	2428	3060	3057	1037	41142	40093	0	400
Inerts (mgVSS/L)	41028	41539	41498	40811	710597	705980	7496	14779
Substrate (mgVSS/L)	0	0	0	0	0	0	0	0
UAP (mgCOD/L)	0	0	0	0	0	0	0	0
BAP (mgCOD/L)	0	0	0	0	0	0	0	0
Acetate (mgCOD/L)	0	0	0	0	0	0	0	0
PCODf (mgVSS/L)	0	0	0	0	0	0	0	0
PCODa (mgVSS/L)	0	0	0	0	0	0	0	0
PCODs (mg2/L)	0	0	0	0	0	0	0	0
NO2-N(mgN/L)	0	0	0	0	0	0	0	0
NO3-N(mgN/L)	0	0	0	1	1	0	121	1
NH4-N(mgN/L)	3833	3790	1263	3891	68966	70340	60500	54140
N2 (mgN/Ld)		0		1		0	0	10
% Difference		1.93%		-4.78%		-0.63%		0.28%